ASAE Memo. No. 5

CoA Memo. No. 165

ADVANCED SCHOOL OF AUTOMOBILE ENGINEERING

THE DESIGN AND STRESS ANALYSIS OF AN INTEGRAL LAND ROVER STRUCTURE

- by -

G.H. Tidbury

R 37,254

ASAE Memo. No. 5

CoA Memo. No.165

November, 1968

Advanced School of Automobile Engineering

The Design and Stress Analysis of an Integral Land Rover Structure.

- by -

G.H.Tidbury, B.Sc., D.I.C., C.Eng., M.I.Mech.E., A.F.R.Ae.S.

SUMMARY

This report gives in detail the calculation of the distribution of forces in an integral structure by the matrix force method. The design of a full scale structure to test the theoretical results is described in an Appendix but test results will be given in a separate report. The method of analysis is suitable for a small first generation digital computer and would now be superceded by 'automatic' programs on large computers.

ERRATA

p.7. 1.23:

Figure 18 shows the breakdown of each plane of the structure into the chosen systems while Figure 18a - o show the load distribution in one of each of the systems due to a given internal load.

p.13. 1.7:

The six columns of the R matrix (page 14) are the six loading cases ....

P.44. 1.10:

$$\frac{f_r}{E_t} = 2.46 \left(\frac{.128}{2.375} \right)^2 = .0716$$

Contents | Page No.

Introduction

Integral vehicle structures have been developed largely on a trial and error basis and are normally constructed of spot welded sheet metal. The present investigation was commenced in 1961 to obtain information on the possible weight saving on a typical vehicle if it were constructed of aluminium alloys of high strength (aircraft specification) and if the sizes of the members were determined by using the stress analysis methods current in the aircraft industry at that time. It was hoped that some light would be thrown on the possibility of reducing the trial and error approach for normal sheet steel vehicles as well as evolving a design that could be made as a full scale model for detailed investigation of the theoretical results.

The essential differences between vehicle structures and aircraft structures from the point of view of analysis are :-

1) The irregular nature of the vehicle structure, usually a mixture of beams and panels.

2) The smaller size of the vehicle structure removing the possibility of using repeated similar structural sections.

3) The lack of reliable information on the load envelope the structure can be expected to work in.

The first two points would suggest the use of a displacement method of analysis and this has been adopted by other workers in the field. McKenna (Ref.1) at General Motors in America, Allwood and Norville (Ref.2) on behalf of the Ford Motor Company in Great Britain. Only the McKenna paper was available when the project started and his method consists of reducing the structure to a three dimensional framework with stiff joints, shear panels being represented by extra framework members disposed across the diagonals. For a realistic idealisation this method required the solution of a large number of simultaneous equations and the paper referred to the need for considerable test work to establish characteristics of the framework to give a good theoretical model for the structural behaviour of the body.

The present investigation was tied to the use of the Pegasus Computer at the College of Aeronautics and this made the use of a force method essential as the store capacity of approximately 6,000 matrix elements limits the number of simultaneous equations that can be solved, if standard matrix manipulation methods are to be used in the solution.

The problem then became one of mating the idealised structure of shear panels and end load carrying members with the separate beams having no shear deformability. It is interesting to note that the Japanese workers Kirioka (Ref.3) and Kawai and Koganai (Ref.4) have developed very similar combinations of structural members when using matrix force methods on vehicle body structures and have shown that good agreement can be reached between theory and practical sheet steel bodies.

Work was carried out concurrently by students at the A.S.A.E. under the guidance of the writer developing these idealisations on simplified small scale model structures, notably Mann (Ref.5), Marsden (Ref.6) and Crawford (Ref.7). Crawford's work, however, was influenced by Kirioka and he has used the forces at actual cuts in rings as redundants rather than the type of system used here which are "self-equilibrating" local sections of the structure as proposed by Argyris and Kelsey (Ref.8).

This report can be regarded as an amplification of Ref.9 and some repetition is inevitable in order to make this report complete. The main divisions of that report are used and in particular the seven steps listed for the analysis are given in detail.

Design of the Structure

Since the structure was designed with a view to checking the theoretical analysis it was possible to use well defined straight structural members and flat panels. The outline of the structure and the structure itself are shown in Figs. 1a and 1b, and can be compared to the non-load carrying Land Rover Estate Car body reproduced in Fig.2.

Several simplifications have been made in the design :

1) The second door opening in the side has been deleted.

2) The windscreen pillar has been made vertical.

3) The floor is flat instead of being raised behind the driver's seat - this is made possible by the saving of depth in the chassis members.

4) The shock absorber attachment points and bump stop reactions are assumed to be at the same point in the structure.

5) The spring hanger points are taken at the same horizontal level.

6) Solid panels are assumed at the scuttle instead of footwells.

The basic idea in the design was to keep a shallow frame, assumed to be loaded in bending only which would serve as a basic system in the analysis and which could be used to attach the running gear in much the same way as the present chassis. The main bending loads should be carried as far as possible by the deep beams formed at the front by the side panels of the engine bay and behind this by the main side frames of the vehicle. Referring to Fig.3 this means that the bending load must be transferred from the plane of the main longitudinal (points 1 to 11) to the side frame (points 13, 56, 61, 18). The cross members are assumed to transfer this load in bending only, assisted by the torque box at the scuttle section (points 4, 5, 22, 21, 68, 69, 44, 43) and the structure round the rear wheel arch. The assumptions made by Kirioka ignored the problem of the rear wheel arch and while it is true that in passenger cars the rear spring attachment points are more widely spaced they are not in the same plane as the side frame of the vehicle.

The joints between the longitudinals and the cross members have therefore been designed to operate as continuous members in bending but

not in torsion. Although the floor panels do, in fact, close the top hat members, zero torsional stiffness is assumed.

For the analysis the nodes are numbered as shown and, for convenience, the constant shear carrying panels are given a letter and suffix number. The side windows carry numbers b_{18} and b_{21} for use with the cut-out technique proposed by Argyris and Kelsey in Ref.8. Members where bending stiffness is assumed are shown in Figs 4a, b & c.

Preliminary design calculations were confined to ensuring that the main underbody cross members would carry the dead load across the vehicle. This gave a second moment of area for the section. The top hat section was then designed on this basis. The first computer calculations were run assuming the same cross-section for the main longitudinals giving a uniform underfloor grillage made up of 2" x 1·5" x ·08" top hat section.

The results, although containing errors in some parts of the program, indicated that the main bending loads were not sufficiently transferred to the side frame of the structure and it was decided that the simplest way of keeping the stresses within safe levels was to increase the size of the main longitudinals to 3·5" x 1·5" x ·08" top hat section. The joints between the longitudinals and crossmembers were subjected to bending tests with the results given in Appendix IV, and modified until the required strength was obtained. From the final computer results it was found that nodes6 and 8 still carried theoretical bending moments greater than the design figures. These joints have been strengthened locally in the full scale body, on the assumption that the very local changes of section will not materially alter the computed stress distribution over the remainder of the structure. The early program also indicated that the choice of a ·75" x ·75" x 18 swg. square tube for the windscreen pillar was far too small as no load of any significance would be transferred to the roof. The size of this member was therefore increased to 1·5" x 1·5" x 14 swg.

Order of Indeterminacy

A literature search failed to reveal a simple method of finding the degree of indeterminacy (or redundancy) of a structure idealised into beams, end load carrying members, and shear panels. Denke (Ref.10), gives formulae for structures consisting entirely of shear panels and axially loaded bars which contains a term for the number of external loads. General formulae have been obtained by Henderson and Bickley (Ref.11), for frameworks under any loading and these formulae have been extended to include shear panels :-

For 2 dimensional structures

$$n = 3(M - N + 1) + P - r \qquad (1)$$

For 3 dimensional structures

$$n = 6(M - N + 1) + P - r \qquad (2)$$

Where M = Number of linear members

N = Number of nodes

P = Number of panels

r = Number of releases

No satisfactory method could be found for combining these two expressions for a structure of the present type, i.e. three dimensional with the planes containing separate members.

The following rules were evolved for this type of structure:-

1 The value of n for the box-like structure is found using the 3-dimensional formula with each plane face assumed to contain one panel surrounded by end load carrying members.

2 The value of n is then found for each plane in turn from the 2-dimensional formula with the actual breakdown of beams, end load carrying members and panels appropriate to that plane.

3 The sum of the values of n found in 1 and 2 gives the order of redundancy of the structures.

More details and examples of the use of the formulae are given in Ref. 12. In the process of checking the application of these formulae the structure forward of the scuttle section was analysed under various assumptions as follows:

Simplified 3-Dimensional Analysis of Front End Structure

The simplified structure was made statically determinate in all possible planes so that the analysis concentrates on the three dimensional egg box effect, it has been shown that indeterminacies in individual planes can be incorporated simply. For this reason the sections of rudimentary chassis which take bending moment only are left out, further, the outside face of the wing is assumed to be a rectangular panel with no cut out for the wheel.

Three cross members are retained across the bonnet top with no bending stiffness about the z axis.

The structure appears as in Fig.5, with an imaginary panel c_o continuing the vehicle floor across the wheel arch. The order of redundancy of this structure for symmetrical loads is two.

The panel c_o was removed in the computer analysis by the use of the Argyris cut out procedure given in Appendix 1 of Ref. 12. Since the order of redundancy is so low this analysis could be done by pencil and paper methods but it was found that the condensing of the data from the 31 loads defined in the structure to the four coefficients of the two simultaneous equations was time consuming and led to errors. It was, therefore, decided to use Pegasus and to gain experience in using condensation techniques. Since the matrix division was only concerned with 2 x 2 matrices the computer time for this program was only a few minutes. The results are shown in Fig.6.

It was proposed that the basic system for the final calculation should be made up of a set of systems transferring the down loads at the extremities of the cross members to the longitudinals of the rudimentary chassis and each concentrated load on the chassis would then be supported by the axle loads, Fig.7b. This method was adopted for the first program of the simplified front end structure (Fig.8a) but to ensure its accuracy another program was run using basic systems that linked each down load with the support points (nodes 2 and 5, Fig.8b). The results of this program were identical within rounding off limits and the equivalence of the two systems established. It can be seen from Figs.8a and 8b that the first method gives much more simple basic systems.

Since the simplified analysis assumed two redundancies and then effectively removed one of them by making a cut out it seemed reasonable that a program could be written with just one redundancy for the whole front end. Advantage was also taken of the fact that the loading assumed gave no loads in the outside panels b_1 and b_6 or in the remaining floor panel c_1. The structure to be analysed could then be represented as in Fig.9. This analysis also gave the same result showing that the front end structure has only one redundancy due to the three cross members in the bonnet top plane.

Structure in Plane of the Bonnet Top

It was originally proposed to idealise the structure in this plane with a stiff ring round the bonnet opening.

A completely stiff ring in one plane has three redundancies and the computation would be simplified if these could be omitted. The structure was analysed in the two forms shown in Figs. 10a and 10b, with 4 redundancies for the first case and 6 in the second (Fig.11). (The indeterminacy formulae indicate 8 redundancies, but for symmetrical loading 2 on each side will be identical). A symmetrical load was imposed on each system assuming unit tension in the member joining points 69 and 69'. This method of loading is not satisfactory in that the unit external load is divided between direct tension in the member (approx. 0·98 of the load) and the load taken by the remainder of the structure. Since the relative flexibilities of these local paths are different the remainder of the structure is only dealing with approximately ·02 of a unit load and all loads in the members are small.

Redundant system No.2, (Fig.10b) used in the analysis represents the structure in the plane of the bonnet top with no bending stiffness included, and for symmetrical loads it is a sufficient structure. By reducing the load at point 69 in the member 69-44 to the mean value computed for the two redundant structures the comparative table of loads table 1 can be drawn up.

From the table it can be seen that the end loads are within 10% for the three idealisations except for F_{43x} and F_{68x} where the actual loads are small. The errors due to ignoring the corner fixations on the shear loads in panels c_8 and c_9 are approximately 14% but again the actual shear loads are small. The conclusion can therefore be drawn that for symmetrical loading the bending stiffness may be ignored for this structure.

This simplification allows a reduction of 6 redundant systems and 7 loads to be defined in the structure.

The Basic System

A basic system is generally taken as a statically determinate structure which will support the external loads and follow the major load path of the complete structure. It is not essential to the theory that the latter condition should be satisfied and in this case the basic system has been chosen solely for simplicity.

It consists of the rudimentary ladder frame with outriggers, shown in Fig.7a. The outriggers are stepped up where necessary to form the rear wheel arch. The loads carried by the vehicle, and the weight of the vehicle itself, are assumed to be concentrated at the node points shown and transferred to the support points by members in bending only, except for the member 9-63 which has a constant end load. The support points are first considered to be at the axle centre lines which are vertically below nodes 2 and 63.

Since each load case is static, it is possible to allocate this support load between the two ends of the spring and the shock absorber or bump stop. For example, the single support load at node 2 is redistributed so that the spring hangers at nodes 1 and 4 carry a proportion of it and the load at 2 is reduced, Fig.7c.

The Redundant System

The method of determining the order of redundancy indicated the number of redundant systems required in each plane of the structure. The plane redundant systems were then selected in the following way :-

1 Where the four shear panels were adjacent the classical Argyris X systems were used, Fig.13 (see Ref.8).

2 When a shear panel crossed the centre line of the vehicle it was possible to use special X systems with the end load carrying members crossing the centre line having uniform load. These systems were calle X_S systems (Fig.14), since the shear panels cross the centre line could well be deleted the same type of system was used for the bonnet t

3 One or more of the panels could be replaced by a beam having no shear deformability. The most common type is when two panels are replaced by a section of continuous beam and these were called W systems (Figs.12, 13, 16) and with modifications for centre line conditions, W_S systems (Figs.16, 17).

4 When one of the four panels in an X system is replaced by a beam, the system was called a V system (Figs.13, 16) and the modified systems where one of the remaining panels crosses the centre line a V_S system (Fig.14) and where two cross the centre line a V_{SS} system (Fig.14).

5 In the case where 3 panels were replaced by a beam enclosing two sides of the remaining panel it was called a U system (Fig.12).

6 The large door opening on the side of the vehicle is essentially a ring with beams at the top and bottom having shear deformability with shallow shear panels while the front vertical member includes the wind screen pillar and is idealised as having no shear deformability along its complete length. The rear vertical member of the ring consists of the front panels of the panelled section of the side of the vehicle. The three redundant systems for such a ring were chosen by replacing the beam on three of the sides in turn by end load carrying members having a unit end load. These systems were called S systems (Fig.12) and are more local in their effect than the 'cut loads' used by Kirioka when analysing the same problem.

The only redundant systems that were not in a two dimensional plane system were those in the floor acting as a grid in bending. These were essentially the same as the systems used by Lucas in Ref.13, and here called T systems (Fig.15). The beams are here considered to have zero shear deformability and are consequently more simple than those used by Lucas. Variations arose due to the cranked beams over the rear wheel arch but no separate designation was required. The most forward of these self-equilibrating groups involved the torque box at the scuttle section and was called the Y.1. system (Fig.16).

Figure 18 shows the breakdown of each plane of the structure into the chosen systems while Fig.19a-k show the load distribution in one of each of the systems due to a given internal load. The values of the member loads in each of these are the terms in the column of the b_1 matrix corresponding to that particular redundancy.

The b_o and b_1 Matrices

As has been stated, the rows of the b_o and b_1 matrices contain all the loads to be defined in the structure, totalling 231.

There are 22 columns in the b_o matrix corresponding to the number of separate loading points (Fig.7a) and 49 columns in the b_1 matrix corresponding to the order of indeterminacy.

Each column lists the loads in the members for either a unit external load for the b_o matrix, or a "unit load" in a particular redundancy for the b_1 matrix. Theoretically there is complete freedom of choice of the order of the rows but there are considerable advantages in a particular choice of row order. Similarly the order of the columns may be arbitrary, but advantages again accrue from a special choice of column order.

As noted in the description of the simplified 3-dimensional analysis of the front end structure in section "Order of Indeterminacy", the b_o matrix is made up by transferring the unit loads on the outriggers of the basic system to the main longitudinal and then transferring these loads to the support points (Fig.7b). The actual layout of the matrix is shown in Fig.19 where it can be seen that the order has been reversed and

the first block of columns give the bending moments in the main longitudinal (nodes 1 - 11) due to units loads at each node. For instance, the first column represents the bending moments along the beam due to a unit load at node 1 when supported at nodes 2 and 63. The first nine columns are similarly constructed and the next two columns represent the distribution of the support loads between the shock absorber/bump stop node and the spring hangers. The remaining columns give the loads in each cross member due to a unit load at the node given at the head of the column and supported by the main longitudinal.

The loads to be computed in the structure were first listed in numerical order, starting with the end loads in the x direction F_{2x} to F_{74x} and continuing with F_{1y} to F_{64y} etc. then working through the bending moments and shear panels to form the 231 rows. The columns corresponding to the redundancies were then written in any order as column headings, The positionswhere non-zero elements occurred were marked in the matrix. The b_1 matrix formed in this way would not provide the optimum use of the computer store, first because the conditions imposed by condensation techniques would not be fulfilled and second there is no guarantee that any complete zero sub-matrix would be formed.

The rows required by the basic system were listed first and the redundant systems which had terms in these rows were chosen as the first columns in the b_1 matrix. The redundant systems having terms in the first row were listed first, and became the first columns in the b_1 matrix, then any system not already covered having elements in the second row were added as further columns and so on, care being taken to ensure that row sequences required by condensation were preserved. In this way a rough banded matrix was produced (Fig.20).

This type of grouping could have been obtained either by a geographical grouping or by a computer search program, however, since it only had to be performed once it was carried out by hand.

The resulting sub-matrices were very sparse and are given in full in Fig.21a and they were put into the computer by small section blocks. Because of the need for checking the sub-matrices they were output from the computer and used as separate input data tapes in the Part I and Part II programs. This method kept the number of instructions in the main program sufficiently small to be held in the store at the same time as the matrices.

To read in a transposed sub-matrix in blocks each case has to be examined separately but the principles used can be set out as follows :-

1 Clear a store place twice as large as the sub-matrix required.

2 Split up the sub-matrix into small blocks consisting of diagonal matrices, rectangular matrices or scalers where elements occur in an isolation.

3 Read the blocks into the computer in clear spaces, beyond the space to be used for the transposed matrix, in row sections of the original matrix.

4 Transpose each row section back into the reserved space where they become columns stored end-on as required for the complete matrix. A careful count of the beginning store numbers of each block of non-zero elements is necessary.

Example:

To read in sub-matrix b^t_{1aI} starting at store allocation 2.

The complete sub-matrix b_{1aI} is shown in Fig.21a, where the crosses represent the non-zero elements.

The blocks chosen are numbered from 1 to 8, and when assembled in the final transposed sub-matrix will lie as shown in Fig.21b. The numbers on the diagram are store allocation numbers.

The diagonal matrix (1) is stored as seven consecutive numbers and can be read into spaces 794 to 800. If it is then added to a zero square matrix starting at 801 the result will be as shown in Fig.22a. Since the store will have zeros in all spaces from 2 to 1585 a rectangular matrix 7 x 24 starting at 801 will be as shown in Fig.22b. This matrix can now be transposed starting at 2 and will form the first 7 columns of the required b^t_{1aI} matrix.

The next section of the b^t_{1aI} matrix will be the 12 columns containing block matrix $(2)^t$. The cleared section of the store from 850 to 1137 can be used to assemble a 12 x 24 matrix corresponding to rows 8 to 19 of the original b_{1aI} matrix. This would appear as in Fig.23a, from which it can be seen that it is only necessary to read in the block matrix (2) at store No. 910 to give the required 12 x 24 matrix, which, when transposed and placed to start at store number 170 will give the 12 columns required.

The next 5 columns are obtained in a similar way as indicated in Fig.23b, the two scalers (4) and (5) being read into store at the spaces indicated. Note that it is important to transpose Fig.23a back to its correct space in b^t_{1aI} required before reading in the block matrix (3) to begin at store number 1009 since it will overwrite some of the zeros in the previous matrix. The matrix, Fig.23b, is transposed to start at 458.

The final nine columns are prepared as in Fig.23c, and transposed into the spaces 578 to 793 to complete b^t_{1aI}.

The Unassembled Flexibility Matrix

The formula for each term in the flexibility matrix depends on the condensation procedure adopted and the values to be substituted in the formulae depend on the size of the members of the structure. Some measure of choice is allowed at each stage and the actual choices made are given in detail.

The condensation procedure was first given in Ref.14. This is based on the fact that when a continuous member is idealised into a number of separate elements with a linear variation of the load in each element

the whole system can be defined by one load at each node point, see Fig.24. Where an external load is introduced or a point load can arise from another part of the structure the load distribution takes the form shown in Fig.25, and it is clearly necessary to specify the load in the continuous member at each side of the point of discontinuity. This general statement will be true whether the load distribution is a direct load along the member or a bending moment.

In the case of continuous beams in the form of portals or rectangular rings it is important to define the sign of the bending moments in such a way that one figure at each corner will specify the bending moment in both the adjacent arms.

The condensed flexibility matrix was found in each case as follows :-

If the uncondensed column matrix of end loads or bending moments is defined as:

$$S = \{s_{11}, s_{12}, s_{21}, s_{22}, s_{31}, s_{32}, - - - - - s_{n2}\}$$

Where s_{11} and s_{12} refer to the loads at either end of the first structural element.

From the discussion above we can write :

$$s_{11} = s_o$$

$$s_{12} = s_{21} = s_1$$

$$s_{22} = s_{31} = s_2$$

$$s_{32} = s_{41} = s_3$$

$$- \quad - \quad -$$

$$- \quad - \quad -$$

$$- \quad - \quad -$$

$$s_{(n-1)2} = s_{n1} = s_{n-1}$$

$$s_{n2} = s_n$$

The condensed form of the column matrix will be :

$$S_c = \{s_o, s_1, s_2, s_3, - - - - - - s_n\}$$

A transformation or condensation matrix Δ_c can be written which will premultiply S_c to give the original load matrix S.

i.e. $\Delta_c S_c = S.$

or

$$\begin{bmatrix} 1,0,0,- - - - ,0 \\ 0,1,0,- - - - ,0 \\ 0,1,0,- - - - ,0 \\ 0,0,1,- - - - ,0 \\ 0,0,1,- - - - ,0 \\ \\ \\ \\ \\ \\ ,1 \end{bmatrix} \begin{bmatrix} s_o \\ s_1 \\ s_2 \\ s_3 \\ - \\ - \\ \\ \\ s_n \end{bmatrix} = \begin{bmatrix} s_o \\ s_1 \\ s_1 \\ s_2 \\ s_2 \\ - \\ - \\ - \\ - \\ s_n \end{bmatrix} = \begin{bmatrix} s_{11} \\ s_{12} \\ s_{21} \\ s_{22} \\ s_{31} \\ - \\ - \\ - \\ - \\ s_{n2} \end{bmatrix}$$

The same condensation matrix will also condense the b_o and b_1 matrices,

i.e. $\Delta_c b_{oc} = b_o$

and $\Delta_c b_{1c} = b_1$

Now $D = b_1^t f b_1$

$= b_{1c}^t \Delta_c^t f \Delta_c b_{1c}$

$= b_{1c}^t f_c b_{1c}$

Where $f_c = \Delta_c^t f \Delta_c$ is the condensed flexibility matrix.

The same formula can be used to find the flexibility matrix where the load at one end of a member is zero throughout the calculation.

Appendix III gives detailed examples of the continuous members condensed in this way and the corresponding condensed matrices. The suffic 'c' was not used in the partitioned matrix analysis as only condensed systems were considered and a suffix 'c' refers to a partitioned set of rows in that analysis.

The individual terms of the flexibility matrices involve the calculation of the effective cross-section areas and second moments of area of all members.

The members were made up from the top hat sections or angles with plates rivetted to them. The usual assumption of the addition of one sixth of the cross-section area of the adjacent plate was made for the determinatio of the effective area in each case, see Fig.26. For the second moment of are the contribution of a plate normal to the axis under consideration was ignore but one sixth of the width of any plate parallel to the axis was included, see Fig.27. The complete list of effective cross-section areas and second moments of area are given in Table 2.

The Load Matrix

The structure has been designed to carry the full cross country weight of 5,705 lbs. as specified by the Rover Company Limited for the 109" W/B Station Wagon Landrover.

An equipment (engine, gearbox, axles, springs etc.) weight list was obtained and the weight of the model structure estimated. The maximum payload was then determined as the cross country weight less the equipment and structure weight and not the maximum payload of the standard vehicle.

The equipment loads were distributed on the Basic System as shown in Fig.28a, while the structure weight distribution was as shown in Fig.28b.

Six payload cases were chosen, the first case being with the driver and one passenger only, while the remaining five cases were all based on the maximum payload distributed in various positions, Fig.29

Case 1. Driver and Passenger

Case 2. Full payload uniformly distributed on the area between 5-22 and 7-24.

Case 3. Ten people and equipment distributed on seats (i.e. 279 lbs. per seat).

Case 4. Full payload uniformly distributed aft of 5-22.

Case 5. Driver and passenger on front seat plus 2,489 lbs. aft of 64-37

Case 6. Full payload outside main longitudinal members.

Figure 30 shows how the loading condition for Case 5 was applied as point loads on the Basic System.

The total static load on the Basic System for each case was therefore the sum of equipment, structure and payload.

Allowance for the dynamic loading of the structure was vased on the acceleration levels recorded on an 86" W/B Landrover as reported in F.V.R.D.E. Report No. B.R.152/5. Maximum vertical acceleration levels were 1·9g at the front, 0·94g in centre and 2·6g at the rear end of the vehicle. The maximum acceleration on the structure of the vehicle was therefore 3·6g (dynamic plus static), and the load on the test structure was therefore based on 4g acceleration i.e. the total static loads were multiplied by a factor of 4.

These loads were reacted by the spring attachment points and the shock absorber or bump stop. It was assumed that the proportion of axle load carried by the shock absorbers be 25%. In all cases except Case 1 and Case 5 both front and rear springs were compressed against the bump stop and in fact for Case 2 the load carried by the front bump stops is 75% of the axle load.

The six columns of the R matrix (page 13) are the six loading cases and the 22 rows are the loads arranged in a similar manner to the columns of the b_{oa} matrix. The first nine rows are the sum of loads at each cross beam giving the bending distribution on the longitudinal members and end load in member 9-63. The next two rows give the distribution between spring hanger points, while the remaining eleven are the loading conditions along each cross member giving bending of the cross members and end loads in members 8-62 and 10-64.

The Computer Program

The theoretical basis of the force method was developed in Ref.8, and summarised in Ref.12.

Using the notation of Ref.12, the matrix of loads in the structural elements (S) is given by :

$$S = (b_o - b_1 D^{-1} Do)R \quad (1)$$

Where $D = b_1^t f b_1$ (2)

and $D_o = b_1^t f b_o$ (3)

Since there are 231 separate loads (either end loads, shear flows or bending moments), equation (1) has 231 rows. The unassembled flexibility matrix f contains 231^2 or 53,361 elements, that is some eight times the total storage space available in the computer. This problem can be overcome by the use of row partitioning as demonstrated in the example of Appendix I of Ref.12.

The device of column partitioning is also available and the theory has again been developed in Ref.8, and summarised in Appendix I of this memo. The following calculation shows that this is not necessary:-

Assume matrices D (49 x 49 = 2401 elements)

and D_o (49 x 22 = 1078 elements) are available for input.

The matrix $D^{-1}Do$ can be formed by reading in each matrix and dividing, providing the result does not overwrite either of the two matrices. Since $D^{-1}Do$ will contain 1078 elements the total storage space required would be:-

$$2 \times 1078 + 2401 = 4557$$

R MATRIX

	Loads	1 Case 1	2 Case 2	3 Case 3	4 Case 4	5 Case 5	6 Case 6
1	1+19	120	120	120	120	120	120
2	3	933	933	933	933	933	933
3	4	64	64	64	64	64	64
4	5+22	583	1745	583	928	583	928
5	6+23	1210	3699	1747	1740	1210	1740
6	7+24	568	1895	1105	1236	568	1236
7	8+62+35+25	139	139	976	1153	139	1153
8	10+64+37+26	310	310	1426	1255	2799	1255
9	11+27	366	366	924	781	2855	781
10	$(1-b)R_F$ (front spring load)	1313	1313	1313	1313	788	1313
11	$(1-b)R_R$ (rear spring load)	1614	2962	2962	2962	2962	2962
12	9	52	52	331	549	52	52
13	35+25	46	46	324	315	46	553
14	37+26	40	40	598	291	702	513
15	62	5	5	284	146	5	270
16	64	5	5	284	146	5	270
17	19	11	11	11	11	11	11
18	22	344	652	344	435	344	516
19	23	259	850	388	330	259	524
20	24	299	581	428	406	299	633
21	36	35	35	592	316	35	565
22	27	25	25	304	135	686	233

Further, if the number of rows in each partitioned part of b_1 were less than 49 they could be read into the space originally occupied by D and the further multiplication b_1 $(D^{-1}Do)$ performed in the same program.

While the above shows that column partitioning is not strictly necessary, no advantage would then be taken of the organisation of the b_1 matrix into a rough banded form referred to in the section "The b_o and b_1 Matrices".

When such a banded matrix is partitioned by both rows and columns some sub-matrices are formed which are composed entirely of zeros, and these zero b_1 sub-matrices can be ignored in the calculation, thus saving overall computing time. The choice was therfore made to partition the 49 columns into two parts, Part I having 24 columns and Part II the remaining 25 columns.

In order to form the three parts of the D matrix, namely D_I, D_{II} and D_{III} (or D_{III}^t) in one program, limitations on the number of rows in each sub-matrix are imposed by the computer store. The store layout adopted is shown in Fig.31 where the instructions read naturally from left to right in each line and store spaces cn the upper lines are overwritten by matrices appearing directly below.

If χ is the number of rows in any sub-matrix the total store space required will be as follows :-

Read in b^t_{1aI}, $(24 \times \chi) = 24\chi$

Transpose to b_{1aI} $(\chi \times 24) = 24\chi$

Read in f_a $(\chi \times \chi) = \chi^2$

Form $b^t_{1aI}\, f_a$ $(24 \times \chi) = 24\chi$

Form D_{Ia} $(24 \times 24) = 576$

Form $b^t_{1cII}\, f_c$ (from a later stage in the program)

$(25 \times \chi) = 25\chi$

Form D_{IIc} $(25 \times 25) = 625$

Form D^t_{IIIc} $(24 \times 25) = 600$

Total $= \chi^2 + 97\chi + 1801$

It is necessary to carry a zero in the store to clear spaces for the f matrices as required so that the limitation is:-

$$6142 \geq \chi^2 + 97\chi + 1802 \qquad (4)$$

i.e. $33 \geq \chi$

The conditions imposed on the value of χ by overwriting are indicated in Fig.31 and are as follows:-

(a) $D_I \leqslant b_{1aII} f_a$

i.e. $24^2 \leqslant 25\chi \quad \therefore \quad \chi \geqslant 24$

(b) $b_{1cII} \leqslant f_c$

i.e. $25\chi \leqslant \chi^2 \quad \therefore \quad \chi \geqslant 25$

(c) $D_{IId} + D^t_{IId} \leqslant 2\, b_{1dI}$

i.e. $25^2 + 25 \times 24 \leqslant 48\chi$

or $48\chi \geqslant 1225 \quad \therefore \quad \chi \geqslant 26$

Combining all the conditions we have:

$26 \leqslant \chi \leqslant 33$

The 231 row matrix system could therefore be partitioned into 7 equal sub-matrices of 33 rows each. The row partitions were designated by the suffices a to g.

The diagram, Fig.31, shows the actual store layout adopted for the Part I Program. The maximum storage space required for the program was 6092 elements and the remaining spaces were used to increase the number of instructions from 80 to the 95 required to write the complete program. The program is shown in detail in Table 3.

The matrices output from the Part I program were D_I, D_{II}, D^t_{III} and Do_I. The first two should be symmetrical square matrices and a complete check was carried out visually that this was so, enabling any errors in either the program or the data to be found.

The remaining matrices were output in binary form as no checks were possible and time could be saved in output and input to the next part of the program.

The second part of the program completed the calculation of the internal load matrix, S and the displacement matrix, r.

There were no problems of storage allocation and the layout of the store adopted is shown in Fig.32.

Results

The results are plotted as bending moments along each member, Figs. 33-37, end loads along each member, Figs. 38-75, and shear flows in each panel, Figs. 76-81.

In order to ensure that the maximum stress on any members was within the yield limit the maximum and minimum values of end loads and bending moments were selected from the six loading cases and combined to give an overall maximum stress value. The detailed stresses have not been included in this report as it is intended to arrange the practical tests to give results in terms of end loads, bending moments and shear for direct comparison with the results given here.

The checking device used was to calculate both bending moments in the beam and the end loads in members normal to the beams. These end loads, considered as a load distribution on the beam, should give the same bending moment diagram as the output of the computer. An example of the agreement obtained is shown in Fig.82. Certain structural properties have not been included in the idealisation, probably the most important is the torsional stiffness of the cross bearers which become closed sections when the floor is attached. Also the idealisation of a panel and a beam when adjacent is as shown in Fig.83, i.e. the effect on the bending stiffness of the beam of the very deep web attached is ignored. It has been shown by Marsden (Ref.1) that for a simple structure this idealisation will give approximately correct stresses but the calculated displacements will be greater than the actual structure. Marsden suggested an improved idealisation which made some allowance for the stiffening effect of the panel on the beam and obtained the same theoretical stress distribution but the calculated displacements were less than those for the actual structure. It may well be that for a more complicated structure it is more important to include the stiffening effect of the panel on the beam and this could be established when the model has been tested. The displacements calculated along the beam by the present programs are shown in Fig.84.

The most remarkable result of the analysis is the fact that the bending moment in the floor beam is not shared by the inner wall of the rear whell arch. It appears that the sudden change in stiffness at the ends of the arch makes the two beams work against each other instead of sharing the load, (see Fig.85). This result, although satisfying equilibrium and compatibility conditions for the structure as idealised, is a little surprising and the results of the analysis in this area will be carefully checked on the model.

Conclusions

The method of analysis detailed in this report is justifiable only where small digital computers are available. With the availability of large fast computers automatic methods of structural analysis are the rule. Most of these are based on displacements as unknowns but some automatic programs have been developed using force methods (Ref.15). Although these automatic force methods use large computers to organise the data and mathematically select redundancies they still have less equations to solve in the final analysis than displacement methods. The accuracy of the calculated load

distribution in the structure for a given idealisation will be largely independent of the method of computation so that the comparison of the test results when available and the theoretical results given here will be significant.

The real conclusions to this work cannot be written until the test program with the full scale model has been completed.

Acknowledgements

The Fighting Vehicles Research and Development Establishment have sponsored the analysis and design of the structure and the building of the full scale model, together with the static test rig. Professor J.R.Ellis, Director of the Advanced School of Automobile Engineering has given continuous support and guidance to the project.

Many people have assisted in the work of preparing and checking data for the analysis and it would not be possible to name them all. Mr A.J.Robertson carried out the complete detail design of the structure, described in Appendix IV, and supervised the tests on the individual joints. He also assisted in the preparation and checking of the final set of computer input and output data. The test rig to be used for the final tests was designed by Mr.P.Healy who has also assisted in collating the information presented in this report.

References

1	McKenna, E.R.	"Computer Evaluation of Automobile Body Structure". Am. Soc. Body Eng., 1961
2	Allwood, R.J. and Norville, C.C.	"The Analysis by Computer of a Motor Car Underbody Structure". I.Mech.E.Automobile Divn., Paper, March, 1966.
3	Kirioka, K.	"An Analysis of Body Structures". S.A.E.Report No. 979A, 1965.
4	Kawai, H. and Koganei, Y.	"Experimental Analysis of Automobile Bodies". Mitsubishi Technical Review, Part 1, Vol.2, No.1, 1965. Part 2, Vol.2, No.3, 1965.
5	Mann, C.W.	"The Stress Analysis of a Model Car Body". A.S.A.E. Thesis, 1963.
6	Marsden, F.D.	"Analysis of a Structure with a Large Cut-Out by the Matrix Force Method". A.S.A.E. Thesis, 1964.
7	Crawford, R.G.	"Analysis of an Integral Van Body in Bending". A.S.A.E. Thesis, 1965.
8	Argyris, J.H. and Kelsey, S.	"Energy Theorems and Structural Analysis". Butterworths, 1960.
9	Tidbury, G.H.	"A Proposed Integral Land Rover Structure". A.S.A.E. Memo No.4.
10	Denke, P.H.	"A General Digital Computer Analysis of Statically Indeterminate Structures". N.A.S.A. TN. D-1666, 1962.
11	Henderson, J.C. and Bickley, W.G.	"Statistical Indeterminancy of a Structure". Aircraft Engineering, December, 1955.
12	Tidbury, G.H.	"Stress Analysis of Vehicle Structures". A.S.A.E. Memo No.3, July, 1964.
13	Lucas, A.H.	"The Stress Analysis of a Railway Coach by the Argyris Matrix Force Method of Structural Analysis". Engineering, 5th May, 1959.
14	Argyris, J.H. and Kelsey, S.	"Modern Fuselage Analysis and the Elastic Aircraft". Butterworths, 1963.
15	Robinson, J.	"Structural Matrix Analysis and the Engineer". John Wiley & Sons, 1966.

Appendix I

Summary of Theory

In Ref.12, it is shown that if S is a matrix of the internal loads in a structure having one column for each external load condition then:

$$S = b_o R + b_1 X \qquad 1.1$$

Where the b_o, b_1 and R matrices have already been defined and X is an unknown matrix given by the solution of the compatibility equation:-

$$b_1^t f S = 0 \qquad 1.2$$

i.e. $$X = -(b_1^t f b_1)^{-1} (b_1^t f b_o)R \qquad 1.3$$

and the solution for S is:

$$S = (b_o - b_1 D^{-1} D_o)R = b R \qquad 1.4$$

Where $$D = b_1^t f b_1 \qquad 1.5$$

and $$D_o = b_1^t f b_o \qquad 1.6$$

In Appendix I of Ref.12 the theory is extended to include row partitioning and it is shown that if:

$$S = \begin{bmatrix} S_a \\ S_b \\ " \\ " \\ " \end{bmatrix}$$

then $$b = \begin{bmatrix} b_a \\ b_b \\ " \\ " \\ " \end{bmatrix} = \begin{bmatrix} b_{oa} \\ b_{ob} \\ " \\ " \\ " \end{bmatrix} - \begin{bmatrix} b_{1a} \\ b_{1b} \\ " \\ " \\ " \end{bmatrix} D^{-1} D_o$$

Where $$D = b_{1a}^t f_a b_{1a} + b_{1b}^t f_b b_{1b} + - - - - - \qquad 1.7$$

and $$D_o = b_{1a}^t f_a b_{oa} + b_{1b}^t f_b b_{ob} + - - - - - \qquad 1.8$$

If column partitioning is required it can be treated separately for simplicity, e.g. :-

$$S = b_o R + \begin{bmatrix} b_{1I}, & b_{1III} \end{bmatrix} \begin{bmatrix} X_I \\ X_{II} \end{bmatrix} \qquad 1.9$$

Where b_{1I} is the first 24 columns of b_1 and b_{1III} is the next 25 columns of b_1, X_I and X_{II} are the row partitioned sections of the unknown matrix X and solutions must be set up for both parts of the matrix, Equation 1.9 is only true if there are less than 24 columns in the basic system which is the case for the present problem.

Substituting the value of S given by equation 1.9 in equation 1.2:

$$\begin{bmatrix} b_{1I}^t \\ b_{1III}^t \end{bmatrix} f \left[b_o R + \begin{bmatrix} b_{1I}, & b_{1III} \end{bmatrix} \begin{bmatrix} X_I \\ X_{II} \end{bmatrix} \right] = 0$$

i.e.

$$\begin{bmatrix} b_{1I}^t f b_o \\ b_{1III}^t f b_o \end{bmatrix} R + \begin{bmatrix} b_{1I}^t f b_{1I}, & b_{1I}^t f b_{1III} \\ b_{1III}^t f b_{1I}, & b_{1III}^t f b_{1III} \end{bmatrix} \begin{bmatrix} X_I \\ X_{II} \end{bmatrix} = 0 \qquad 1.10$$

writing

$$D_{oI} = b_{1I}^t f b_o$$

$$D_{oII} = b_{1III}^t f b_o$$

$$D_I = b_{1I}^t f b_{1I}$$

$$D_{II} = b_{1III}^t f b_{1III}$$

$$D_{III} = b_{1III}^t f b_{1I}$$

Equation 1.10 becomes:

$$\begin{bmatrix} D_{oI} \\ D_{oII} \end{bmatrix} R + \begin{bmatrix} D_I & D_{III}^t \\ D_{III} & D_{II} \end{bmatrix} \begin{bmatrix} X_I \\ X_{II} \end{bmatrix} = 0 \qquad 1.11$$

Since f is a symmetrical matrix and $b_{1I}^t f b_{1III} = \left[b_{1III}^t f b_{1I} \right]^t$

$$= D_{III}^t$$

Equation 1.11 can be written as two simultaneous equations in X_I and X_{II}.

$$D_I X_I + D_{III}^t X_{II} + D_{oI} R = 0 \qquad 1.12$$

$$D_{III} X_I + D_{II} X_{II} + D_{oII} R = 0 \qquad 1.13$$

Equation 1.13 can be solved for X_{II} as:

$$X_{II} = -D_{II}^{-1} \left[D_{oII} R + D_{III} X_I \right]$$

and equation 1.12 becomes:

$$D_I X_I - D_{III}^t D_{II}^{-1} \left[D_{oII} R + D_{III} X_I \right] = -D_{oI} R$$

i.e. $$X_I = -\left[D_I - D_{III}^t D_{II}^{-1} D_{III} \right]^{-1} \left[D_{oI} - D_{III}^t D_{II}^{-1} D_{oII} \right] R$$

and

$$X_{II} = -D_{II}^{-1} \left[D_{oII} - D_{III} \left[D_I - D_{III}^t D_{II}^{-1} D_{III} \right]^{-1} \left[D_{oI} - D_{III}^t D_{II}^{-1} D_{oII} \right] \right]$$

A new notation is clearly required to make these equations more convenient.

Let $$D_x = D_I - D_{III}^t D_{II}^{-1} D_{III} \qquad 1.14$$

$$D_{ox} = D_{oI} - D_{III}^t D_{II}^{-1} D_{oII} \qquad 1.15$$

$$\therefore \quad X_I = -D_x^{-1} D_{ox} R \qquad 1.16$$

$$X_{II} = -D_{II}^{-1} \left[D_{oII} - D_{III} D_x^{-1} D_{ox} \right] \qquad 1.17$$

The required solution for the unknown internal load matrix S is from equation 1.9:-

$$S = \left\{ b_o - b_{II} D_x^{-1} D_{ox} - b_{III} D_{II}^{-1} \left[D_{oII} - D_{III} D_x^{-1} D_{ox} \right] \right\} R \qquad 1.18$$

If row partitioning is used as well as column partitioning it only affects the calculation of the D matrices which become:-

$$\left.\begin{aligned} D_{oI} &= b_{1aI}^{t} f_a b_{oa} + b_{1bI}^{t} f_b b_{ob} + \text{- - - - - - -} \\ &= D_{oIa} + D_{oIb} + \text{- - - - - - - - - - - - - - -} \end{aligned}\right) \quad 1.19$$

$$\left.\begin{aligned} D_{oII} &= b_{1aII}^{t} f_a b_{oa} + b_{1bII}^{t} f_b b_{ob} + \text{- - - - - -} \\ &= D_{oIIa} + D_{oIIb} + \text{- - - - - - - - - - - - -} \end{aligned}\right) \quad 1.20$$

$$\left.\begin{aligned} D_{I} &= b_{1aI}^{t} f_a b_{1aI} + b_{1bI}^{t} f_b b_{1bI} + \text{- - - - - -} \\ &= D_{Ia} + D_{Ib} + \text{- - - - - - - - - - - - - - -} \end{aligned}\right) \quad 1.21$$

$$\left.\begin{aligned} D_{II} &= b_{1aII}^{t} f_a b_{1aII} + b_{1bII}^{t} f_b b_{1bII} + \text{- - - - -} \\ &= D_{IIa} + D_{IIb} + \text{- - - - - - - - - - - - - - -} \end{aligned}\right) \quad 1.22$$

$$\left.\begin{aligned} D_{III} &= b_{1aII}^{t} f_a b_{1aI} + b_{1bII}^{t} f_b b_{1bI} + \text{- - - - -} \\ &= D_{IIIa} + D_{IIIb} + \text{- - - - - - - - - - - - - - -} \end{aligned}\right) \quad 1.23$$

The equations 1.19 to 1.23 define the matrices D_{oIa} etc. which are used as steps in the computer program. The row partitioning will be carried through to the calculation of the S matrix and equation 1.18 can be written:

$$S = \begin{bmatrix} S_a \\ S_b \\ " \\ " \\ " \\ " \end{bmatrix} = \begin{bmatrix} b_{oa} - b_{1aI} D_x^{-1} D_{ox} - b_{1aII} D_{II}^{-1} \left[D_{oII} - D_{III} D_x^{-1} D_{ox} \right] \\ b_{ob} - b_{1bI} D_x^{-1} D_{ox} - b_{1bII} D_{II}^{-1} \left[D_{oII} - D_{III} D_x^{-1} D_{ox} \right] \\ " \\ " \\ " \\ " \end{bmatrix} R \quad 1.24$$

For the problem described in this report there are seven row partitioned segments (suffices a to g) and of these the following sub-matrices are zero:-

$$b_{ob} = b_{oc} = b_{od} = b_{of} = b_{og} = 0 \quad)$$
$$b_{1aII} = b_{1bII} = 0 \quad)$$
$$b_{1fI} = b_{1gI} = 0 \quad) \qquad 1.25$$

Substituting equation 1.25 into equations 1.19 to 1.23 we have:-

$$D_{oI} = D_{oIa} \qquad 1.26$$

$$D_{oII} = 0 \qquad 1.27$$

$$D_I = D_{Ia} + D_{Ib} + D_{Ic} + D_{Id} + D_{Ie} \qquad 1.28$$

$$D_{II} = D_{IIc} + D_{IId} + D_{IIe} + D_{IIf} + D_{IIg} \qquad 1.29$$

$$D_{III} = D_{IIIc} + D_{IIId} + D_{IIIe} \qquad 1.30$$

and from equation 1.15: $D_{ox} = D_{oI}$ 1.31

With the considerable simplification introduced by the zero sub-matrices the required partitioned sections of the load matrix are:-

$$S_a = \left[b_{oa} - b_{1aI} D_x^{-1} D_{oI} \right] R \qquad 1.32$$

$$S_b = \left[-b_{1bI} D_x^{-1} D_{oI} \right] R \qquad 1.33$$

$$S_c = \left[-b_{1cI} D_x^{-1} D_{oI} + b_{1cII} D_{II}^{-1} D_{III} D_x^{-1} D_{oI} \right] R \qquad 1.34$$

$$S_d = \left[-b_{1dI} D_x^{-1} D_{oI} + b_{1dII} D_{II}^{-1} D_{III} D_x^{-1} D_{oI} \right] R \qquad 1.35$$

$$S_e = \left[-b_{1eI} D_x^{-1} D_{oI} + b_{1eII} D_{II}^{-1} D_{II} D_x^{-1} D_{oI} \right] R \qquad 1.36$$

$$S_f = \left[b_{1fII} D_{II}^{-1} D_{III} D_x^{-1} D_{oI} \right] R \qquad 1.37$$

$$S_g = \left[b_{1gII} D_{II}^{-1} D_{III} D_x^{-1} D_{oI} \right] R \qquad 1.38$$

As described in section "The Computer Program" of the main report, Part 1 of the program prepared the D matrices given by equations 1.26, 1.28

1.29 and 1.30 (with $D_{III}{}^t$ being computed instead of D_{III}) while Part 2 of the program worked out equations 1.32 to 1.38.

Part 2 of the program also calculated the displacement of the load points relative to the support points when the complete structure is loaded. This displacement matrix is called the r matrix and is given in Ref.12 as:

$$r = b_o{}^t f S \qquad 1.39$$

When row partitioning is used equation 1.39 becomes:

$$r = b_{oa}{}^t f_a S_a + b_{ob}{}^t f_b S_b - - - - - + \text{etc.} \qquad 1.40$$

Since, in this case $b_{ob}{}^t = b_{oc}{}^t = - - - - = 0$

the expression for r is simply:

$$r = b_{oa}{}^t f_a S_a \qquad 1.41$$

Appendix II

Internal Load Sign Convention

1. END LOAD CARRYING MEMBERS

Tension $+^{ve}$

2. SHEAR PANELS

Shear force acting on a panel in the positive direction of an axis with the most positive value of the other axis gives a positive shear i.e.

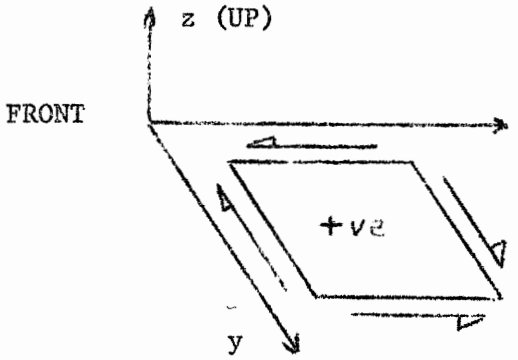

(c PANELS)

x y plane

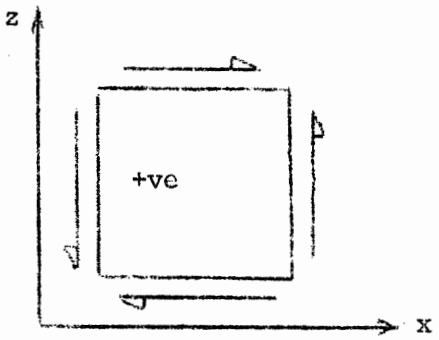

(b PANELS)

x z plane

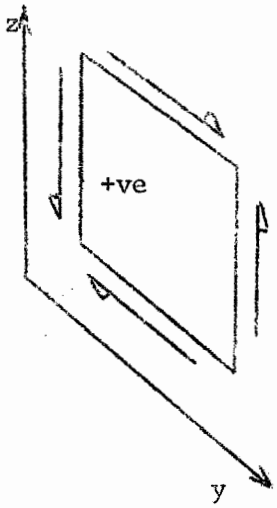

(a PANELS)

y z plane

fig.(i)

3. BENDING MOMENTS

Each "continuous beam" must be treated separately as follows:

Crossmembers. M_{1x}, M_{5x}, M_{6x}, M_{7x}, M_{11x}.

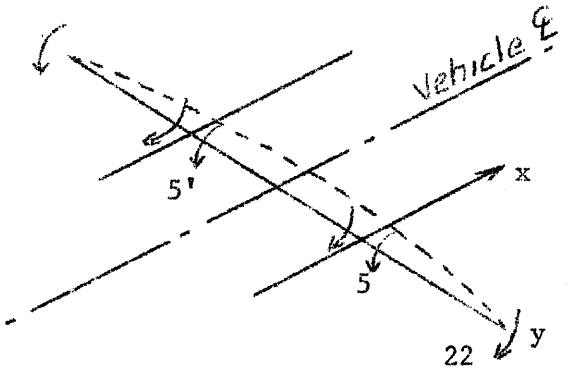

HOGGING B.M's +ve
(Loading on the beam)

fig.(ii)

Cranked Crossmembers. M_{8x}, M_{62x}, M_{9x}, M_{10x}, M_{64x}.

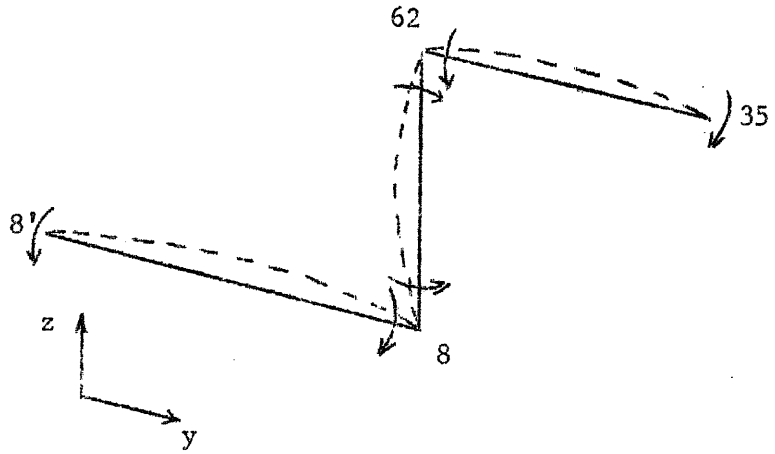

HOGGING +ve on 35-62
and 8-8'
SAGGING +ve in y
direction on 8-62

fig.(iii)

M_{9x} indicates the complete system:-

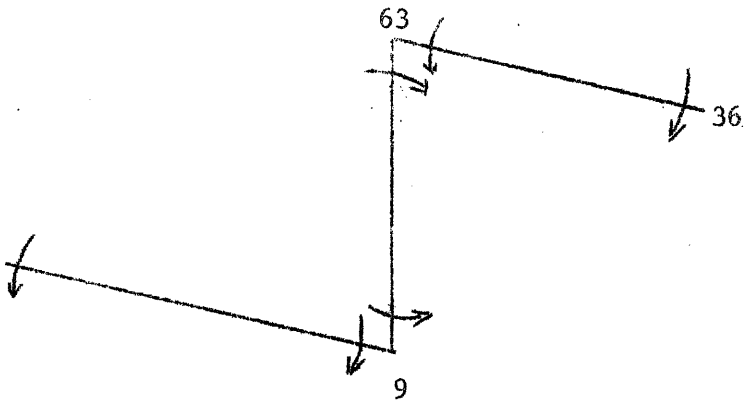

Directions as above
M_{9x} always equals M_{63x}

fig.(iv)

Lateral Bending Moments, Screen Pillar.

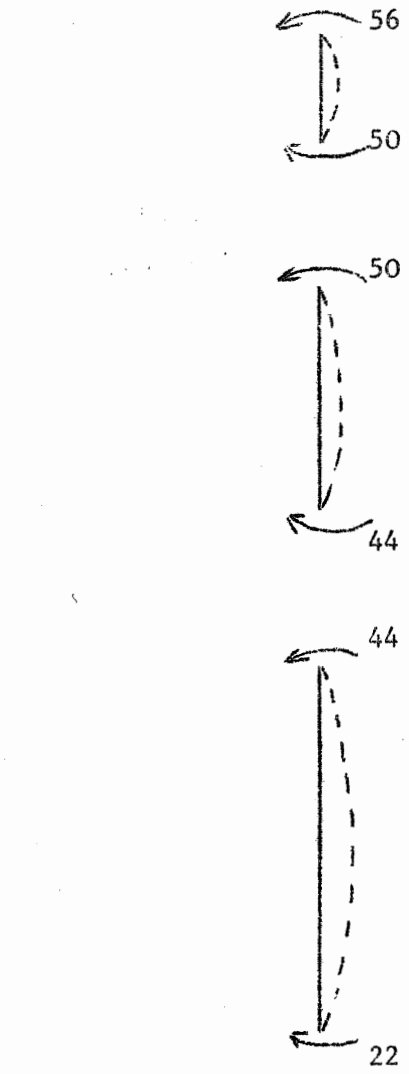

+ve B.M's shown

Hogging +ve in y direct

M_{44x}, M_{50x}

fig.(v)

Main Longitudinal

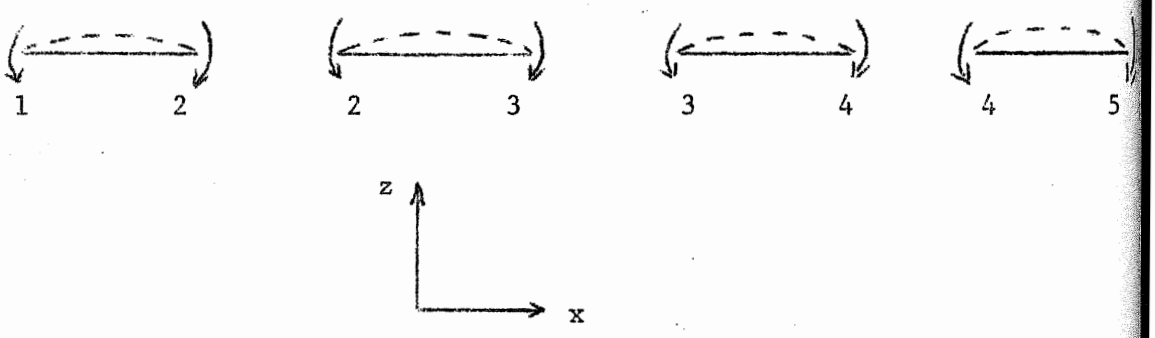

fig.(vi)

Hogging B.M.'s +ve

i.e. M_{2y} - - - - - - - - M_{10y} +ve as shown

Front Wing-Wheel Arch

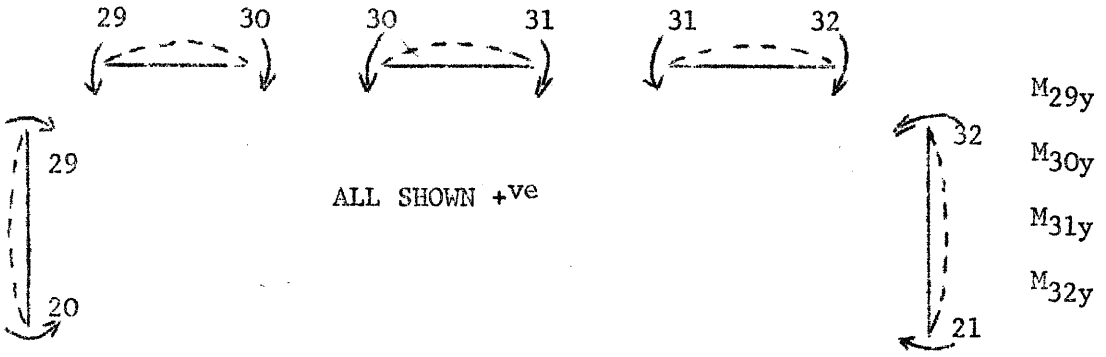

fig.(vii)

OR Forces Acting on Arch

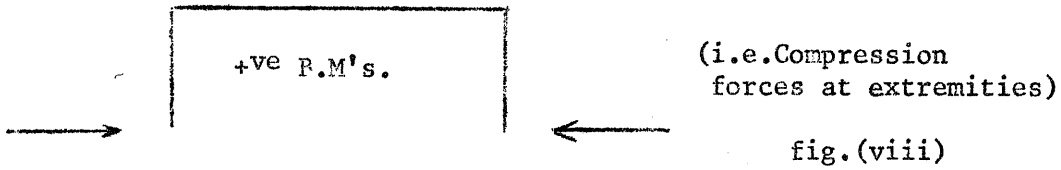

fig.(viii)

Front Door Post

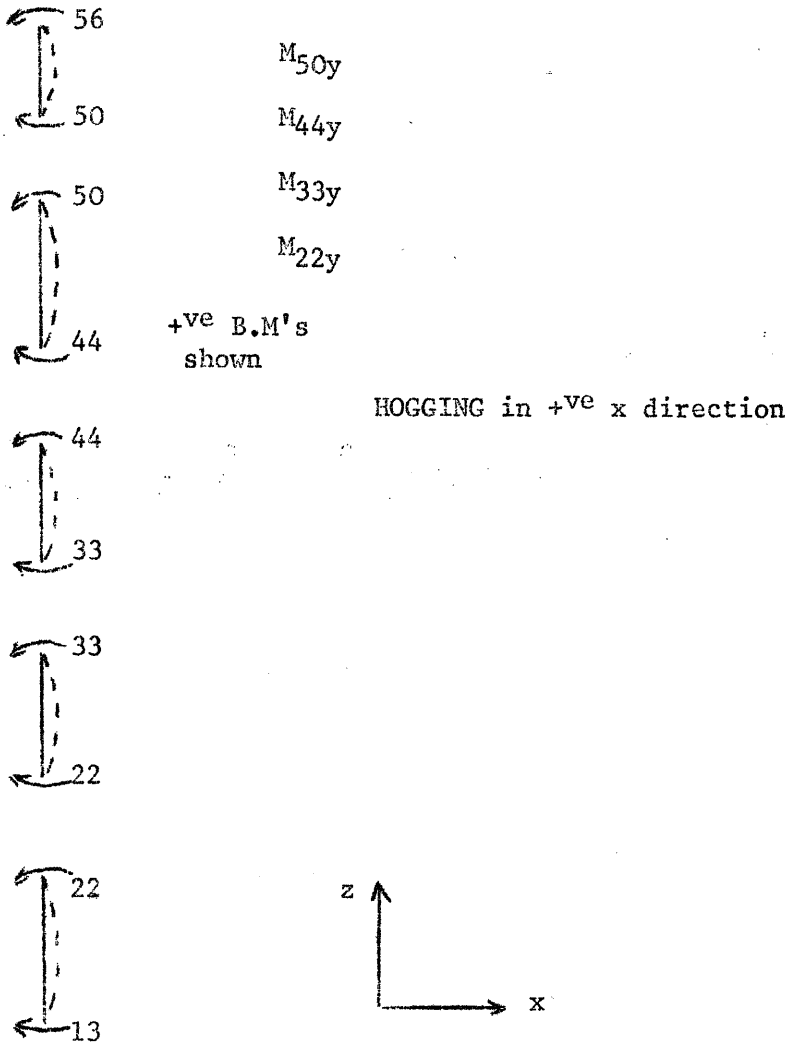

fig.(ix)

Rear Wheel Arch

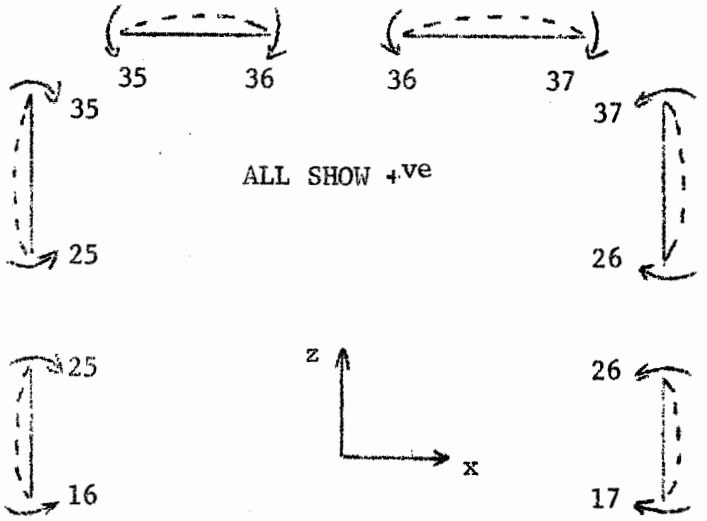

M_{25y}
M_{35y}
M_{36y}
M_{37y}
M_{26y}

fig.(x)

Scuttle Portal in Floor

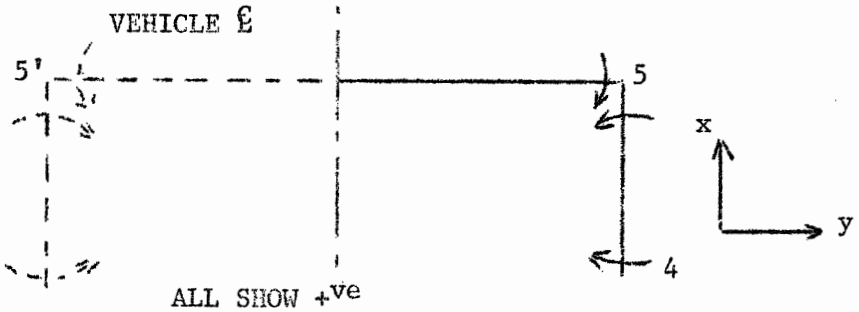

fig.(xi)

M_{5z} B.M. between 5 and 5' always constant

Rear Wheel Cut Out

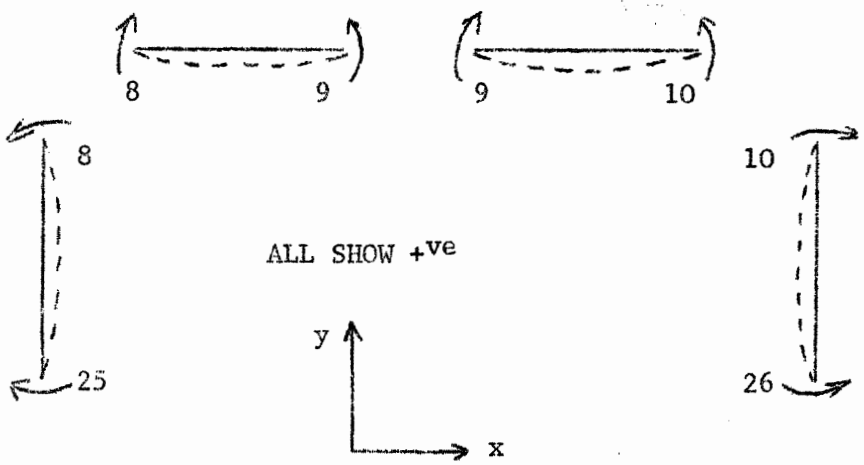

M_{8z}
M_{9z}
M_{10z}

fig.(xii)

This last may be better seen if drawn with the axes as for the scuttle portal

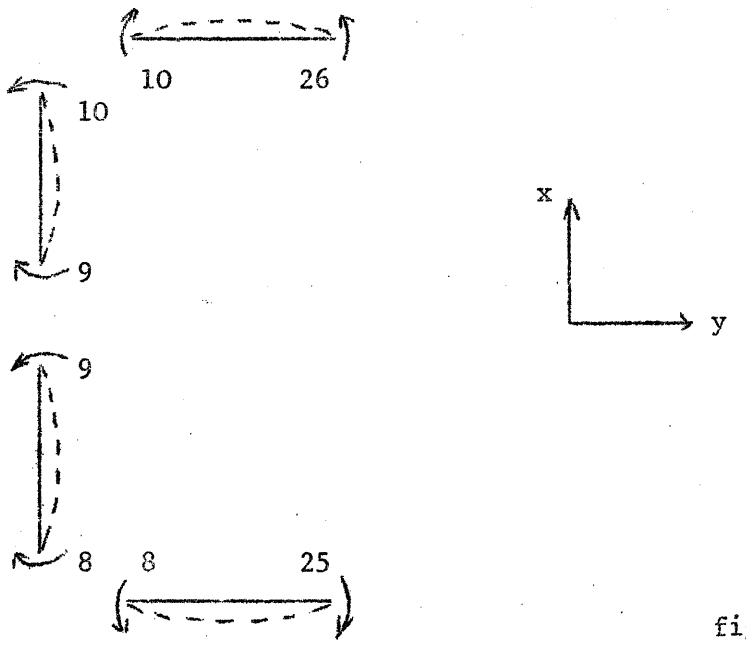

fig.(xiii)

Now 8-9 and 9-10 have hogging B.M. $+^{ve}$ for $+^{ve}y$ as does 4-5 in the other system.

Appendix III

Condensation

The end load distribution on the main longitudinal would have the form:

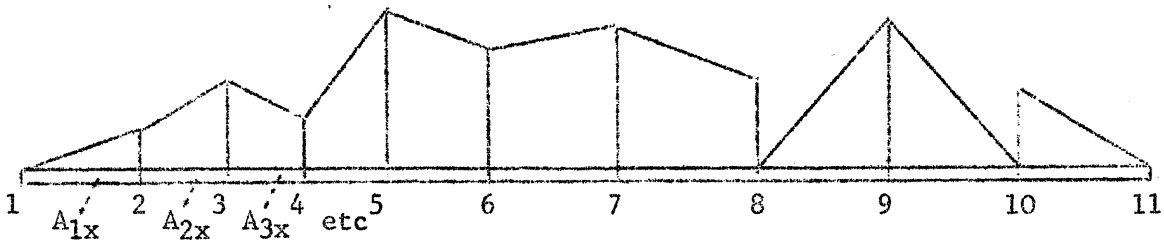

fig.(i)

The discontinuities at nodes 8 and 10 being caused by the horizontal portal at the rear wheel arch.

The section 1 to 8 will form one chain having the condensed flexibility matrix:

Condensed Flexibility Sub-Matrix 1

Row Designation	
F_{2x}	$\frac{1}{E}\Big[(\frac{l_1}{3A_{1x}} + \frac{l_2}{3A_{2x}}),\ \frac{l_2}{6A_{2x}}$
F_{3x}	$\frac{l_2}{6A_{2x}},\ (\frac{l_2}{3A_{2x}} + \frac{l_3}{3A_{3x}}),\ \frac{l_3}{6A_{3x}}$
F_{4x}	$\frac{l_3}{6A_{3x}},\ (\frac{l_3}{3A_{3x}} + \frac{l_4}{3A_{4x}}),\ \frac{l_4}{6A_{4x}}$
F_{5x}	$\frac{l_4}{6A_{4x}},\ (\frac{l_4}{3A_{4x}} + \frac{l_5}{3A_{5x}}),\ \frac{l_5}{6A_{5x}}$
F_{6x}	$\frac{l_5}{6A_{5x}},\ (\frac{l_5}{3A_{5x}} + \frac{l_6}{3A_{6x}}),\ \frac{l_6}{6A_{6x}}$
F_{7x}	$\frac{l_6}{6A_{6x}},\ (\frac{l_6}{3A_{6x}} + \frac{l_7}{3A_{7x}}),\ \frac{l_7}{6A_{7x}}$
F_{8-7x}	$\frac{l_7}{6A_{7x}},\ \frac{l_7}{3A_{7x}}\Big]$

The above rows must be placed next to each other in the matrix calculation.

No row need be defined in the matrix for the load F_{8-9x}, nor for F_{10-9x}, and one value at F_{9x} determines the 'roof' distribution with one value of flexibility

$$f_{ax} = \frac{l_8}{3A_{8x}E} + \frac{l_9}{3A_{9x}E}$$

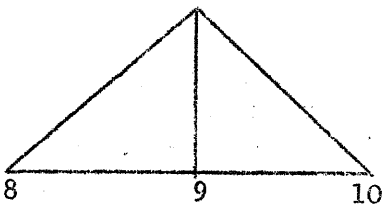

fig.(ii)

This single row designated F_{9x} can be put at any place in the matrices.

The final section of the main longitudinal distribution carries the row designation F_{10-11x} and is again a separate row with a flexibility

for row $F_{10-11x} = \frac{l_{10}}{3A_{10x}E}$

All the remaining end loads in the x direction can be made by combining the properties of the above three condensations. The correspondence between the suffices of the lengths and the effective areas cannot be maintained but from the above example it is clear which cross-section is applicable in each case.

F_y Rows

These rows involve members crossing the ℄ of the vehicle. For bending loads the ℄ is fixed and the uncondensed flexibility matrix for the load distribution illustrated will be:-

fig.(iii)

Load at ℄ $\quad f = \frac{1}{E}$

$F_{1-℄y}$	$\frac{2d_1}{6A_{1y}}$	$\frac{d_1}{6A_{1y}}$		
	$\frac{d_1}{6A_{1y}}$	$\frac{2d_1}{6A_{1y}}$		
F_{1-19y}			$\frac{2d_2}{6A_{19y}}$	$\frac{d_2}{6A_{19y}}$
F_{19y}			$\frac{d_2}{6A_{19y}}$	$\frac{2d_2}{6A_{19y}}$

Since the value of the load F_{1y} only need be specified the condensed flexibility is:

$$\frac{d_1}{A_{1y}E} + \frac{d_2}{6A_{19y}E}$$

At node point 4 there is only an outrigger 4-21 with zero end load at node 21. The flexibility is:

$$f_{4y} = \frac{d_2}{3A_{4y}E}$$

The next cross member has a discontinuity of end load at node 5 and an end load at node 22 provided by the bending stiffness in the windscreen pillar.

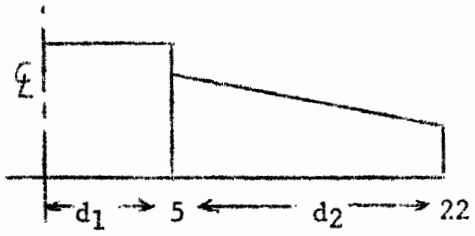

fig.(iv)

This system can be split into two, one constant end load across the ℄ of the vehicle, designated F_{5y}, where the flexibility $f_{5y} = \frac{d_1}{A_{5y}E}$

The remainder of the cross member required two rows for definition and the square flexibility matrix is:

Row No:

$$\begin{matrix} F_{5-22y} \\ F_{22y} \end{matrix} = \frac{1}{6A_{22y}E} \begin{bmatrix} 2d_2 & d_2 \\ d_2 & 2d_2 \end{bmatrix}$$

The other cross members at floor level are combinations of the above.

At scuttle level the cross member 44-69 requires two loads to define the distribution and the condensed flexibility sub-matrix is:

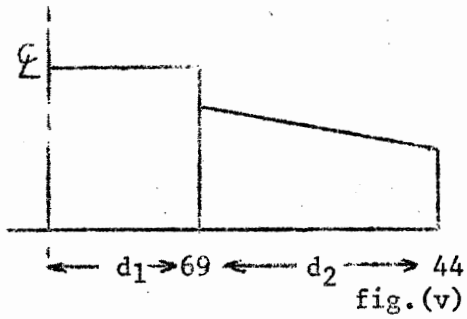

fig.(v)

Row No:

$$\begin{matrix} F_{44y} \\ F_{69y} \end{matrix} = \frac{1}{E} \begin{bmatrix} \frac{d_2}{3A_{44y}} & \frac{d_2}{6A_{44y}} \\ \frac{d_2}{6A_{44y}} & \left(\frac{d_2}{3A_{44y}} + \frac{d_1}{A_{69y}}\right) \end{bmatrix}$$

The member across the top of the windscreen has a constant end load since there is no shear in the panels between it and the roof. (These panels do not appear in the calculations for bending). Consequently only one row is allocated to the load in this member.

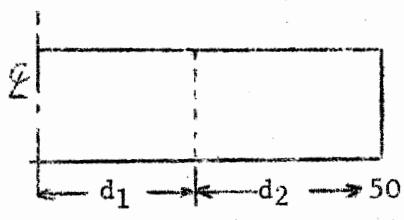

fig.(vi)

The corresponding flexibility is:

$$f_{50y} = \frac{d_1 + d_2}{A_{50y}E}$$

Assuming constant effective cross section area across the vehicle.

The remaining cross member end loads have the same form as those detailed above.

F_z Rows

The condensed flexibilities for the various continuous and isolated end load members in the vertical direction can be made up from the same types as were discussed for the F_x rows. There are no cases of constant end load as occur for the cross members.

M_x Rows

The M_x bending moments will occur on the cross members and for straight cross members the rows required to specify the loads and the form of the flexibility matrix are the same as for the F_y rows e.g.

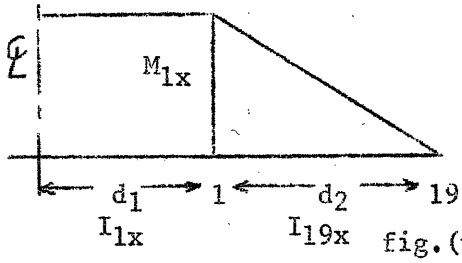

fig.(vii)

for the M_{1x} row

$$\text{Flexibility} = \frac{d_1}{E\ I_{1x}} + \frac{d_2}{3E\ I_{19x}}$$

Where the cross member is cranked over the rear wheel arch two separate cases have to be considered. At the ends of the wheel arch (members 8, 62, 35 and 10, 64, 37) the bending moment at point 62, say, is different from point 8 due to the shear in the end panels of the wheel arch whereas in the centre of the wheel arch the bending moment is the same at points 9 and 63.

For the ends of the wheel arch two adjacent rows will be necessary,

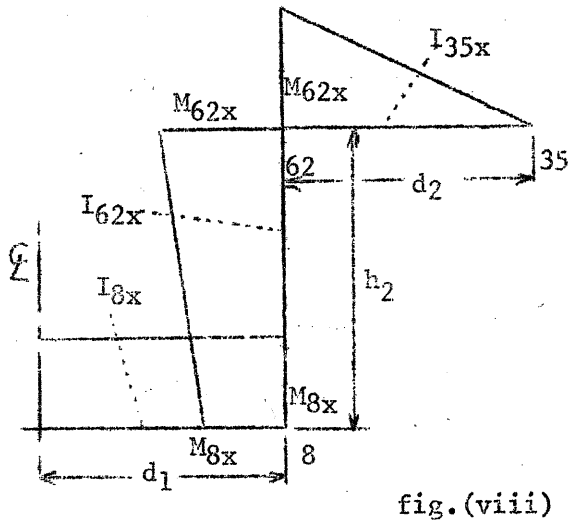

fig.(viii)

M_{8x}

M_{62x}

Having the condensed flexibility matrix

$$\frac{1}{E}\begin{bmatrix} \frac{d_1}{I_{8x}} + \frac{h_2}{3I_{62x}}, & \frac{h_2}{6I_{62x}} \\ \frac{h_2}{6I_{62x}}, & \frac{h_2}{3I_{62x}} + \frac{d_2}{3I_{35x}} \end{bmatrix}$$

For the centre cross members only one row is necessary, M_{9x} with the corresponding flexibility

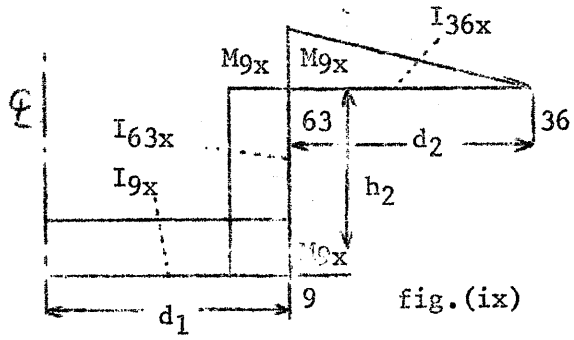

fig.(ix)

$$\frac{d_1}{EI_{9x}} + \frac{h_2}{EI_{63x}} + \frac{d_2}{3EI_{36x}}$$

The windscreen pillar and its continuation has also lateral bending stiffness with a distribution as shown:

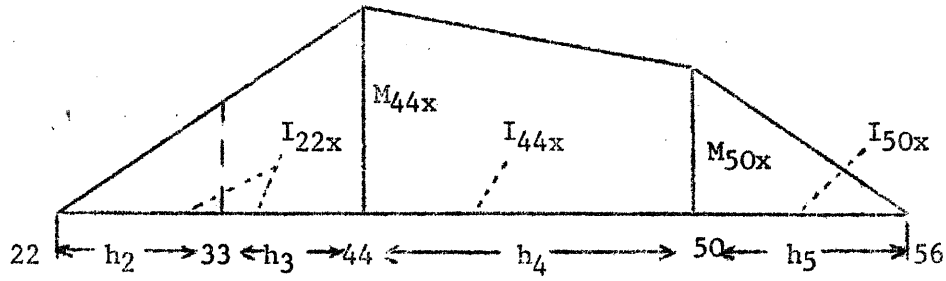

fig.(x)

and a flexibility matrix for the two rows:-

$$\begin{matrix} M_{44x} \\ M_{50x} \end{matrix} \quad \frac{1}{E} \begin{bmatrix} \frac{h_2 + h_3}{3I_{22x}} + \frac{h_4}{3I_{44x}} & , & \frac{h_4}{6I_{44x}} \\ \frac{h_4}{6I_{44x}} & , & \frac{h_4}{3I_{44x}} + \frac{h_5}{3I_{50x}} \end{bmatrix}$$

M_y Rows

The bending moment distribution on the main longitudinal member is continuous with zero moments at points 1 and 11 and the flexibility matrix has the same form as for end loads except that the discontinuity at the rear wheel arch does not exist. The rows M_{2y} to M_{10y} must therefore be kept together. The windscreen pillar has fore and aft bending stiffness over a greater length than for lateral loads and there is a load input at point 33 giving a change in slope of the bending moment distribution at this point.

The wheel arch surrounds are treated as continuous beams with flexibility sub-matrices as shown:-

Front Wheel Arch

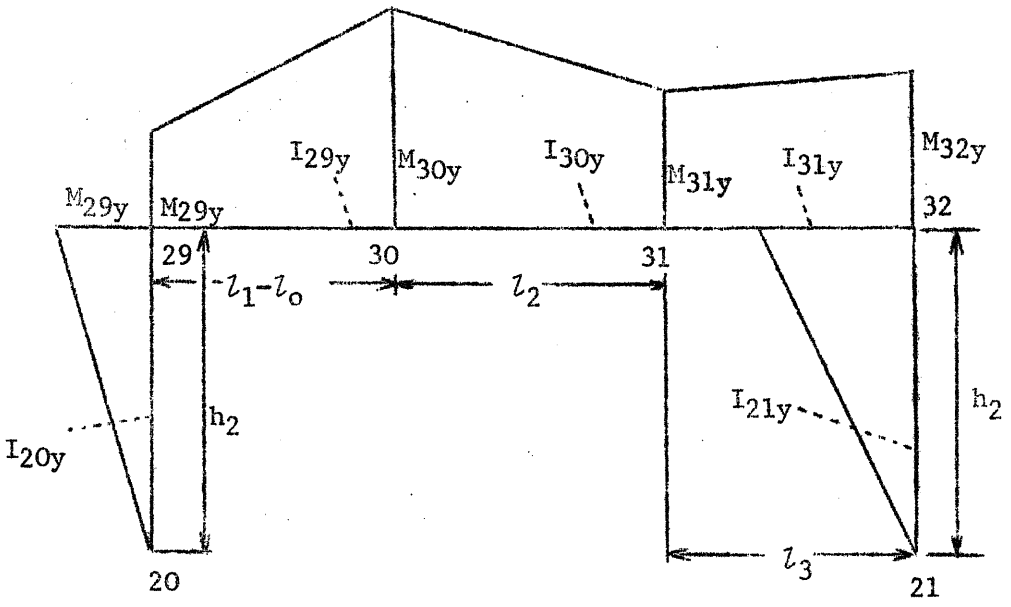

fig.(xi)

Rows

Flexibility

$$
\begin{array}{ll}
M_{29y} & \frac{1}{E}\left[\begin{array}{ccc}
\frac{h_2}{3I_{20y}} + \frac{l_1-l_0}{3I_{29y}}, & \frac{l_1-l_0}{6I_{29y}} & \\
\frac{l_1-l_0}{6I_{29y}}, & \frac{l_1-l_0}{3I_{29y}} + \frac{l_2}{3I_{30y}}, & \frac{l_2}{6I_{30y}} \\
 & \frac{l_2}{6I_{30y}}, & \frac{l_2}{3I_{30y}} + \frac{l_3}{3I_{31y}}, \quad \frac{l_3}{6I_{31y}} \\
 & & \frac{l_3}{6I_{31y}}, \quad \frac{l_3}{3I_{31y}} + \frac{l_2}{3I_{21y}}
\end{array}\right] \\
M_{30y} & \\
M_{31y} & \\
M_{32y} &
\end{array}
$$

Rear Wheel Arch

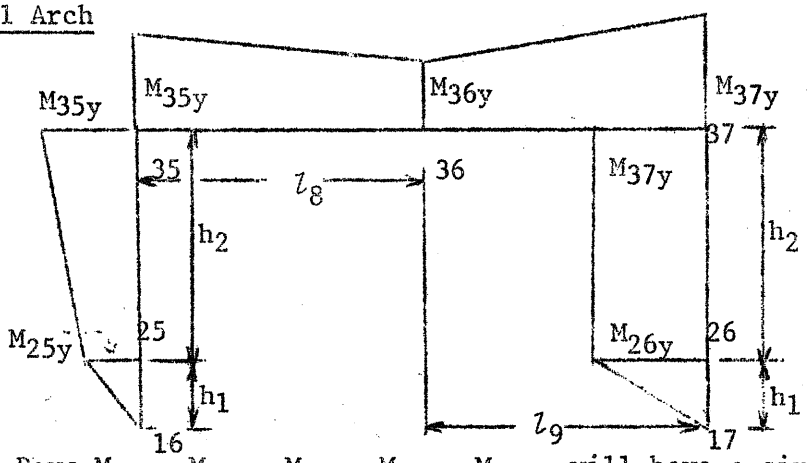

fig.(xii)

Rows M_{25y}, M_{35y}, M_{36y}, M_{37y}, M_{26y} will have a similar form to the front wheel arch.

M_z Rows

There are only two portal members with stiffness about the z axis. One is at floor level across the vehicle at the scuttle section to react shear in the floor panel of the footwell box. The symmetrical bending moment distribution shown requires only one row to define it.

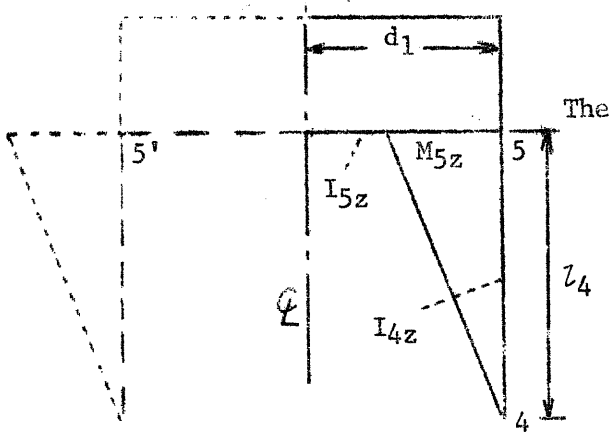

fig.(xiii)

The flexibility for this row is:

$$\frac{d_1}{EI_{5z}} + \frac{l_4}{EI_{4z}}$$

The horizontal portal frame at the bottom of the rear wheel arch is the other M_z member with a distribution as shown:-

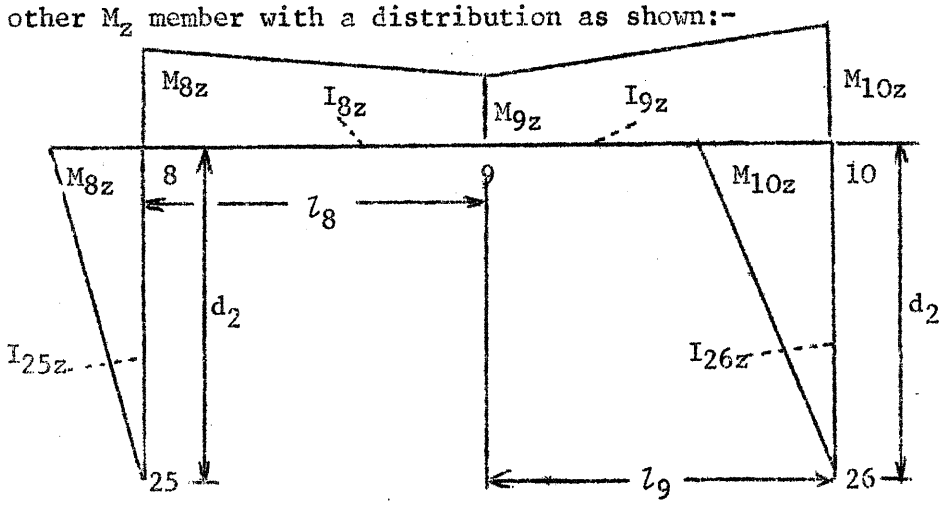

fig.(xiv)

Leading to the flexibility sub-matrix:-

Row — Flexibility

$$
\begin{array}{ll}
M_{8z} & \frac{1}{E}\left[\begin{array}{ccc}
\frac{d_2}{3I_{25z}} + \frac{l_8}{3I_{8z}}, & \frac{l_8}{6I_{8z}} & \\
\frac{l_8}{6I_{8z}}, & \frac{l_8}{3I_{8z}} + \frac{l_9}{3I_{9z}}, & \frac{l_9}{6I_{9z}} \\
 & \frac{l_9}{6I_{9z}}, & \frac{l_9}{3I_{9z}} + \frac{d_2}{3I_{26z}}
\end{array}\right] \\
M_{9z} & \\
M_{10z} &
\end{array}
$$

Appendix IV

Detail Design and Sample Tests of Floor Structure

Overall Design Considerations

It was decided to construct the model of high grade aluminium alloy material using as far as possible existing production equipment available at Cranfield. This equipment consisted of folding machines, a small fly-press and basic hand tools while the heat-treatment facilities consisted of only a very small furnace.

With these factors in mind and also the fact that extruded aluminium alloy sections are only produced with relatively low strength alloys it was decided to manufacture the model using high grade alloy sheet. The main members being made straight and folded from sheet on the existing equipment. This method also allowed sections most suited to this application to be used, standard extrusions not being of desirable shapes.

The material chosen therefore was 2 L 72 Alclad sheet in the solution treated condition which has a reasonable strength and is also ductile enough to allow bending operations to be carried out without cracking. After bending it would have been desirable to bring the properties of 2 L 72 up to 2 L 73 by precipitation treatment giving an increase of 40% in the proof stress and 8% in the ultimate stress. The lack of furnace facilities however, prevented this being carried out.

A rivetted and bolted method of joining components was chosen as this could be carried out cheaply and only needed the purchase of a few air-line drills and rivetters. Construction of this type has the advantage that if modifications are required it is relatively easy to drill out rivets or remove bolts and replace with new components. An alternative construction would have been to use spot welds. This would have meant the purchase of more costly equipment and also promote corrosion and future modification problems.

Allowable stress levels have been based on $^2/_3$ of the ultimate. The ultimate tensile stress of 2 L 72 is 56,000 lb/in^2 giving a working stress 37,300 lb/in^2 which corresponds to 0.3% proof stress.

Design stress levels have been calculated from static loads factored by 4 for the dynamic condition. This high acceleration factor is 11% above any measured level on a vehicle of this type used in cross-country operations. It was therefore considered satisfactory to equate design stress levels to the maximum working stress without further factors.

c Detail Design Considerations

The length of 168 inches of the model structure and the limited production facilities of the A.S.A.E. dictated that the main longitudinal members 1 - 11 had to be manufactured in four sections. Ideally, a continuous

beam with a tapered section at node 4 is required giving uniform stiffness over lengths in front and behind this node point. This could have been achieved if large press equipment had been available. However, by making these members in relatively short lengths the work was handled on existing folding machines.

The positions for the joints were chosen at nodes 4, 7, and 9, which enabled the basic floor structure to be made in three sub-assemblies, with members 1 - 4 being attached as individual items. These positions also avoided the areas of high bending stress at nodes 6, 8, and 10 and the need for large joint reinforcing. In addition to the joints in the longitudinal members reinforcing has had to be added to these members at cross member connections even where the longitudinal members are continuous. (As at nodes 5, 6, 7 and 11). Over the rear wheel arch the cross members of course have two 90^{o} bends which required joint arrangements.

The design of the rivetted joints has been based on basic text book rivet group loading calculations with design loads based on the computed results of bending moments, end loads, and shear loads. A typical analysis of joint stressing is shown below.

As indicated in Section "Design of the Structure", and fig (i), the basic beams are loaded beyond their design figures at nodes 6 and 8. Local reinforcing has been added at these points in order to carry the higher loads. At node 8 the bending on the crossmember is also too high for the basic member and reinforcing has been added to this as well.

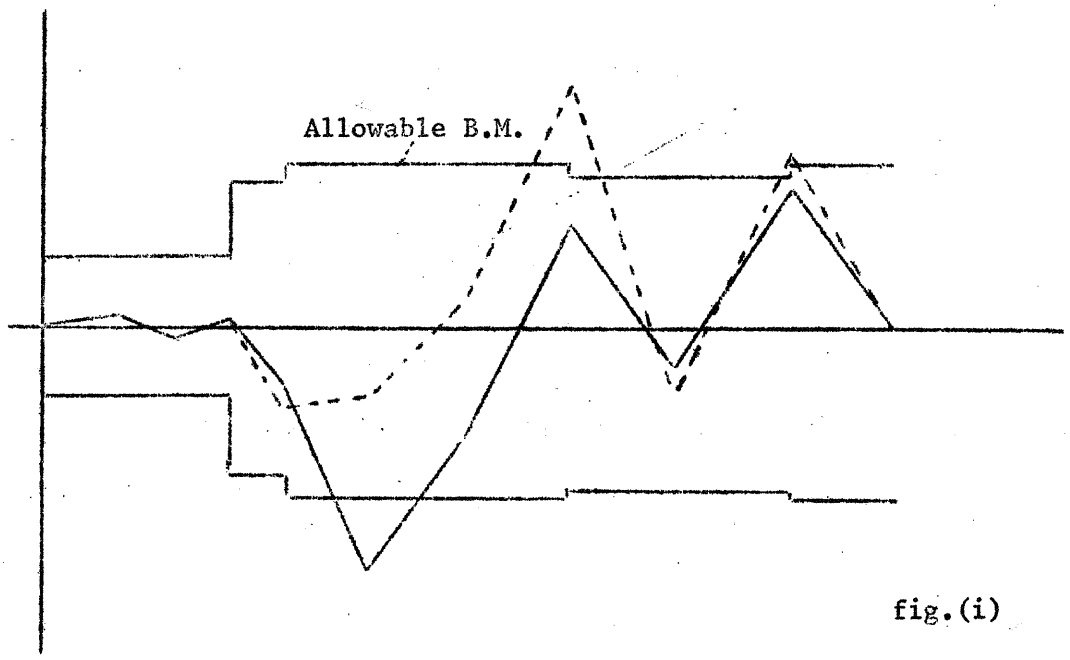

fig.(i)

In designing this floor structure it was considered wise to investigate these joints by conducting tests on typical joint assemblies. Two points which needed verifying were (1) the compressive/buckling characteristics of the floor panel over the crossmembers as shown in Fig.1, App.IV. (2) the stiffening effect of the reinforcing on the basic beam.

Two longitudinal member joints were tested, one similar to joint at node 5 and the other similar to joint at node 7. Two types of angled joint for the cross members were also tested.

The tests showed that a reinforcing plate on top of the floor panel was required to avoid buckling and some indication of the stiffening effect was obtained. Redesign of the right angled cross member joint was also found necessary. However, due to to subsequent computer calculations the joints used for the actual model have been modified from the test joint design and if time had been available further tests should bave been conducted. As these tests were not carried out no alterations to the flexibility matrix have been considered.

To obtain the most efficient design considerable computer, design, workshop and testing time would be required as this is an iterative process involving design and testing large numbers of joint assemblies and investigating their effect on the overall flexibility of the structure.

Design Calculations for Joint 7

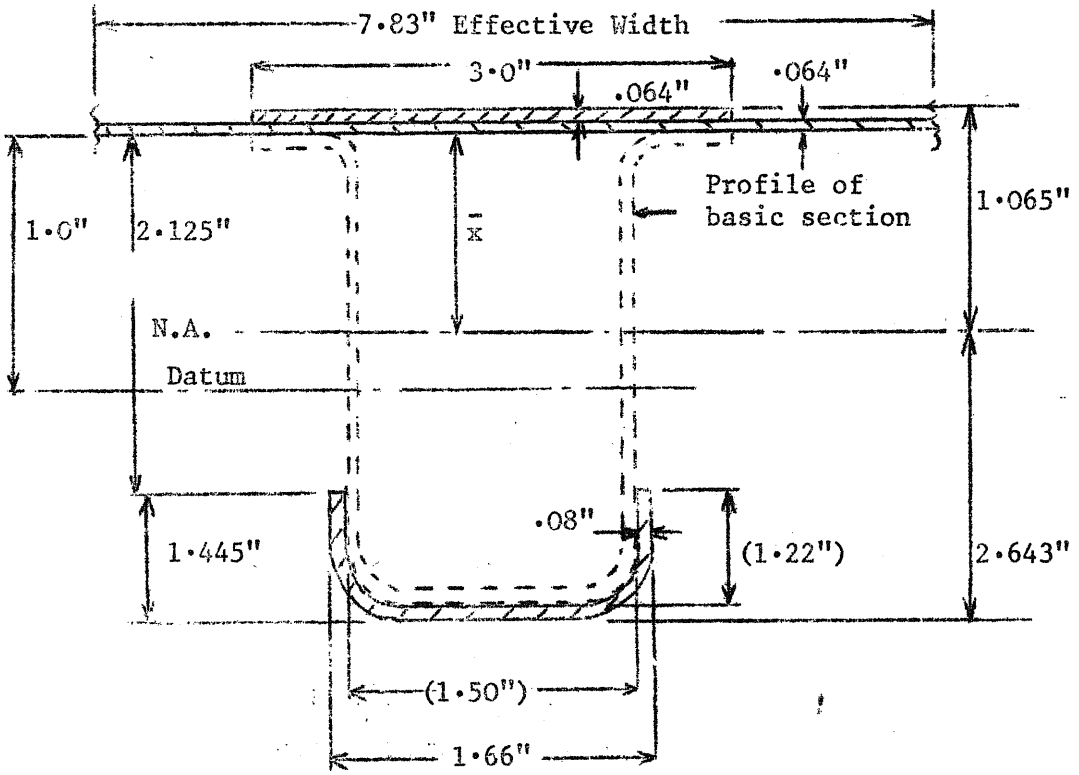

fig.(ii)

Position of Neutral Axis

$\bar{x}$ = ·937 ins.

Area A = 1·008 in^2

Second moment of area about N.A.

$I_{N.A.}$ = 2·1415 in^4

Loading Case is Case 2 from computer results

Bending Moment = -24,385 lb-in

End Load = -2,442 lbs.

Shear Force (from bending moments) = +2,009 lbs.

Stress Distribution due to Bending

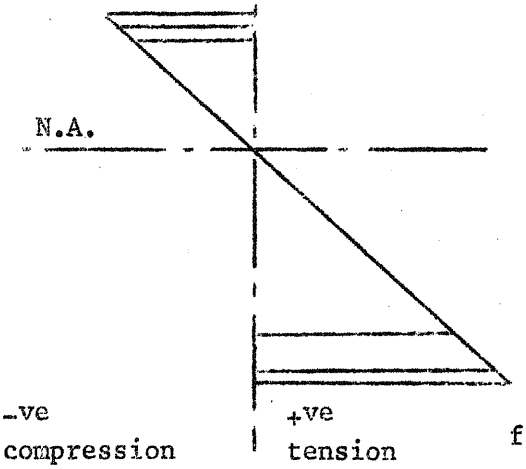

fig.(iii)

$$fc = -24,385 \times \frac{1\cdot065}{2\cdot1415}$$

$$= -12,110 \text{ lbs/in}^2$$

$$ft = 24,385 \times \frac{2\cdot643}{2\cdot1415}$$

$$= 30,100 \text{ lbs/in}^2$$

Stress Distribution due to End Load

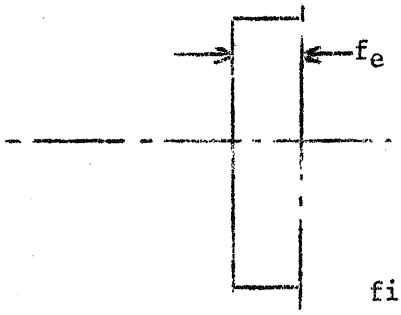

fig.(iv)

$$fe = \frac{-2442}{1\cdot008} = -2425 \text{ lb/in}^2$$

Note: End load assumed to act at N.Axis Computed loads assumed to act at Datum. An eccentricity of ·063 has been ignored.

Resultant Stress Distribution

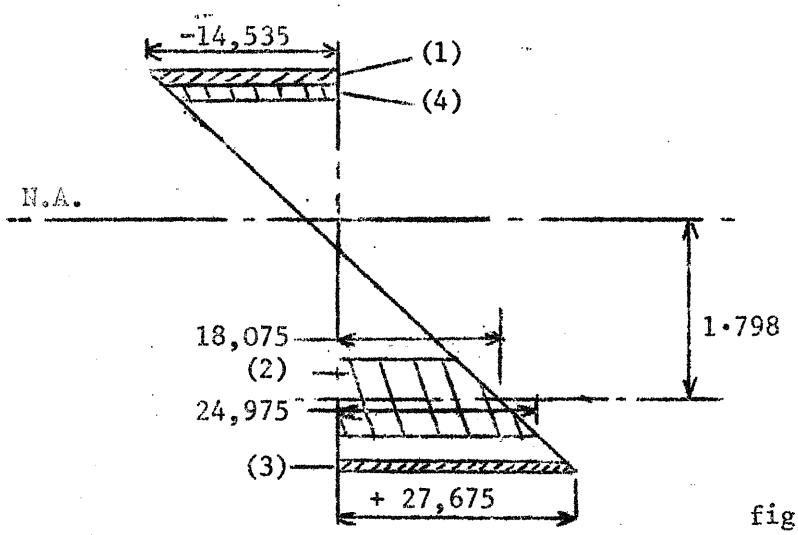

fig.(v)

This is equivalent to:-

(1) End load in top reinforcing

Mean stress = -14,205 lb/in^2

End load = -14,205 x ·64 x 3 = <u>-2725 lbs</u>

Strength of bolts and rivets attaching top reinforcing = <u>5028 lbs</u>
(Based on 2/3 ultimate strength)

$$R.F. = \frac{5028}{2725} = 1\cdot85$$

(2) This is equivalent to end load and moment

End load = mean stress x area
= 3525 lb

Moment = $\frac{fI'}{y}$ (applied to side parts of reinforcing)

= (24975 - 18075) $\frac{\cdot 0242}{\cdot 61}$

= 274 lb-in

(3) End load in base of reinforcing

End load = 27,225 x ·12 = 3275 lb

Combining (2) and (3) and applying forces and moments to rivet group we get:-

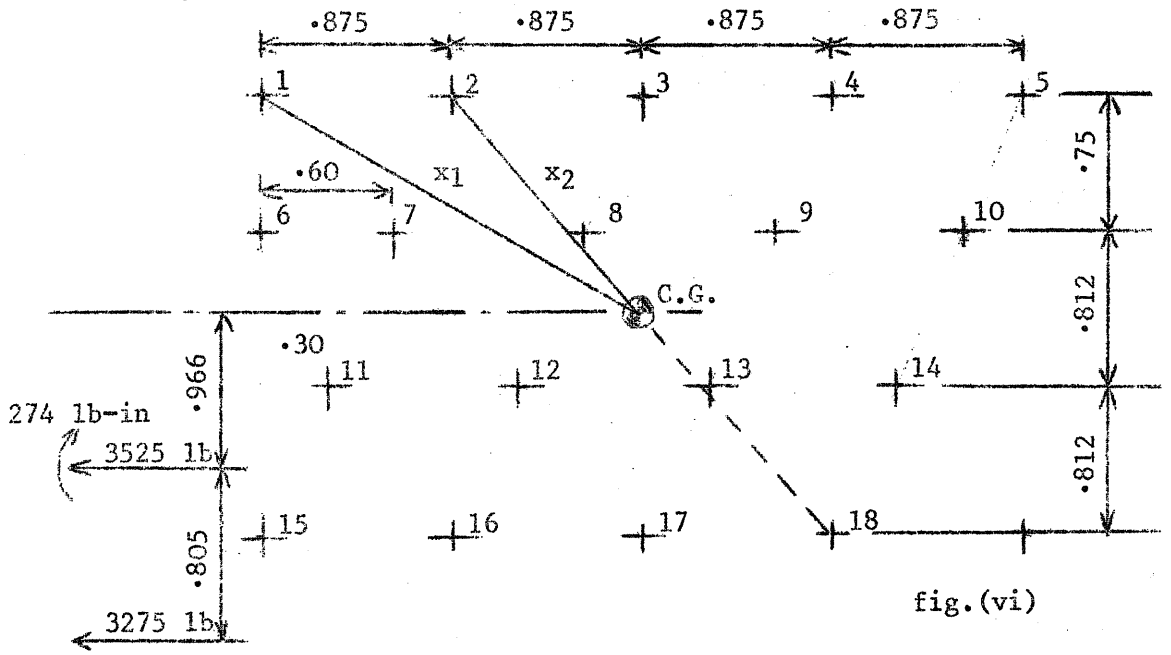

fig.(vi)

Moment applied to rivet group

= (3275 x 1·771) + (3525 x ·966) + 274

= 5800 + 3405 + 274

= 9479 lb/in

Resisting moment of rivet groups = $2\frac{W_n}{x_n}$ $(x_1^2 + x_2^2 - - - - - - - x_{18}^2)$
(2 rivet groups, one each side of beam)

where W_n = load on rivet n

Load on rivets due to end load = $\frac{(3525 + 3275)}{36}$

= 189 lbs

Load due to shear force = $\frac{2009}{36}$ = 56 lbs.

Combining these loads by vectors gives rivet 18 as most severely loaded rivet.

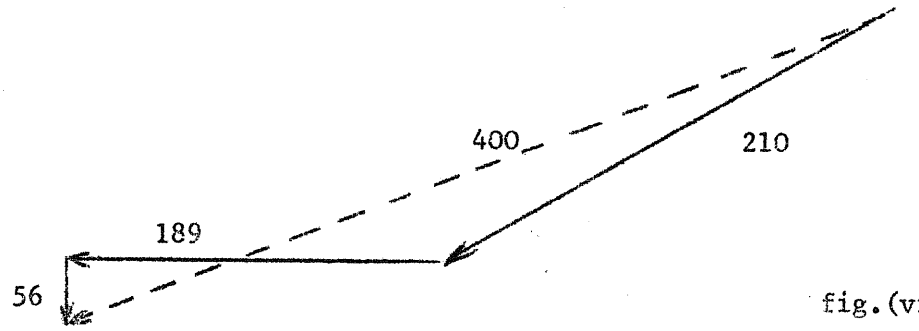

fig.(vii)

Resultant load on rivet 18 = 400 lb.

Ultimate single shear load on AGS 2045/508 rivet in 14 SWG plate = 625 lbs.

Allowable shear load = $^2/_3 \times 625$ = 416 lb.

Reserve factor = $\frac{416}{400}$ = 1·04

Buckling of Floor and Reinforcing over Joint

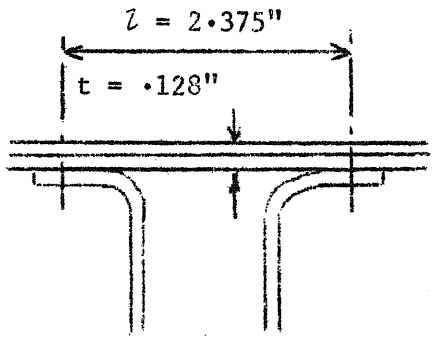

fig.(viii)

Stress when buckling occurs

$f_r = KE_t(\frac{t}{l})^2$ where K is a factor dependent on end fixing

E_t = tangent modulus

Using data based on R.Ae.S. Data Sheet 02.01.15 we get

$$\frac{f_r}{E_t} = 2{\cdot}46 \quad \frac{{\cdot}128}{2{\cdot}375}^2 = {\cdot}0716$$

$$f_r = 30{,}000 \text{ lb/in}^2$$

Bending Moment at this section to give this stress level

$$M = \frac{30{,}000 \times 2{\cdot}1415}{1{\cdot}065} = 60{,}300 \text{ lb-in}$$

Without reinforcing buckling will occur at approximately one third of this value.

Test Method

The two main longitudinal ieces were tested (one similar to joint 5 - reinforcing only - and one similar to joint 7 - complete join - for Floor Longitudinal Members) by the conventional circular bending test arranged as shown in Fig.2/fig (ix) App. IV. Loads were applied in either direction i.e. to induce both sagging and hogging bending moments. Fig.2 App.IV shows the hogging moments applied to test joint 5. Deflections were measured under each load point and under the centre of the joint.

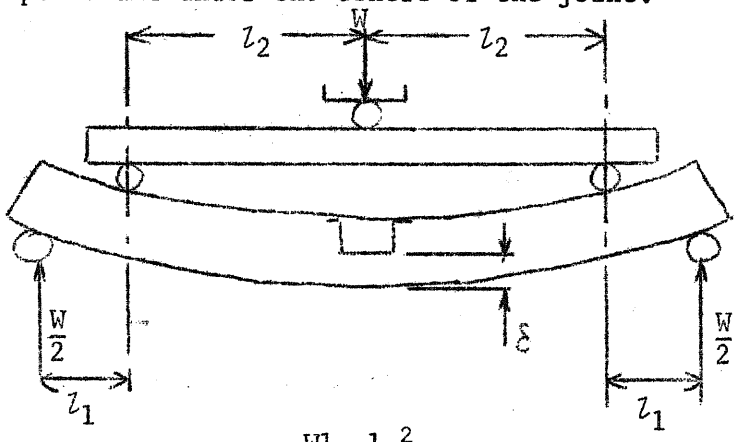

fig.(ix)

$$\text{Theoretical } \delta = \frac{W l_1 l_2^2}{4 EI}$$

$$l_1 = 8{\cdot}5$$

$$l_2 = 10{\cdot}5$$

$$\text{Giving Theoretical } \delta = \frac{234W}{EI}$$

Local reinforcing was fitted to the beams at each loading point to prevent local buckling.

These two joints at nodes 5 and 7 are both loaded with sagging moments, however, hogging moment loading was applied to the test pieces up to the ·15% proof loading of the basic beam.

Basic Beam and Floor Plate of Test Beams

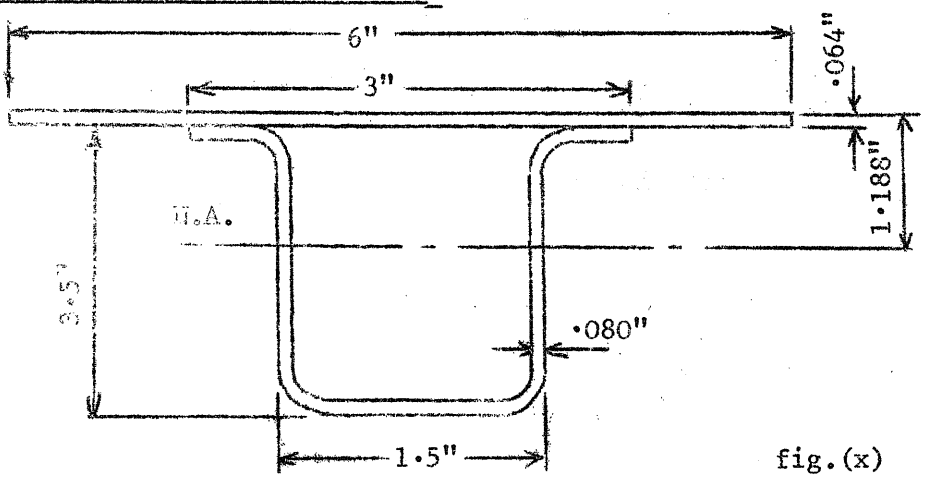

fig.(x)

N.Axis is as shown 1·188" below top face of plate

$$I_{NA} = 1{\cdot}886 \text{ in}^4$$

Allowable Bending Moments

$$0{\cdot}1\% \text{ Proof} \quad M = \frac{33{,}600 \quad 1{\cdot}886}{2{\cdot}376} = 26{,}600 \text{ lb-in}$$

$$0{\cdot}5\% \text{ Proof} \quad M = \frac{39{,}200 \quad 1{\cdot}886}{2{\cdot}376} = 31{,}100 \text{ lb-in}$$

$$\text{Ultimate} \quad M = \frac{56{,}000 \quad 1{\cdot}886}{2{\cdot}376} = 44{,}500 \text{ lb-in}$$

Summary of Results

Test Joint 5 Figs.1, 2, App.IV

Without reinforcing on floor, beam failed at a sagging moment of 19,600 lb-in (Floor panel buckled).

With reinforcing on floor, beam was satisfactory up to 30,000 lb-in sagging and hogging bending moments.

The equivalent value of I for the length of beam under circular bending ≈ 2·50 in^4 showing an increase in stiffness of 32% over basic beam. Load deflection test results are shown in Fig.3, App.IV.

Test Joint 7 Fig.4, App.IV

With no reinforcing on floor the beam failed as a sagging moment of 20,600 lb-in. (Floor panel buckled).

With reinforcing, failure did not occur until a sagging moment of 35,000 lb-in was applied.

In the hogging condition, the test was stopped at 43,000 lb-in bending moment at which stage no failure had occurred. Load deflection test results are shown in Fig.5,App.IV.

The equivalent I values are 3·09 in^4 (sagging) and 2·4 in^4 (hogging) which are 64% and 26% increases over the basic beam stiffness.

Note:- Figs.3 & 5, App.IV are plotted such that any permanent set incurred by the sagging moments is not shown in plotting the hogging moments.

Test Method for Right Angled Joint (Joints 8, 9, & 10)

Fig.6, App.IV

This test piece can be idealised into the system shown:-

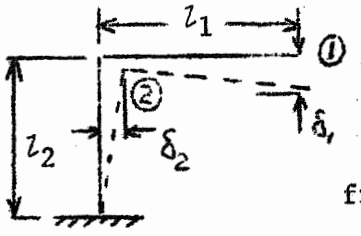

fig.(xi)

l_1 = 7·54 in Measured along theoretical N. Axis

l_2 = 5·29 in

Theoretically $\delta_1 = \frac{Wl_1}{EI} \left\{ l_1 l_2 + \frac{l_1^2}{3} \right\}$

$$\delta_2 = \frac{Wl_1 l_2^2}{2\,EI}$$

Measurements were taken at points (1) and (2) up to a bending moment at point 2 of 15,400 lb-in. The results are shown in Fig.7, App.IV.

Basic Beam of Right Angled Test Piece.

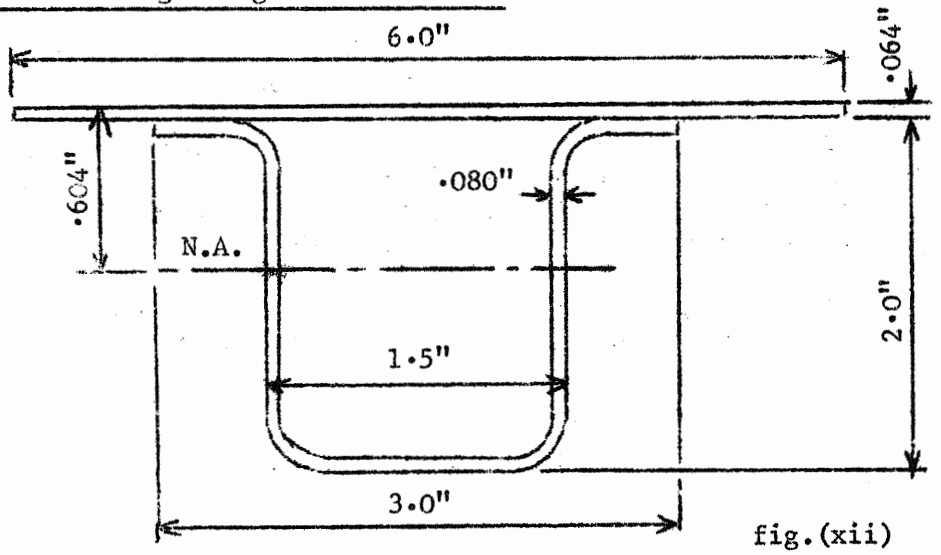

fig.(xii)

$I_{NA} = \cdot 499\ in^4$

Allowable Bending Moments

0·1% Proof $M = \frac{33,600 \quad \cdot 499}{1 \cdot 46} = 11,500$ lb-in

0·5% Proof $M = \frac{39,200 \quad \cdot 499}{1 \cdot 46} = 13,400$ lb-in

Ultimate $M = \frac{56,000 \quad \cdot 499}{1 \cdot 46} = 19,100$ lb-in

From this test the equivalent I of the beam measured between load point and built-in end is:-

$I = \cdot 162\ in^4$

This is a reduction in stiffness of 67·5% from the basic beam and is unacceptable.

Summary

These tests confirmed that the joints in the longitudinal members i.e. joints 5 and 7 were satisfactory up to their nominal proof load.

Yielding of the members was becoming noticable at proof load conditions. The preliminary tests of these members confirmed that the floor buckling predicted would occur and that reinforcing on the floor panels was necessary. No visible damage was incurred by any of the rivet groups.

The large increase in member stiffness is perhaps undesirable and as indicated on page 41 of this appendix, much more work is required to produce the most efficient structure.

However, it was therefore concluded that these types of joints and their analysis were satisfactory for this structure.

The right angled test piece was however less satisfactory as the stiffness of the joint was considerably reduced. Inspection of the reinforcing bracket revealed that yielding of the flanges had occurred and this was the main cause for the high deflections.

In the light of this test, the joint was redesigned as a closed box section for the actual structure. This is shown in Fig.8, App.IV.

TABLE 1

Comparison of loads in bonnet top for three idealisations

Loads Defined in the Structure	Non-redundant Basic System 2	Bonnet top 1	Bonnet top 2
$F_{69 - 69'y}$	+1	+ .983	+ .983
M_{69z}	+0	+ .000199	+ .000208
M_{68z}	+0	+0	- .0000745
M_{67z}	+0	+0	+ .0000490
M_{66z}	+0	- .000897	- .0000923
F_{65y}	- .0278	- .0291	- .0293
$F_{66 - 41y}$	+ .0445	+ .0460	+ .0459
F_{67y}	+0	+ .0000089	+ .0000264
F_{68y}	+0	- .0000199	- .0000405
$F_{69 - 44y}$	- .0167	- .0169	- .0166
F_{41x}	- .0295	- .0308	- .0310
F_{42x}	- .0197	- .0210	- .0215
F_{43x}	- .0098	- .00924	- .00859
F_{66x}	+ .0295	+ .0308	+ .0310
F_{67x}	+ .0197	+ .0211	+ .0215
F_{68x}	+ .0098	+ .00924	+ .00859
C_6	- .00164	- .00171	- .00172
C_7	+ .00098	+ .000975	+ .000945
C_8	+ .00098	+ .000925	+ .000861
C_9	+ .00098	+ .000924	+ .000858
$F_{66 - 66'y}$	+ .0445	+ .0460	+ .0459

TABLE 2

Effective Cross Sectional Area			Second Moments of Area		
$A_{1x} = .884$	$A_{1y} = .722$	$A_{1z} = .344$	$I_{1x} = .419$	$I_{1y} = .419$	
$A_{2x} = .884$		$A_{2z} = .288$			
$A_{3x} = .884$		$A_{3z} = .233$			
$A_{4x} = 1.209$		$A_{4z} = .358$		$I_{4y} = 1.729$	$I_{4z} = .536$
$A_{5x} = 1.244$	$A_{5y} = 1.015$	$A_{5z} = .519$	$I_{5x} = .455$	$I_{5y} = 2.028$	
			$I_{5'x} = .451$		
$A_{6x} = 1.244$	$A_{6y} = 1.111$		$I_{6x} = .500$	$I_{6y} = 2.028$	
$A_{7x} = 1.244$	$A_{7y} = .887$		$I_{7x} = .511$	$I_{7y} = 2.028$	
$A_{8x} = 1.352$	$A_{8y} = .972$	$A_{8z} = .988$	$I_{8x} = .485$	$I_{8y} = 1.927$	$I_{8z} = .551$
			$I_{8'x} = .525$		
$A_{9x} = 1.352$	$A_{9y} = .933$	$A_{9z} = .993$	$I_{9x} = .531$	$I_{9y} = 1.927$	$I_{9z} = .551$
			$I_{9'x} = .531$		
$A_{10x} = 1.244$	$A_{10y} = .940$	$A_{10z} = .988$	$I_{10'x} = .516$	$I_{10y} = 2.028$	
	$A_{11y} = .695$	$A_{11z} = .306$	$I_{11x} = .458$		
			$I_{11'x} = .458$		
$A_{12x} = .301$		$A_{12z} = .181$			
$A_{13x} = .301$		$A_{13z} = .545$		$I_{13y} = .359$	
$A_{14x} = .301$		$A_{14z} = .633$			
$A_{15x} = .301$		$A_{15z} = .681$			
		$A_{16z} = .269$		$I_{16y} = .006$	
$A_{17x} = .094$		$A_{17z} = .210$		$I_{17y} = .004$	
		$A_{18z} = .210$			
$A_{19x} = .225$	$A_{19y} = .885$	$A_{19z} = .206$			
		$A_{20z} = .078$		$I_{20y} = .001$	
$A_{21x} = .654$	$A_{21y} = .332$	$A_{21z} = .279$		$I_{21y} = .006$	
$A_{22x} = .482$	$A_{22y} = .995$	$A_{22z} = .577$	$I_{22x} = .204$	$I_{22y} = .210$	
$A_{23x} = .482$	$A_{23y} = .887$				

TABLE 2

(continued)

Effective Cross Sectional Area

$A_{24x} = .662$ $A_{24y} = .951$ $A_{24z} = .338$

$A_{25y} = .377$ $A_{25z} = .369$

$A_{26x} = .407$ $A_{26y} = .345$ $A_{26z} = .345$

$A_{27y} = .849$ $A_{27z} = .345$

$A_{28x} = .160$ $A_{28z} = .206$

$A_{29x} = .110$ $A_{29z} = .144$

$A_{30x} = .110$ $A_{30z} = .184$

$A_{31x} = .110$ $A_{31z} = .160$

$A_{32x} = .160$ $A_{32y} = .160$ $A_{32z} = .361$

$A_{33y} = .160$ $A_{33z} = .713$

$A_{34x} = .234$ $A_{34z} = .338$

$A_{35x} = .319$ $A_{35y} = .940$ $A_{35z} = .439$

$A_{36x} = .319$ $A_{36y} = .994$ $A_{36z} = .455$

$A_{37x} = .234$ $A_{37y} = .940$ $A_{37z} = .415$

$A_{38z} = .345$

$A_{39x} = .238$ $A_{39y} = .235$

$A_{40x} = .238$ $A_{40y} = .144$

$A_{41x} = .238$ $A_{41y} = .184$

$A_{42x} = .238$ $A_{42y} = .160$

$A_{43x} = .238$ $A_{43y} = .385$

$A_{44y} = .558$ $A_{44z} = .497$

$A_{45x} = .343$ $A_{45z} = .338$

$A_{46x} = .195$ $A_{46z} = .291$

$A_{47x} = .195$ $A_{47z} = .159$

$A_{48x} = .343$ $A_{48z} = .267$

$A_{49z} = .345$

$A_{50x} = .163$ $A_{50y} = .163$ $A_{50z} = .489$

Second Moments of Area

$I_{25y} = .006$ $I_{25z} = .006$

$I_{26y} = .006$ $I_{26z} = .006$

$I_{29y} = .001$

$I_{30y} = .001$

$I_{32y} = .006$

$I_{62-35x} = .485$ $I_{35y} = .007$

$I_{36y} = .007$

$I_{44x} = .163$ $I_{44y} = .146$

$I_{50x} = .007$ $I_{50y} = .006$

TABLE 2

(continued)

Effective Cross Sectional Area		Second Moments of Area	
$A_{51x} = .300$		$A_{51z} = .543$	
$A_{52x} = .163$		$A_{52z} = .352$	
$A_{53x} = .163$		$A_{53z} = .455$	
$A_{54x} = .300$		$A_{54z} = .328$	
	$A_{55y} = .240$	$A_{55z} = .345$	
$A_{56x} = .192$	$A_{56y} = .409$		
$A_{57x} = .192$	$A_{57y} = .543$		
$A_{58x} = .192$	$A_{58y} = .352$		
$A_{59x} = .192$	$A_{59y} = .455$		
$A_{60x} = .192$	$A_{60y} = .328$		
	$A_{61y} = .210$		
$A_{62x} = .364$			
$A_{63x} = .364$			
$A_{65x} = .361$	$A_{65y} = .204$		
$A_{66x} = .361$	$A_{66y} = .204$		
$A_{67x} = .361$			
$A_{68x} = .361$			
	$A_{69y} = .478$		
$A_{70x} = .463$	$A_{70y} = .409$		
$A_{71x} = .463$	$A_{71y} = .543$		
$A_{72x} = .463$	$A_{72y} = .352$		
$A_{73x} = .463$	$A_{73y} = .455$		
$A_{74x} = .463$	$A_{74y} = .328$		
	$A_{75y} = .265$		
	$A_{76y} = .163$	$A_{76z} = .546$	

TABLE 3

```
D
N
LAND ROVER SYM PART  1

T63.6
1045 --00
0

J64.0

(0)→1                                          zero
(1)x(2,25x111)→2
(0,33x17)→794                                  b1aI
(794,33x24)*→2
(0,66/)→2708                                   fa diagonals
(2708,33/)+(1586,33x33)→1586
(2741,33/)+(1587,33x33)→1587
(2741,33/)+(1619,33x33)→1619
(2,24x33)x(1586,33x33)→2675
(2675,24x33)x(794,33x24)→3467
(0,33x22)→794                                  boa
(2675,24x33)x(794,33x22)→4043
(4043,24x22)∪→1                                                DOIa binary
(0,33x24)→794                                  b1bI
(794,33x24)*→2
(1)x(1586,20x60)→1586
(0,47/)→2708                                   fb diagonals
(2708,33/)+(1586,33x33)→1586
(2741,33/)+(1587,33x33)→1587
(2741,33/)+(1619,33x33)→1619
(2,24x33)x(1586,33x33)→2675
(2675,24x33)x(794,33x24)→4043
(3467,24x24)+(4043,24x24)→3467
(0,33x24)→794                                  b1cI
(794,33x24)*→2
(1)x(1586,20x60)→1586
(0,66/)→2708                                   fc diagonals
(2708,33/)+(1586,33x33)→1586
(2741,33/)+(1587,33x33)→1587
(2741,33/)+(1619,33x33)→1619

(2,24x33)x(1586,33x33)→2675
(2675,24x33)x(794,33x24)→4043
(3467,24x24)+(4043,24x24)→3467
(0,25x33)∪→2                                   b*1cII binary
(2,25x33)x(1586,33x33)→4043
(2,25x33)*→1586
(4043,25x33)x(1586,33x25)→4868
(2675,24x33)x(1586,33x25)→5493
(0,33x24)→794                                  b1dI
(794,33x24)*→2
```

Table 3 (contd)

	Input	Output
(1)x(1586,20x60)→1586		
(0,66/)→2708	f_d diagonals	
(2708,33/)+(1586,33x33)→1586		
(2741,33/)+(1587,33x33)→1587		
(2741,33/)+(1619,33x33)→1619		
(2,24x33)x(1586,33x33)→2675		
(2675,24x33)x(794,33x24)→4043		
(3467,24x24)+(4043,24x24)→3467		
(0,25x33)∪→2	b^t_{ldII} binary	
(2,25x33)x(1586,33x33)→4043		
(2,25x33)*→1586		
(4043,25x33)x(1586,33x25)→2		
(4868,25x25)+(2,25x25)→4868		
(2675,24x33)x(1586,33x25)→630		
(630,24x25)+(5493,24x25)→5493		
(1)x(2,25x111)→2		
(0,33x9)→1289	b_{leI}	
(794,33x24)*→2		
(0,66/)→2708	f_e diagonals	
(2708,33/)+(1586,33x33)→1586		
(2741,33/)+(1587,33x33)→1587		
(2741,33/)+(1619,33x33)→1619		
(2,24x33)x(1586,33x33)→2675		
(2675,24x33)x(794,33x24)→4043		
(3467,24x24)+(4043,24x24)→3467		
(3467.24x24)→0		D_I
(0,25x33)∪→2	b^t_{leII} binary	
(2,25x33)x(1586.33x33)→4043		
(2,25x33)*→1586		
(4043,25x33)x(1586,33x25)→2		
(2,25x25)+(4868,25x25)→4868		
(2675,24x33)x(1586,33x25)→630		
(630,24x25)+(5493,24x25)→5493		D^t_{II} binary
(5493,24x25)∪→1		
(0,25x33)∪→2	b^t_{lfII} binary	
(1)x(1586,20x60)→1586		
(0,66/)→2708	f_f diagonals	
(2708,33/)+(1586,33x33)→1586		
(2741,33/)+(1587,33x33)→1587		
(2741,33/)+(1619,33x33)→1619		
(2,25x33)x(1586,33x33)→4043		
(2,25x33)*→1586		
(4043,25x33)x(1586,33x25)→2		
(2,25x25)+(4868,25x25)→4868		
(0,25x33)∪→2	b^t_{lgII} binary	
(1)x(1586,20x60)→1586		
(0,56/)→2708	f_g diagonals	

Table 3 (contd)

Input	Output
(2708,33/)+(1586,33x33)→1586	
(2741,33/)+(1587,33x33)→1587	
(2741,33/)+(1619,33x33)→1619	
(2,25x33)x(1586,33x33)→4043	
(2,25x33)*→1586	
(4043,25x33)x(1586,33x25)→2	
(2,25x25)+(4868,25x25)→4868	
(4858,25x25)→0	D_{II}
*	
S	

Table 3 (contd)

```
D

N
LAND ROVER SYM PART 2

J64.0
```

	Input	Output
(0)→1	+0	
(0,24x25)∪→2	D^{t}_{III} binary	
(2,24x25)*→602		
(0,25x25)→1202	D_{II}	
(1202,25x25),(602,25x24)→1827		
(2,24x25)x(1827,25x24)→2427		
(0,24x24)→2	D_{I}	
(2,24x24)-(2427,24x24)→3003		
(0,24x22)∪→1202	D_{OI}	
(3003,24x24),(1202,24x22)→2427		
(1827,25x24)x(2427,24x22)→602		
(0,33x22)→1152	b_{oa}	
(1)x(2955,33x24)→2955		
(0,33x17)→2955	b_{1aI}	
(2955,33x24)x(2427,24x22)→3747		
(1152,33x22)*→4473		
(1152,33x22)-(3747,33x22)→1152		
(0,22x6)→2	R	
(1152,33x22)x(2,22x6)→1878		
(1878,33x6)(5)→0		S_a
(1)x(2955,30x40)→2955		
(0,66/)→4077	f_a diagonals	
(4077,33/)+(2955,33x33)→2955		
(4110,33/)+(2956.33x33)→2956		
(4110,33/)+(2988,33x33)→2988		
(4473,22x33)x(2955,33x33)→5199		
(5199,22x33)x(1878,33x6)→2955		
(2955,22x6)(5)→0		r
(0,33x24)→2955	b_{1bI}	
(0)→134	1	
(2955,33x24)x(2427,24x22)→3747		
(134)x(3747,33x22)→1152		
(1152,33x22)x(2,22x6)→1878		
(1878,33x6)(5)→0		S_b
(0,33x24)→2955	b_{1cI}	
(2955,33x24)x(2427,24x22)→3747		
(0,25x33)∪→4473	b^{t}_{1cII} binary	
(4473,25x33)*→5298		
(5298,33x25)x(602,25x22)→4473		

Table 3 (contd)

	Input	Output
(4473,33x22)-(3747,33x22)→1152		
(1152,33x22)x(2,22x6)→1878		
(1878,33x6)(5)→0		S_c
(0,33x24)→2955	b_{1dI}	
(2955,33x24)x(2427,24x22)→3747		
(0,25x33)∪→4473	b^t_{1dII} binary	
(4473,25x33)*→5298		
(5298,33x25)x(602,25x22)→4473		
(4473,33x22)-(3747,33x22)→1152		
(1152,33x22)x(2,22x6)→1878		
(1878,33x6)(5)→0		S_d
(1)x(2955,33x24)→2955		
(0,33x9)→3450	b_{1eI}	
(2955,33x24)x(2427,24x22)→3747		
(0,25x33)∪→4473	b^t_{1eII} binary	
(4473,25x33)*→5298		
(5298,33x25)x(602,25x22)→4473		
(4473,33x22)-(3747,33x22)→1152		
(1152,33x22)x(2,22x6)→1878		
(1878,33x6)(5)→0		S_e
(0,25x33)∪→4473	b^t_{1fII} binary	
(4473,25x33)*→5298		
(5298,33x25)x(602,25x22)→4473		
(4473,33x22)x(2,22x6)→1878		
(1878,33x6)(5)→0		S_f
(0,25x33)∪→4473	b^t_{1gII} binary	
(4473,25x33)*→5298		
(5298,33x25)x(602,25x22)→4473		
(4473,33x22)x(2,22x6)→1878		
(1878,33x6)(5)→0		S_g

*

S

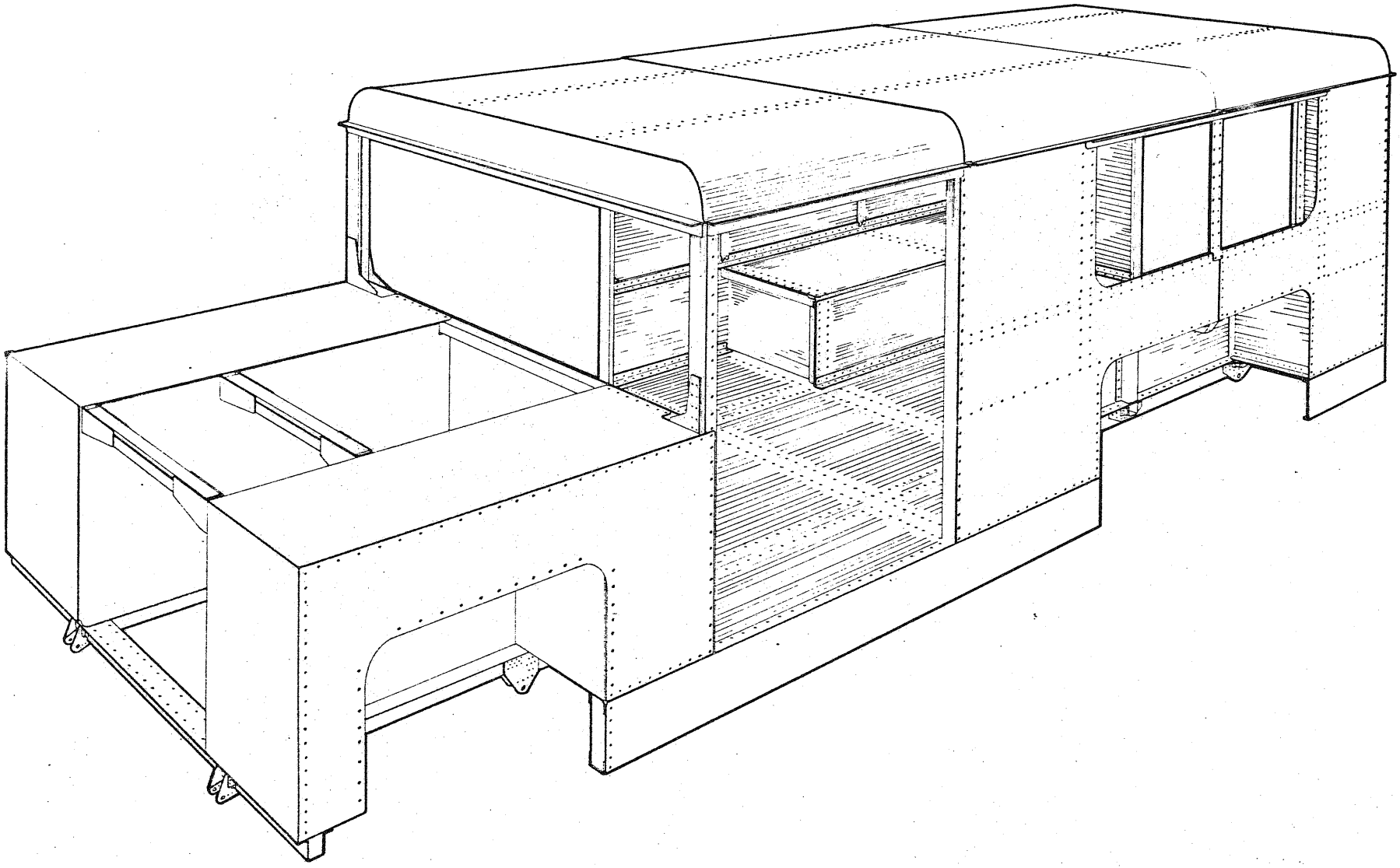

FIG. 1a

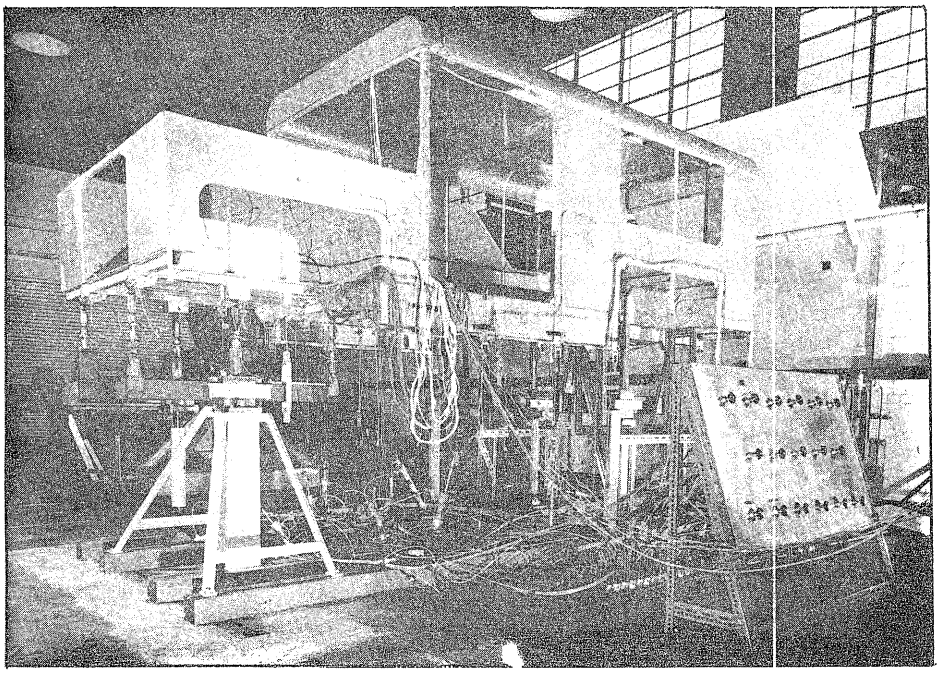

FIG. 1b

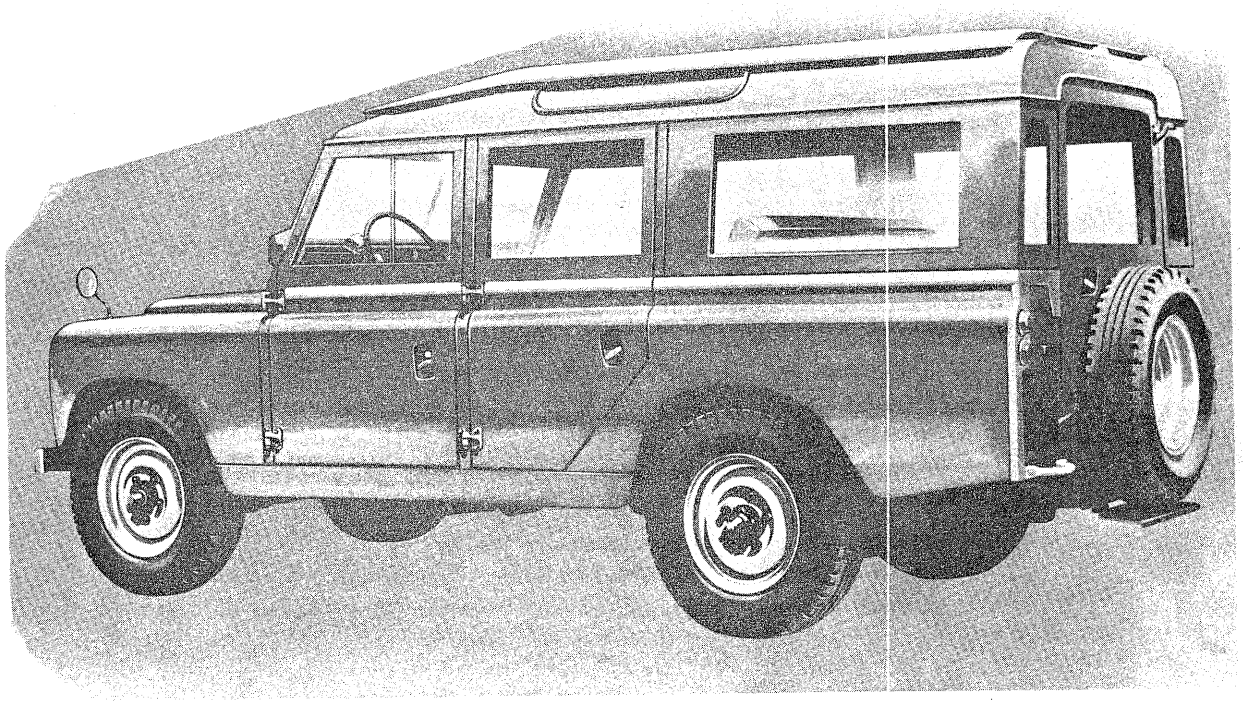

FIG. 2.

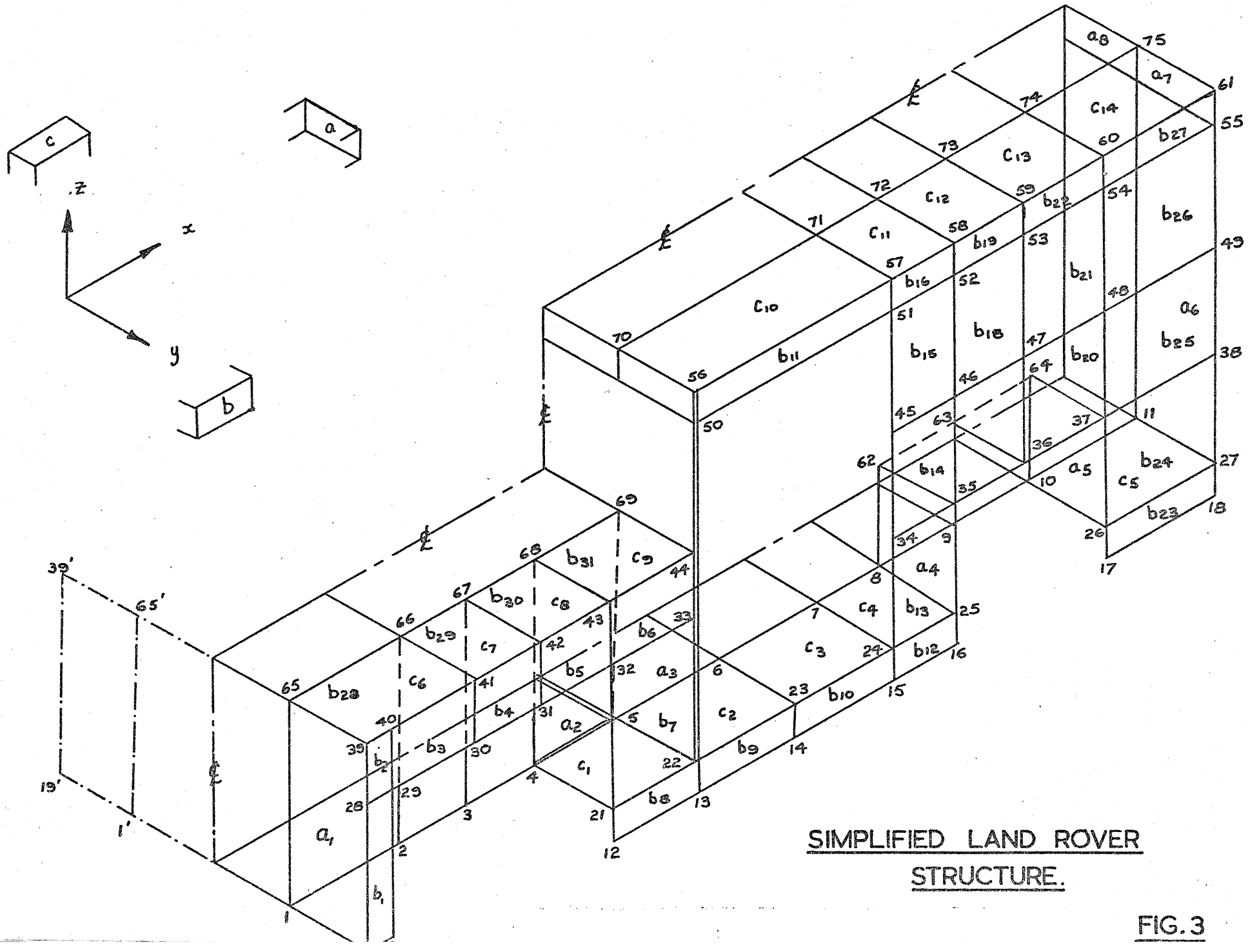

SIMPLIFIED LAND ROVER STRUCTURE.

FIG. 3

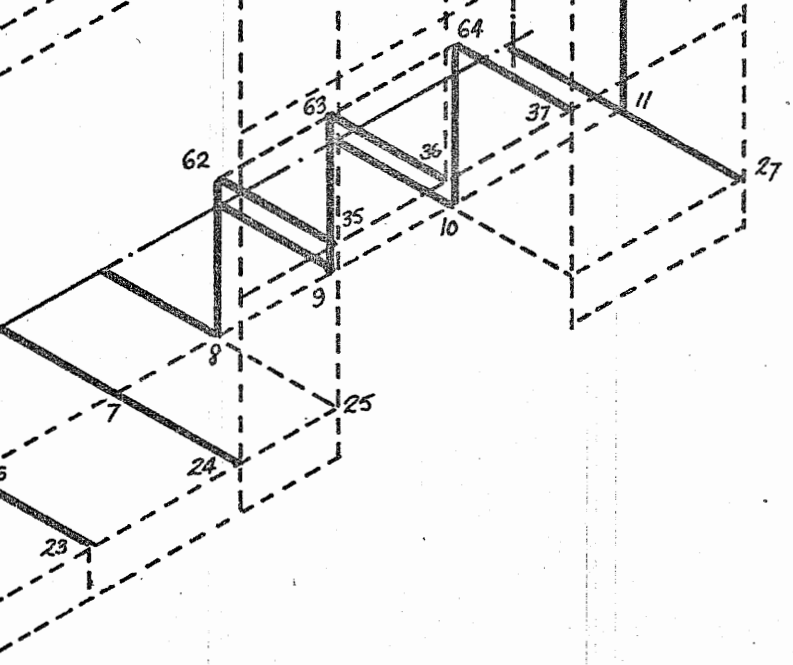

FIG. 4a.

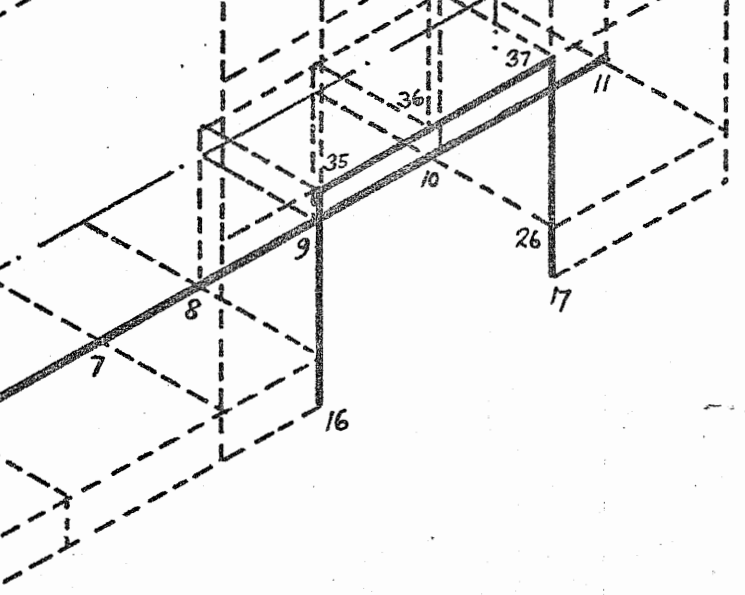

FIG. 4b.

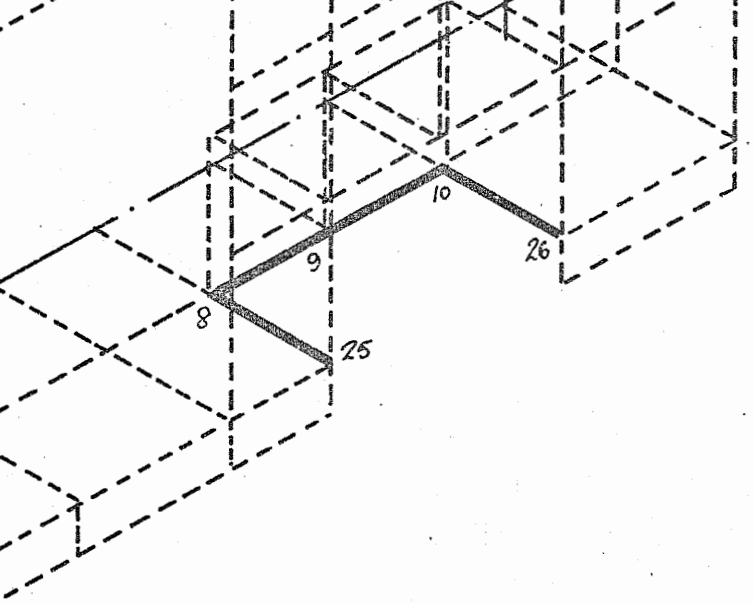

FIG. 4c

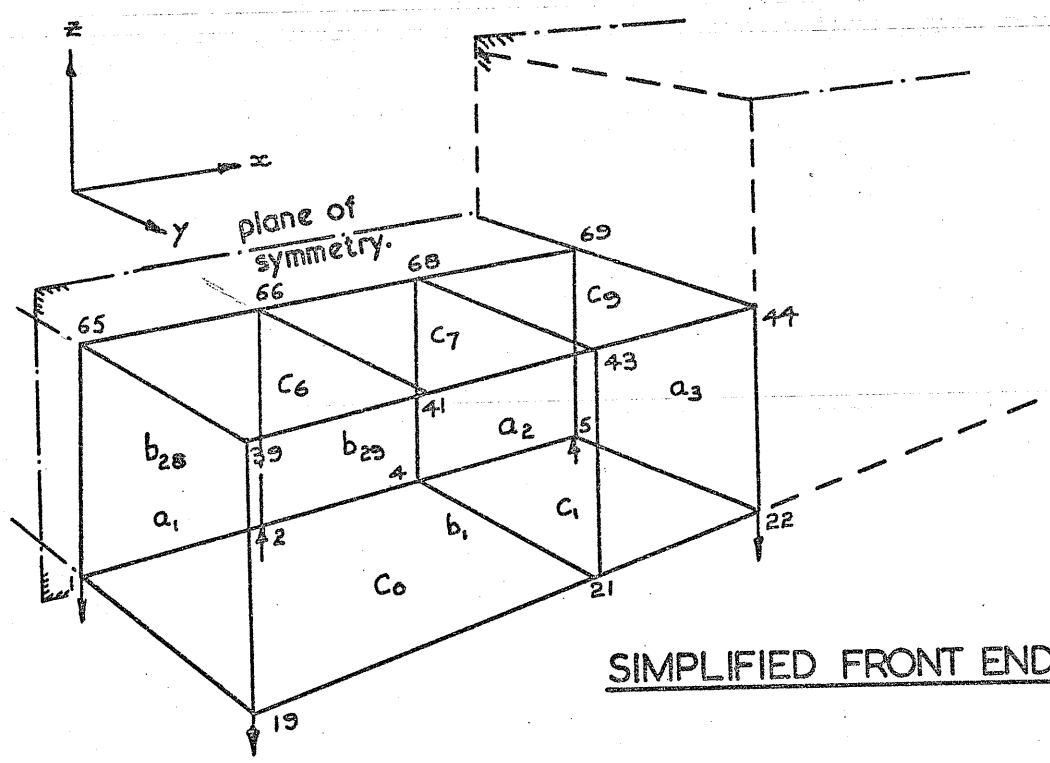

SIMPLIFIED FRONT END.

FIG. 5

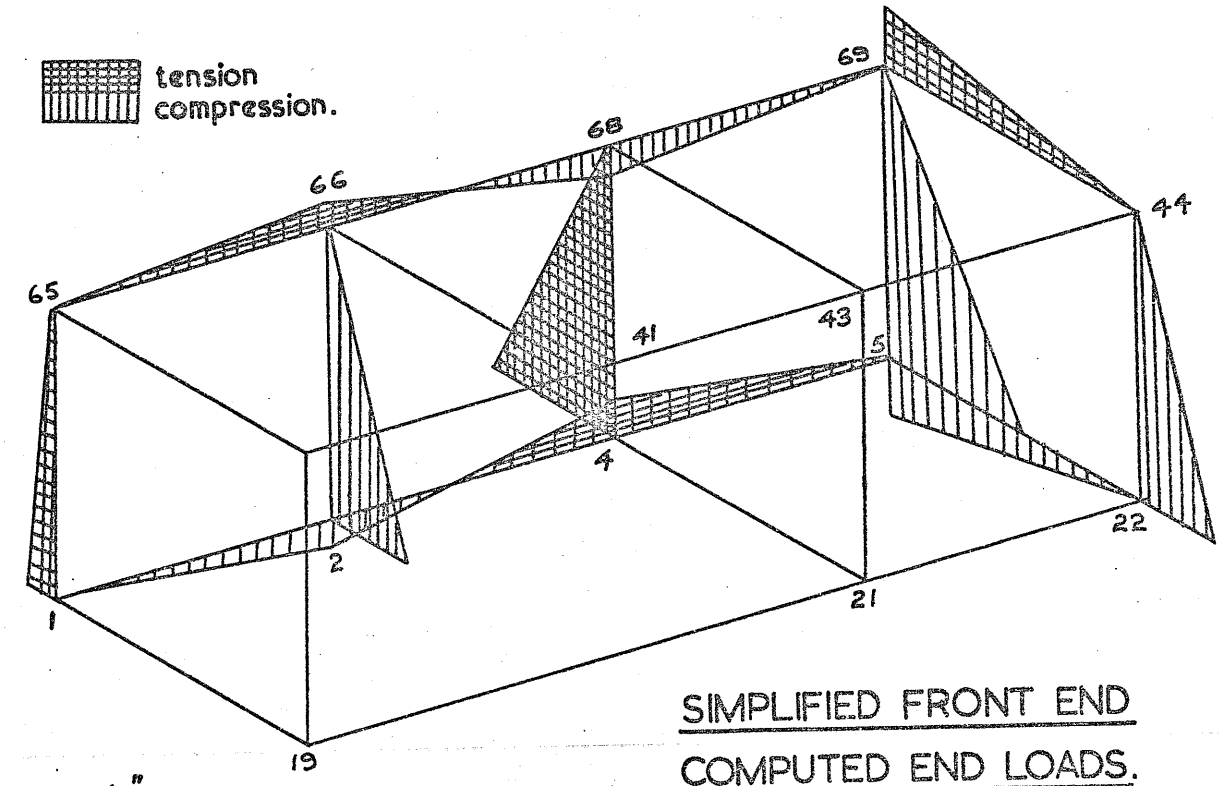

scale $\frac{1}{8}$" = 25 lb. app.

SIMPLIFIED FRONT END
COMPUTED END LOADS.

FIG. 6

BASIC SYSTEM

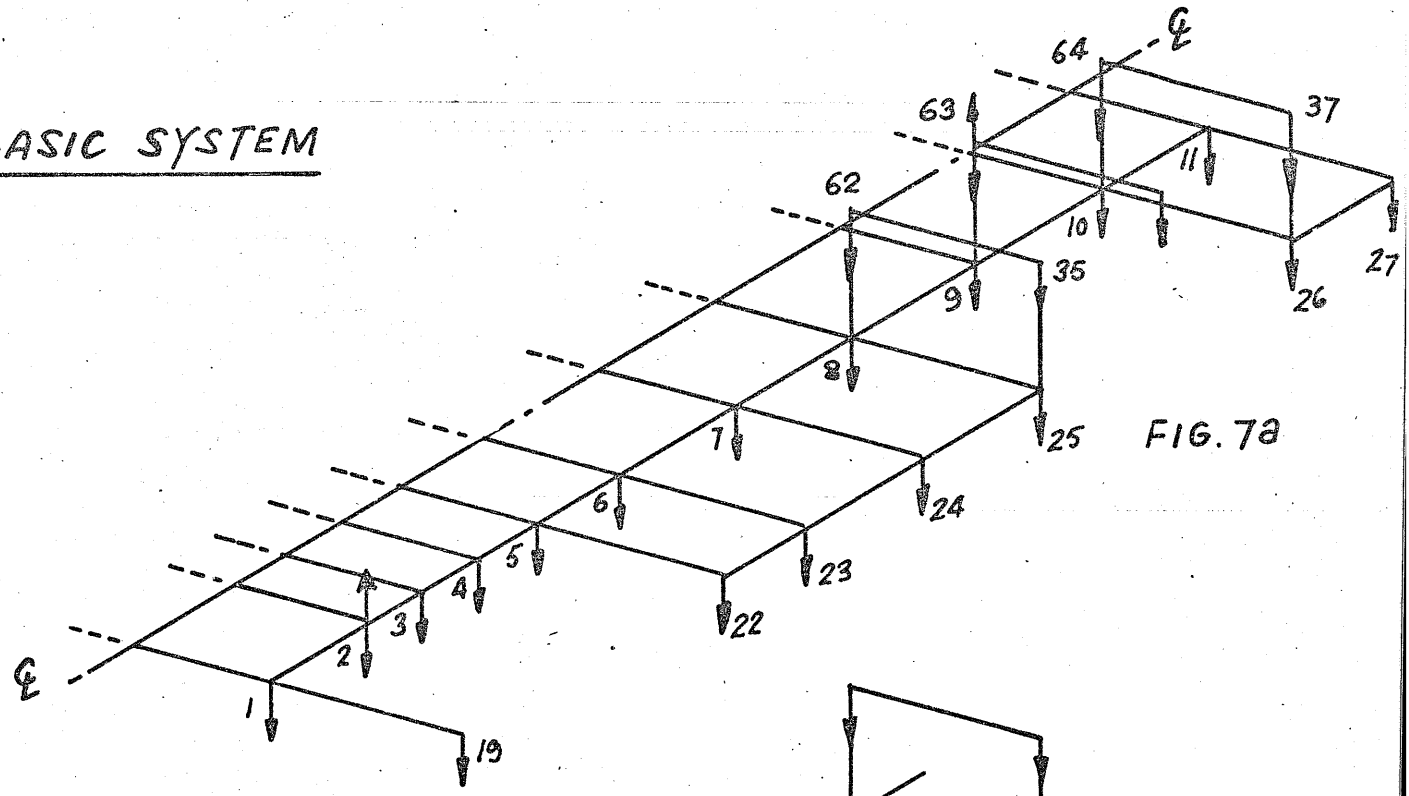

FIG. 7a

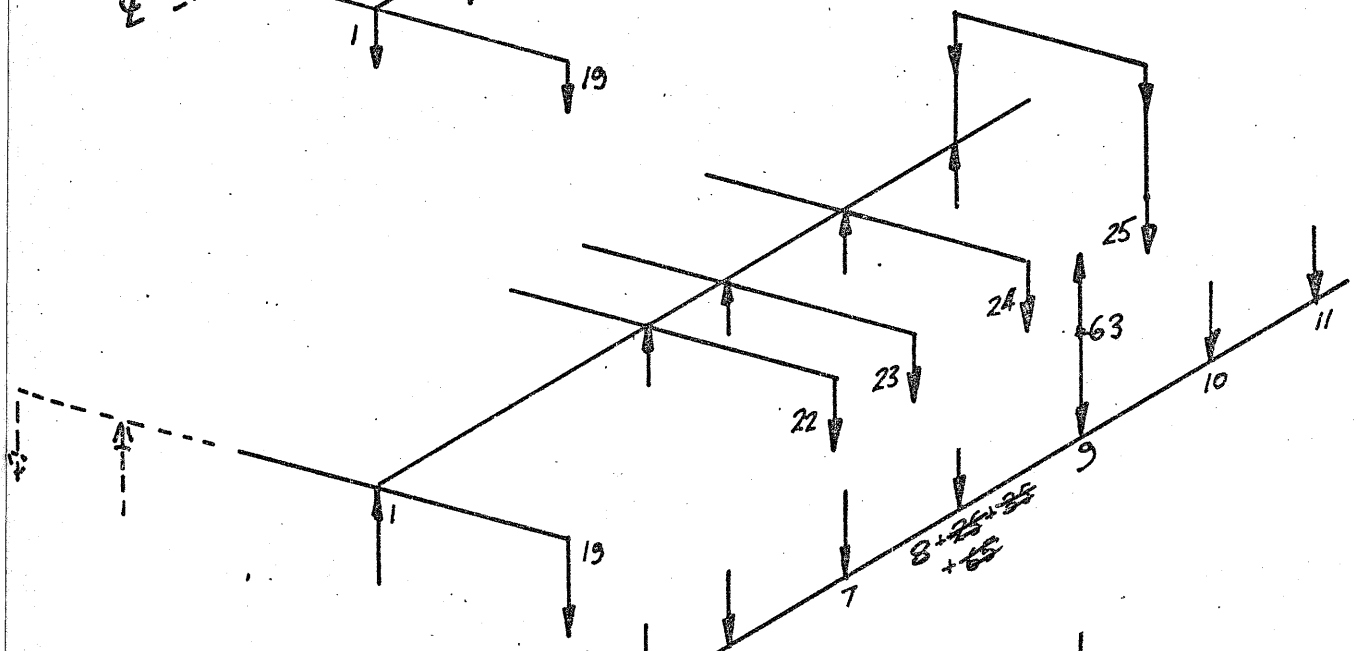

FIG. 7b

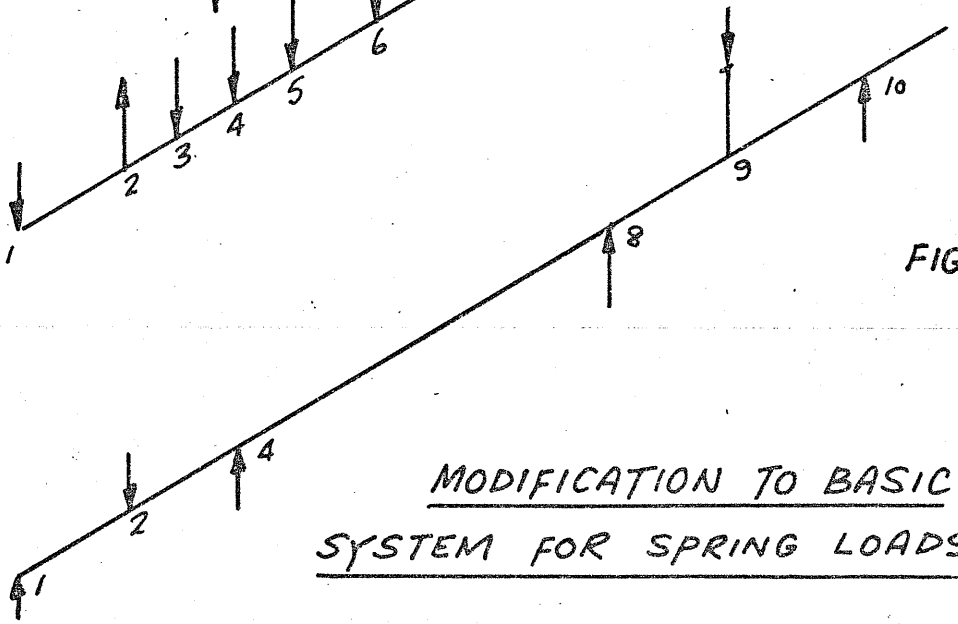

FIG. 7c

MODIFICATION TO BASIC SYSTEM FOR SPRING LOADS.

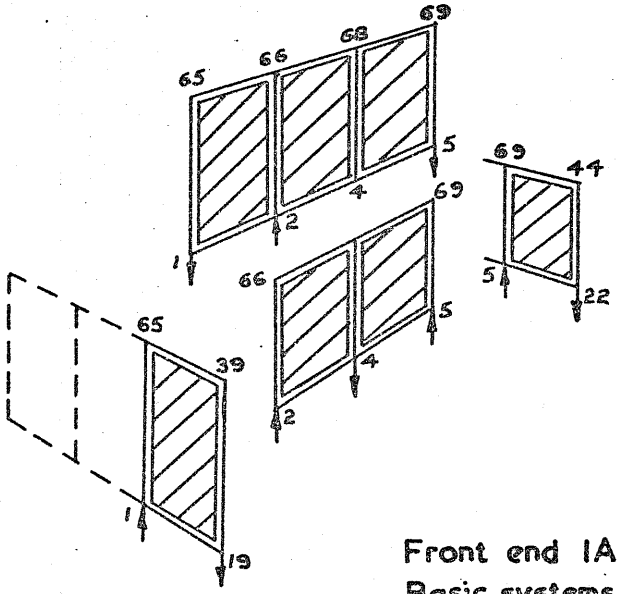

Front end 1A
Basic systems.

FIG. 8a.

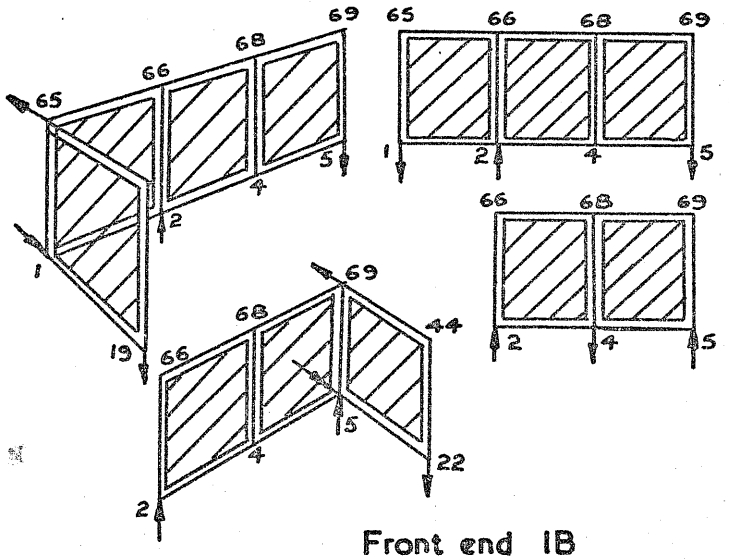

Front end 1B
Basic systems.

FIG. 8b.

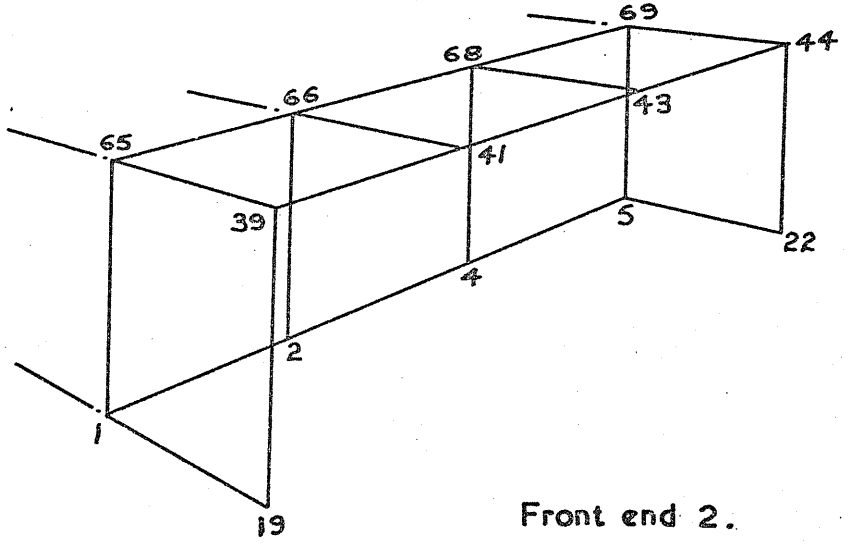

Front end 2.

FIG. 9.

Bonnet Top 1

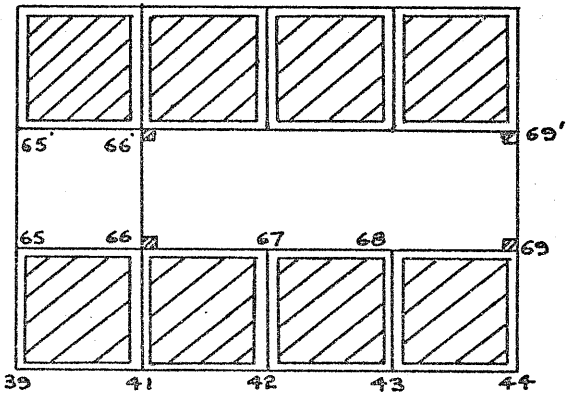

M=29 N=20 P=8

$n_s = 3(M-N+1)+P = 38$

$r = 2M - N - 4$ Bending Fixations = 34

$n = 4$

FIG10a

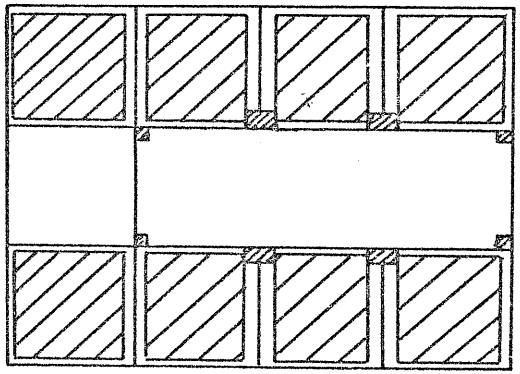

Bonnet Top 2

$n_s = 38$

$r = 30$

$n = 8$

FIG. 10b

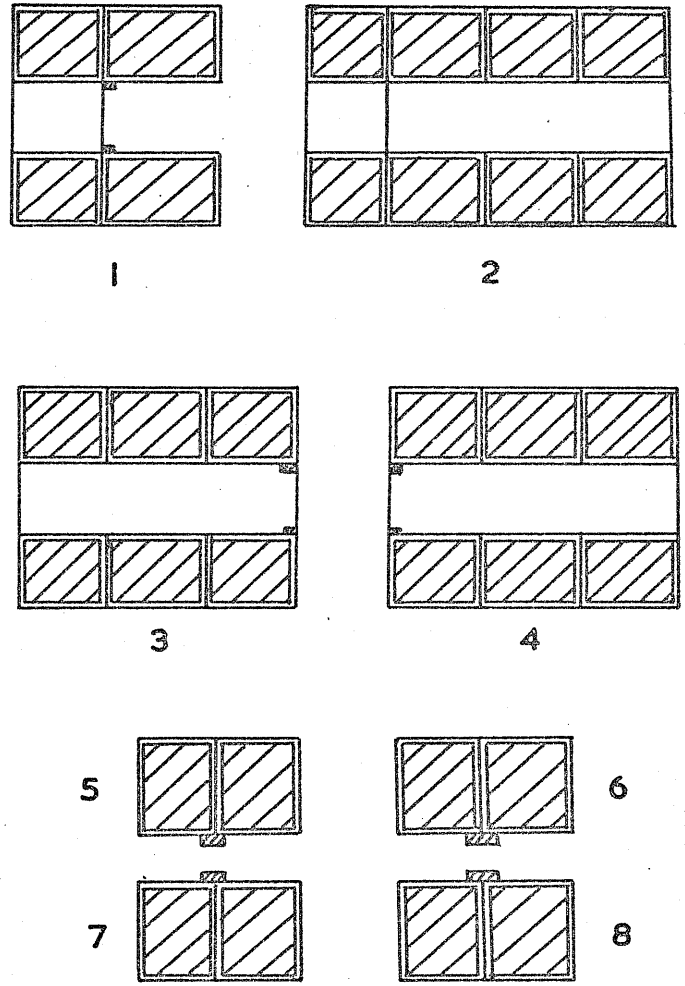

BONNET TOP REDUNDANT SYSTEMS.

FIG. 11

REAR WHEEL ARCH

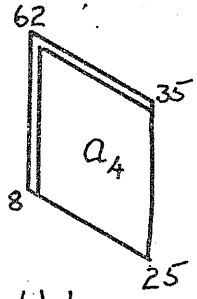

U1

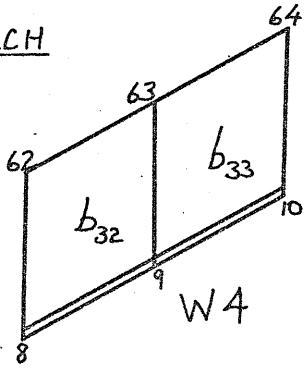

W4

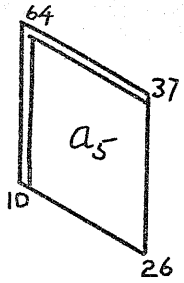

U2

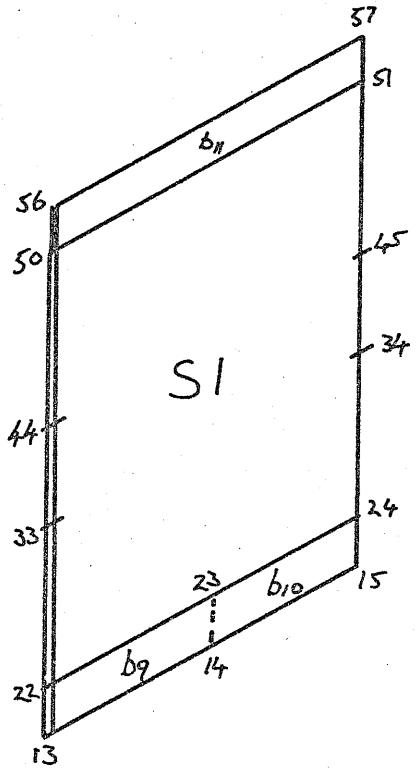

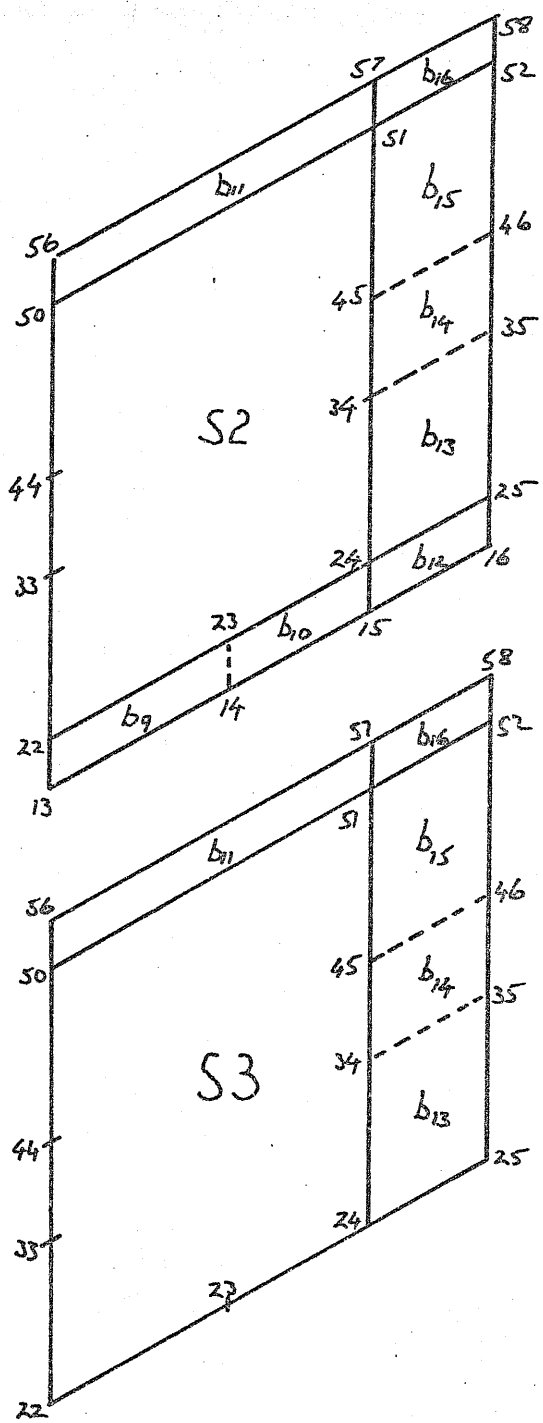

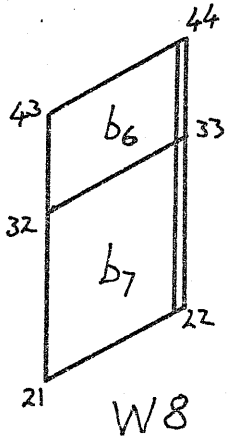

W8

W7

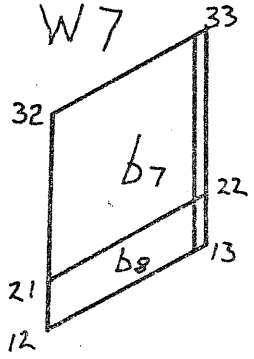

BODY SIDE REDUNDANCIES T

fig. 1

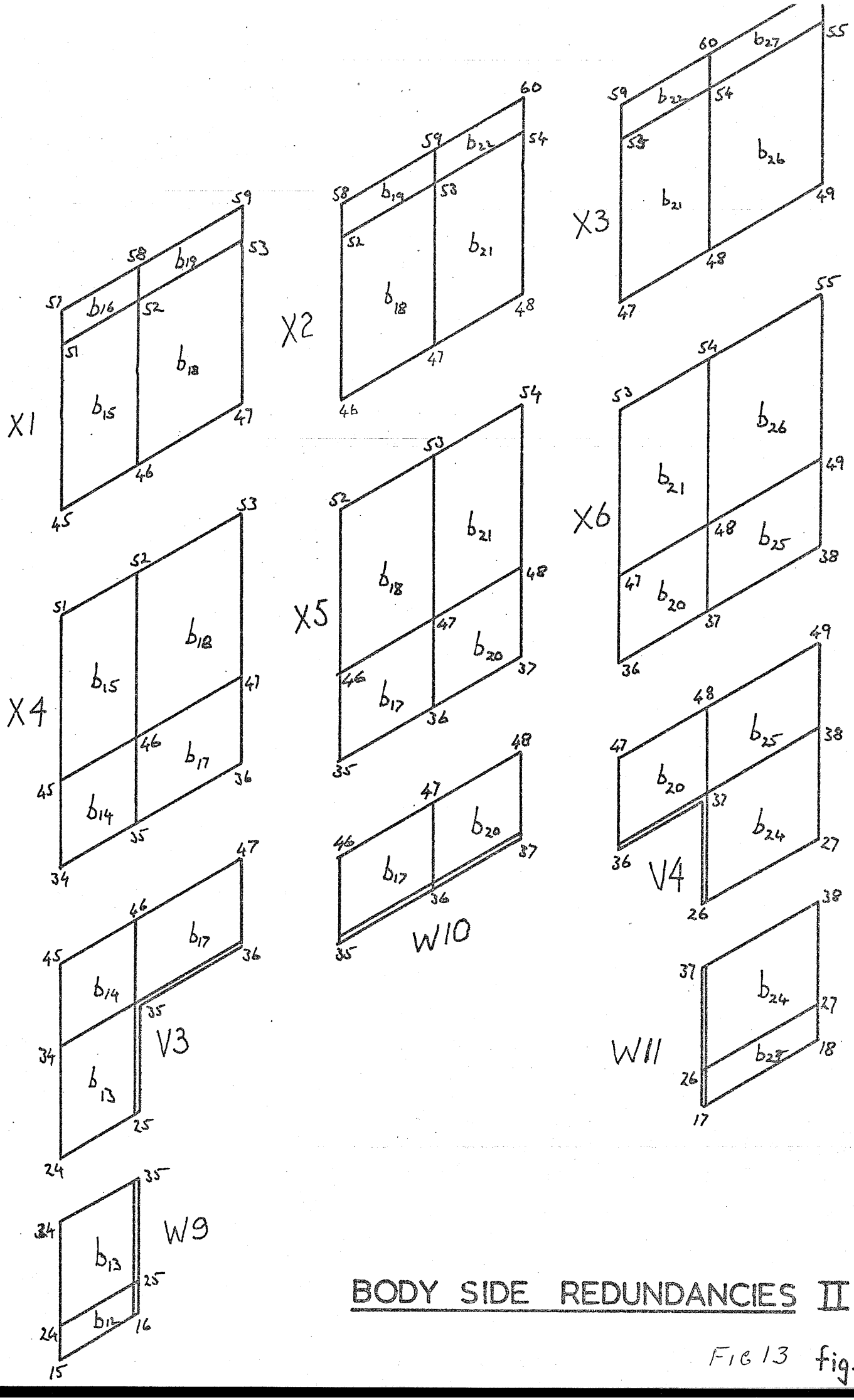

BODY SIDE REDUNDANCIES II

Fig 13 fig.

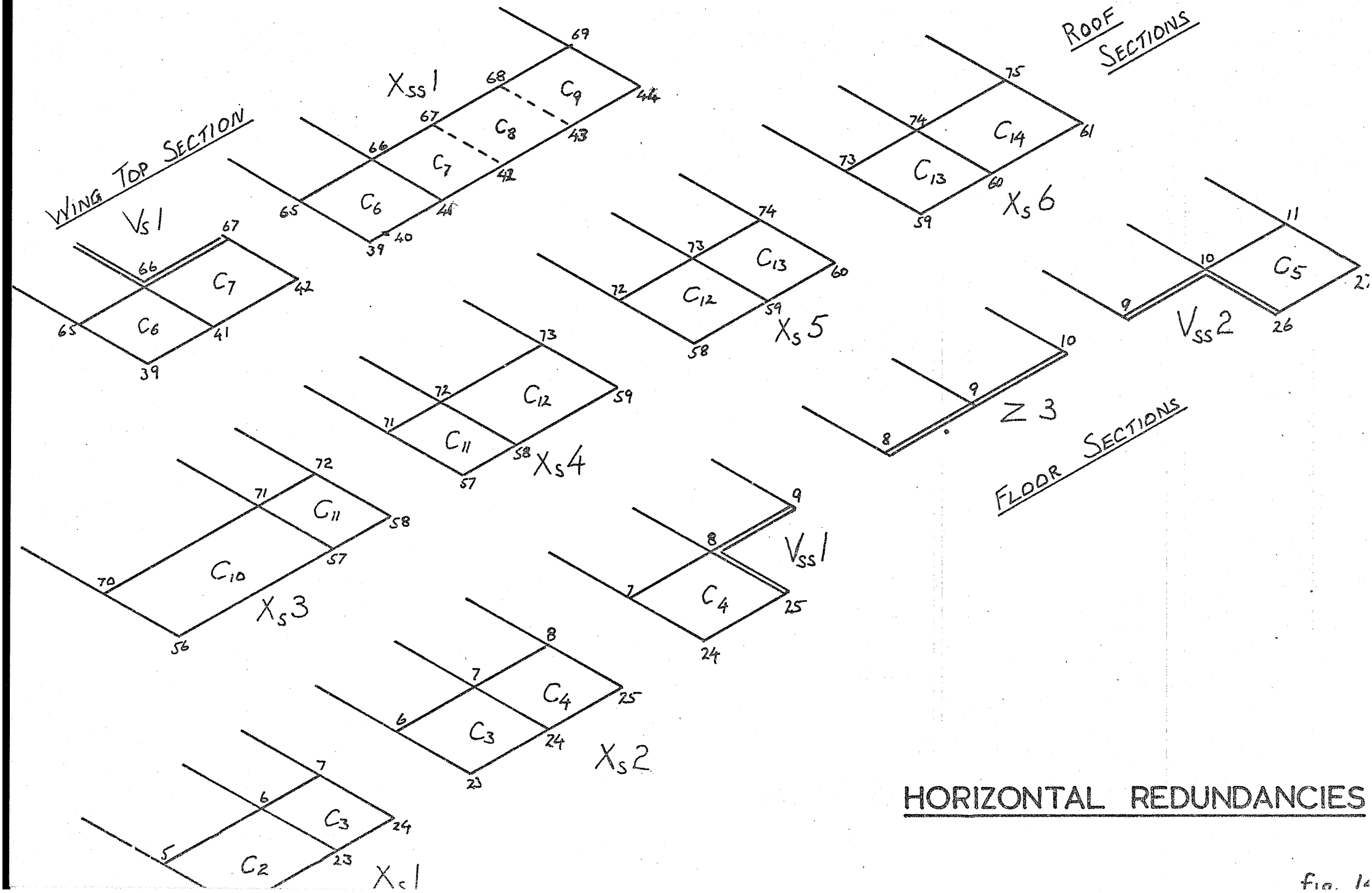

HORIZONTAL REDUNDANCIES

fig. 14

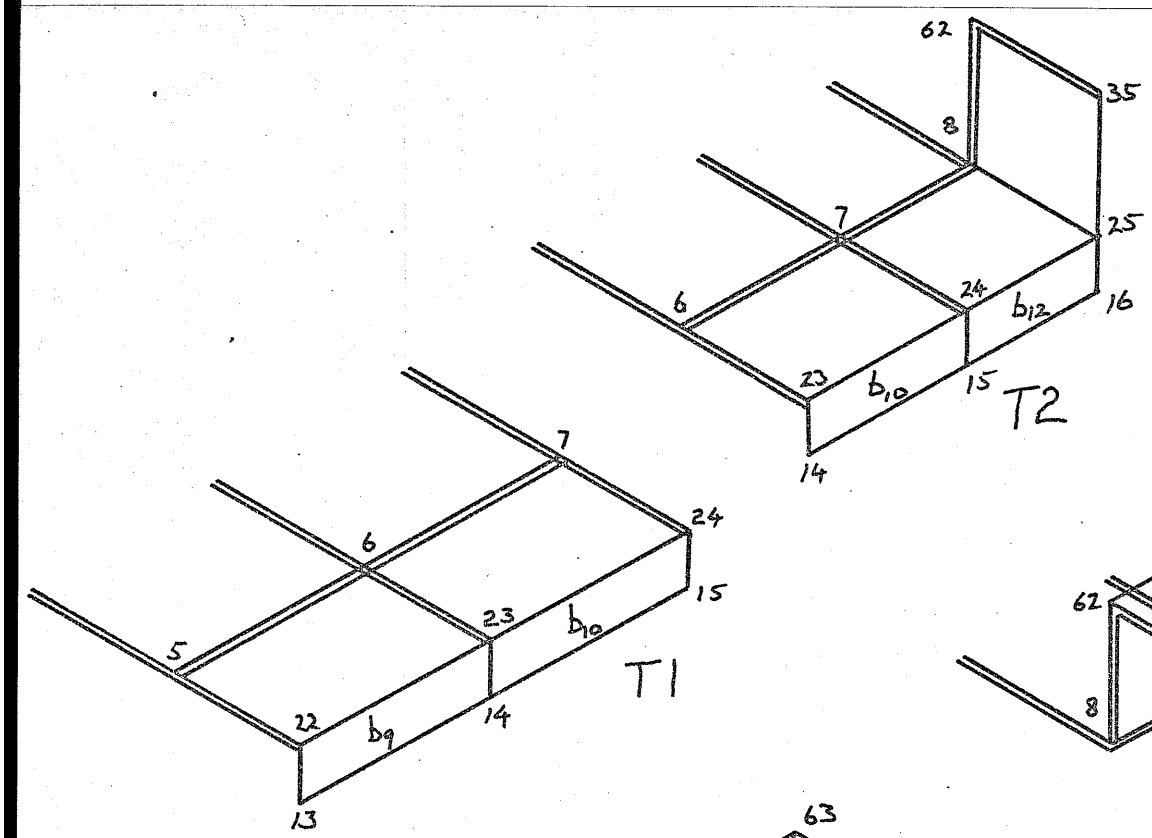

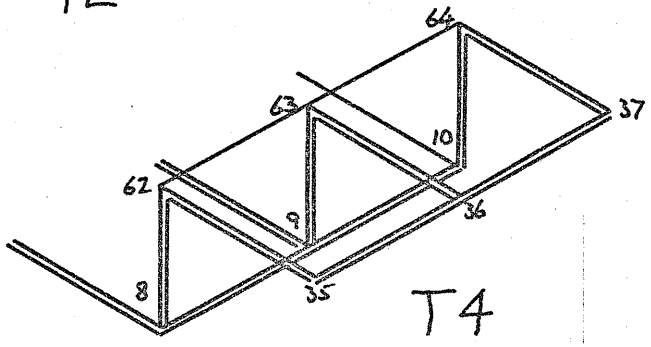

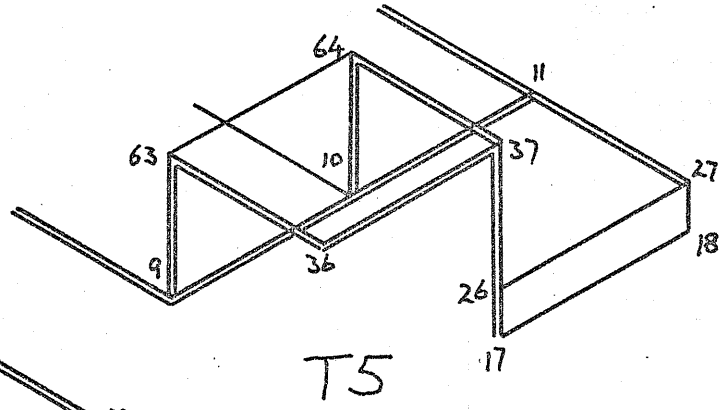

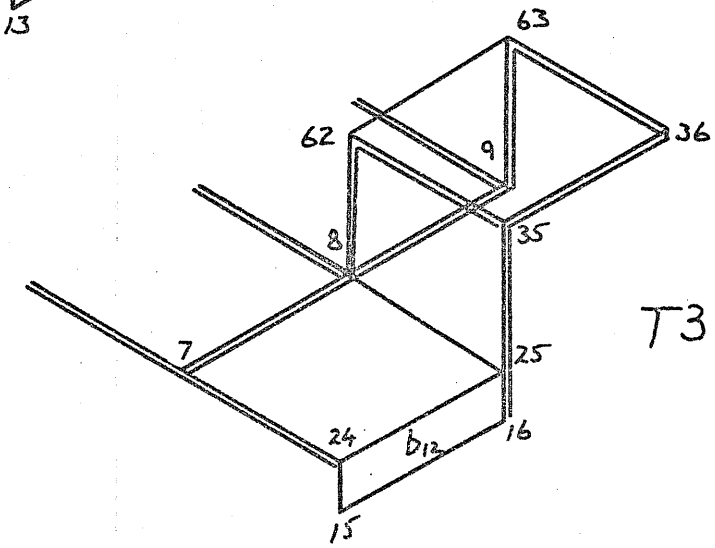

FLOOR BENDING REDUNDANCIES

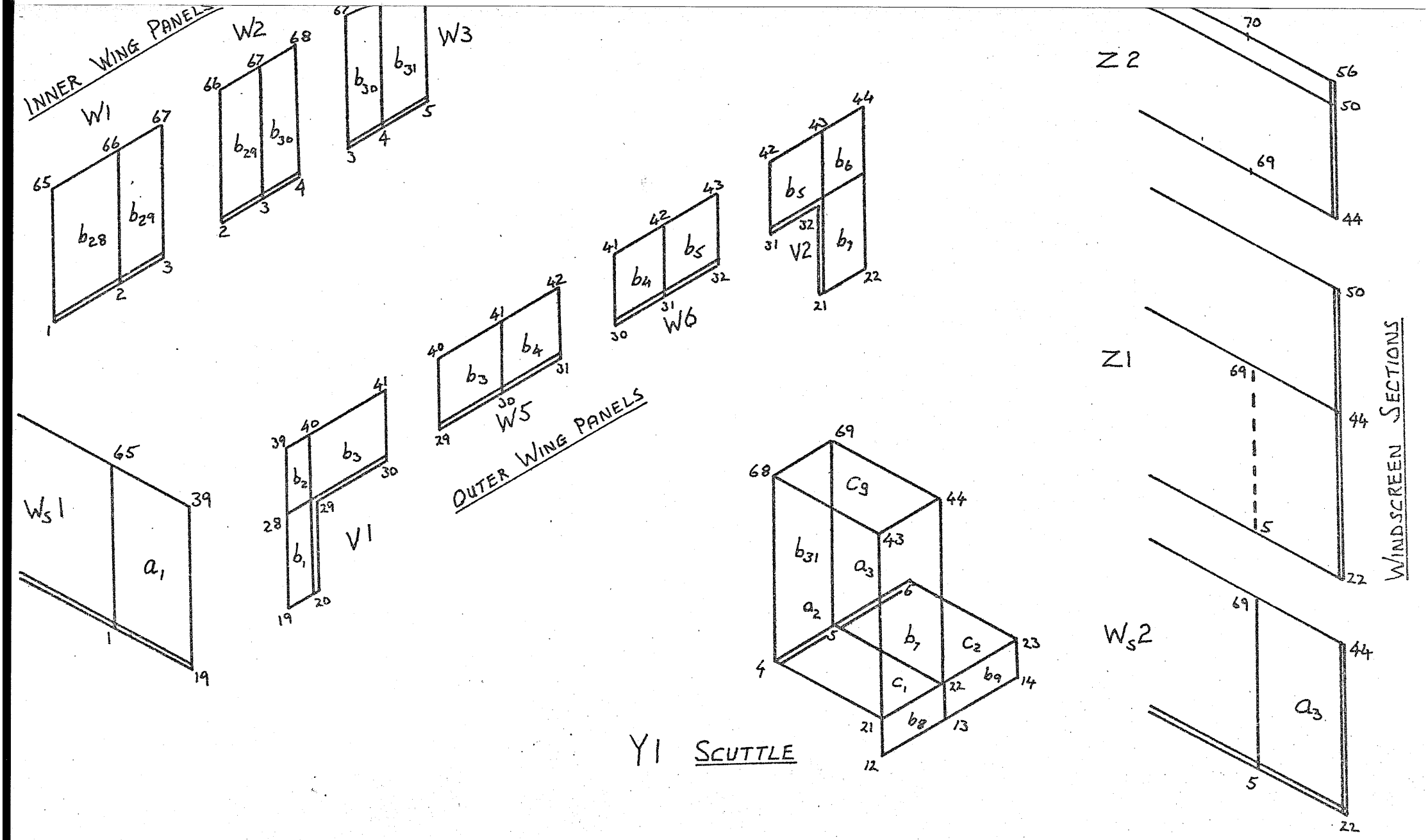

FRONT END REDUNDANCIES

fig 16

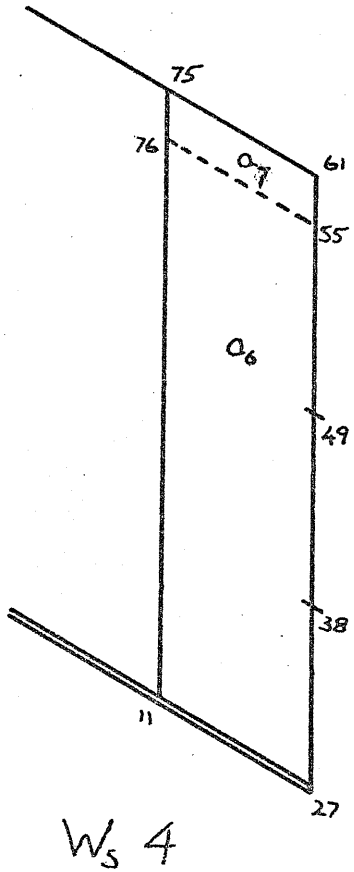

W_S 4

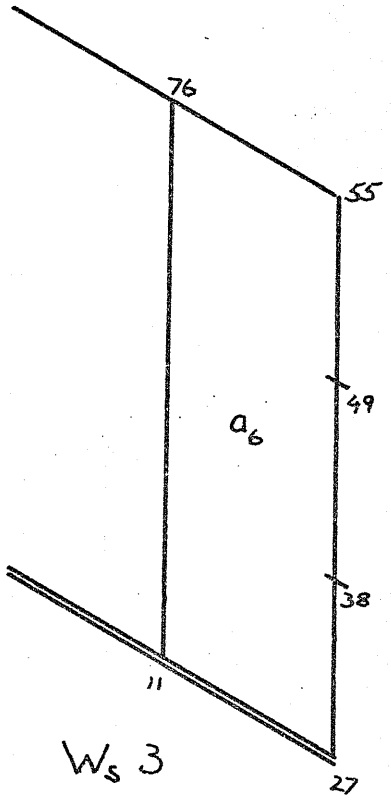

W_S 3

REAR END REDUNDANCIES

fig. 17

BODY SIDE STRUCTURE – IDEALISATION

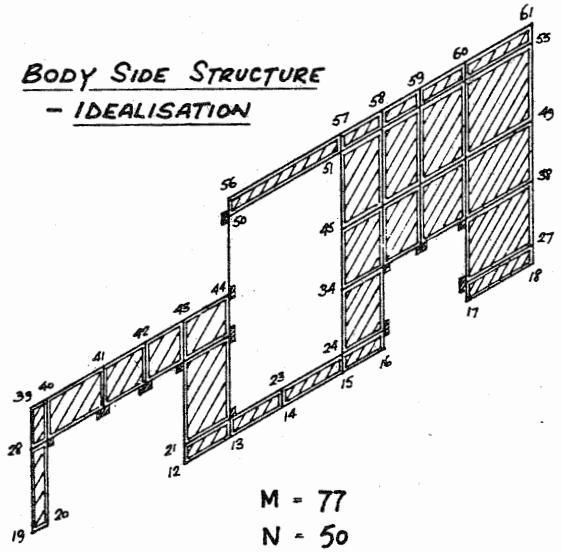

M = 77
N = 50
P = 27
n_s = 111
r = 91
n = 20

(Order of Redundancy)

ORDER of REDUNDANCY of TRANSVERSE PLANE STRUCTURES.

FRONT CROSS SECTION
M = 10
N = 8
P = 2
n_s = 11
r = 10
n = 1

SCUTTLE CROSS SECTION
M = 16
N = 12
P = 2
n_s = 17
r = 14
n = 1

REAR END CROSS SECTION
M = 17
N = 12
P = 4
n_s = 22
r = 20
n = 2

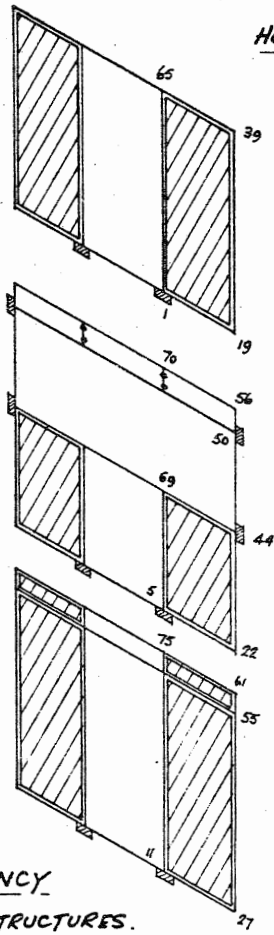

ORDER of REDUNDANCY of HORIZONTAL PLANE STRUCTURES

M = 38
N = 24
P = 15
n_s = 60
r = 52
n = 8

FOR SYMMETRICAL LOADS - Order of Redundancy = 4

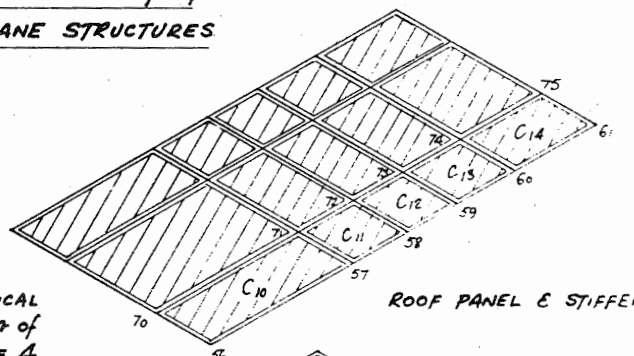

ROOF PANEL & STIFFENERS

M = 29
N = 20
P = 8
n_s = 38
r = 38
n = 0

(SYMMETRICAL LOADS ONLY)

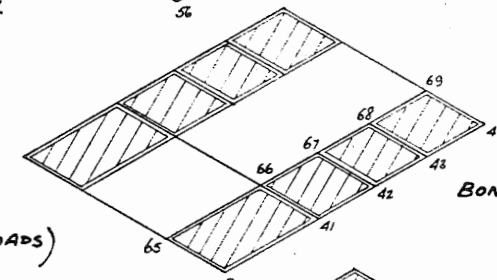

BONNET TOP

M = 45
N = 30
P = 16
n_s = 64
r = 52
n = 12

FOR SYMMETRICAL LOADS - Order of Redundancy = 6

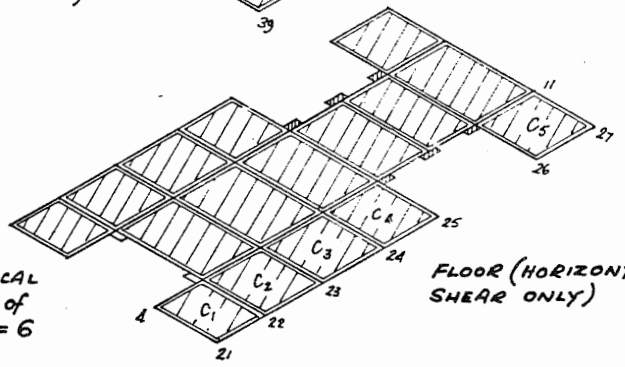

FLOOR (HORIZONTAL SHEAR ONLY)

FIG. 18.

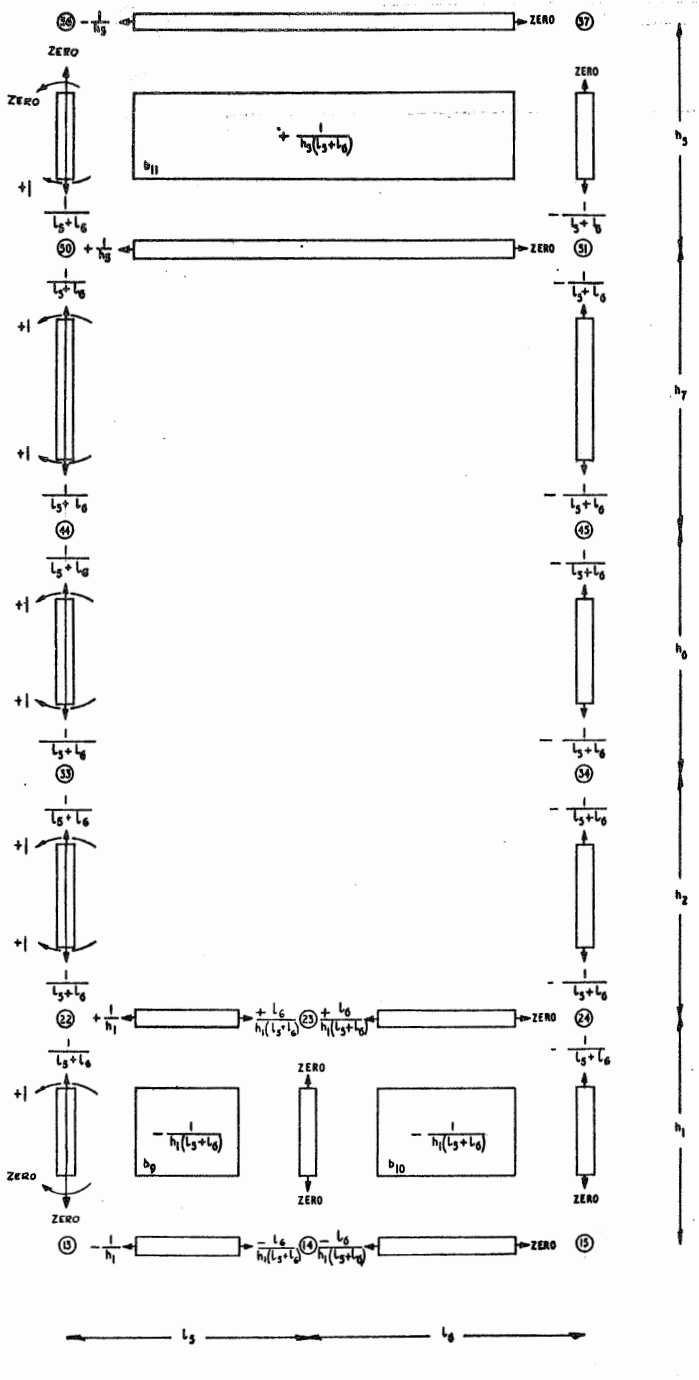

REDUNDANCY S.I.

fig. 18a

KEY TO FIGURES *18a-o*

MEMBERS WITH LINEARLY VARYING END-LOADS ONLY

MEMBERS WITH LINEARLY VARYING BENDING MOMENTS ONLY

MEMBERS ACTING AS TWO ELEMENTS CARRYING LINEARLY VARYING END-LOADS AND BENDING MOMENTS

ARROWS ALWAYS SHOW +VE DIRECTION OF FORCE (OR MOMENT) SIGNS INDICATE ACTUAL DIRECTION OF FORCE (OR MOMENT)

SEE APPENDIX II

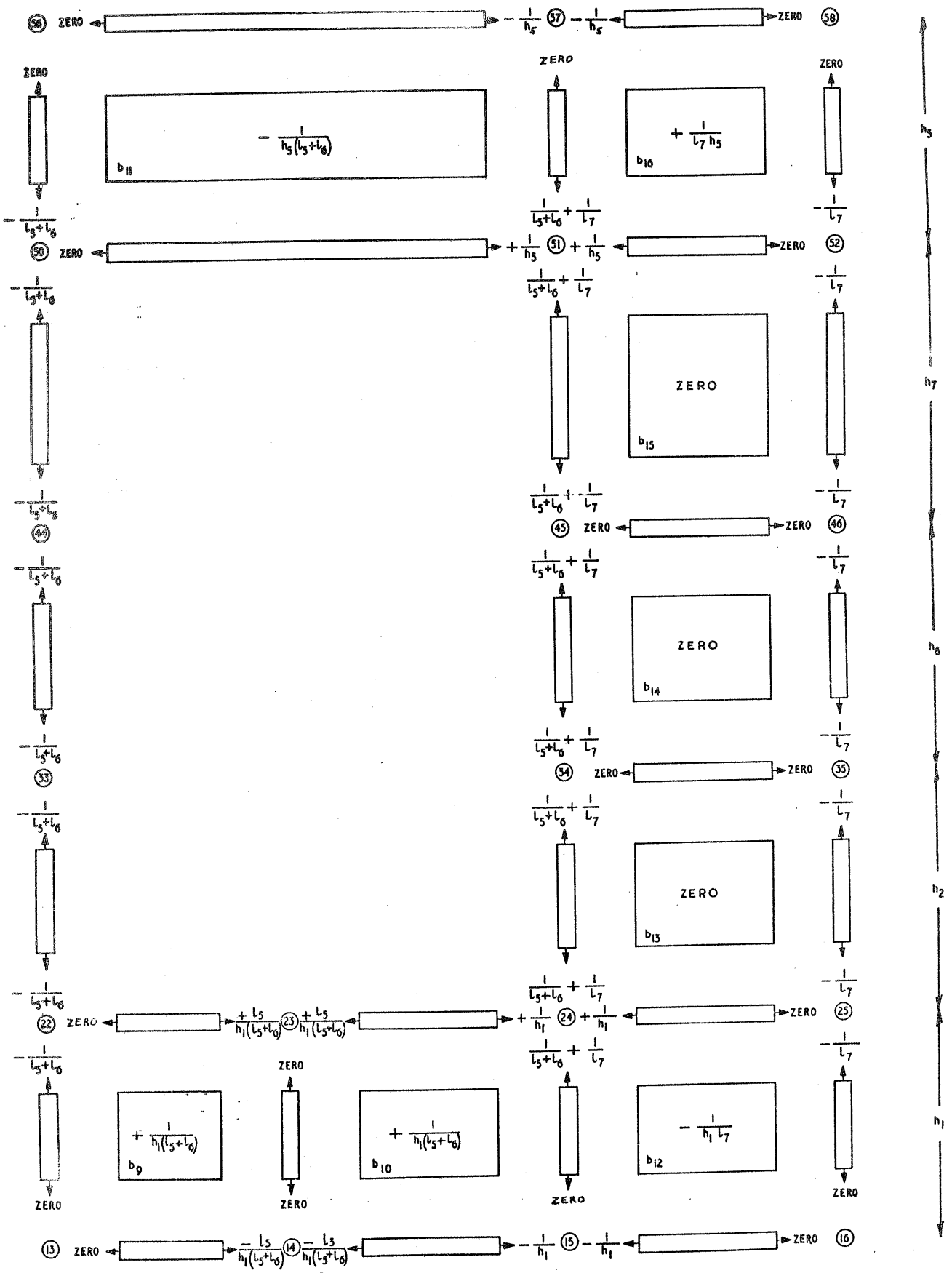

REDUNDANCY S. 2.

fig. 18b

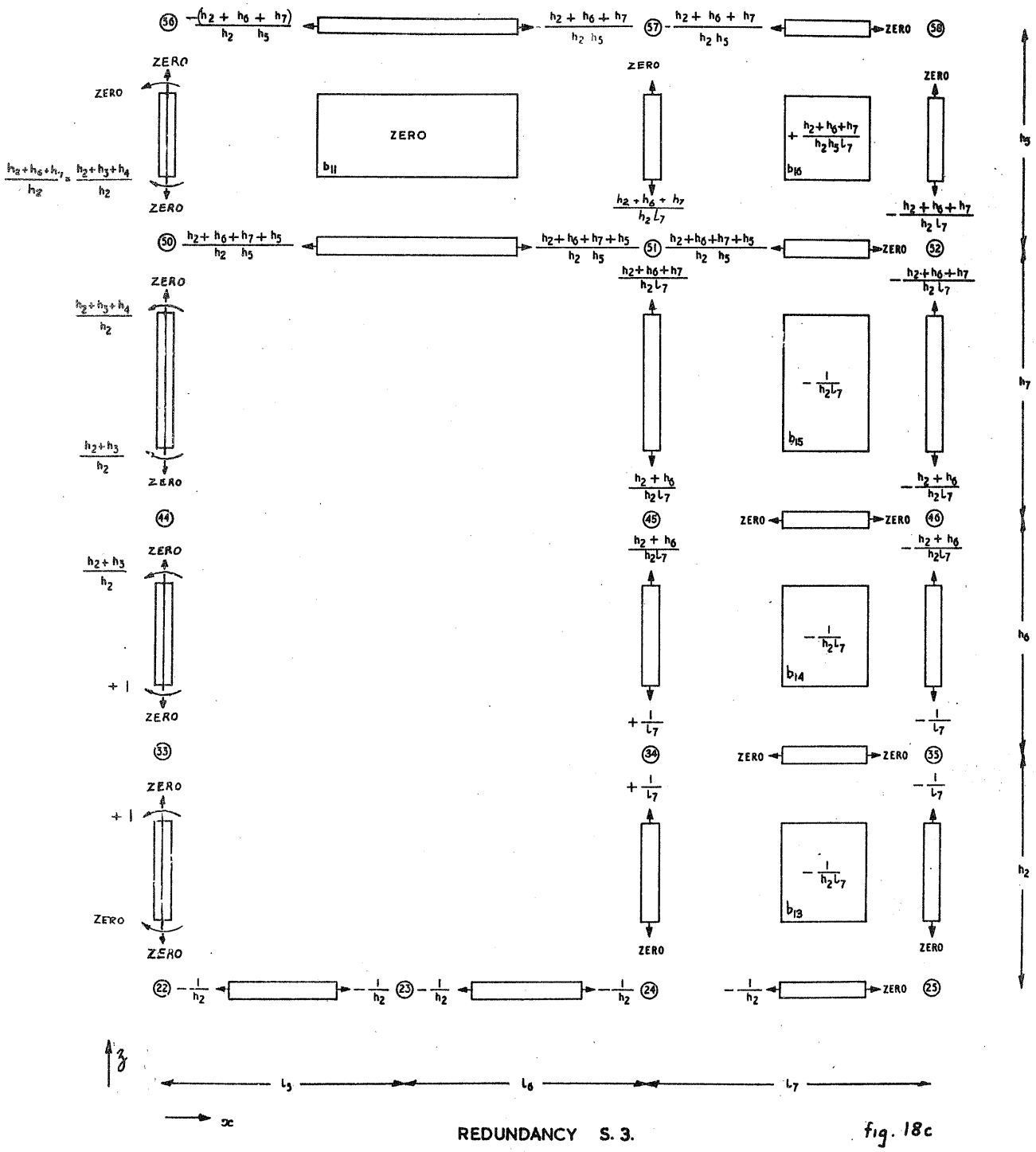

REDUNDANCY S. 3.

fig. 18c

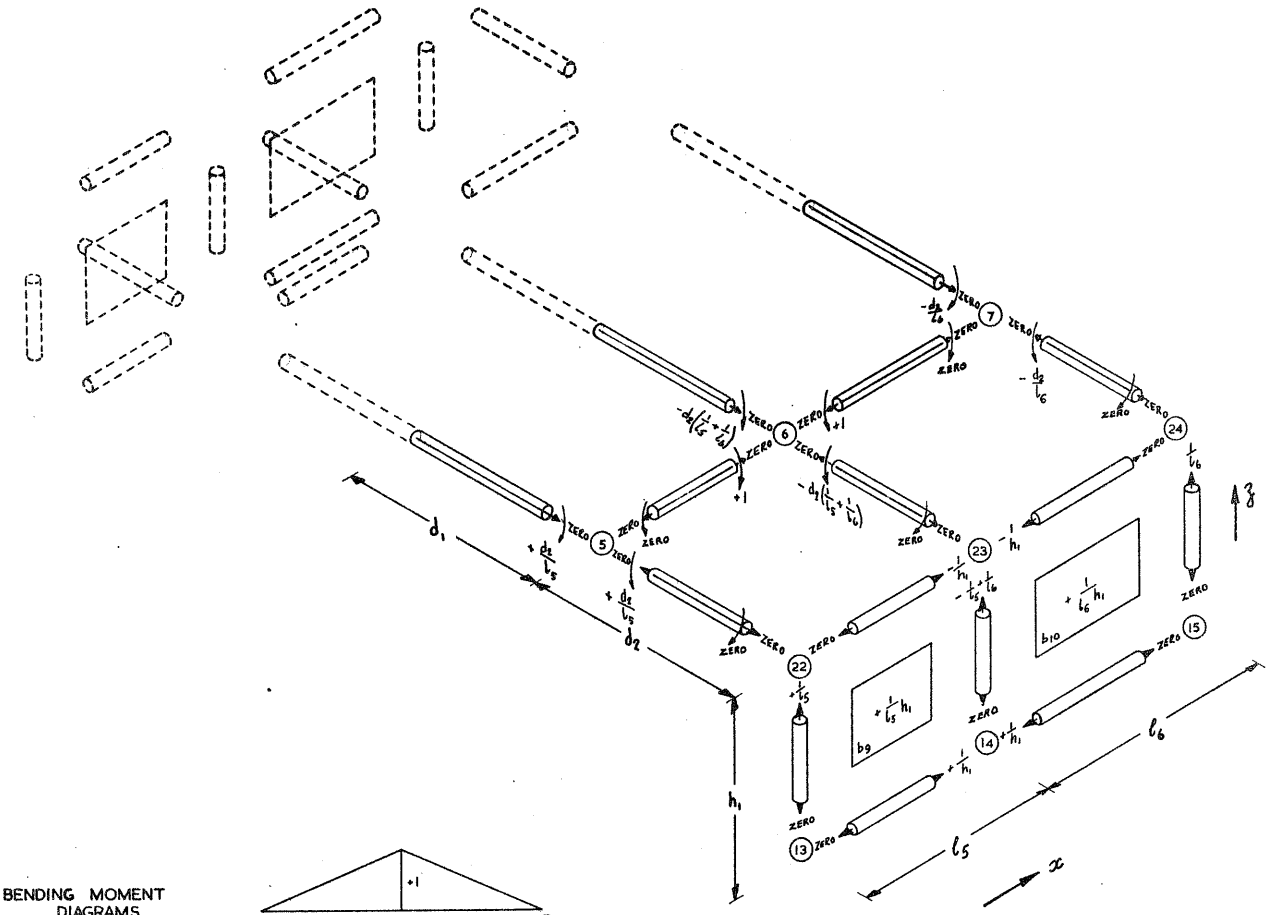

BENDING MOMENT DIAGRAMS

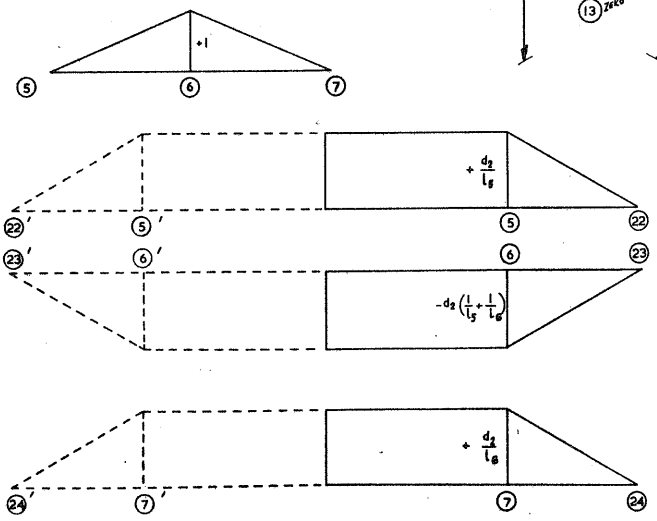

REDUNDANCY T_1

fig. 18d

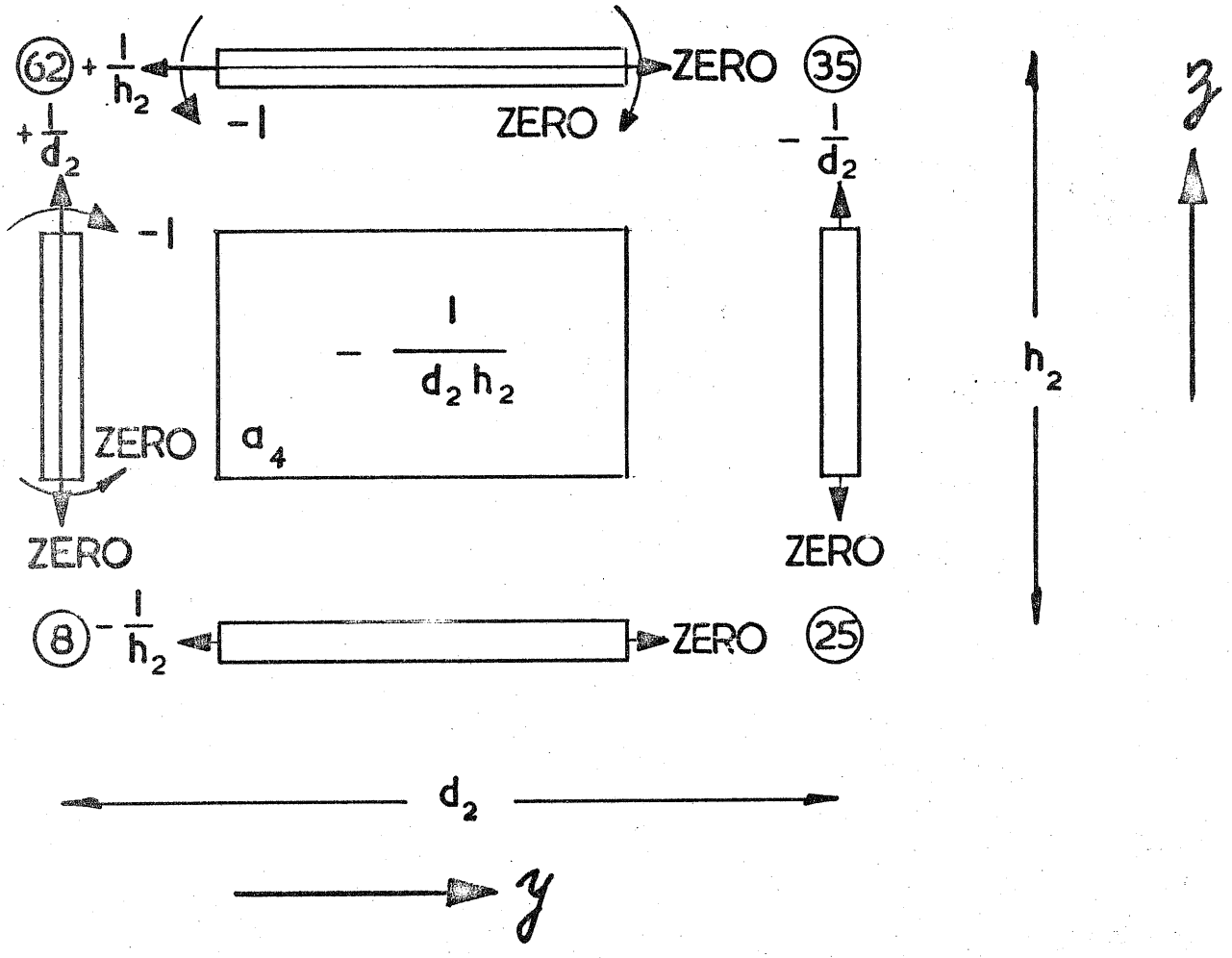

REDUNDANCY U_1

fig. 18e

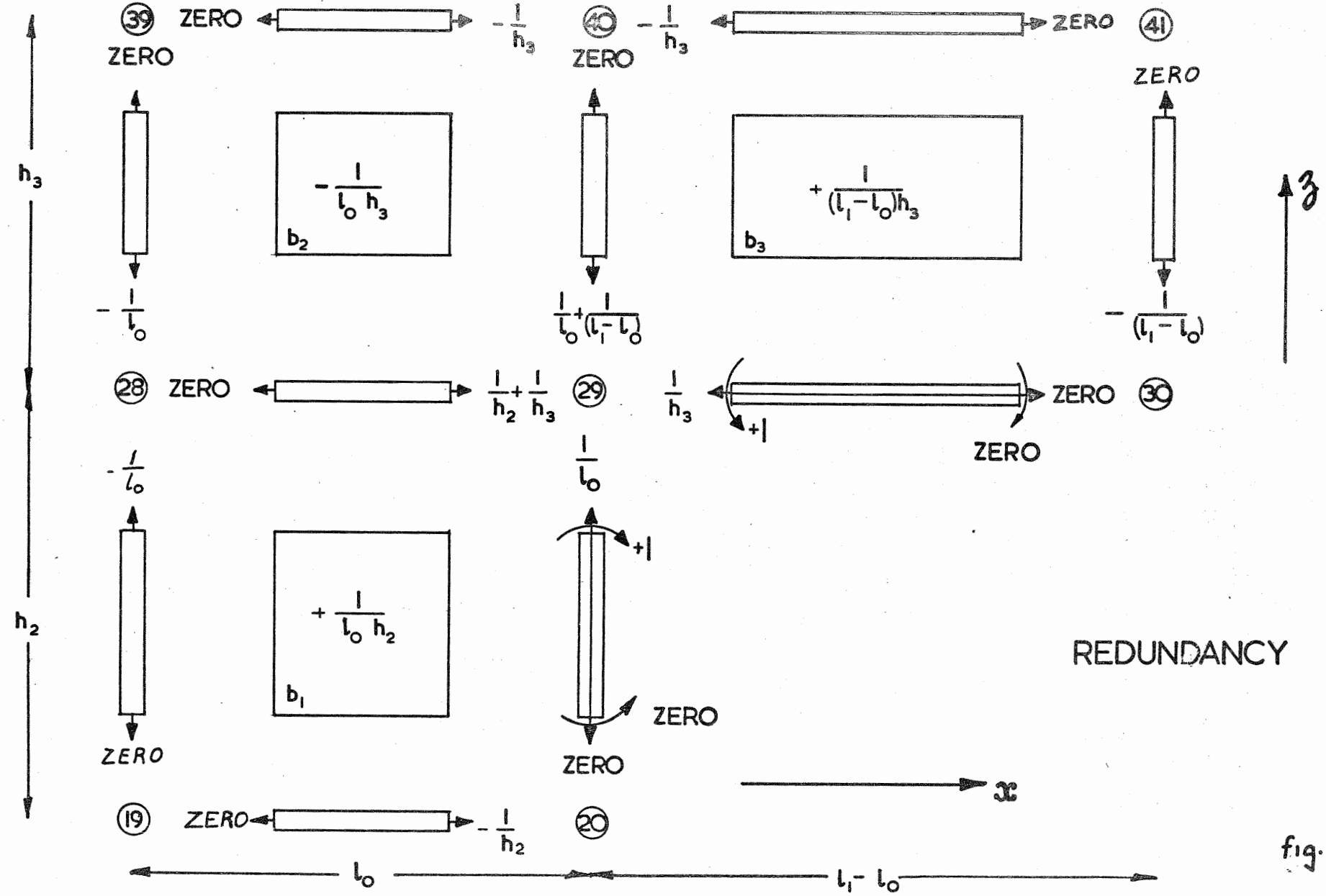

REDUNDANCY V.I.

fig. 18f

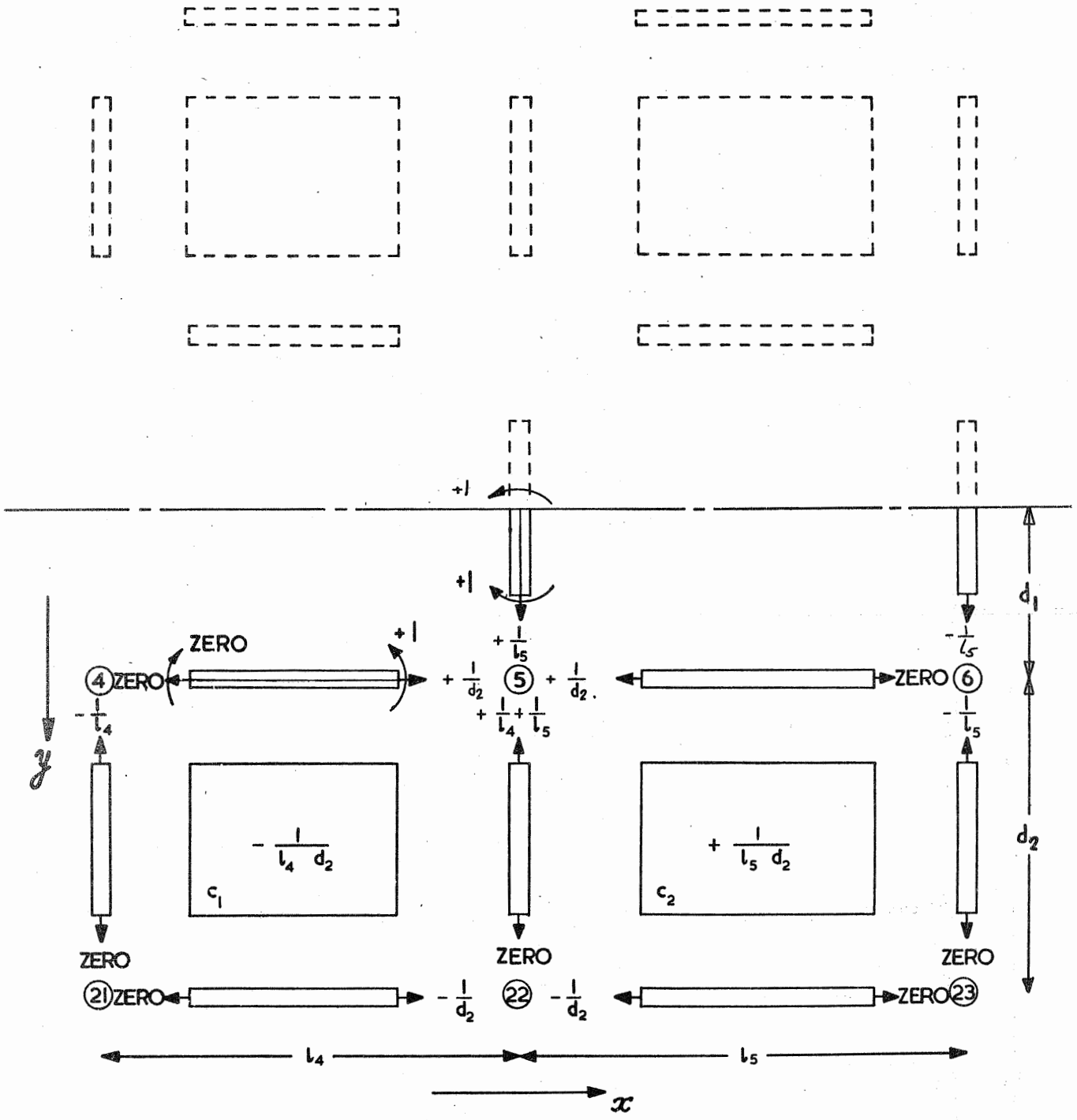

REDUNDANCY Vs I.

fig. 18g

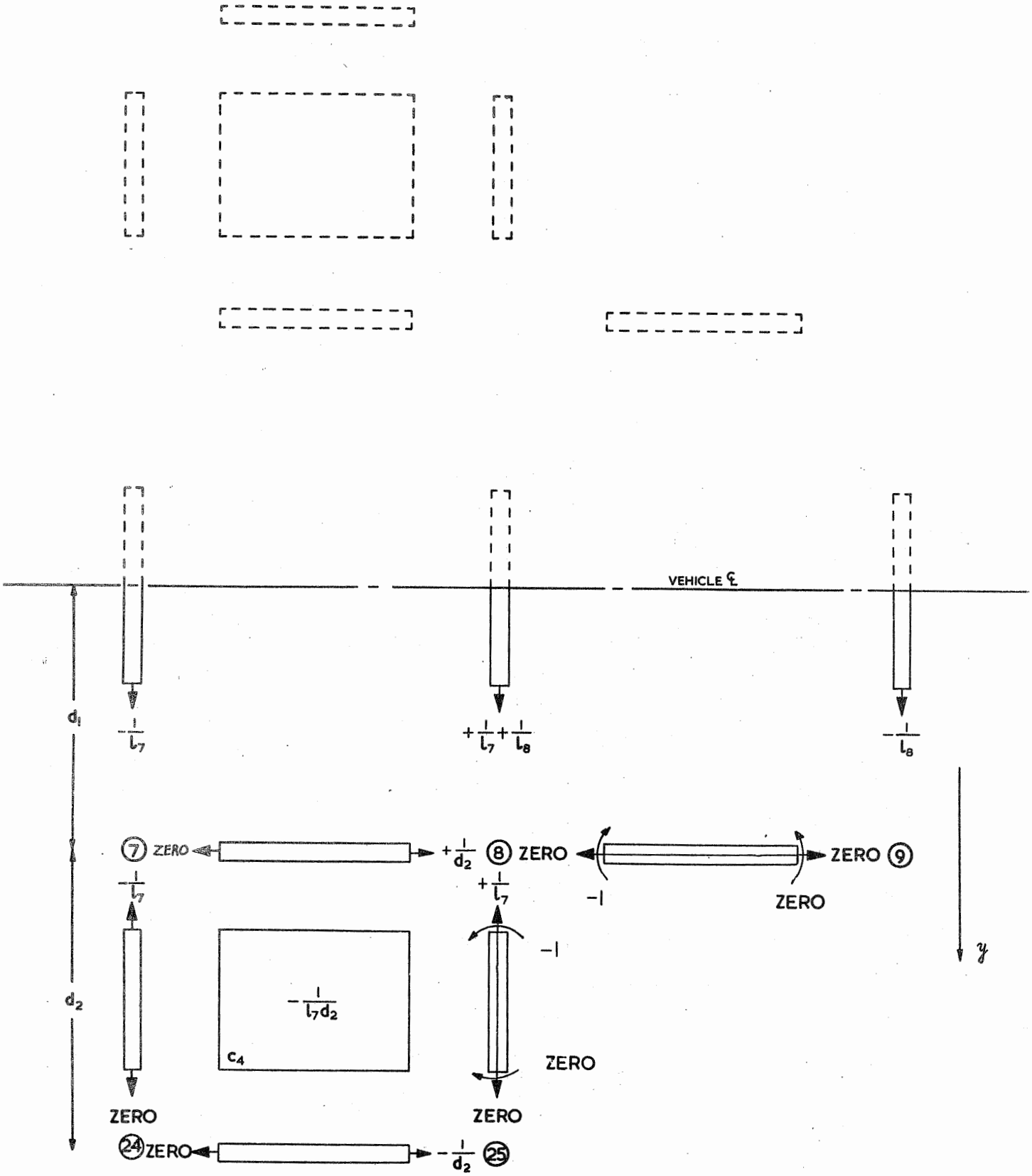

REDUNDANCY $V_{ss}1$

fig. 18h

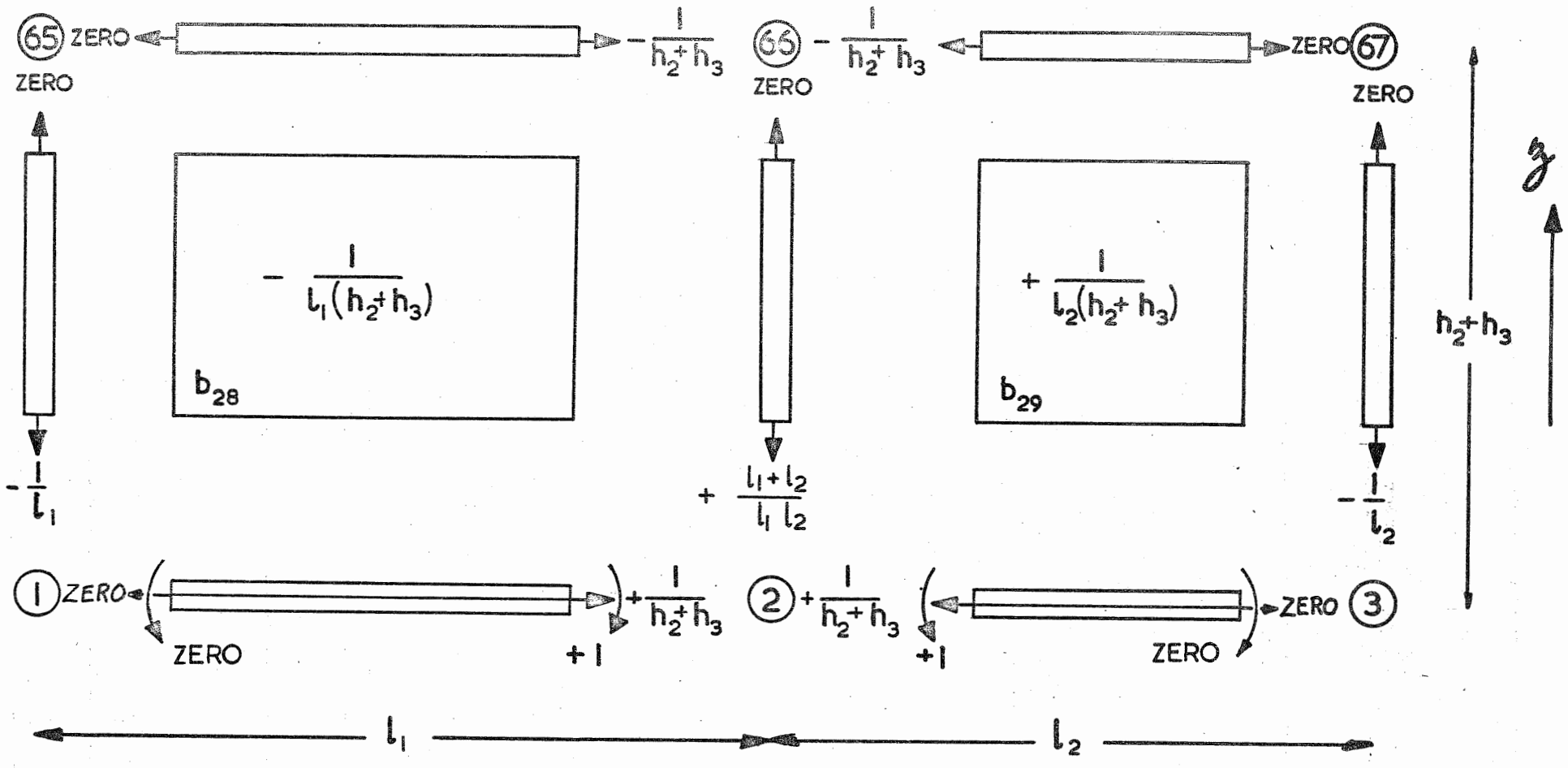

REDUNDANCY W_1

fig. 18i

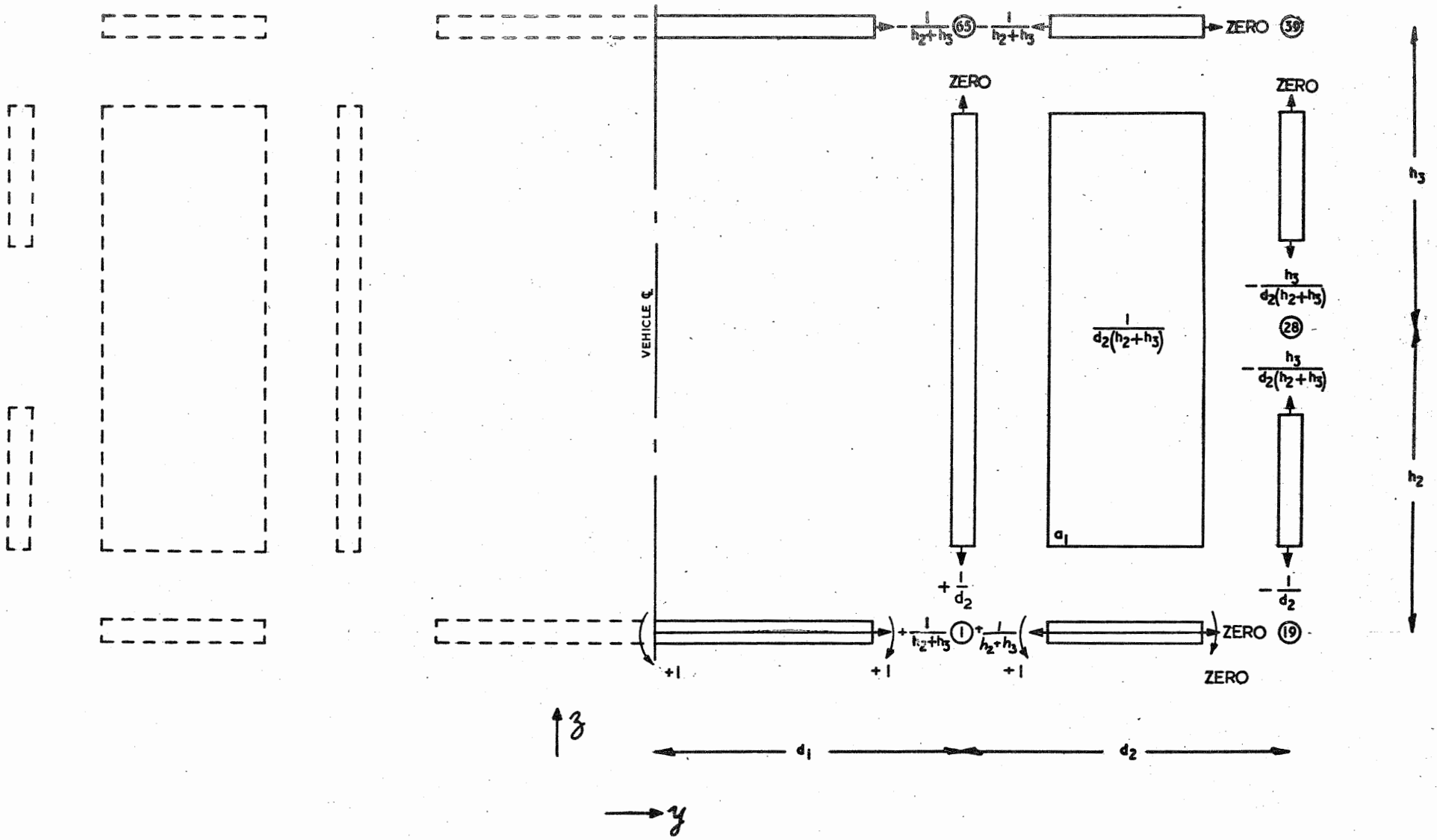

REDUNDANCY W_S I

fig. 18j

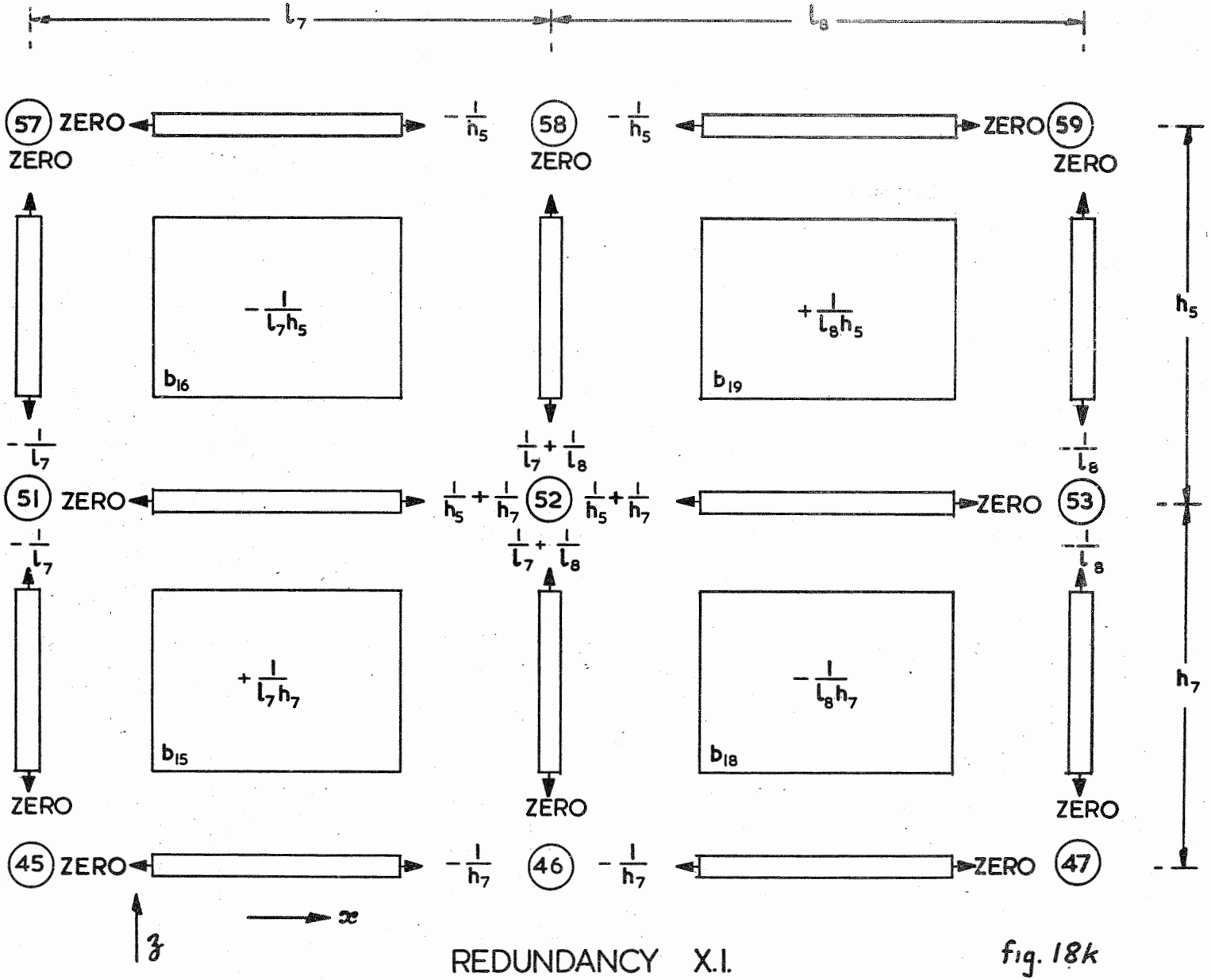

REDUNDANCY X.I.

fig. 18k

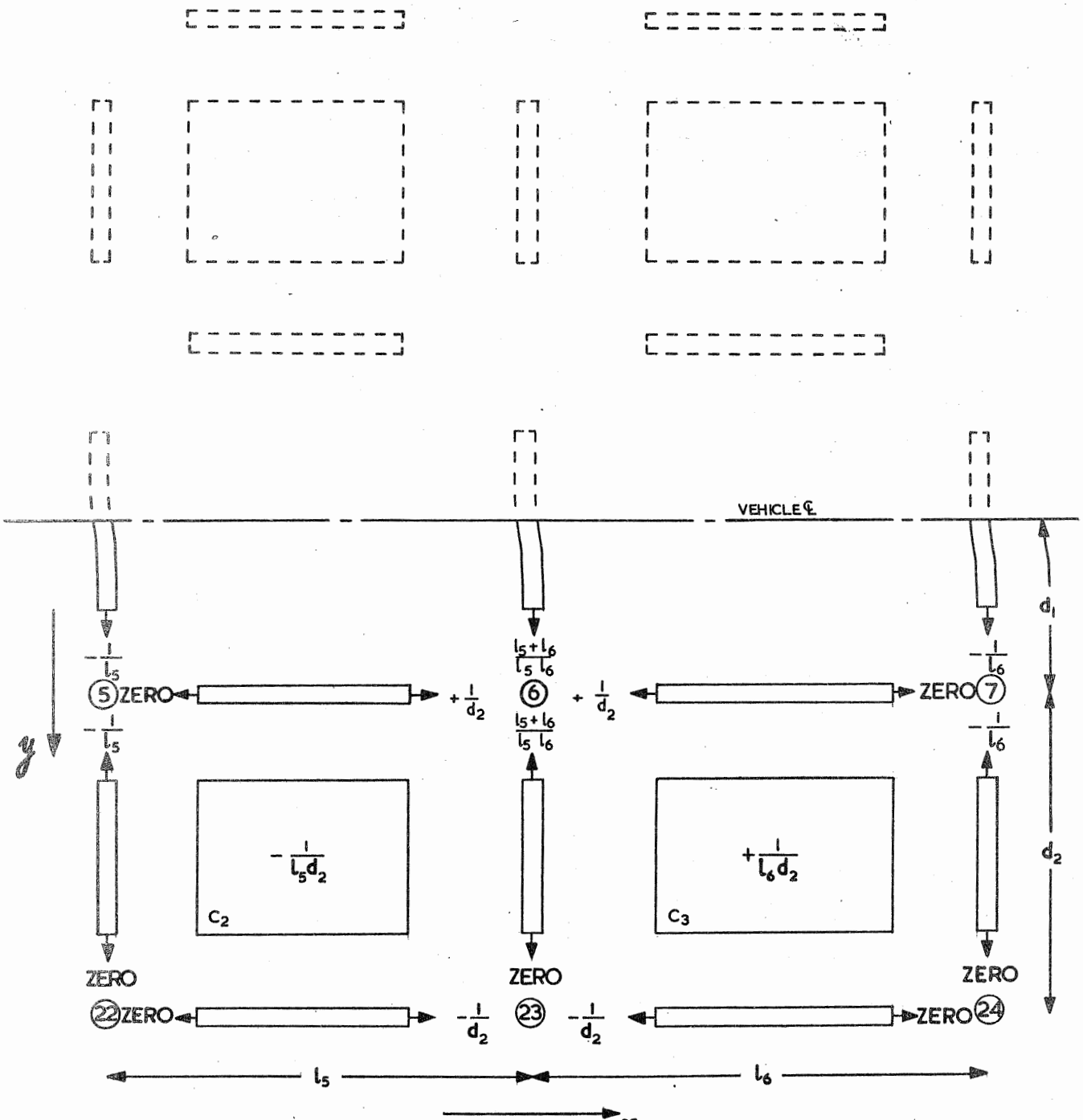

REDUNDANCY X_5 I

fig. 18l

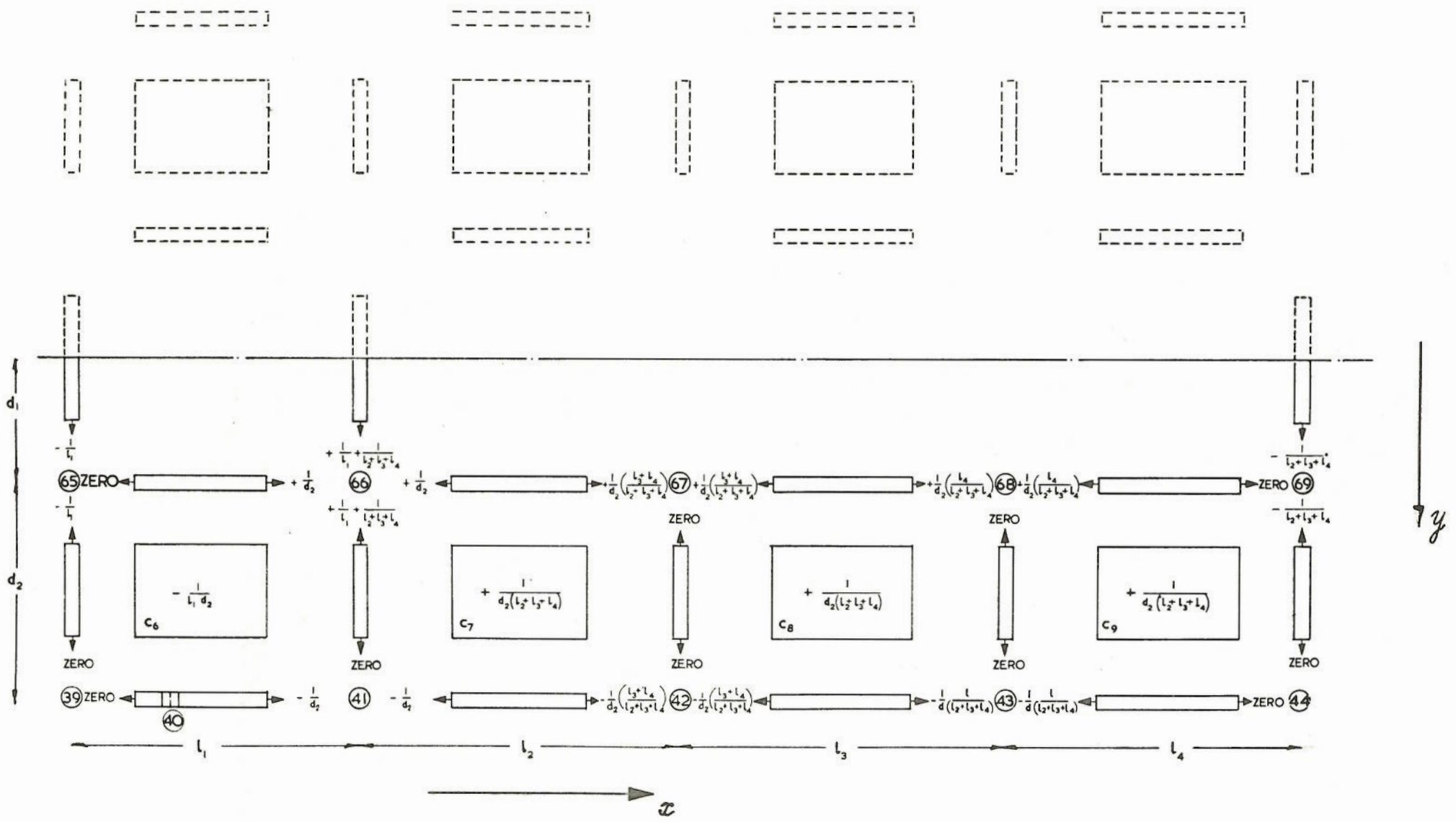

REDUNDANCY $X_{ss.}$ 1.

fig. 18m

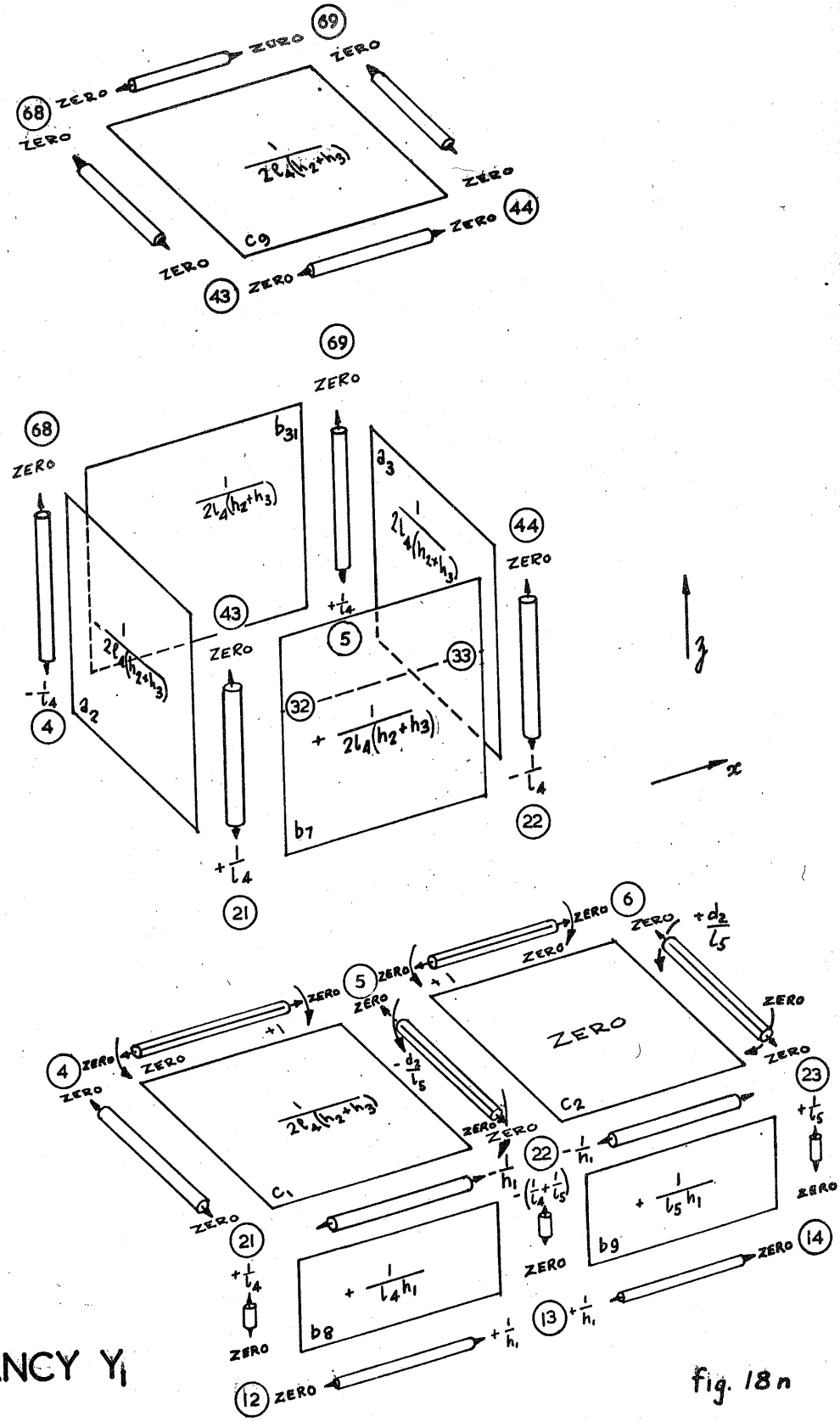

REDUNDANCY Y_1

fig. 18n

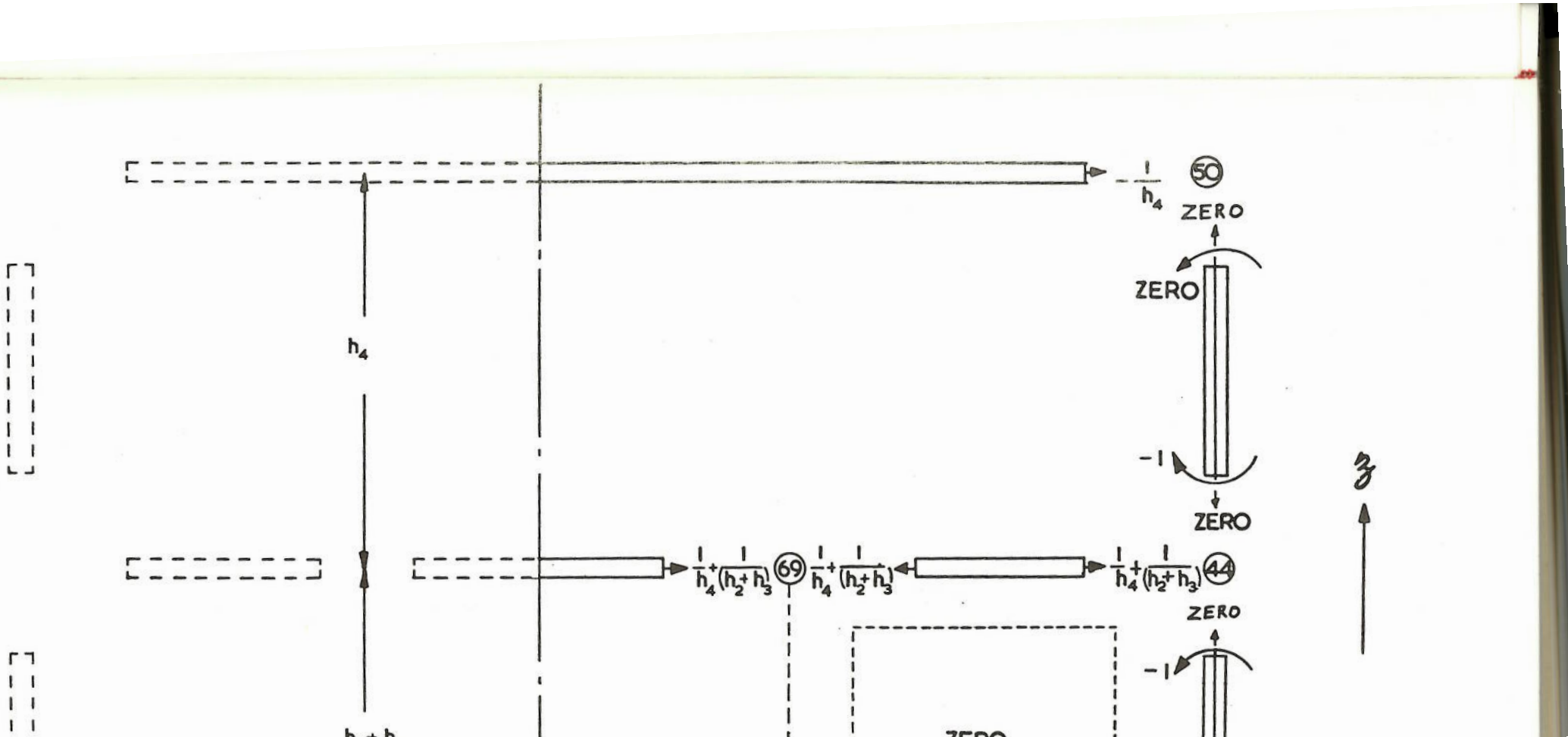
$\frac{1}{h_4}$
50
ZERO
ZERO
-1
ZERO
h_4
$\frac{1}{h_4+(h_2+h_3)}$
69
$\frac{1}{h_4+(h_2+h_3)}$
$\frac{1}{h_4+(h_2+h_3)}$
44
ZERO
-1
z

b_{CA} SUB MATRIX

COLUMN No.		1	2	3	4	5	6	7	8	9	10	11	12	13	14	15	16	17	18	19	20	21	22
NODE WHERE UNIT LOAD IS POSITIONED		1	3	4	5	6	7	8	10	11	$(1-b_2)R_F$	$(1-b_2)R_R$	9	$35+25$	$37+26$	62	64	19	22	23	24	36	27
	M_{2y}	+18.0									-9.4737												
	M_{3y}	+16.6364	-9.0909	-8.1818	-7.2727	-5.909	-4.0	-2.0909	+2.0909	+3.7273	-4.7368												
	M_{4y}	+114.727	-8.1818	-16.364	-14.545	-11.818	-8.0	-4.1818	+4.1818	+7.4545													
	M_{5y}	+13.091	-7.2727	-14.545	-21.818	-17.727	-12.0	-6.2727	+6.2727	+11.1812													
	M_{6y}	+10.636	-5.9091	-11.818	-17.272	-26.59	-18.0	-9.4091	+9.4091	+16.773													
	M_{7y}	+7.20	-4.00	-8.00	-12.00	-18.00	-26.4	-13.38	+13.80	+24.60													
	M_{8y}	+3.7636	-2.0909	-4.1818	-6.2727	-9.409	-13.80	-18.191	+18.191	+32.427													
	M_{9y}								+23.00	+41.00		-11.50											
	M_{10y}									+18.0													
	F_{9z}	-.16364	+.0909	+.1818	+.2727	+.403	+.60	+.7309	+1.2091	+1.3727		-1.00	+1.00										
	F_{62z}	-.16364	+.0909	+.1818	+.2727	+.403	+.60	+.7309	+1.2091	+1.3727		-1.00	+1.00										
	M_{8x}													+17.0									
	M_{62x}													+17.0									
	M_{10x}														+17.0								
	M_{64x}														+17.0								
	F_{8z}															-1.00							
	F_{64z}															-1.00							

	b_0	b_1	
		I	II
		24	25
a_{33}	b_{0a}	b_{1aI}	b_{1aII} = ZERO
b_{33}	ZERO	b_{1bI}	b_{1bII} = ZERO
c_{33}	ZERO	b_{1cI}	b_{1cII}
d_{33}	ZERO	b_{1dI}	b_{1dII}
e_{33}	ZERO	b_{1eI}	b_{1eII}
f_{33}	ZERO	b_{1fI} = ZERO	b_{1fII}
g_{33}	ZERO	b_{1gI} = ZERO	b_{1gII}

fig 20

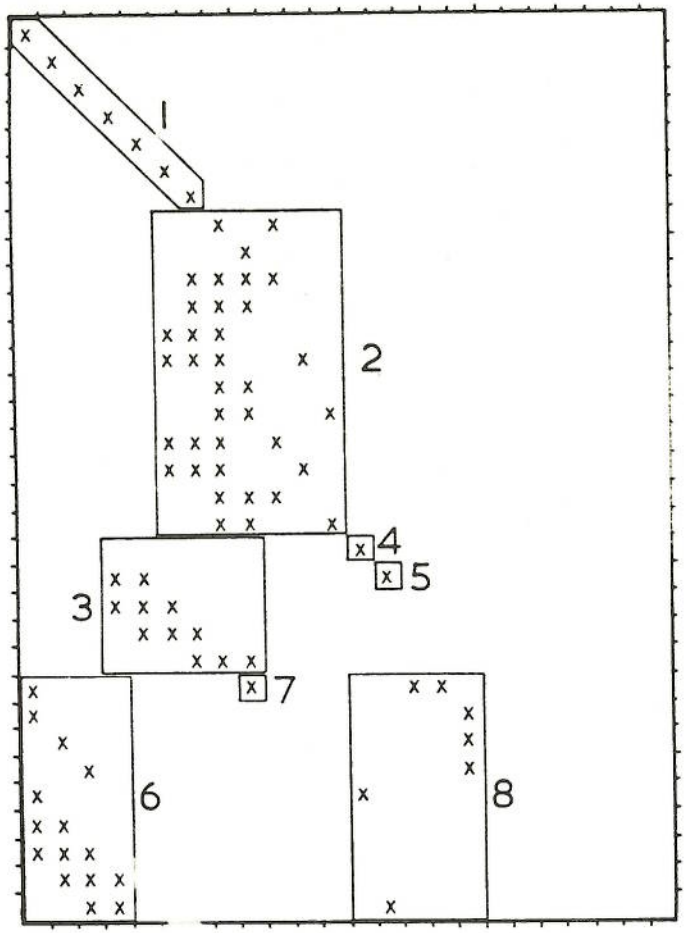

FIG. 21a

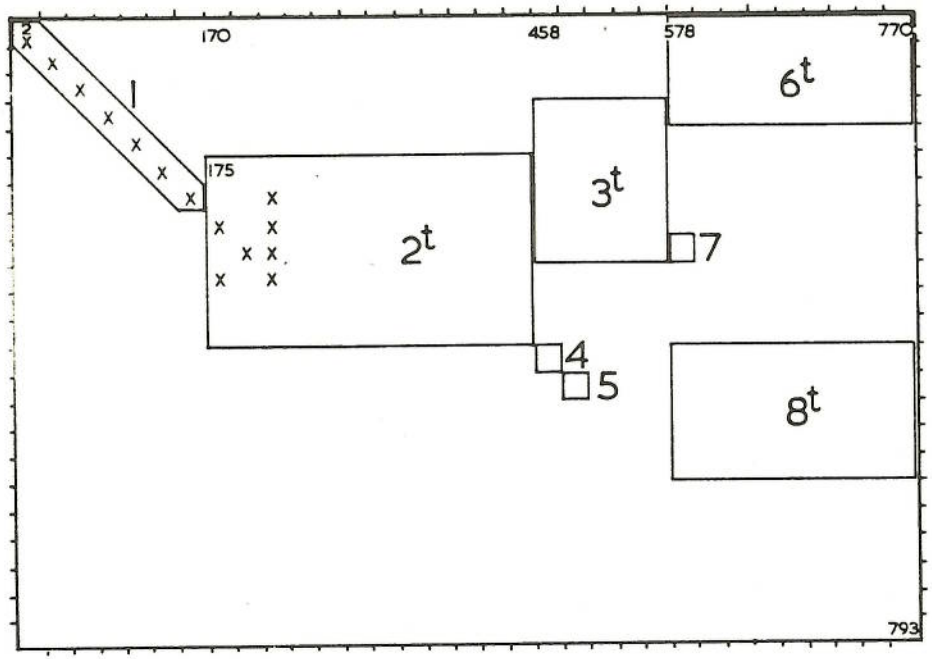

FIG. 21b

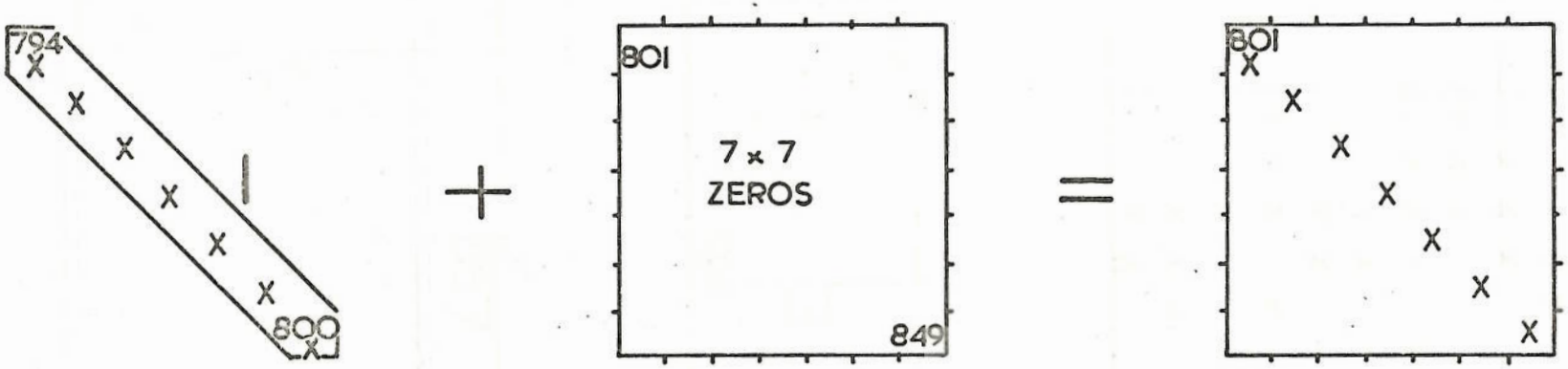

FIG 22a

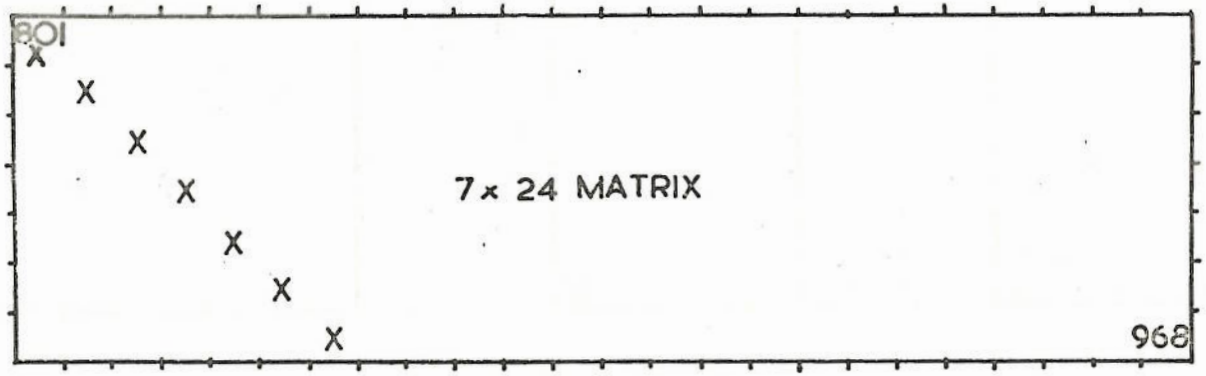

FIG 22b

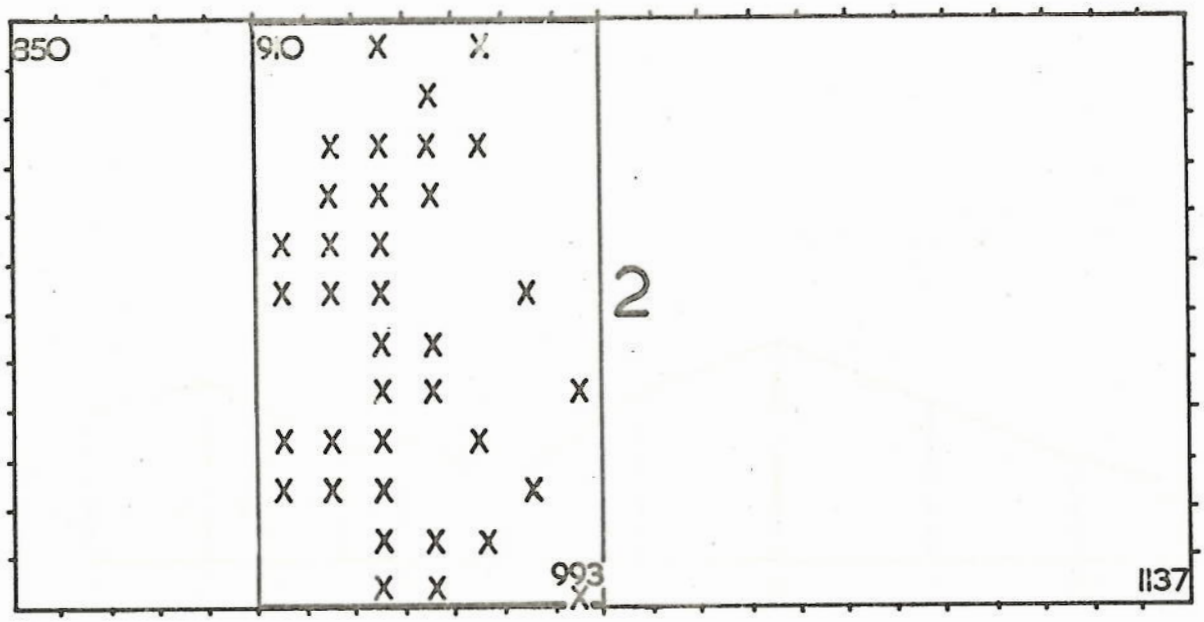

FIG 23a.

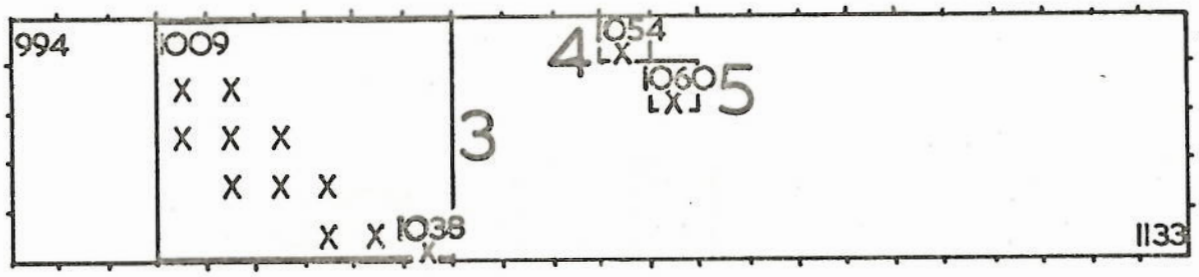

FIG 23b.

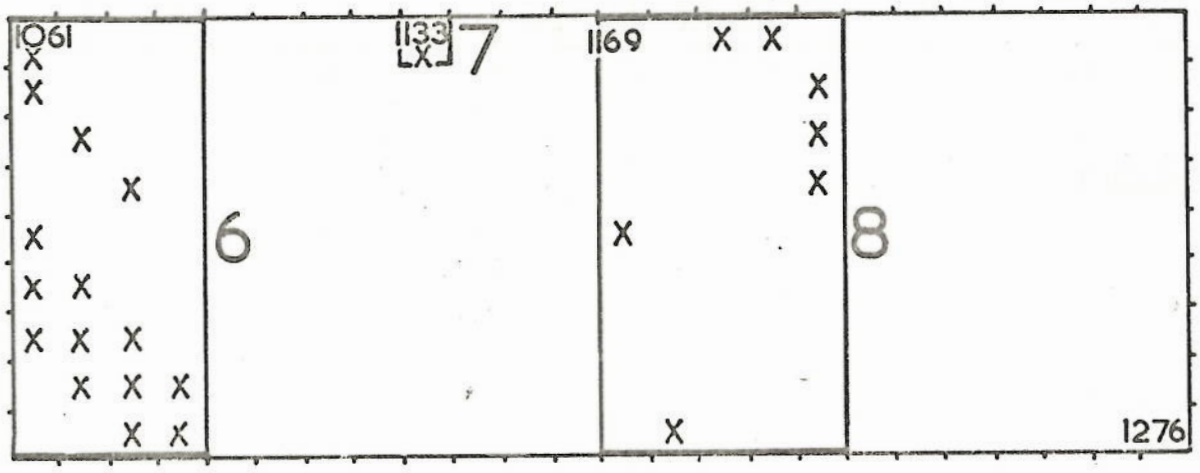

FIG 23c.

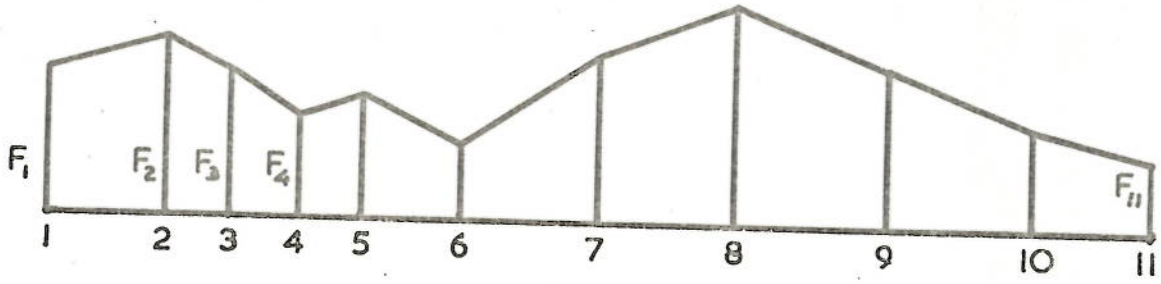

DIRECT LOAD OR BENDING MOMENT DISTRIBUTION

FIG 24

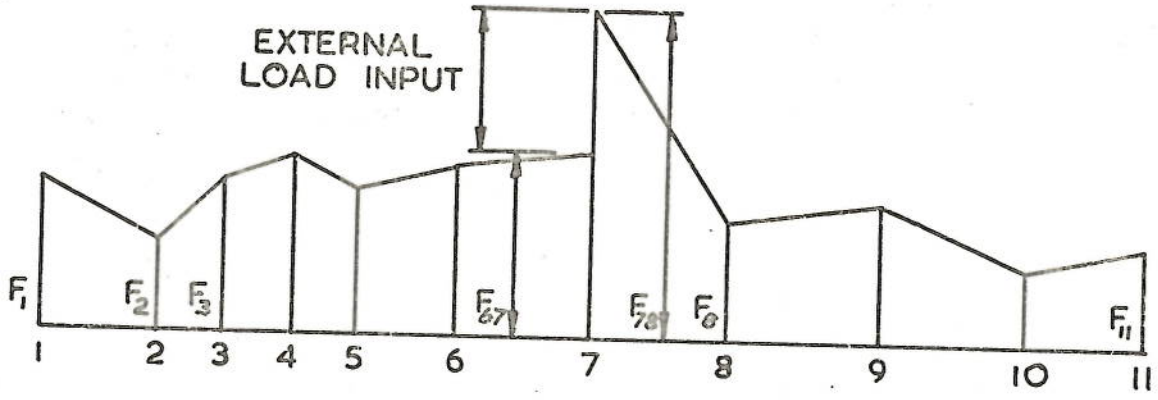

FIG 25

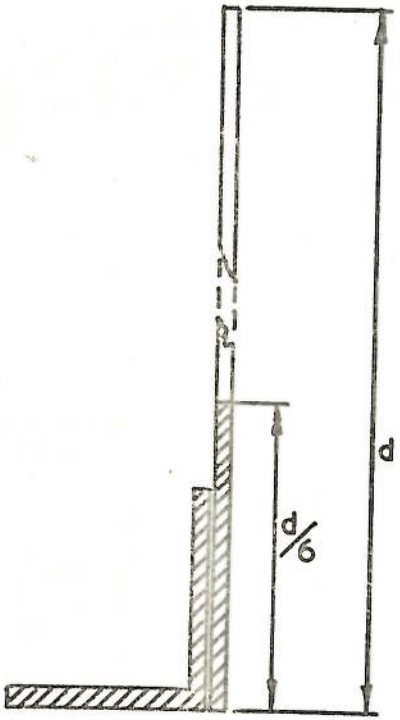

FIG 26

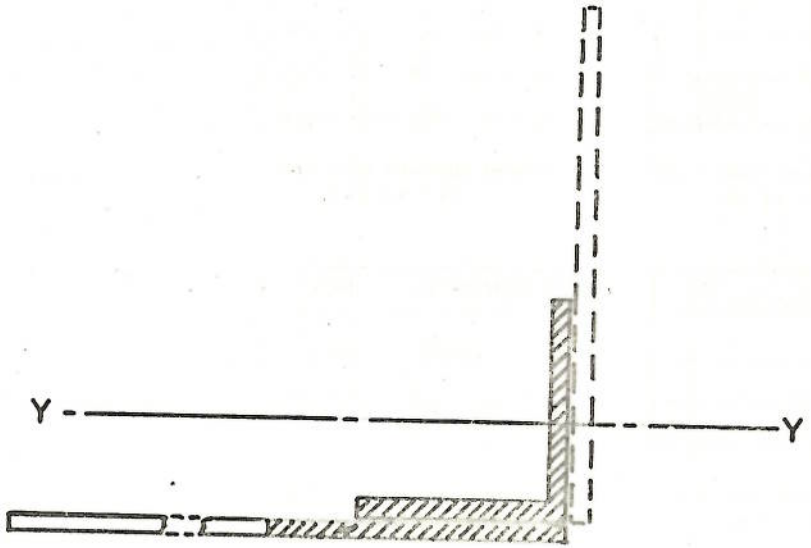

I_{YY} INCLUDES EFFECT OF HATCHED AREA

FIG 27

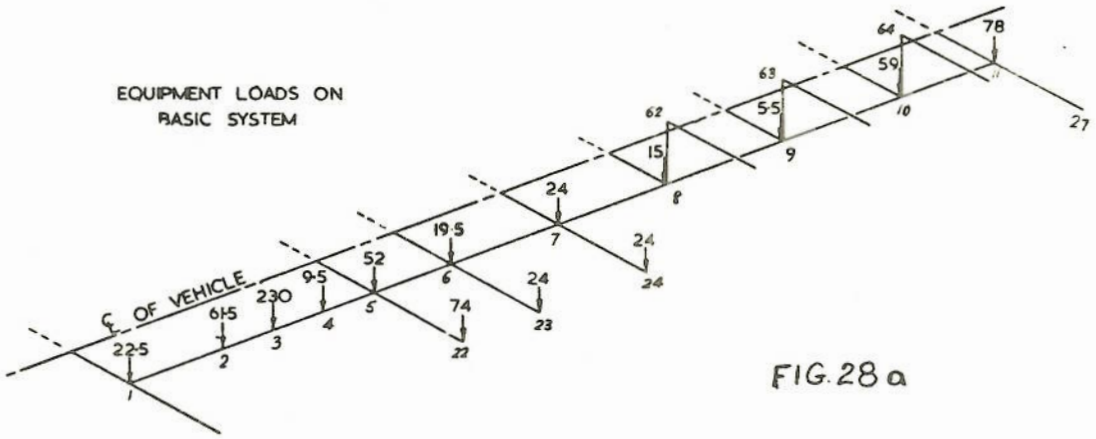

FIG. 28a

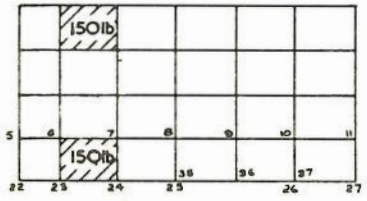

Case 1. Driver and Passenger.

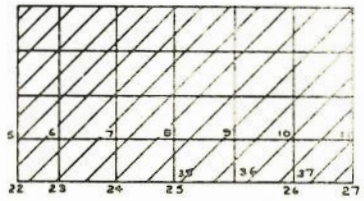

Case 4. Uniformly distributed load aft 5·22.

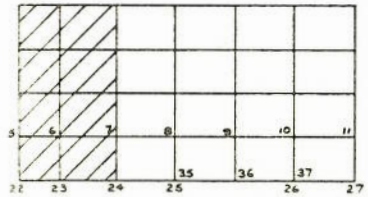

Case 2. Load distributed between 5·22 and 7·24.

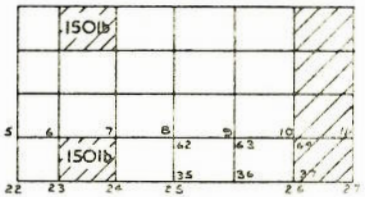

Case 5. Driver, Passenger + 248 9lb. aft 64 37.

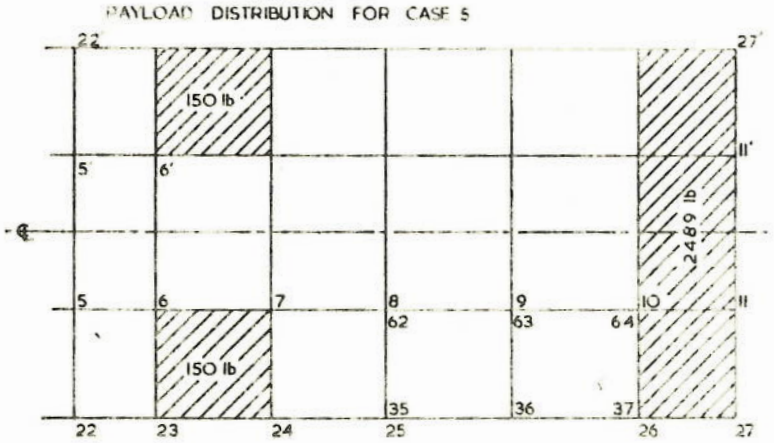
PAYLOAD DISTRIBUTION FOR CASE 5
150 lb
2489 lb
150 lb

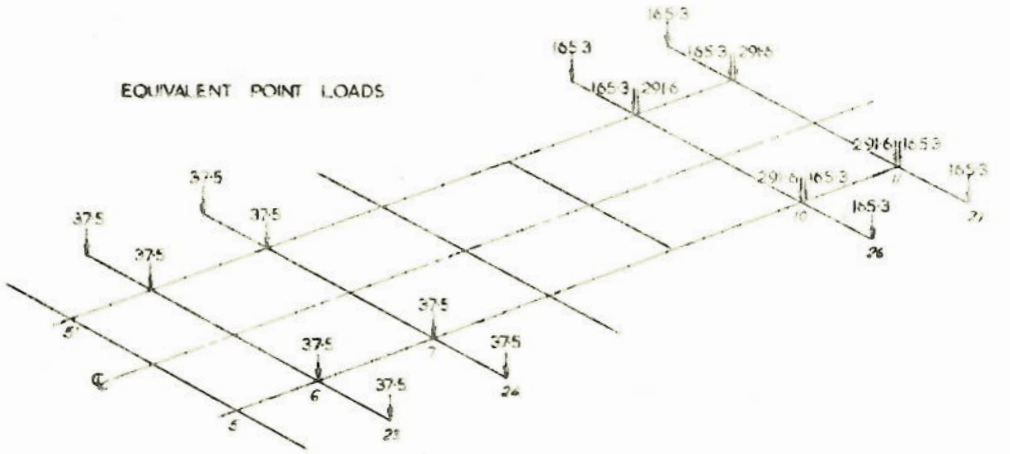
EQUIVALENT POINT LOADS
375
165.3
291.6

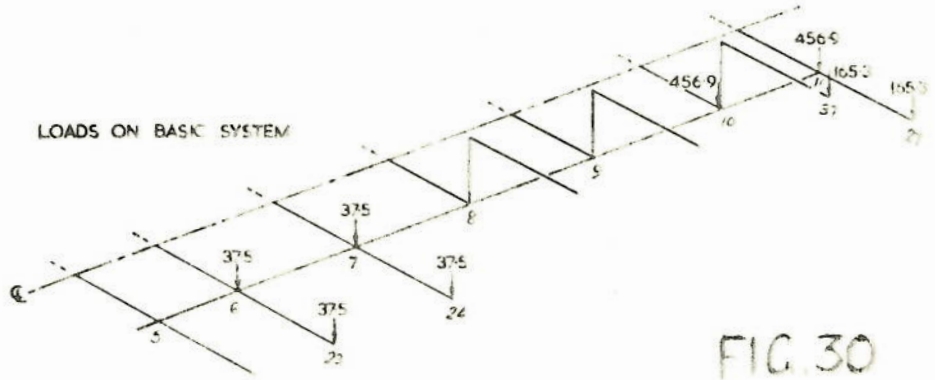
LOADS ON BASIC SYSTEM
375
456.9
165.3

FIG. 30

COMPUTER STORE ALLOCATION DIAGRAM PART I PROGRAMME.

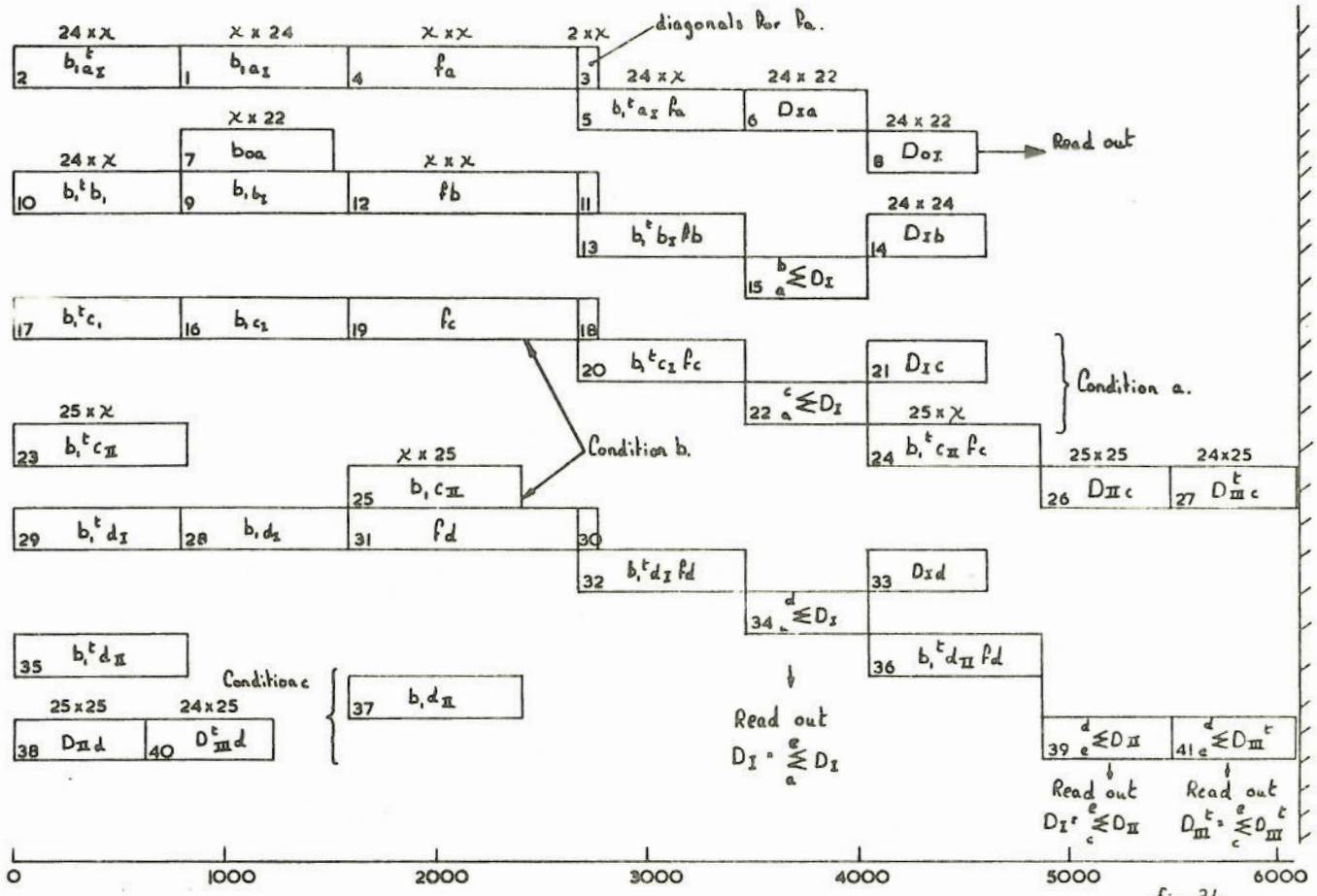

fig 31.

FIG. 31

COMPUTER STORE ALLOCATION DIAGRAM PART II PROGRAM.

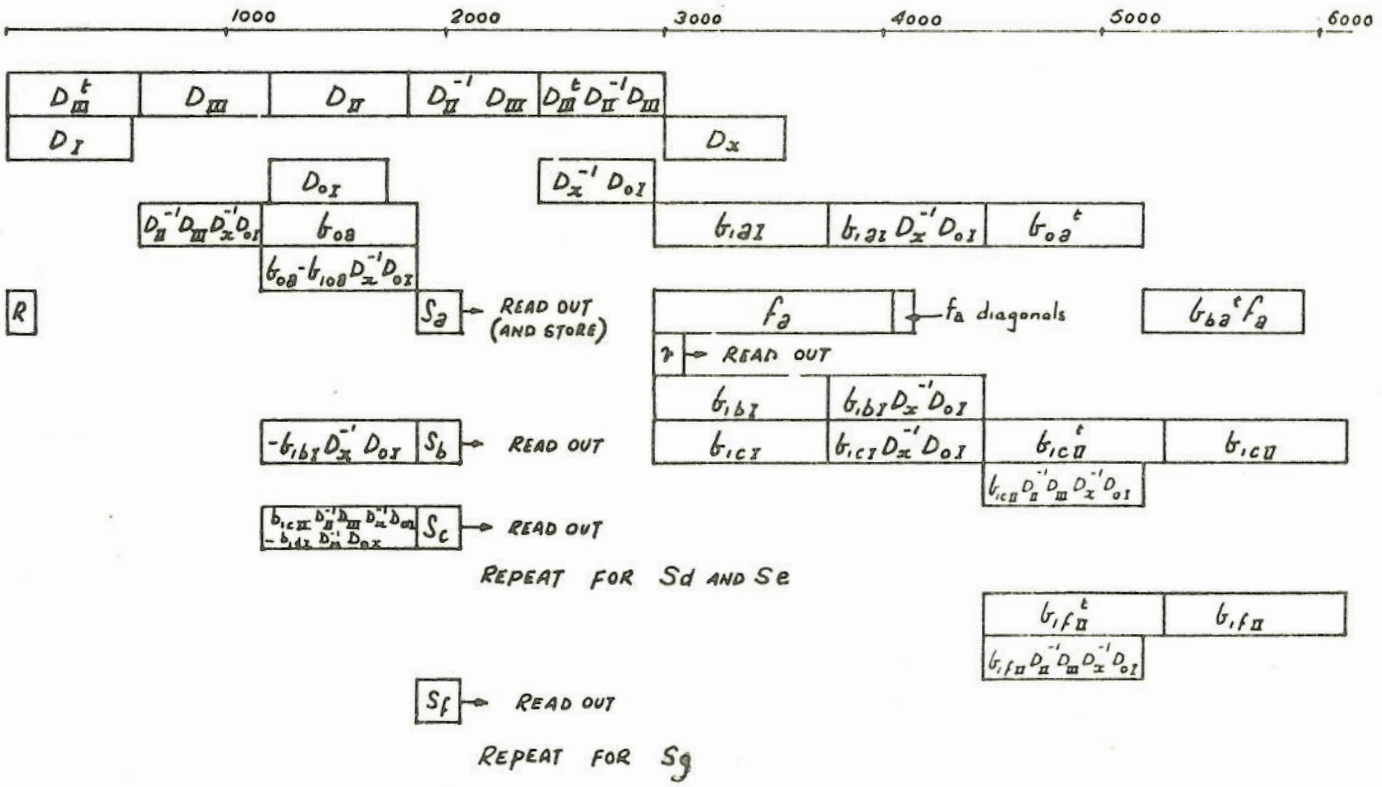

FIG. 32

BENDING MOMENTS ON MEMBER 1-11

[BENDING LOAD CASE ONLY- (NO TORSION)]

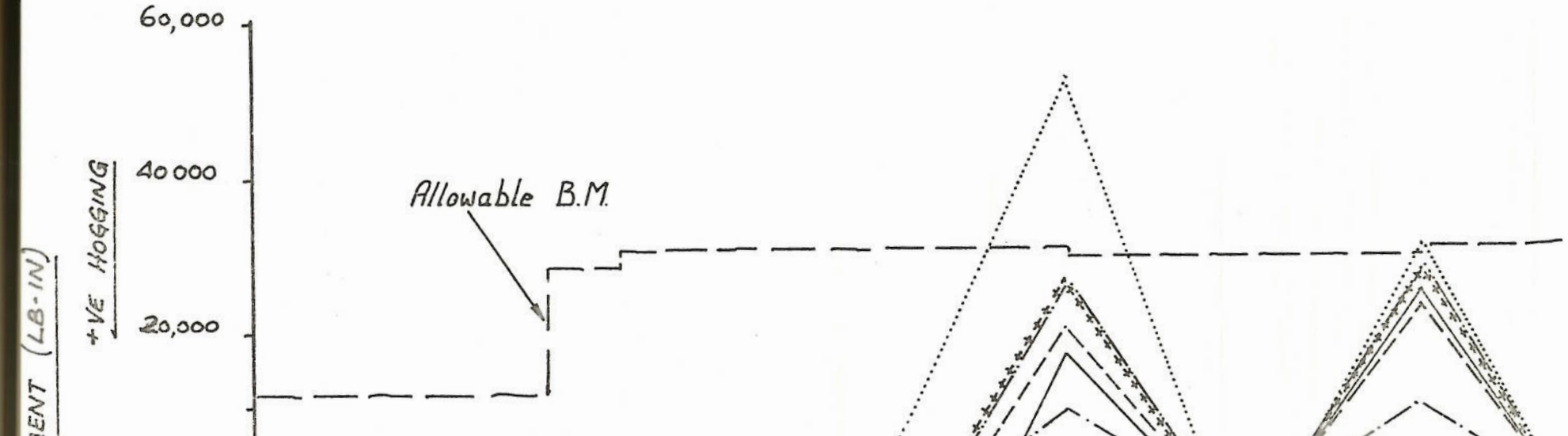

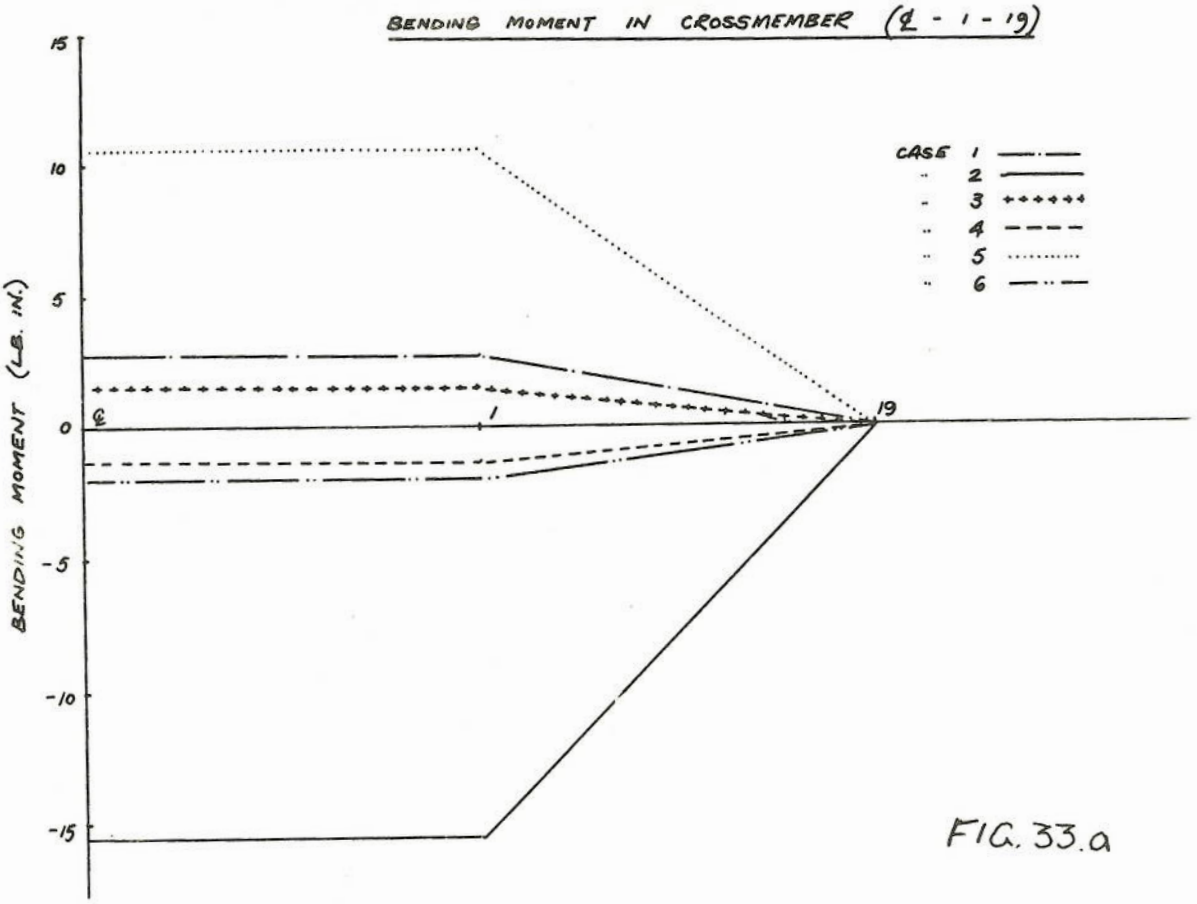

FIG. 33.a

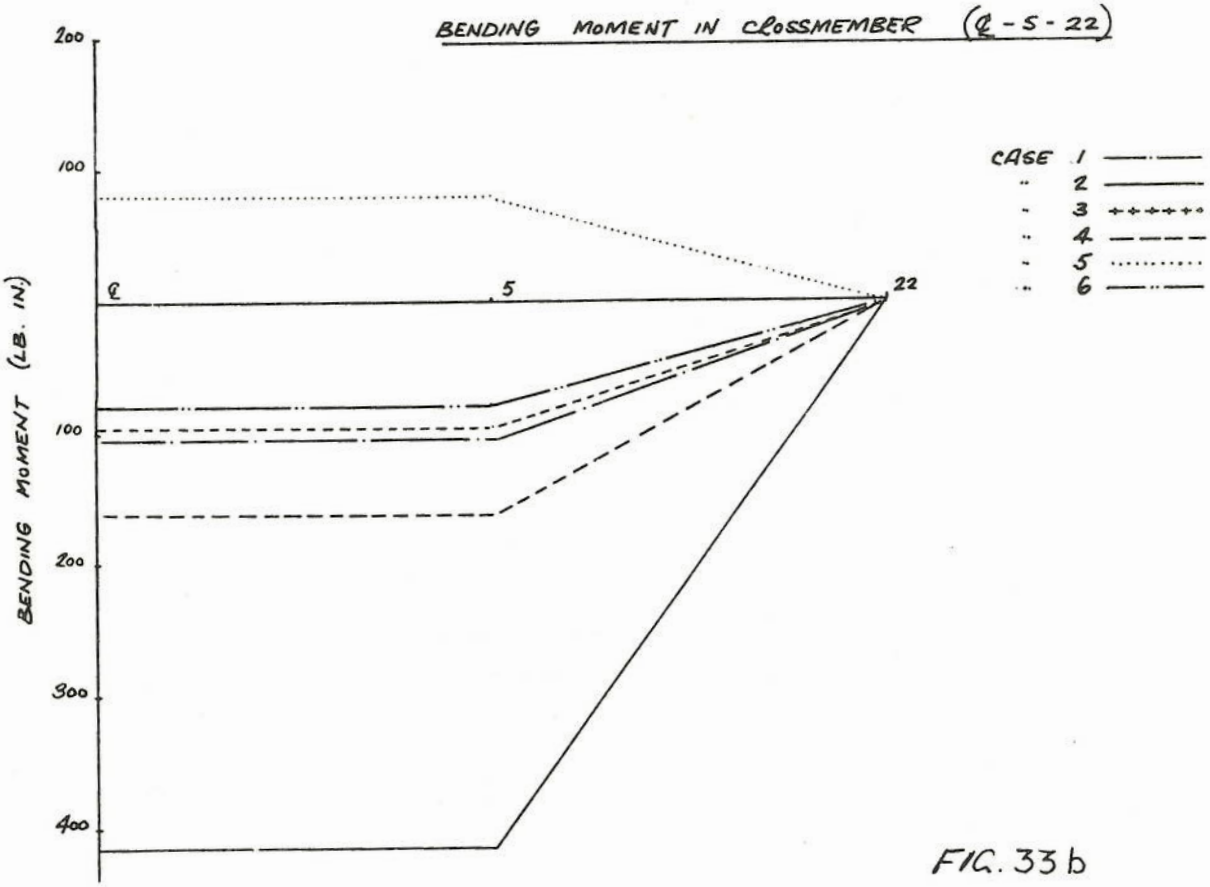

FIG. 33 b

BENDING MOMENT IN CROSSMEMBER (℄ - 6 - 23)

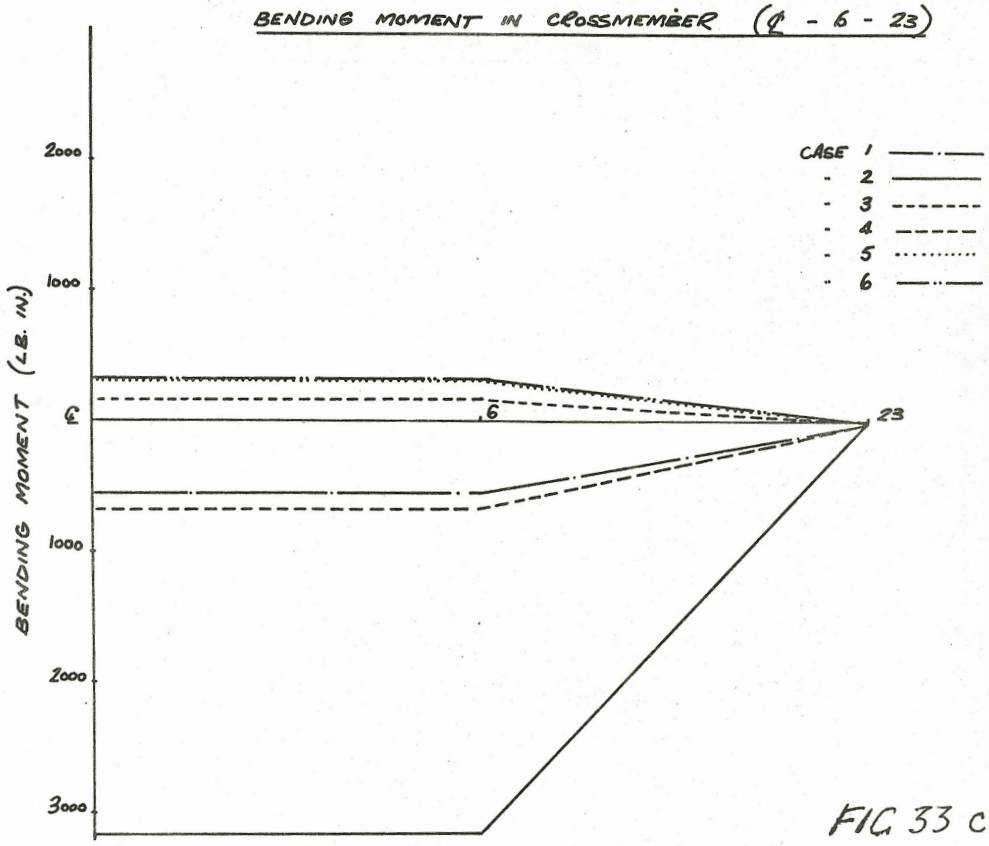

FIG 33 c

BENDING MOMENTS IN CROSSMEMBER (℄ - 7 - 24)

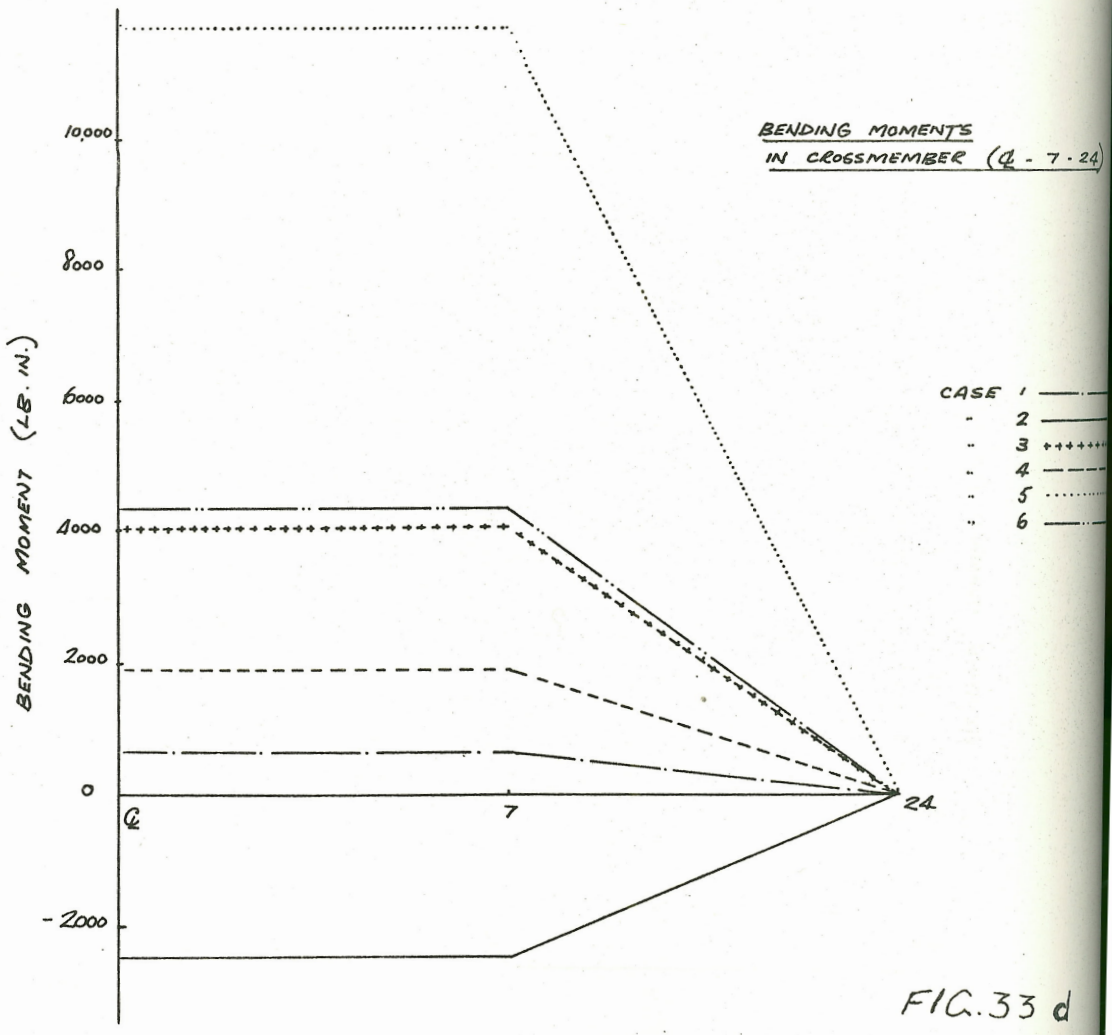

FIG. 33 d

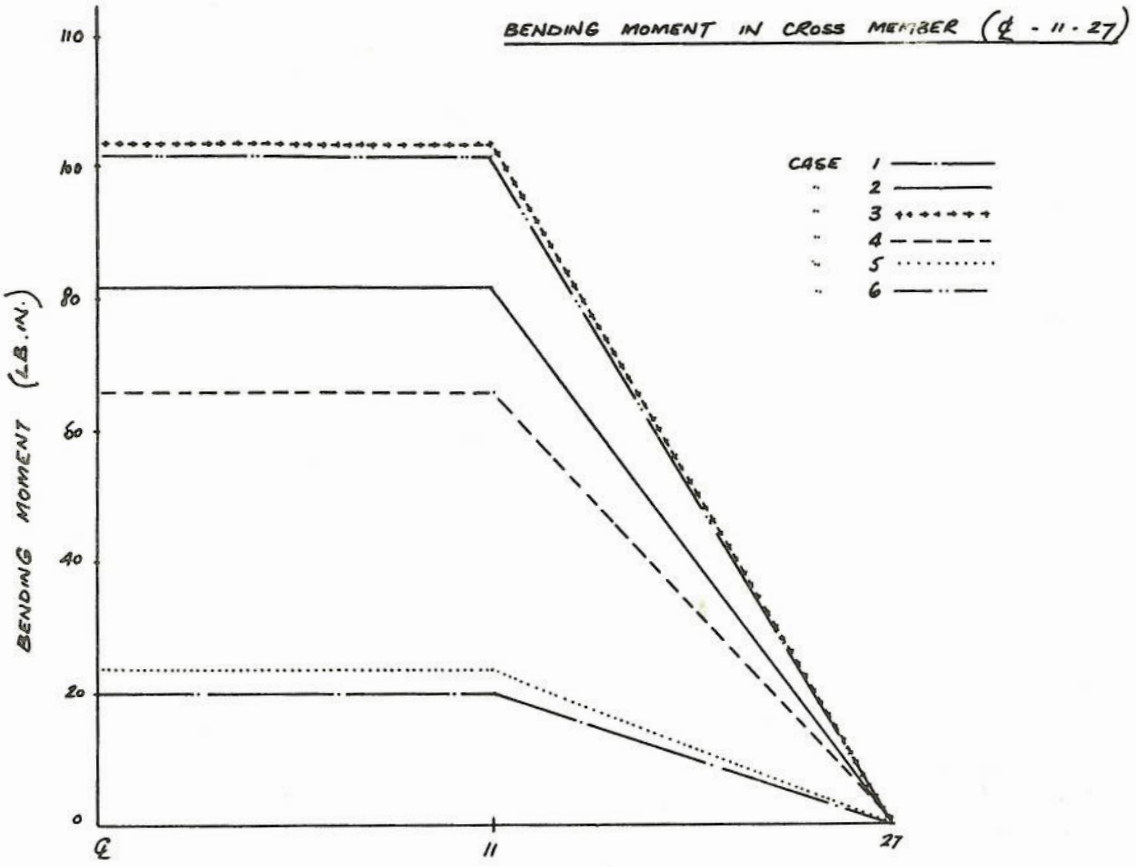
BENDING MOMENT IN CROSS MEMBER (℄ - 11 - 27)
BENDING MOMENT (LB. IN.)
110
100
80
60
40
20
0
℄
11
27
CASE 1
2
3
4
5
6

FIG 33 e

BENDING MOMENTS ON CROSS MEMBER (8, 62, 35)

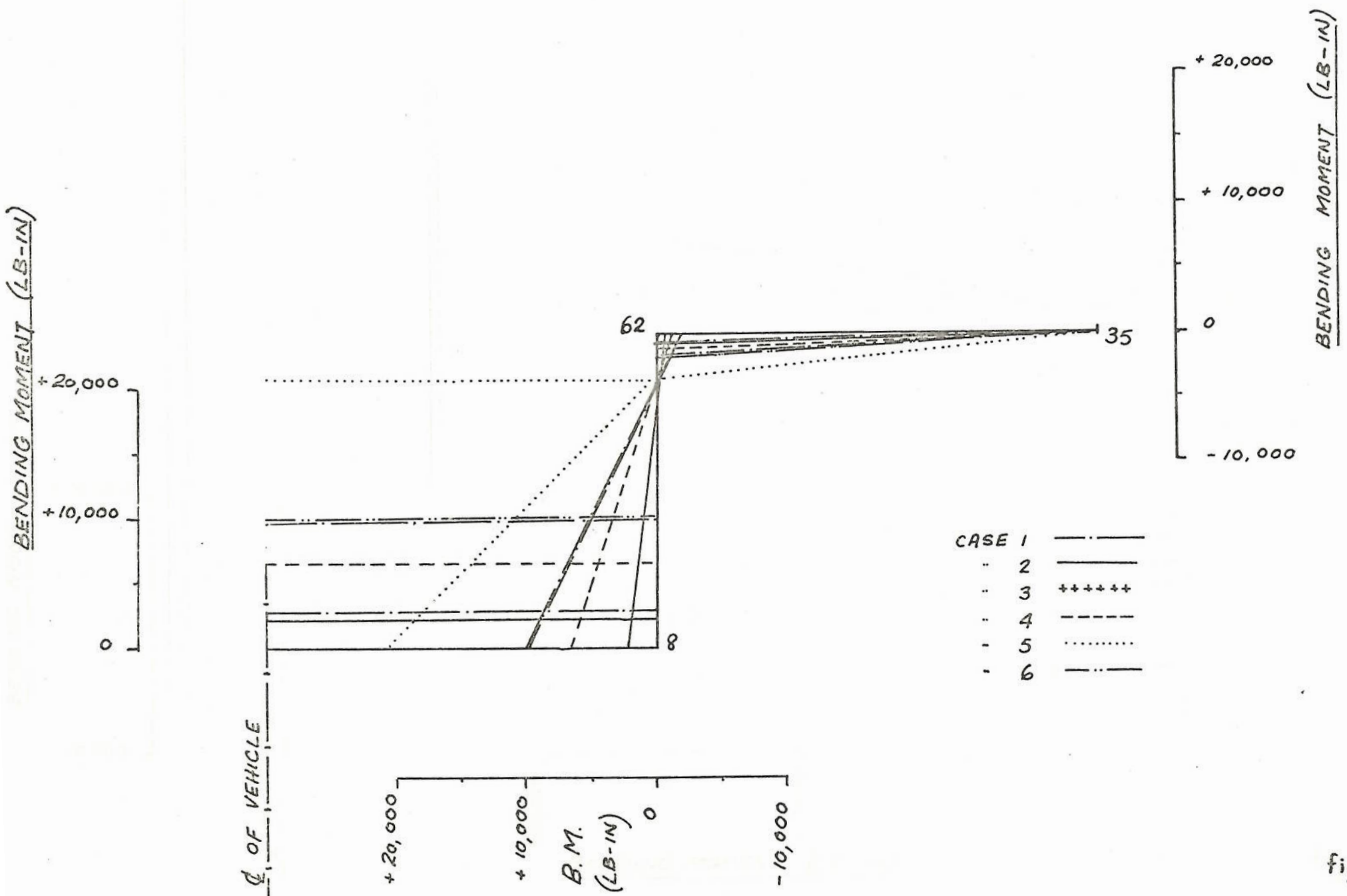

Fig. 34

BENDING MOMENTS ON CROSS MEMBER 9-63-36

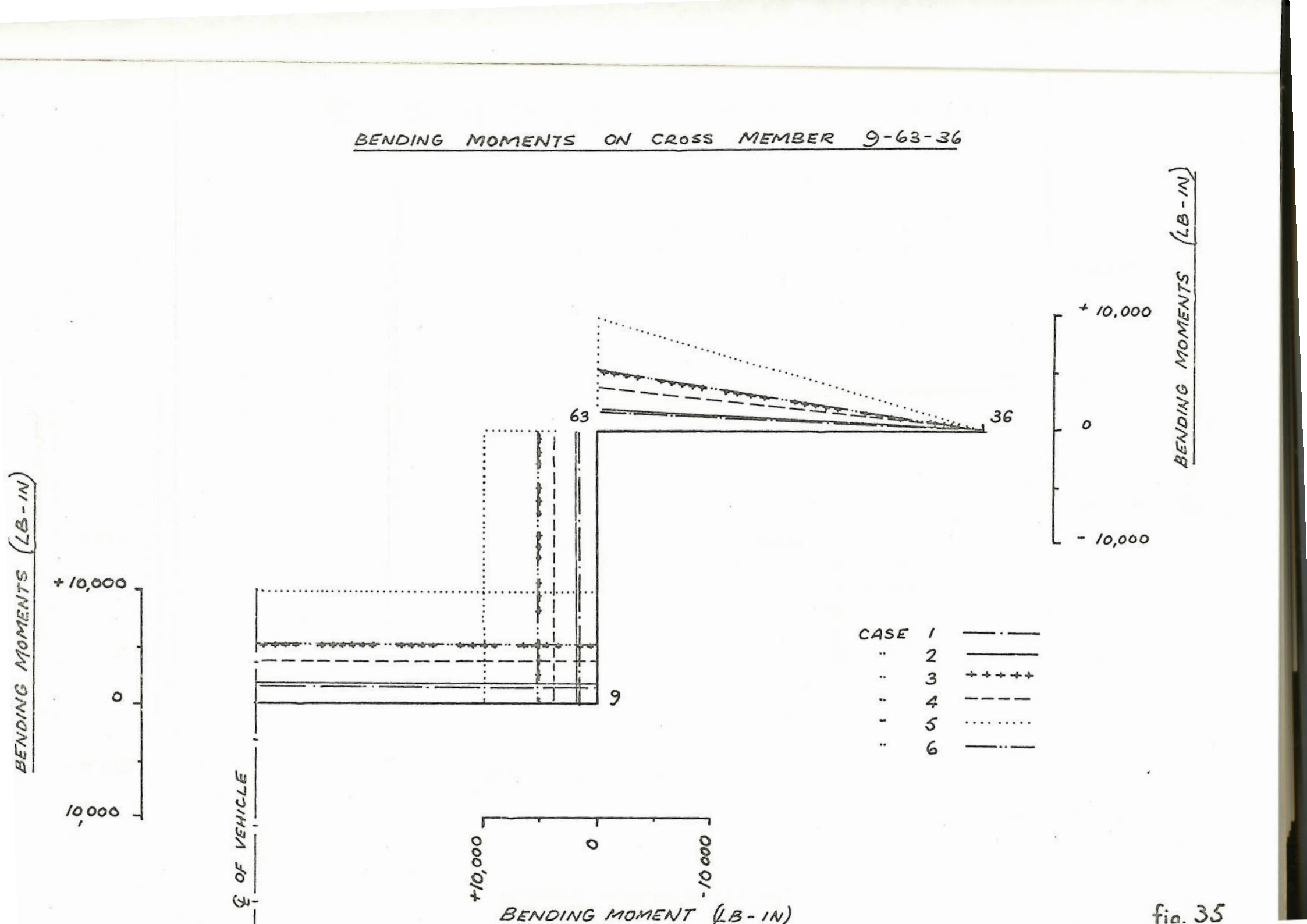

fig. 35

BENDING MOMENTS ON CROSS MEMBER 10-64-37

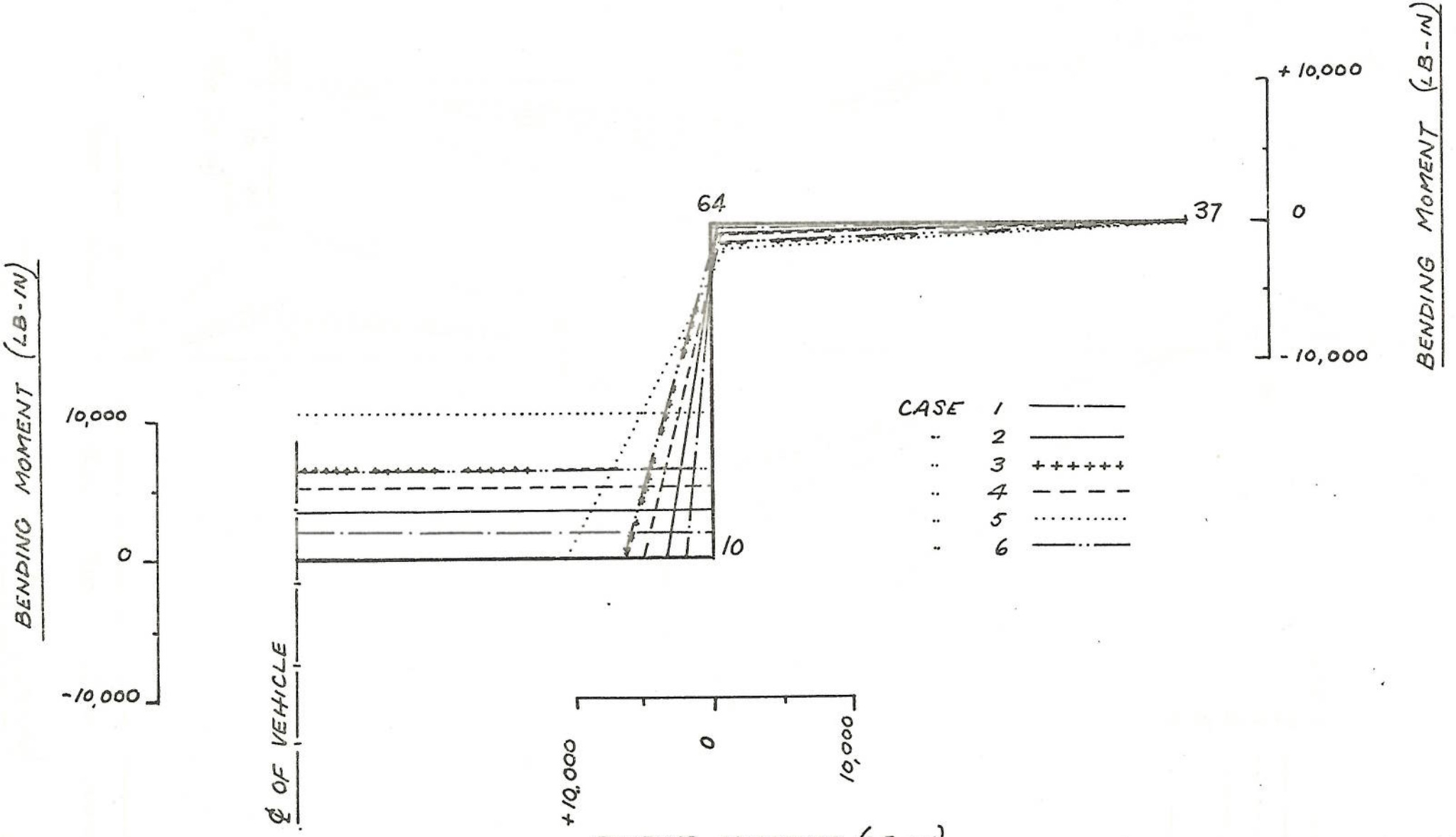

fig. 36

Mx & My BENDING MOMENTS ON DOOR PILLAR 13-56

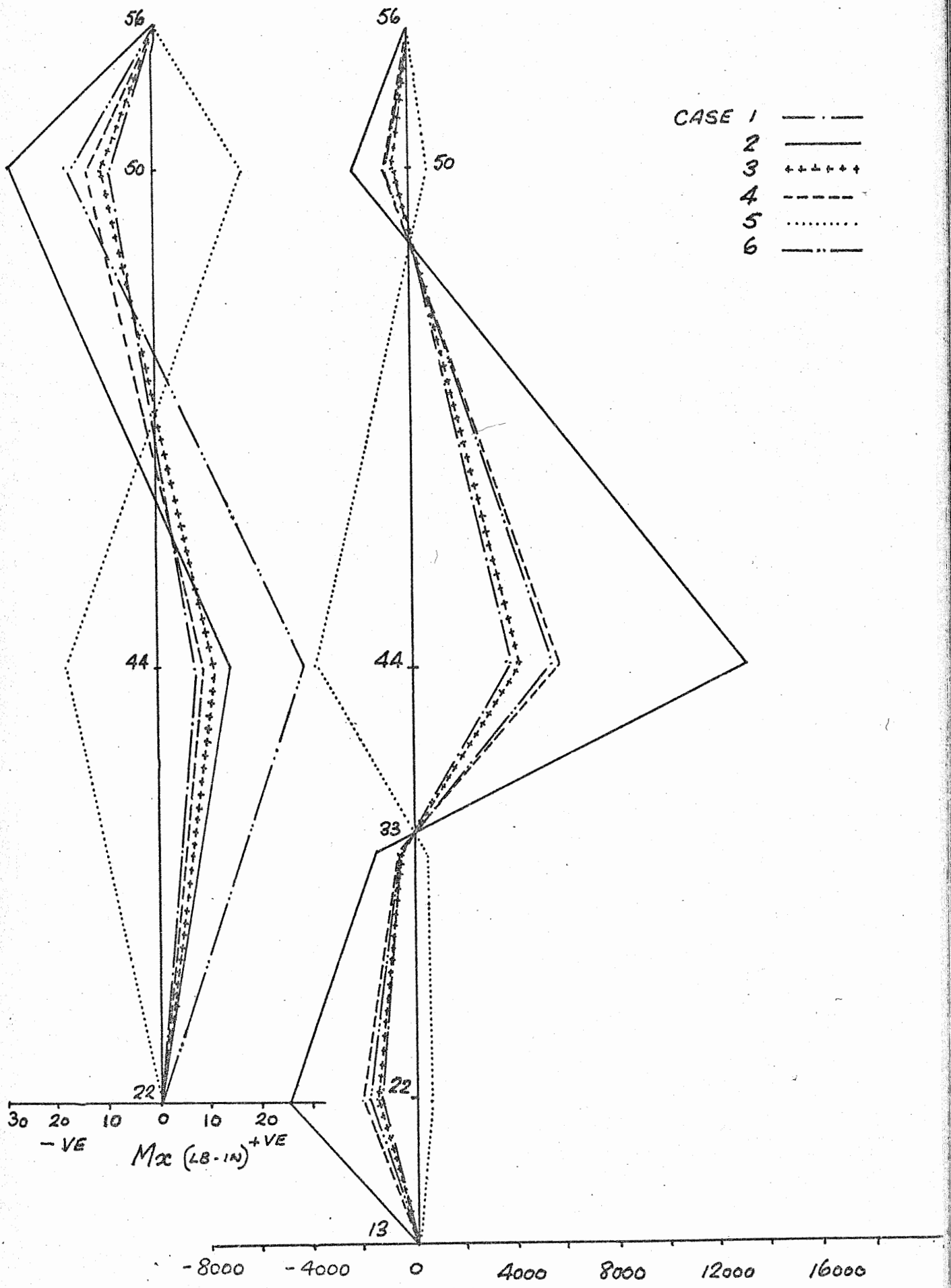

fig. 37

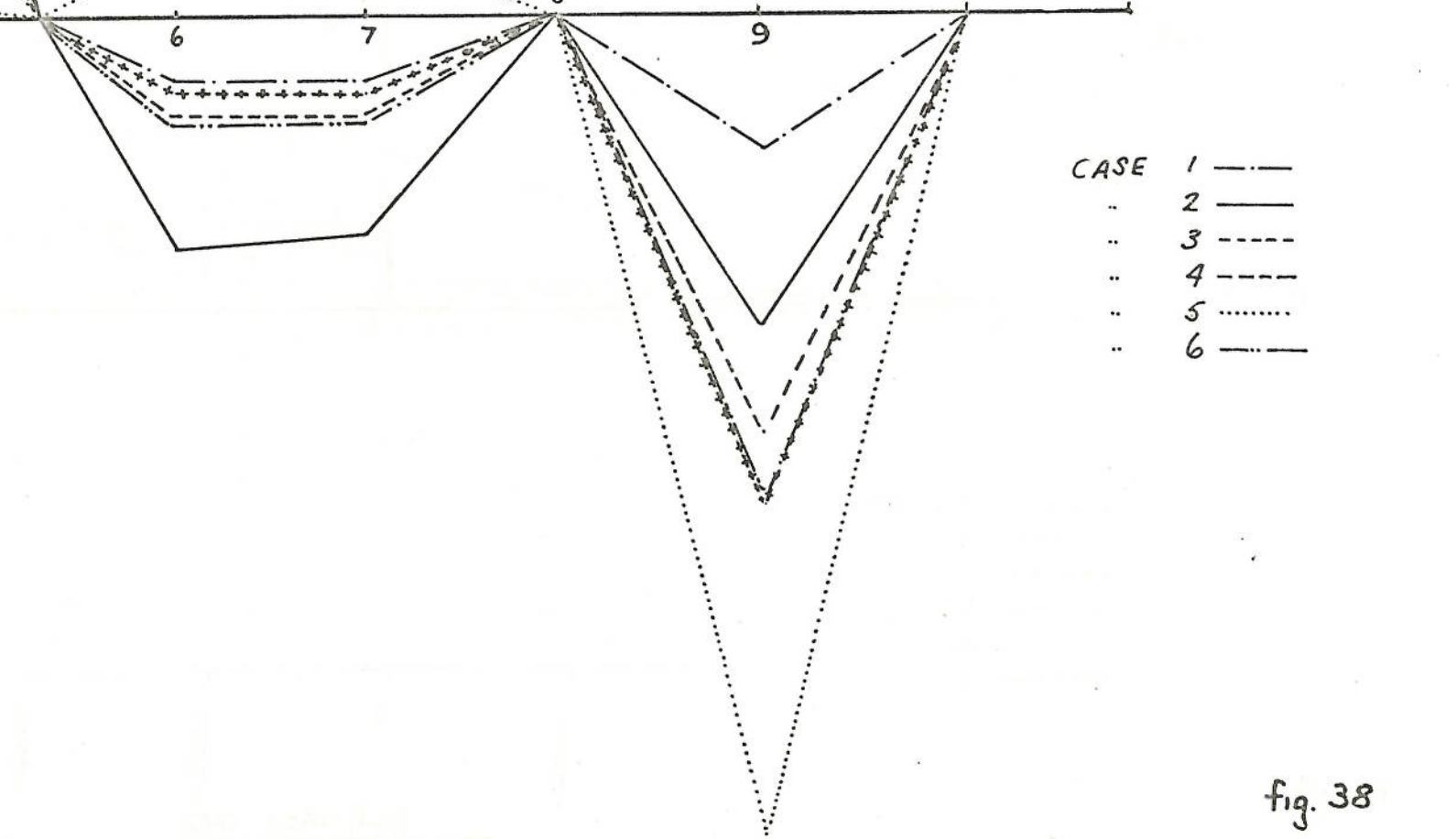

fig. 38

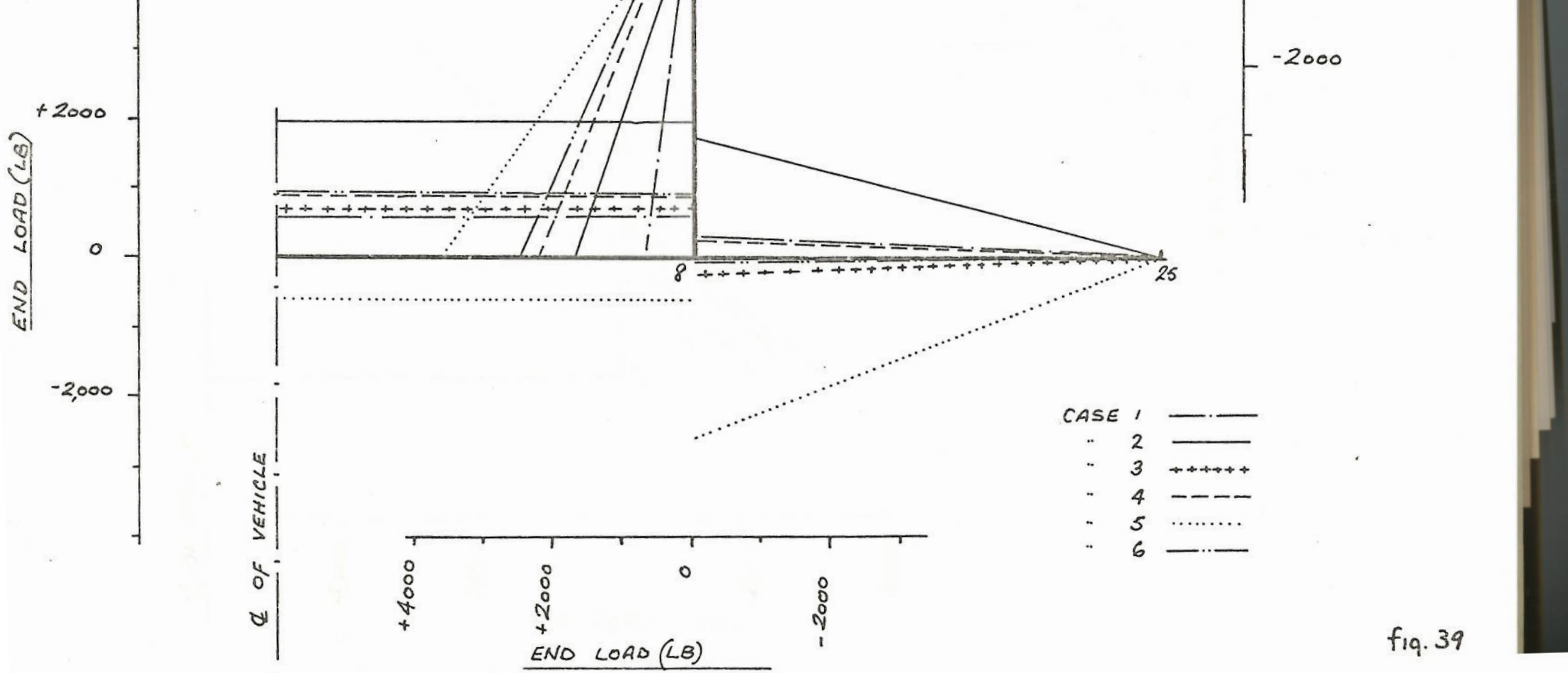
+2000
0
-2,000
END LOAD (LB)
-2000
8
25
CASE 1
2
3
4
5
6
℄ OF VEHICLE
+4000
+2000
0
-2000
END LOAD (LB)

fig. 39

END LOAD IN CROSS MEMBERS 9-63-36

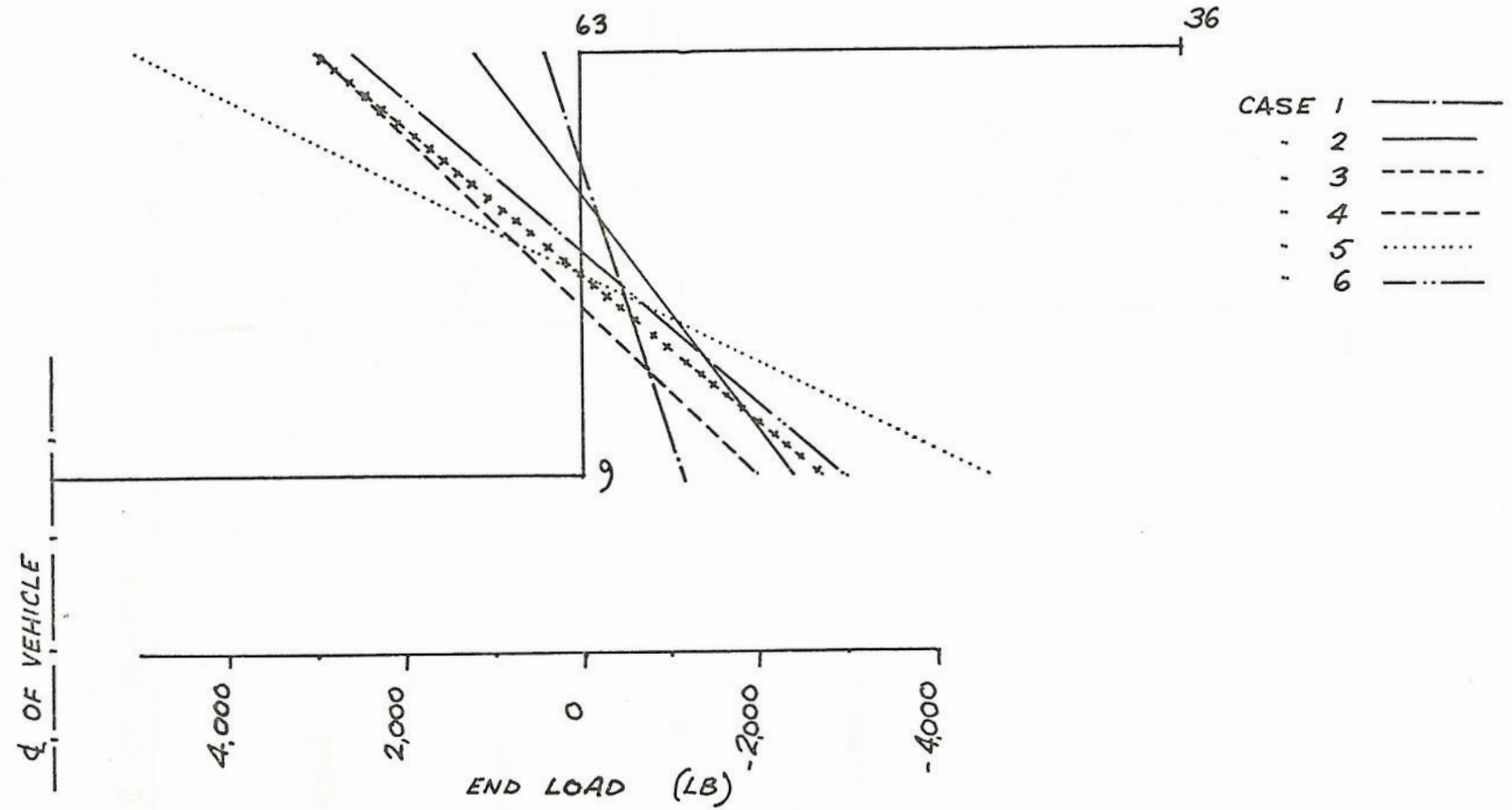

fig 40

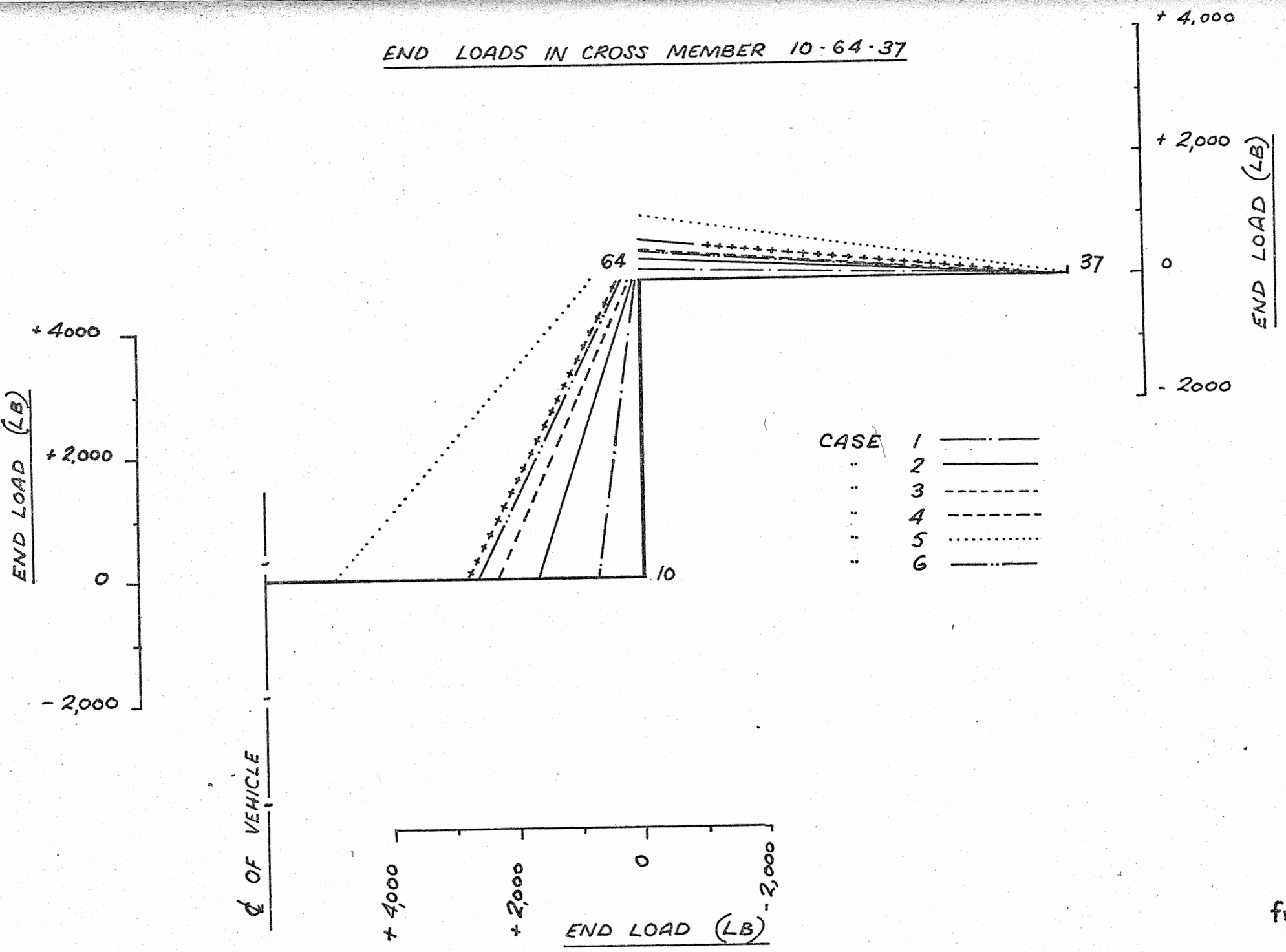
END LOADS IN CROSS MEMBER 10-64-37
+ 4,000
+ 2,000
0
- 2000
END LOAD (LB)
64
37
10
CASE 1
2
3
4
5
6
+4000
+2,000
0
- 2,000
END LOAD (LB)
℄ OF VEHICLE
+ 4,000
+ 2,000
0
- 2,000
END LOAD (LB)

fig 41

END LOADS IN TOP OUTER WING MEMBER 39 - 44

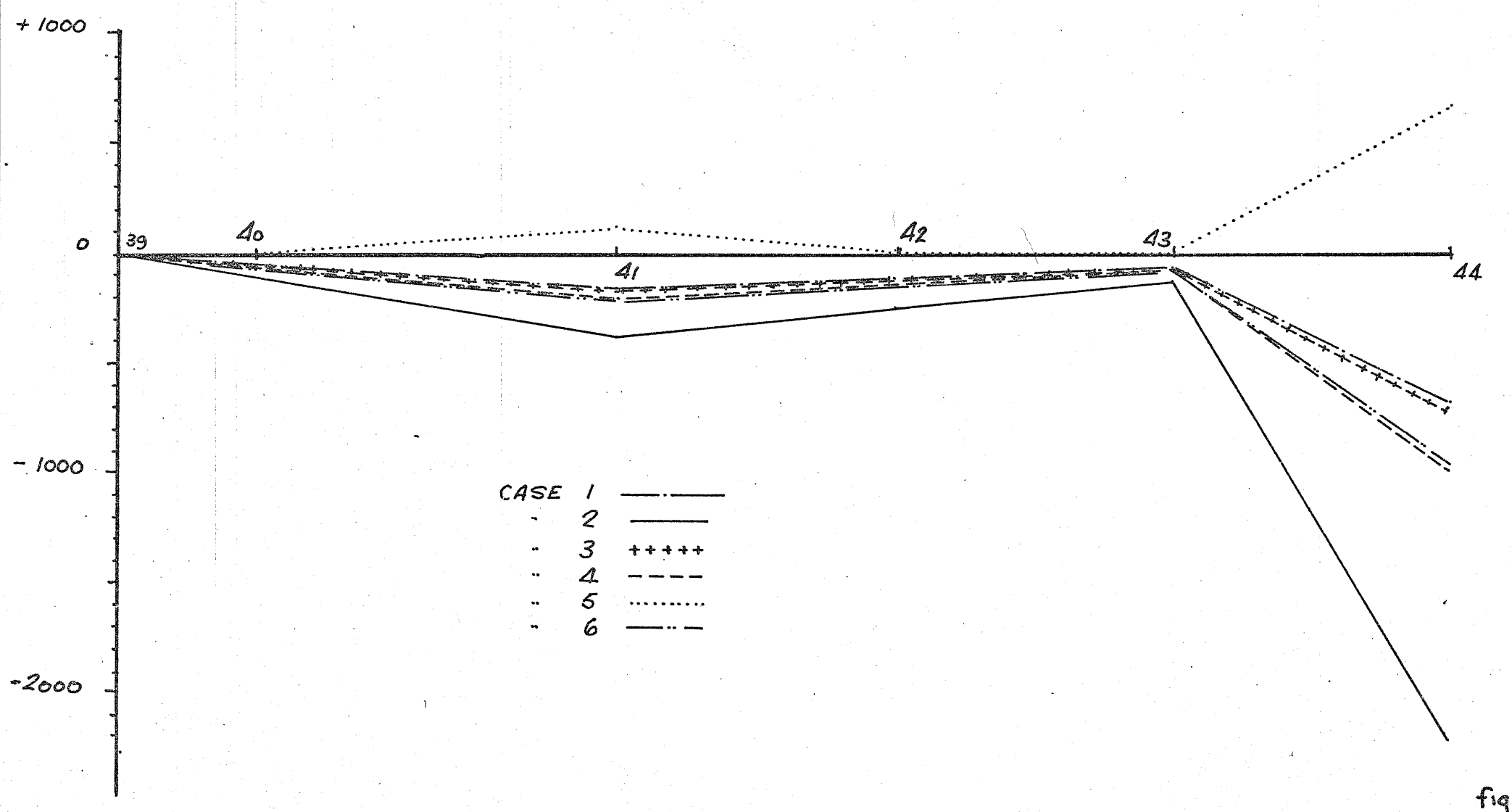

fig. 42

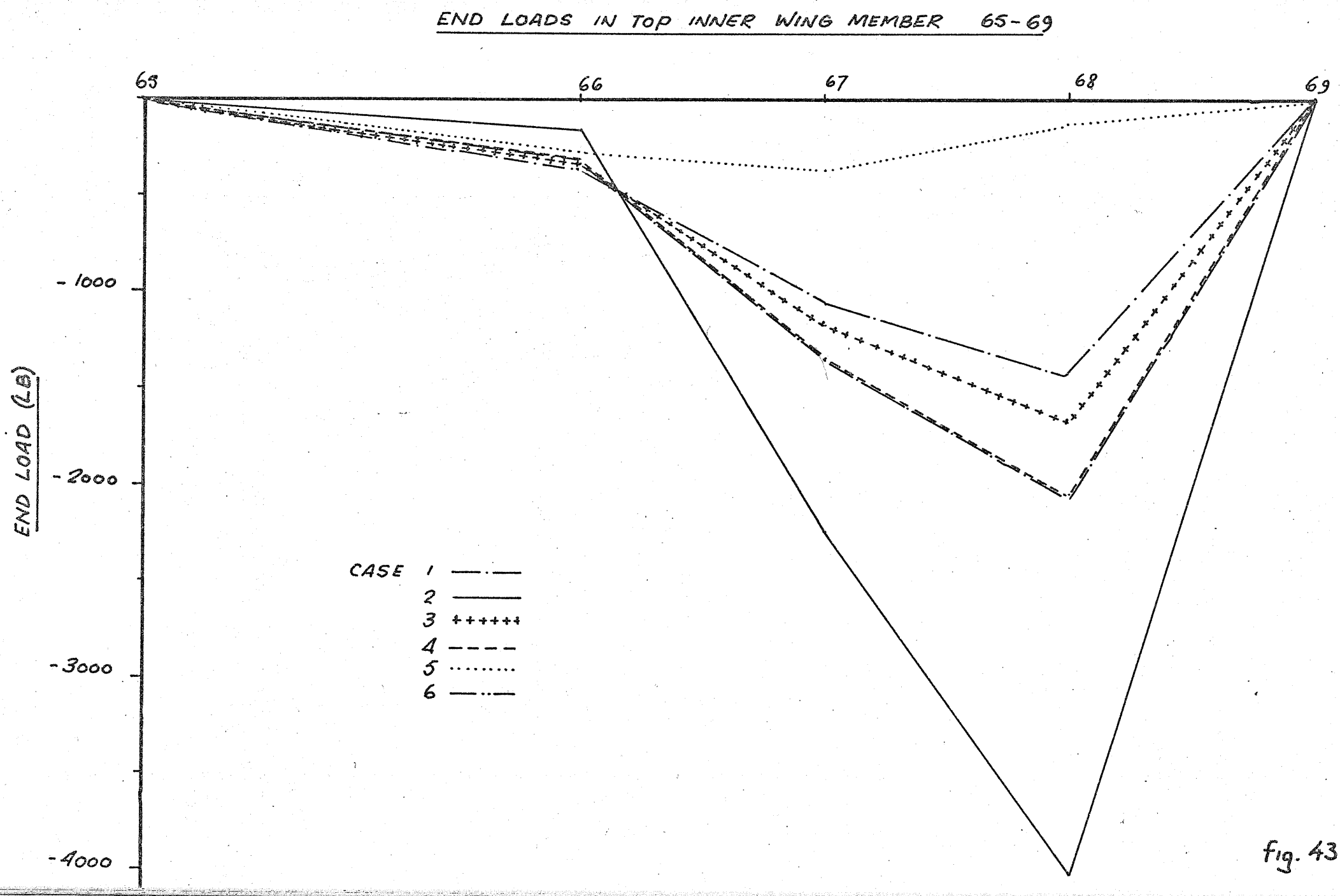
END LOADS IN TOP INNER WING MEMBER 65-69
65
66
67
68
69
-1000
-2000
-3000
-4000
END LOAD (LB)
CASE 1
2
3
4
5
6

Fig. 43

END LOADS IN SILL MEMBERS 21-25 & 12-16

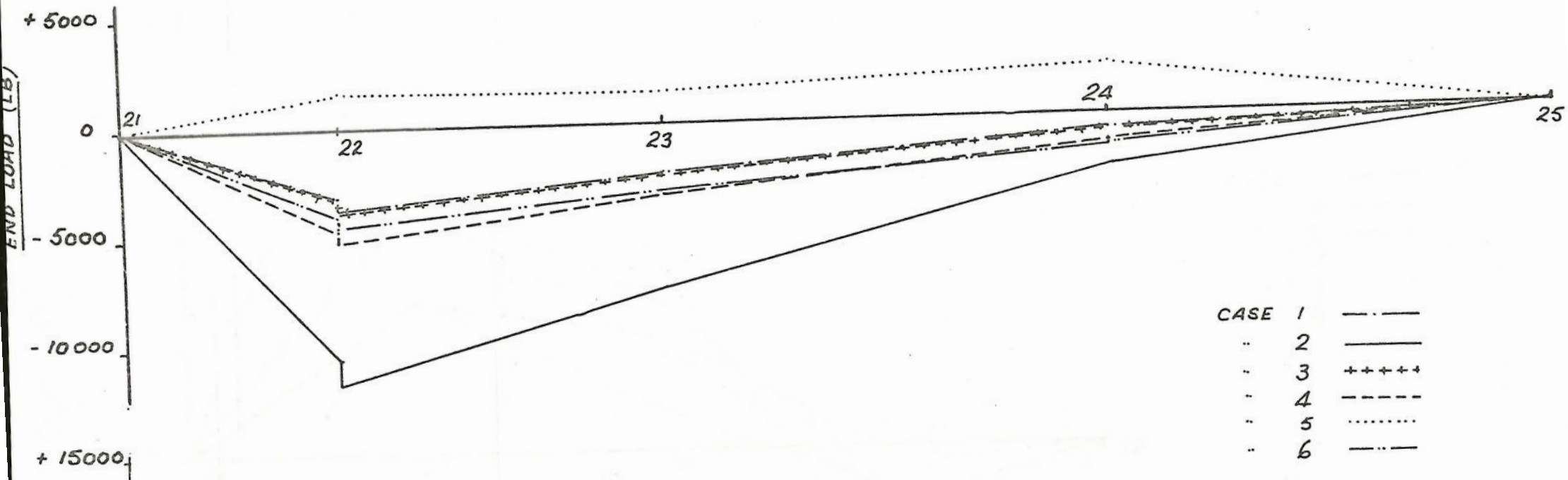

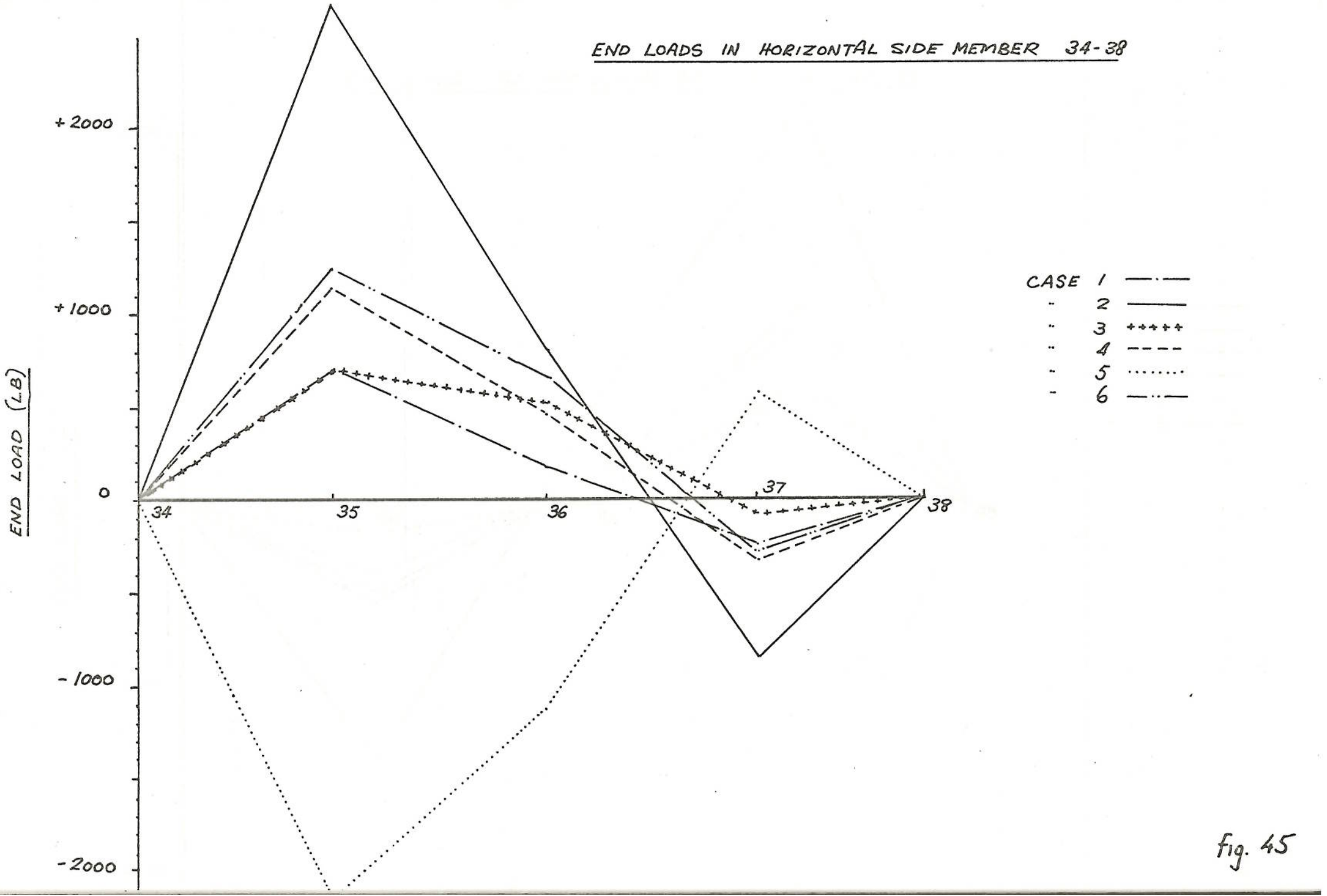
END LOADS IN HORIZONTAL SIDE MEMBER 34-38
+2000
+1000
0
-1000
-2000
END LOAD (LB)
34
35
36
37
38
CASE 1
2
3
4
5
6

Fig. 45

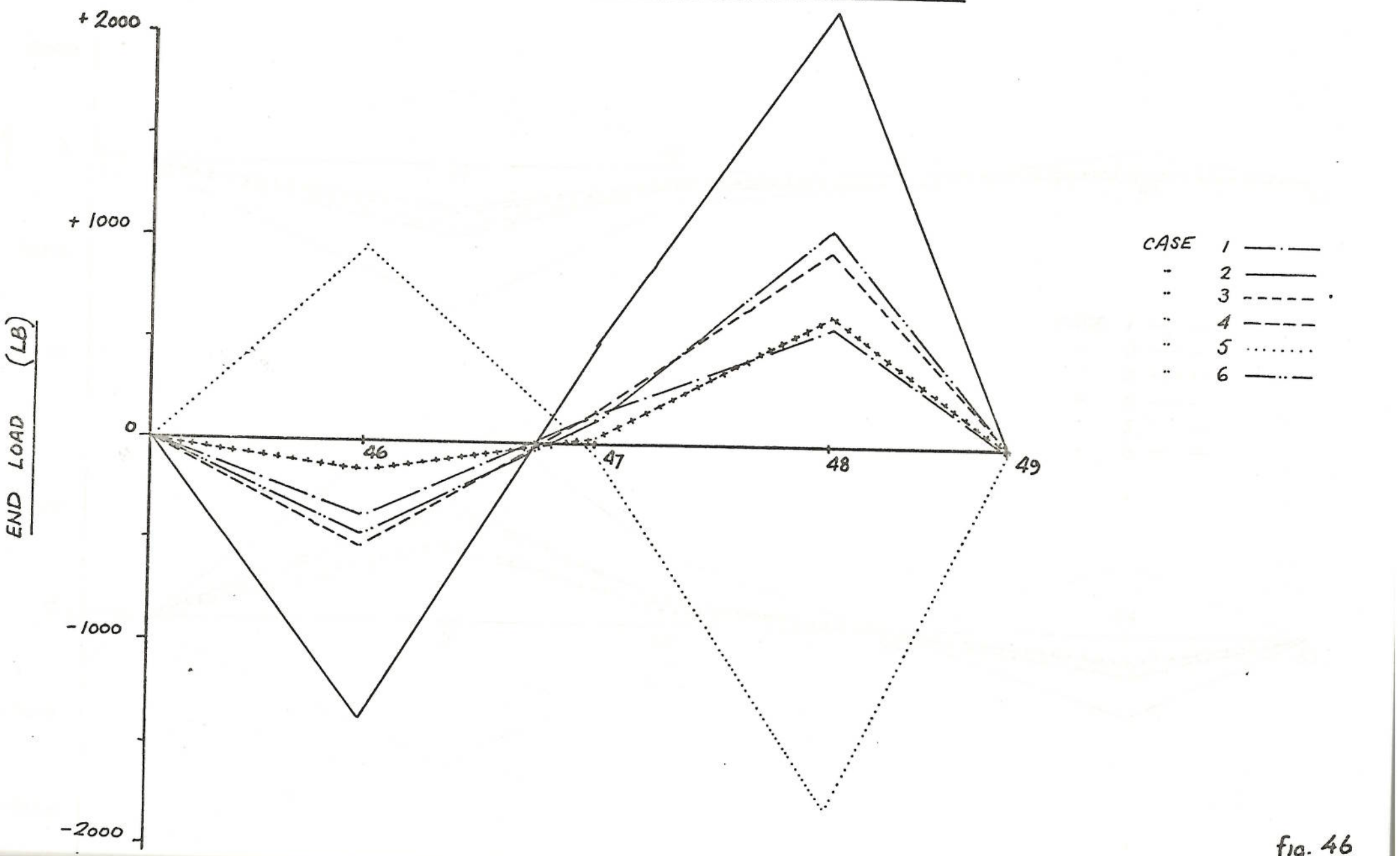
END LOADS IN HORIZONTAL SIDE MEMBER 49 - 49
+ 2000
+ 1000
0
-1000
-2000
END LOAD (LB)
46
47
48
49
CASE 1
2
3
4
5
6

fig. 46

END LOADS IN MEMBERS 56 - 61 & 50 - 55

(BENDING LOAD CASE - NO TORSION)

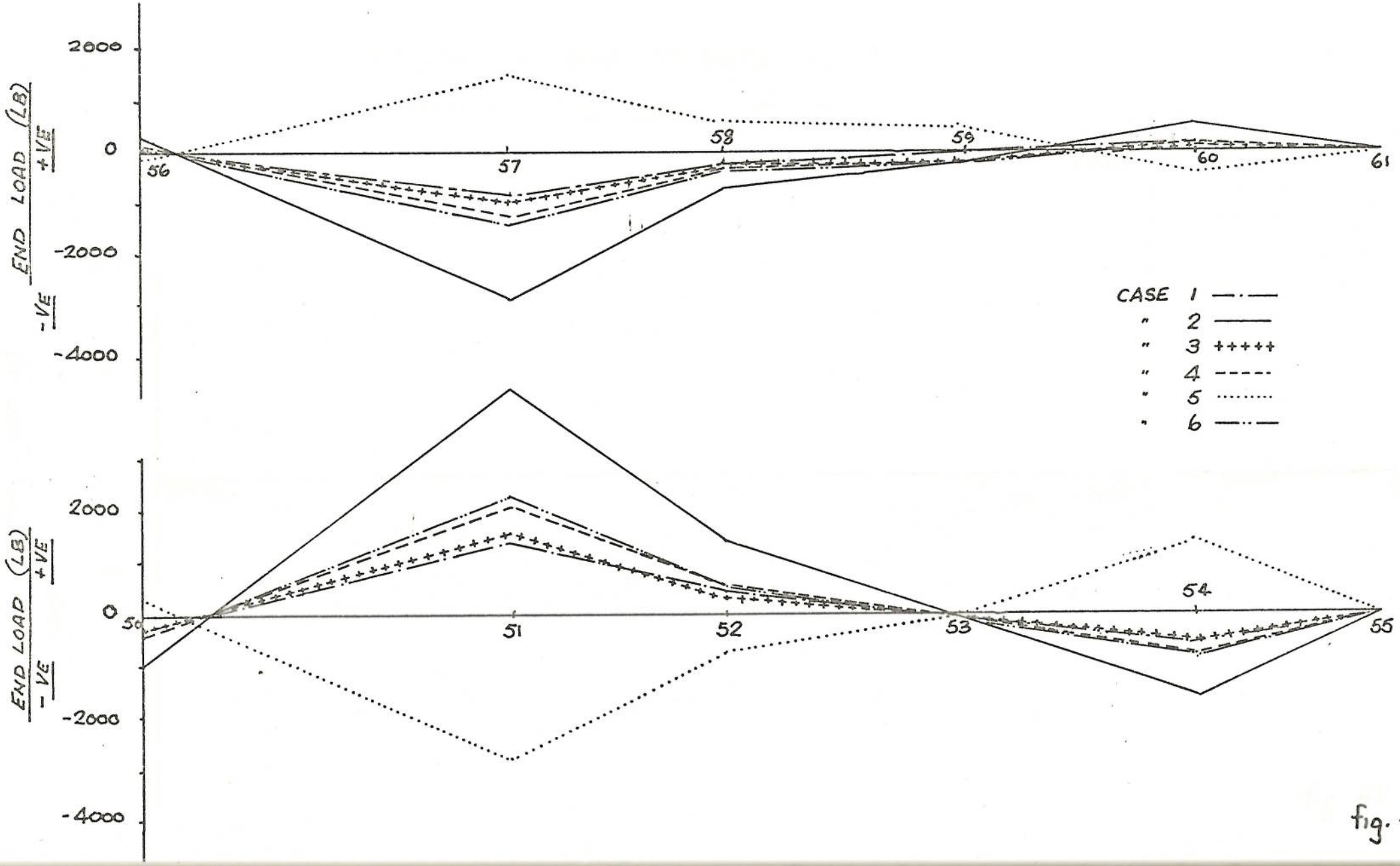

fig. 47

END LOAD IN ROOF MEMBERS 70-75

[BENDING LOAD CASE - NO TORSION]

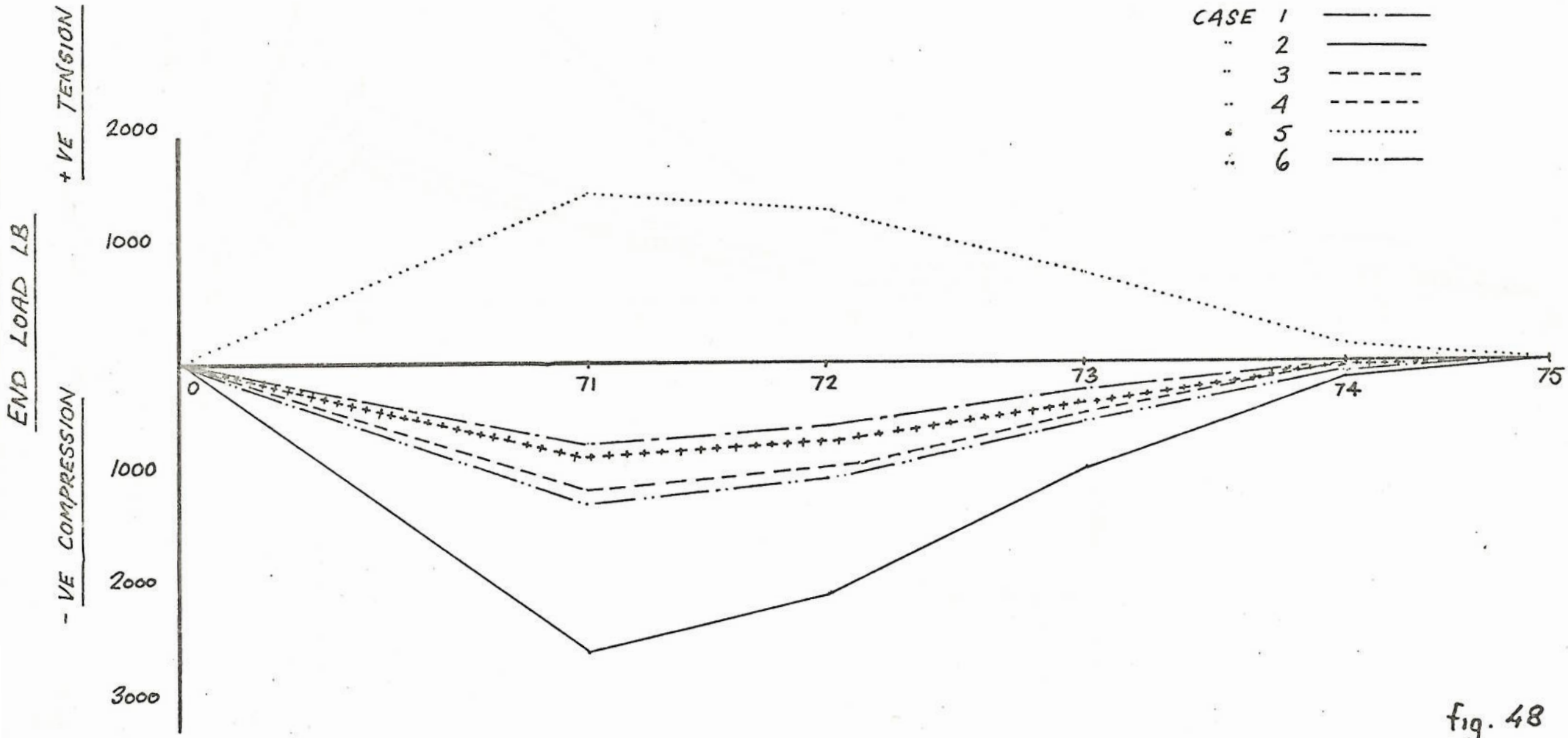

fig. 48

END LOADS IN DOOR / WSCREEN PILLAR 13-56

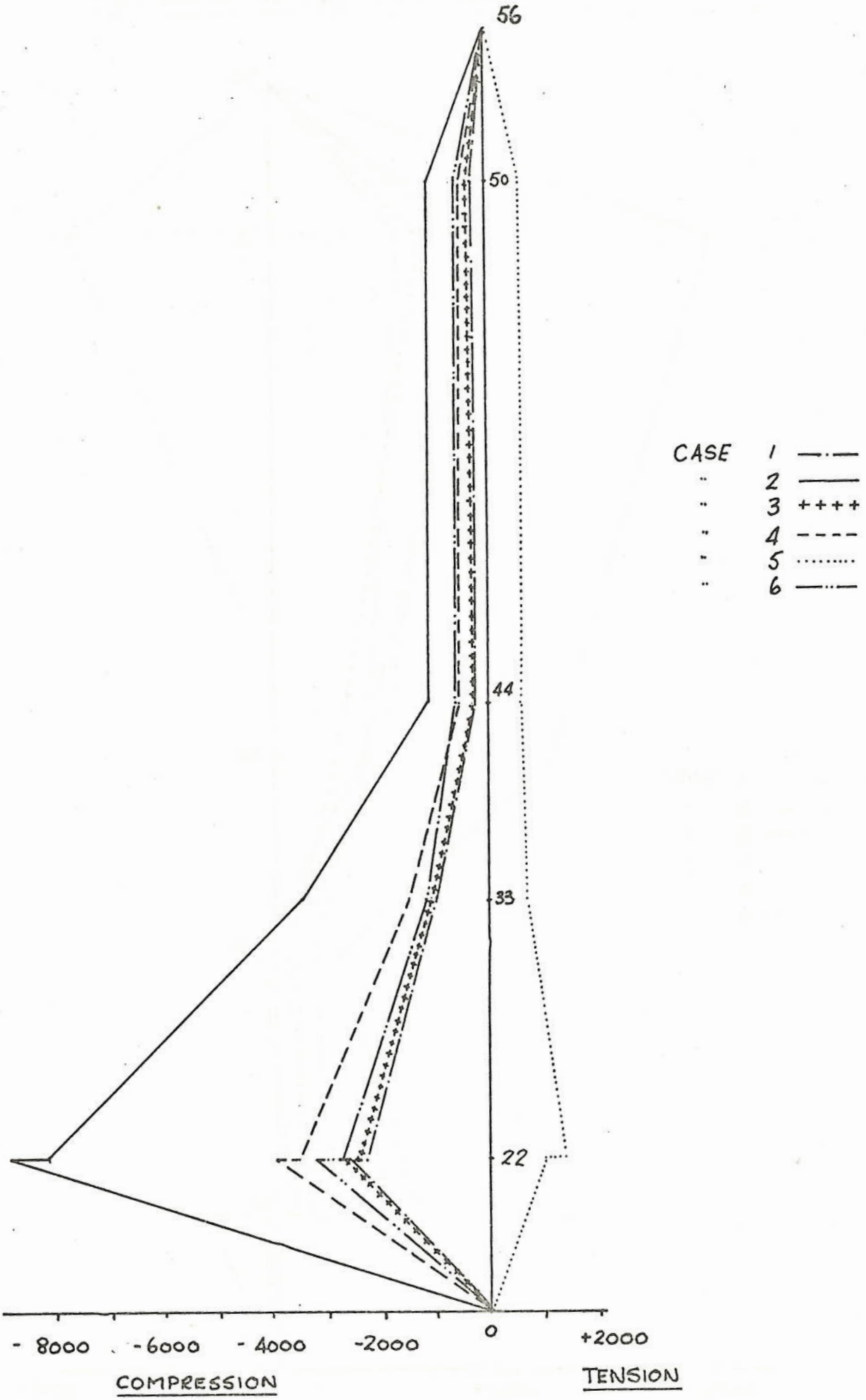

fig. 49

END LOADS IN SIDE DOOR REAR PILLAR 15-57

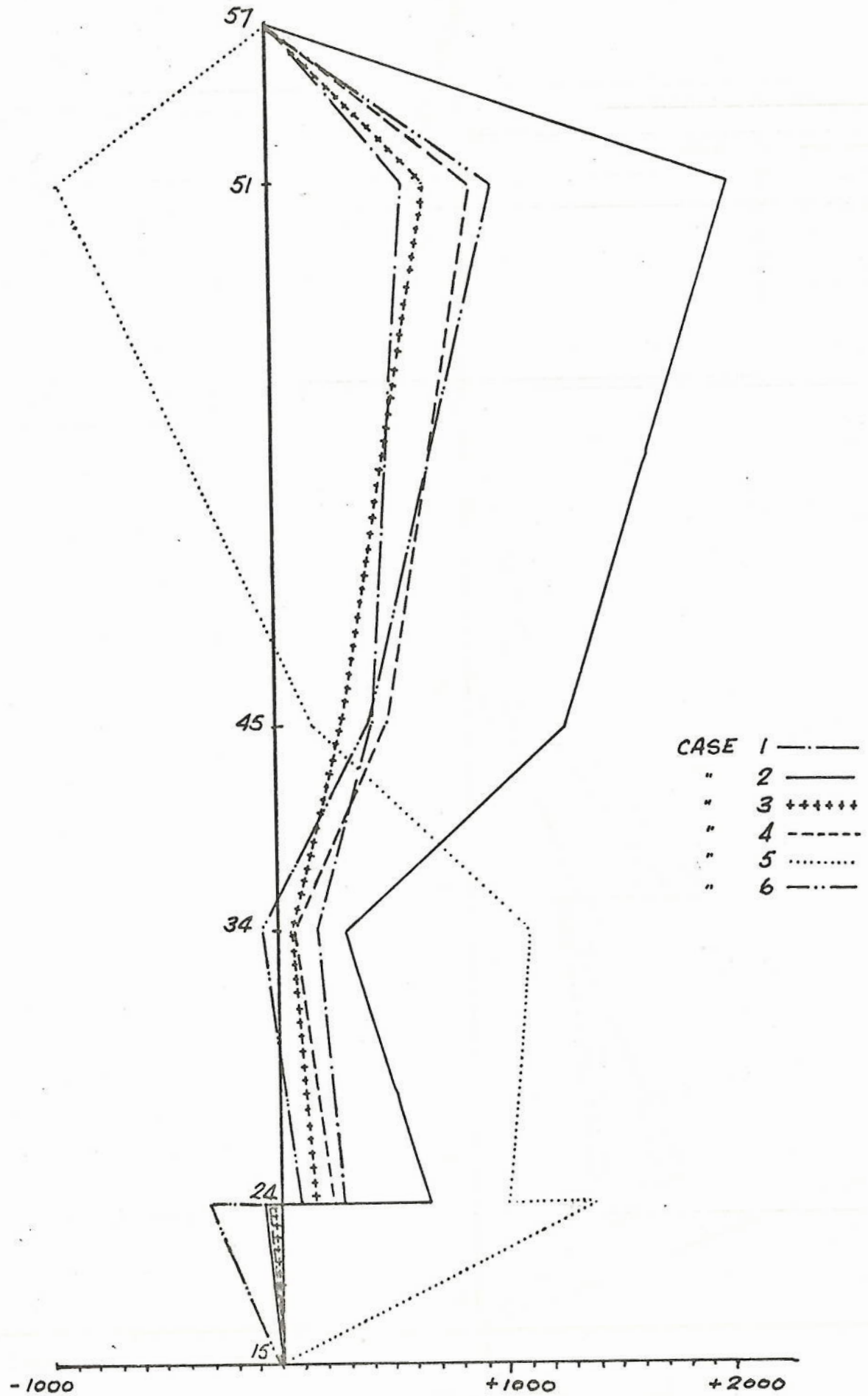

fig. 50

END LOADS IN VERTICAL SIDE MEMBER 16-58

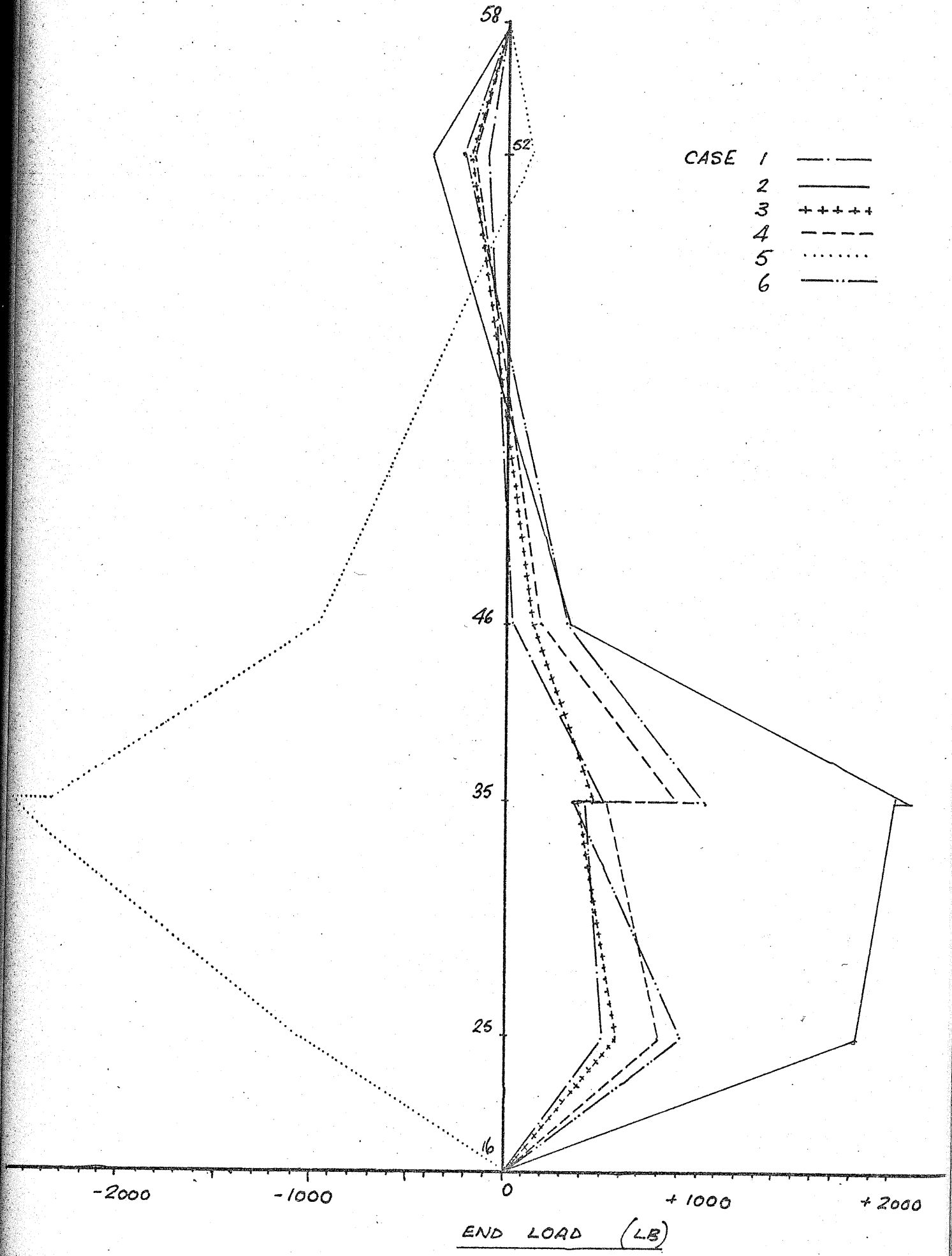

fig. 51

END LOADS IN VERTICAL SIDE MEMBER 36 - 59

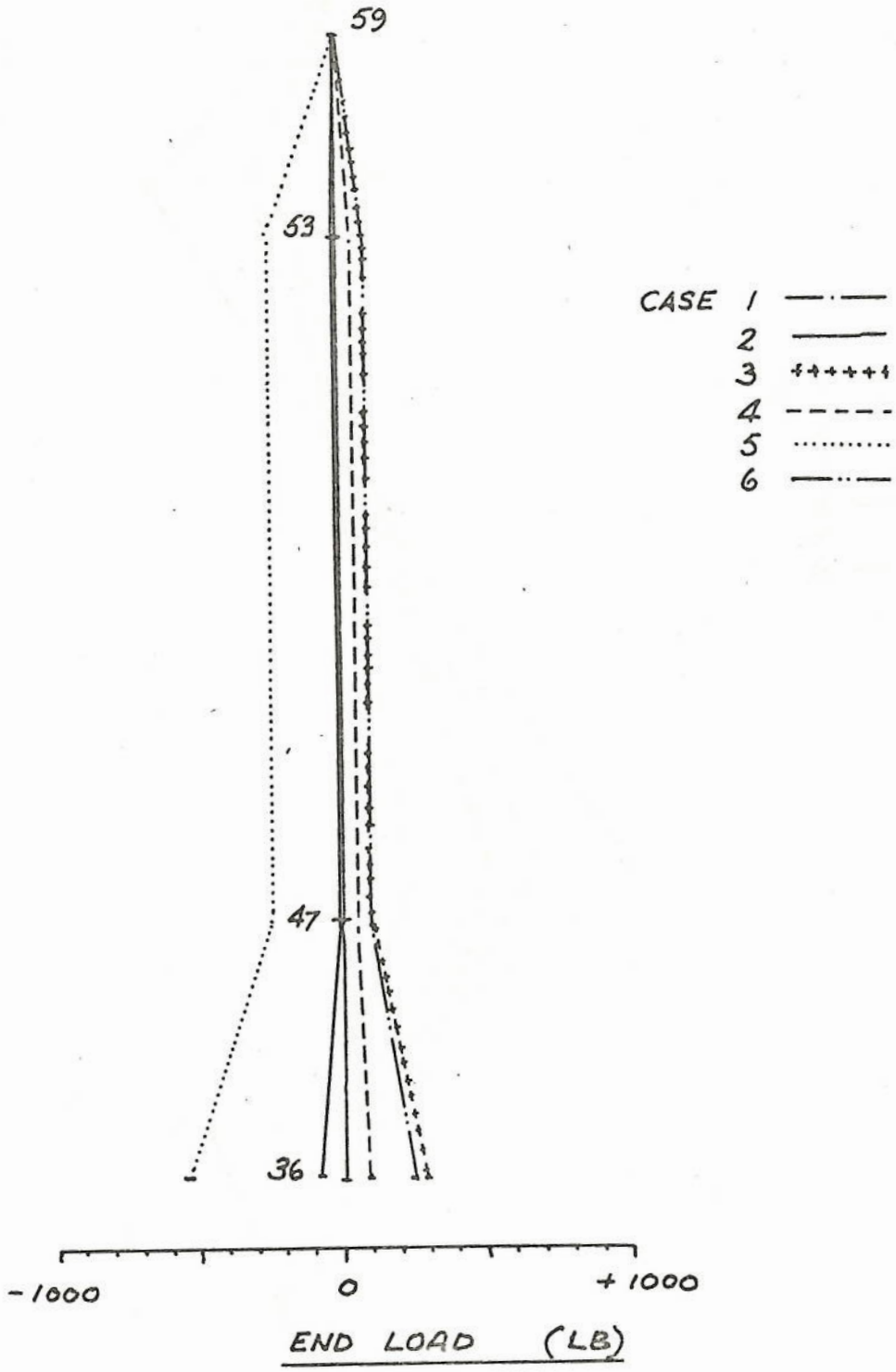

fig 52

END LOAD IN VERTICAL SIDE MEMBER 17 - 60

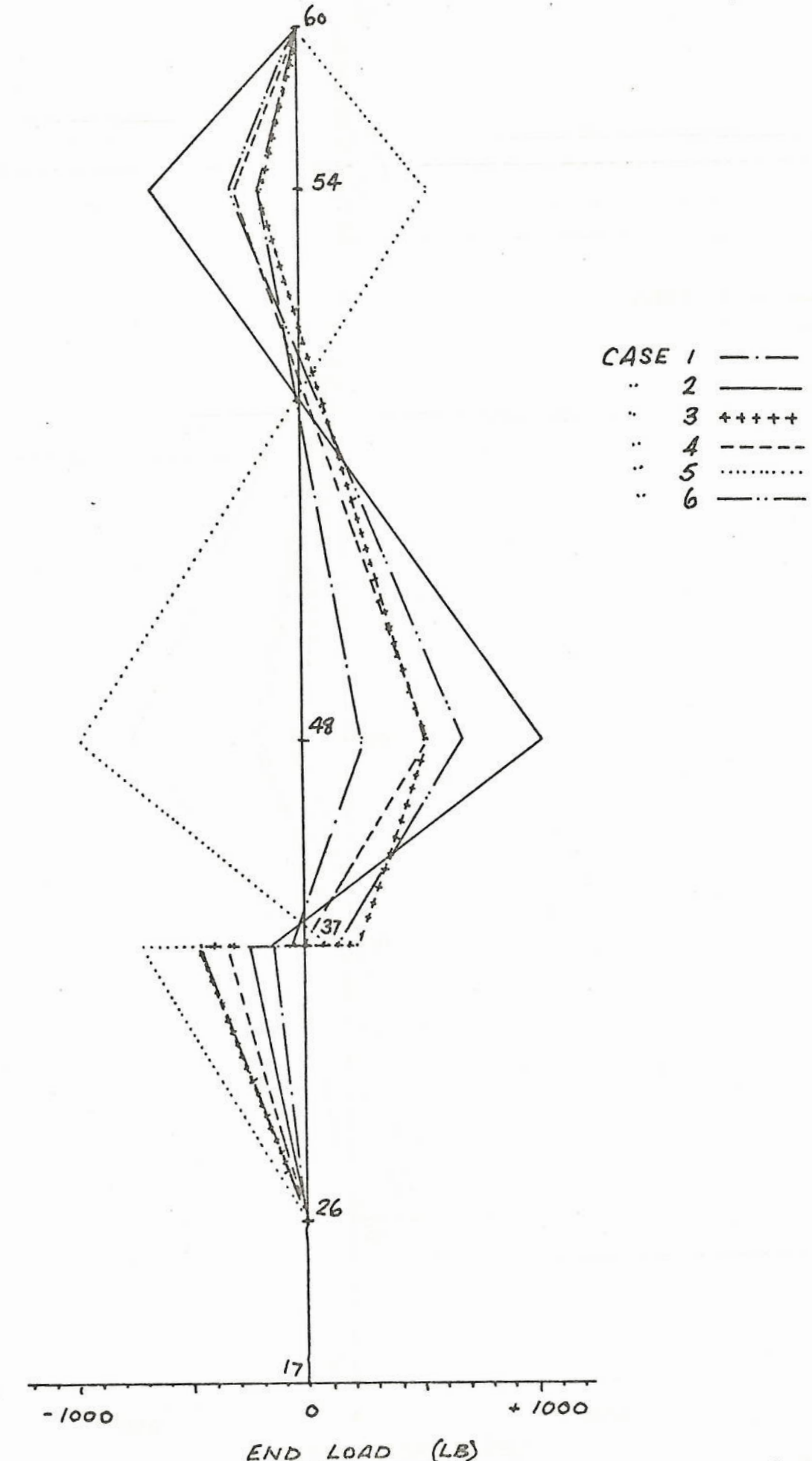

fig. 53

END LOADS IN VERTICAL CORNER MEMBER 18-61

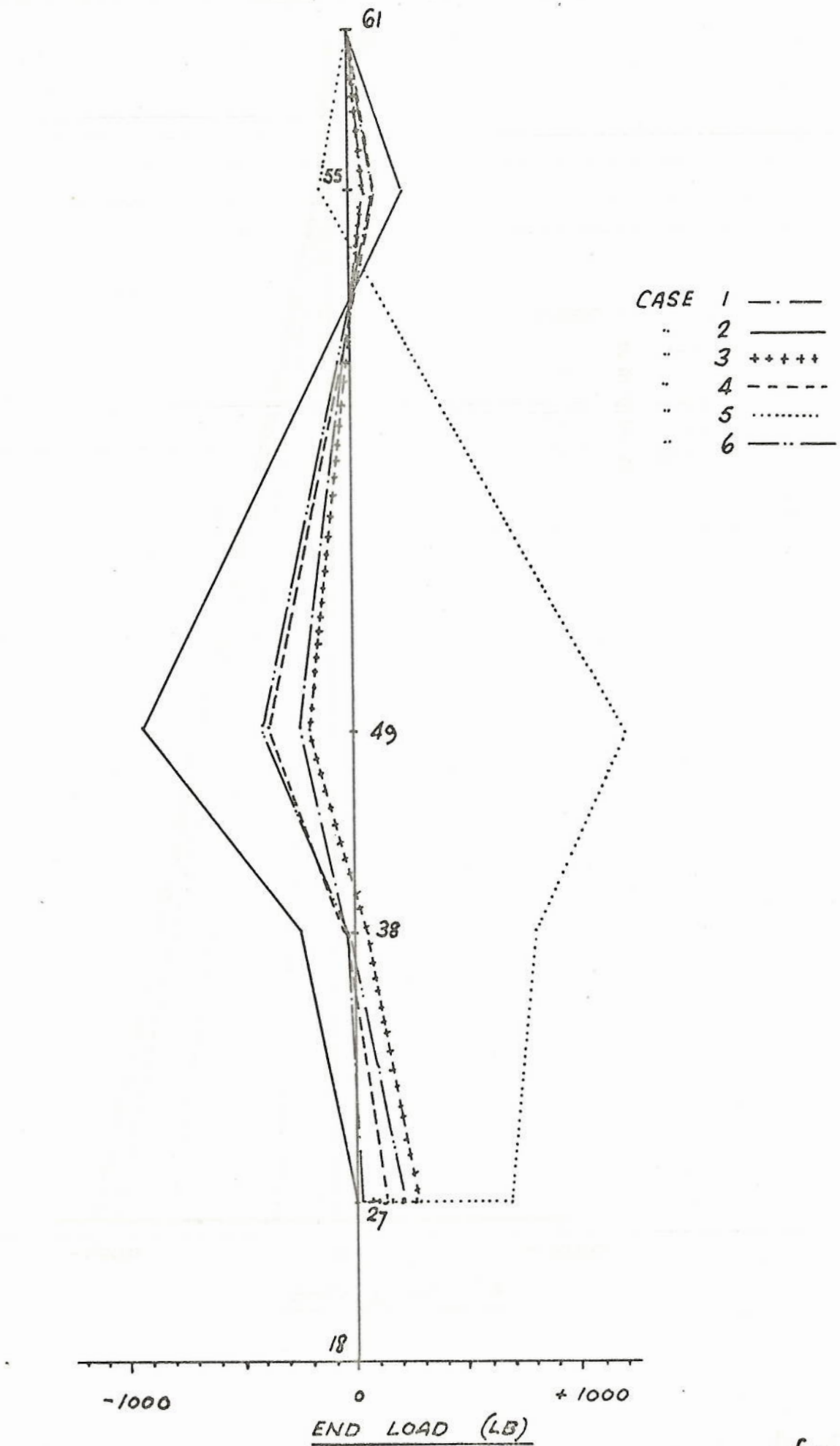

fig. 54

END LOADS IN REAR DOOR PILLAR 11-75

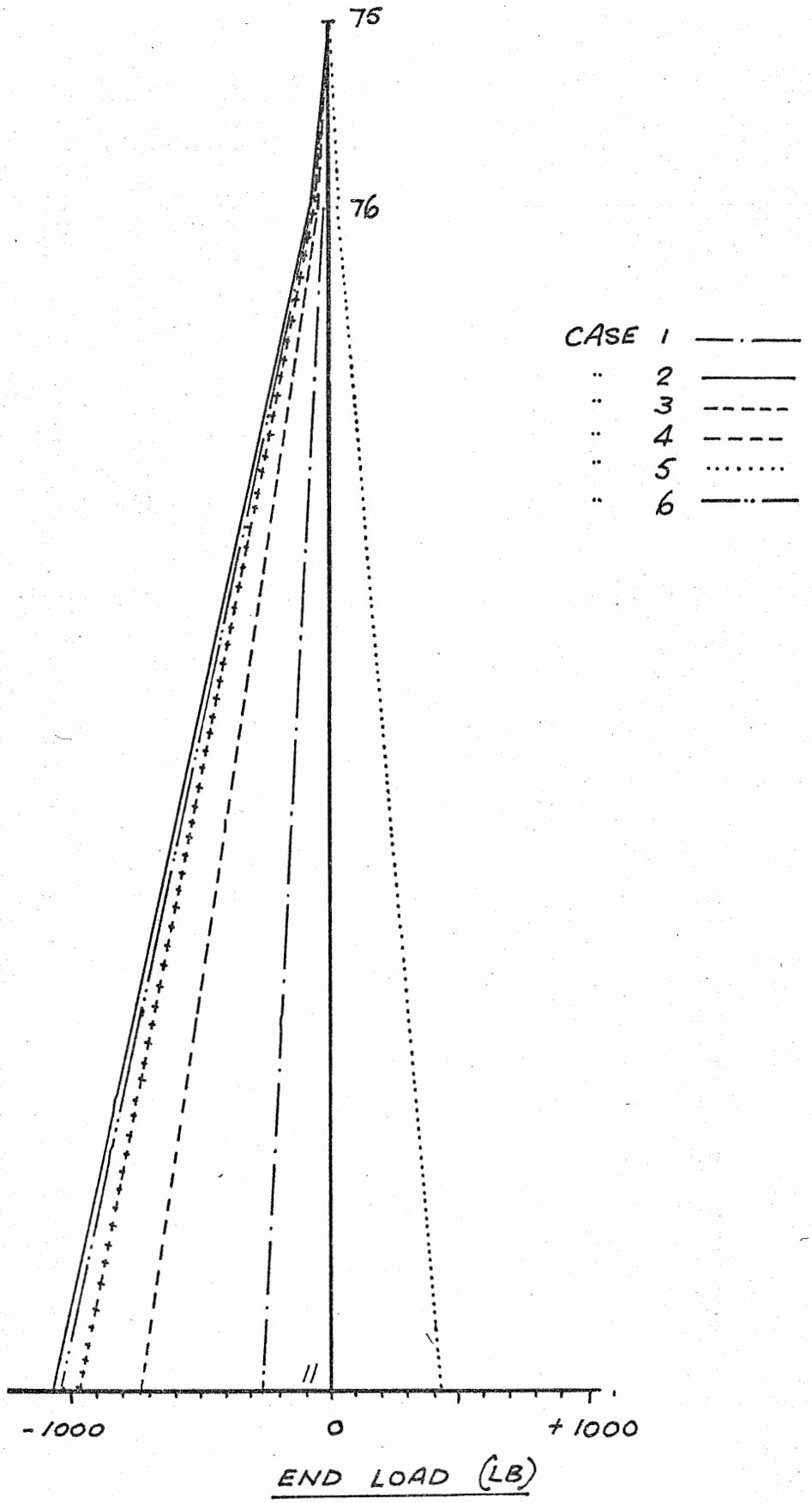

fig. 55

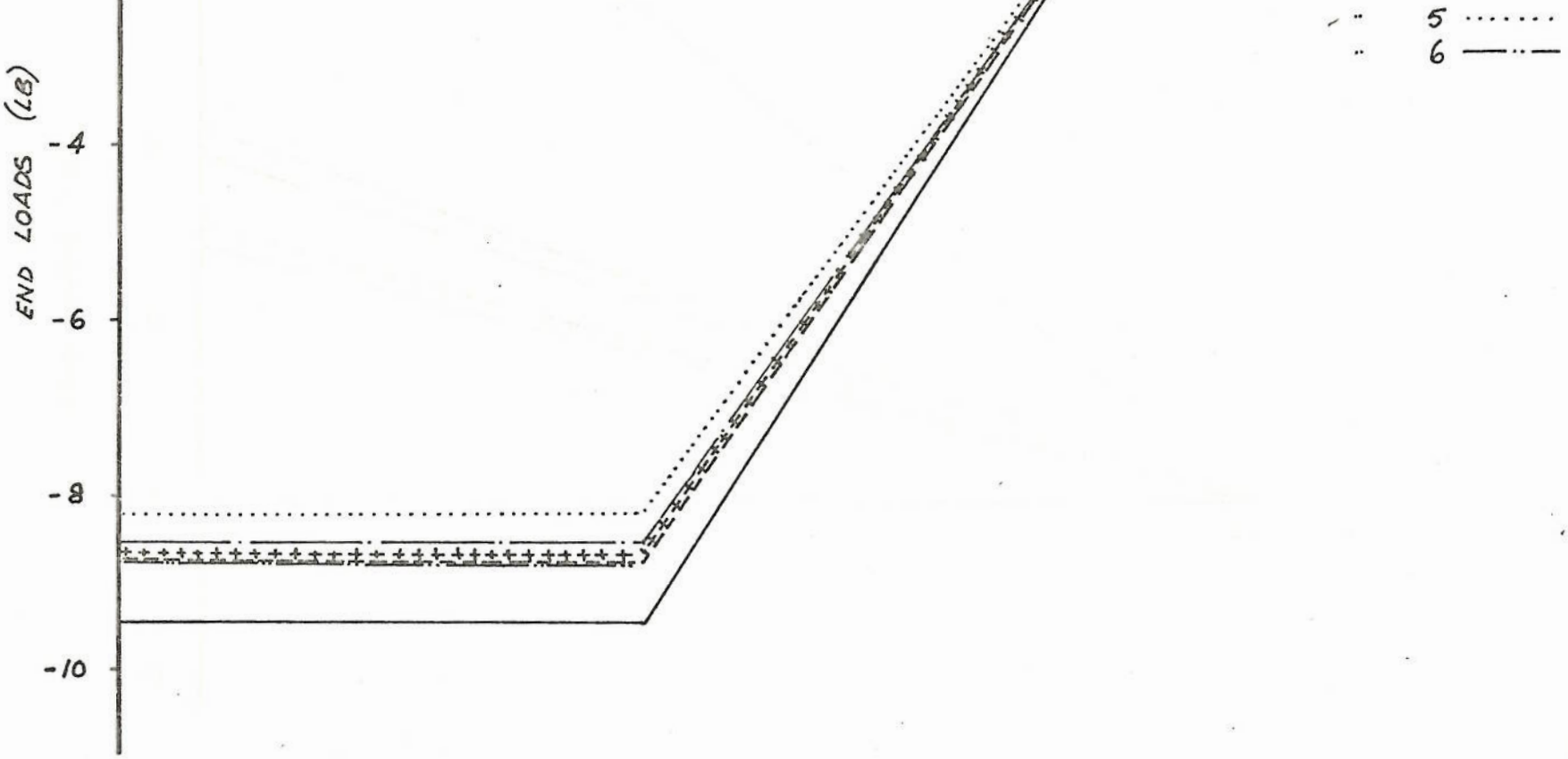

fig. 56

END LOADS & CROSSMEMBERS (4 - 21)

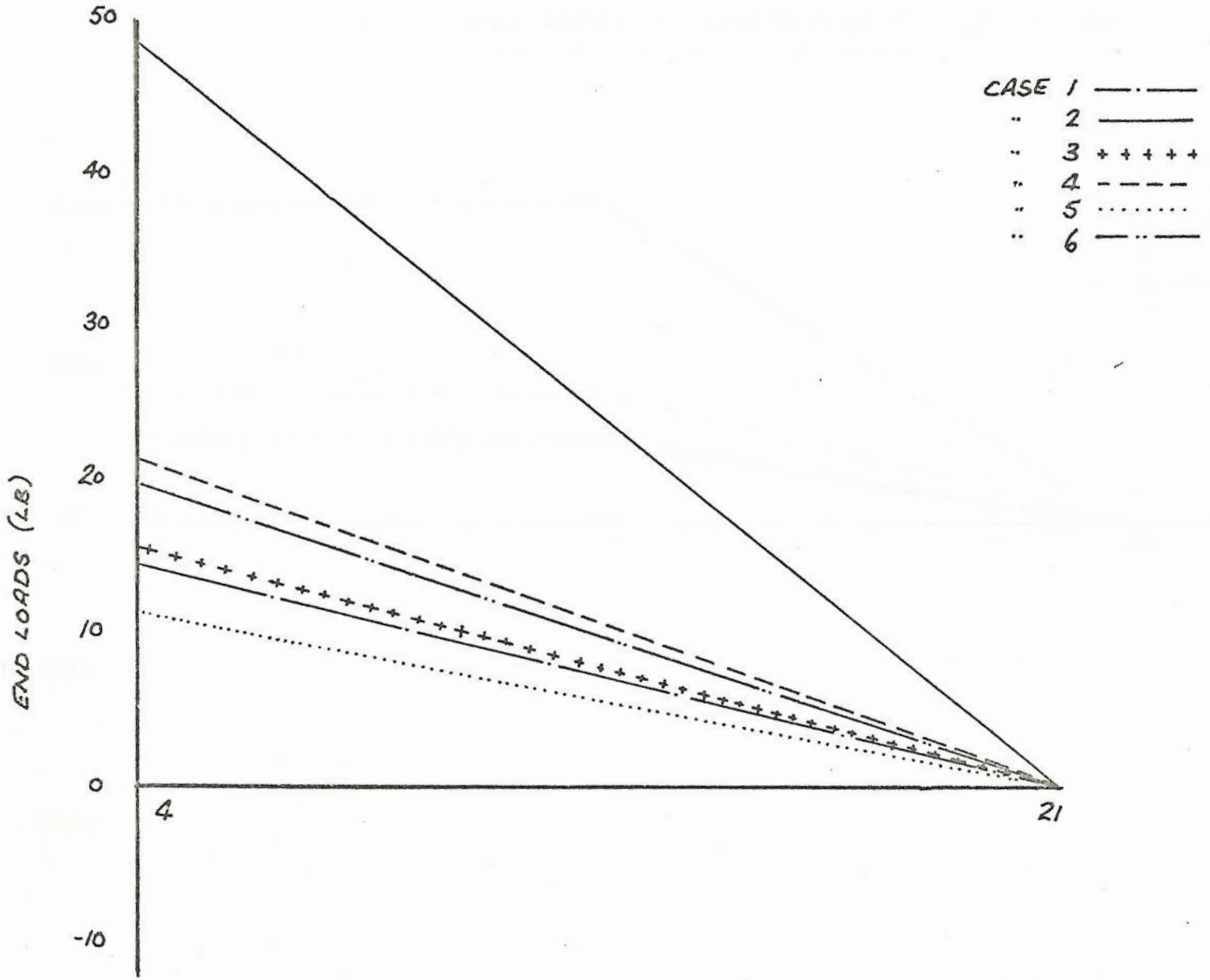

fig. 57

END LOADS IN CROSSMEMBER (℄ - 5 - 22)

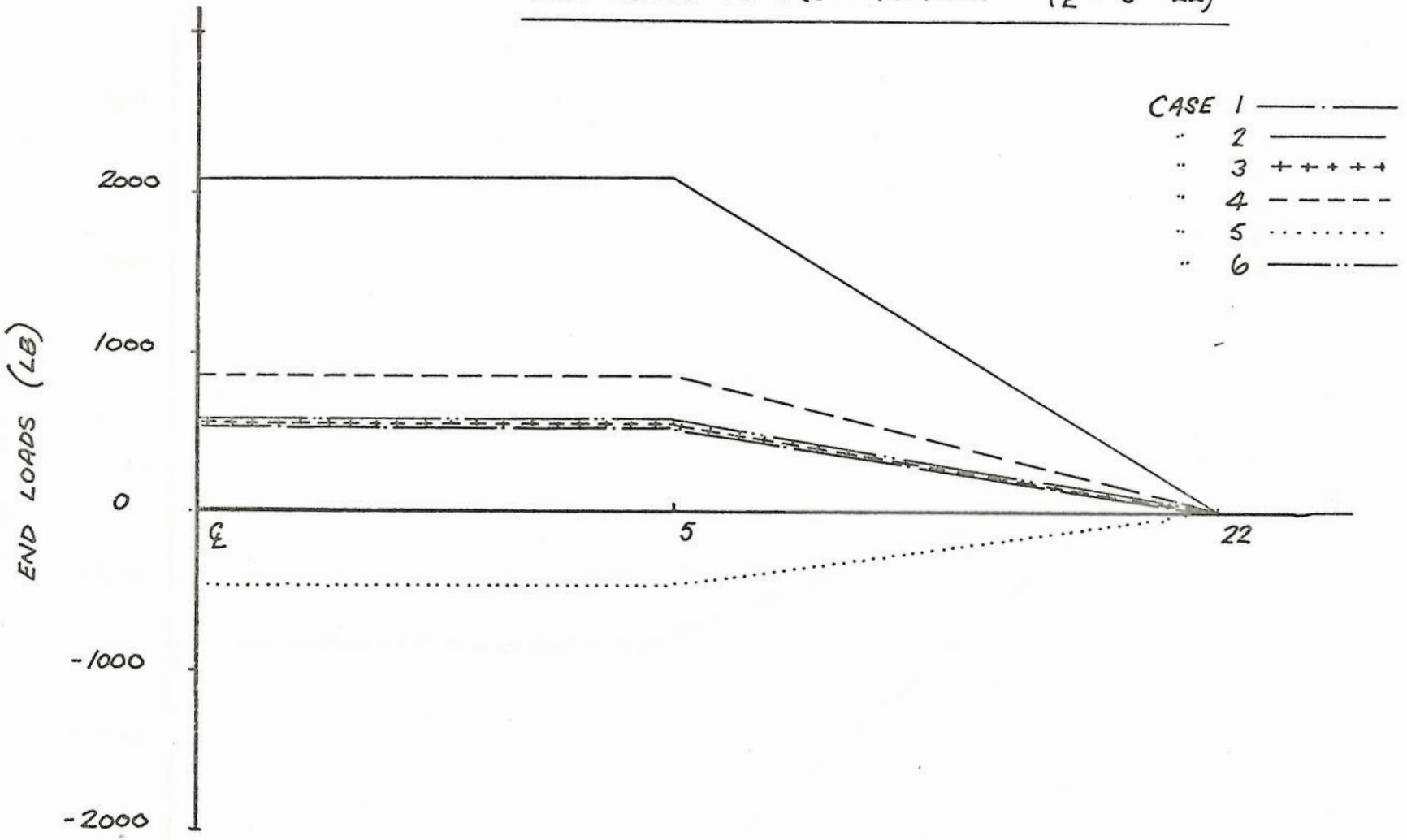

Fig. 58

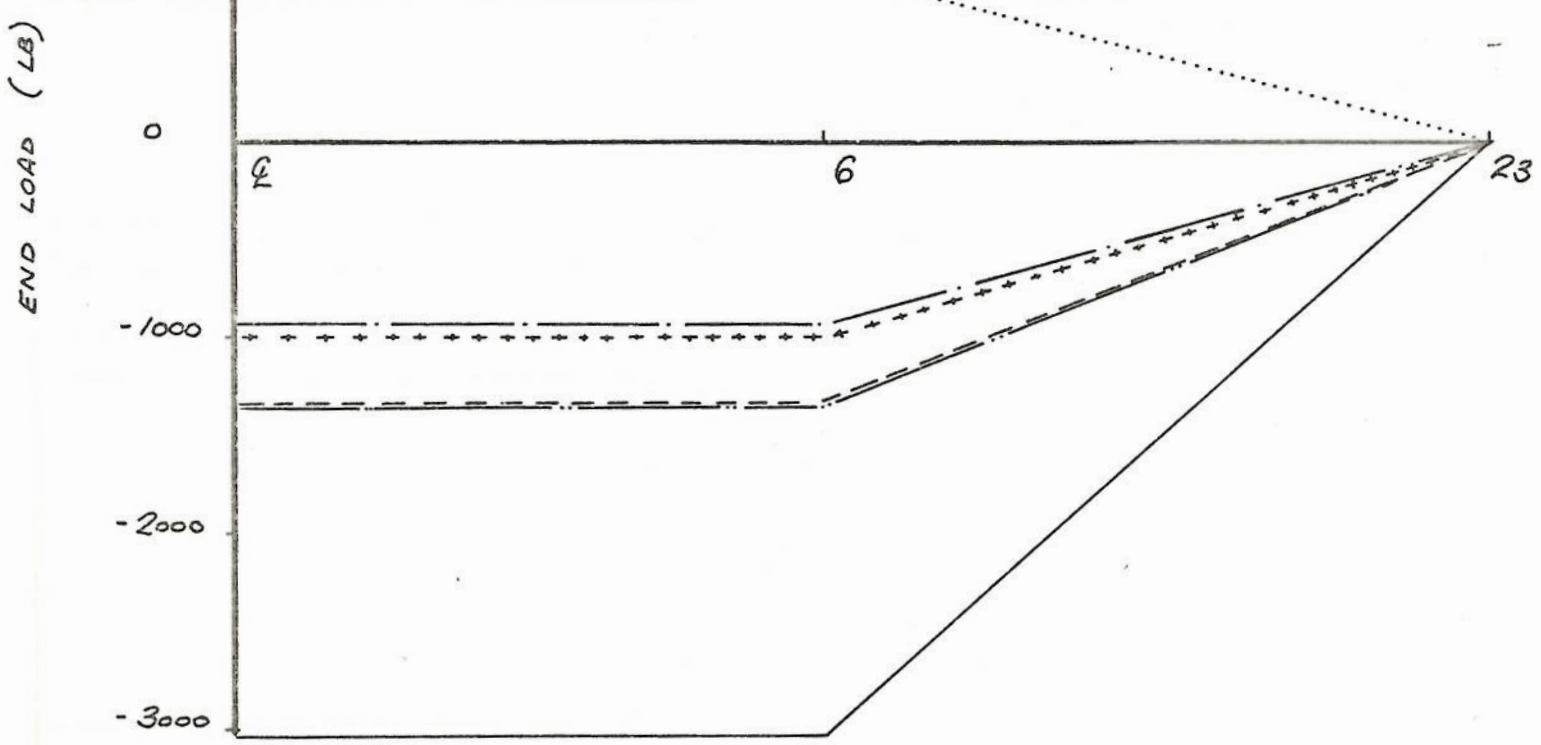

fig. 59

END LOADS IN CROSS MEMBER (℄ - 7 - 24)

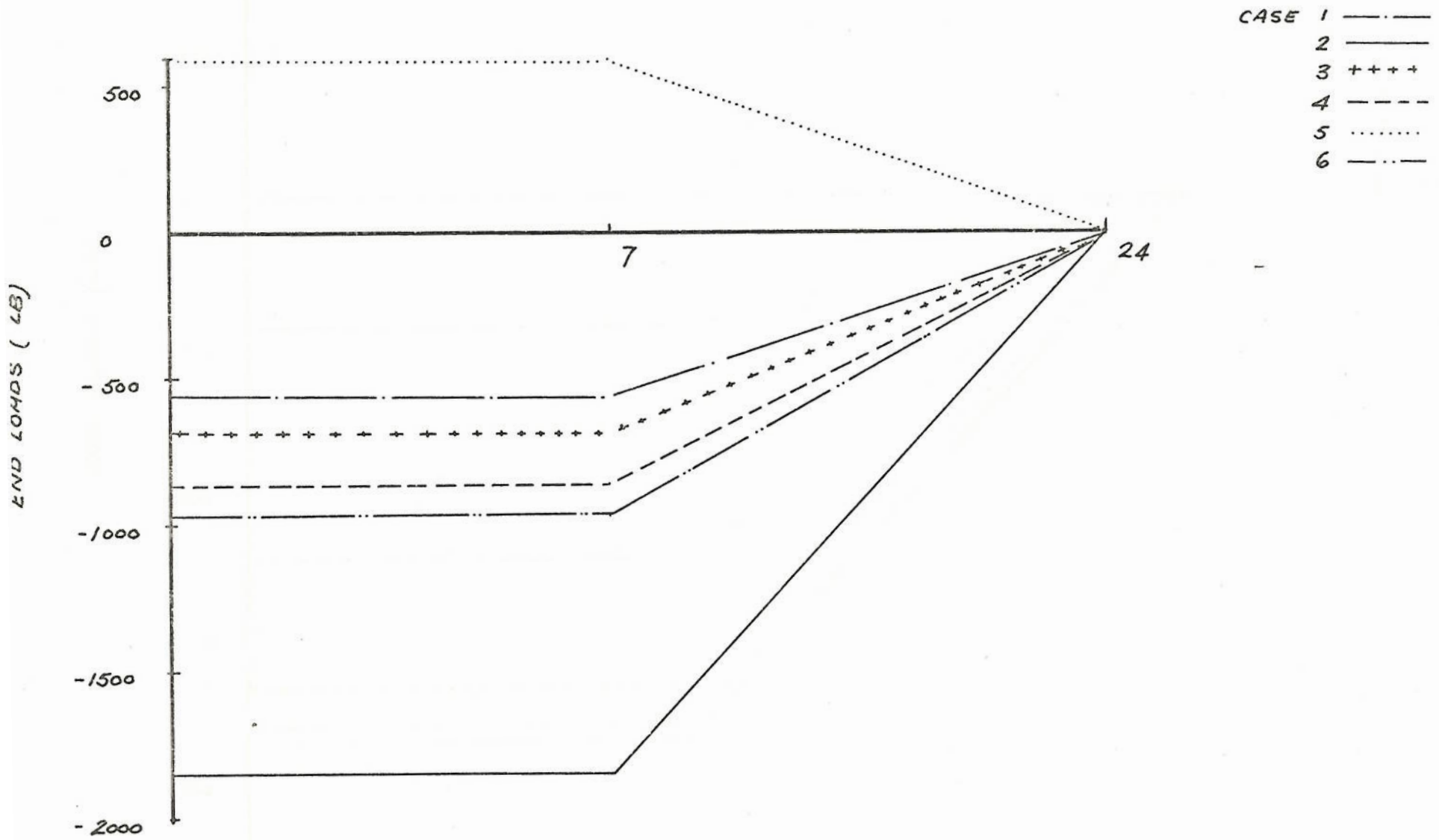

fig. 60

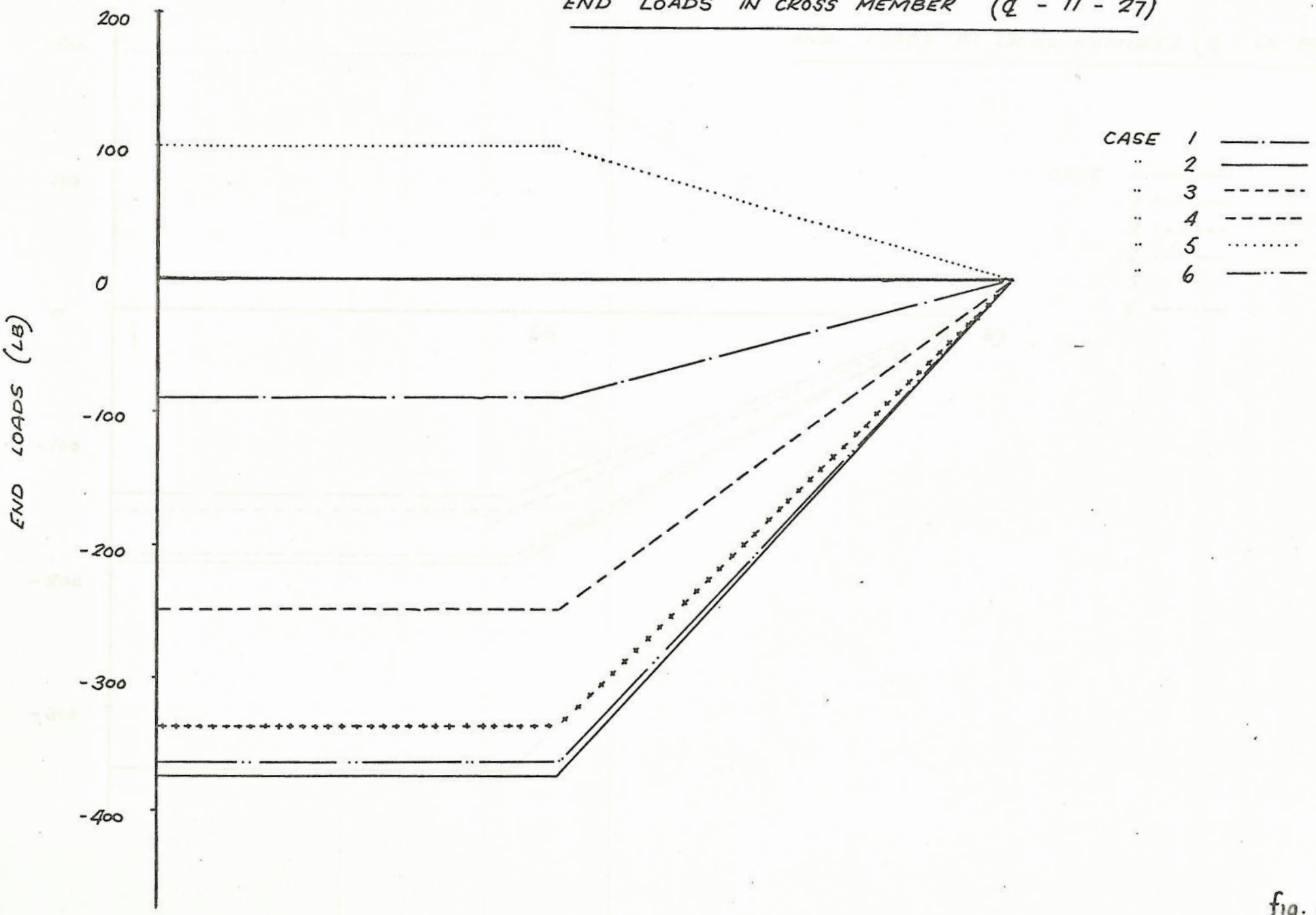
END LOADS IN CROSS MEMBER (℄ - 11 - 27)
200
100
0
-100
-200
-300
-400
END LOADS (LB)
CASE 1
" 2
" 3
" 4
" 5
" 6

fig. 61

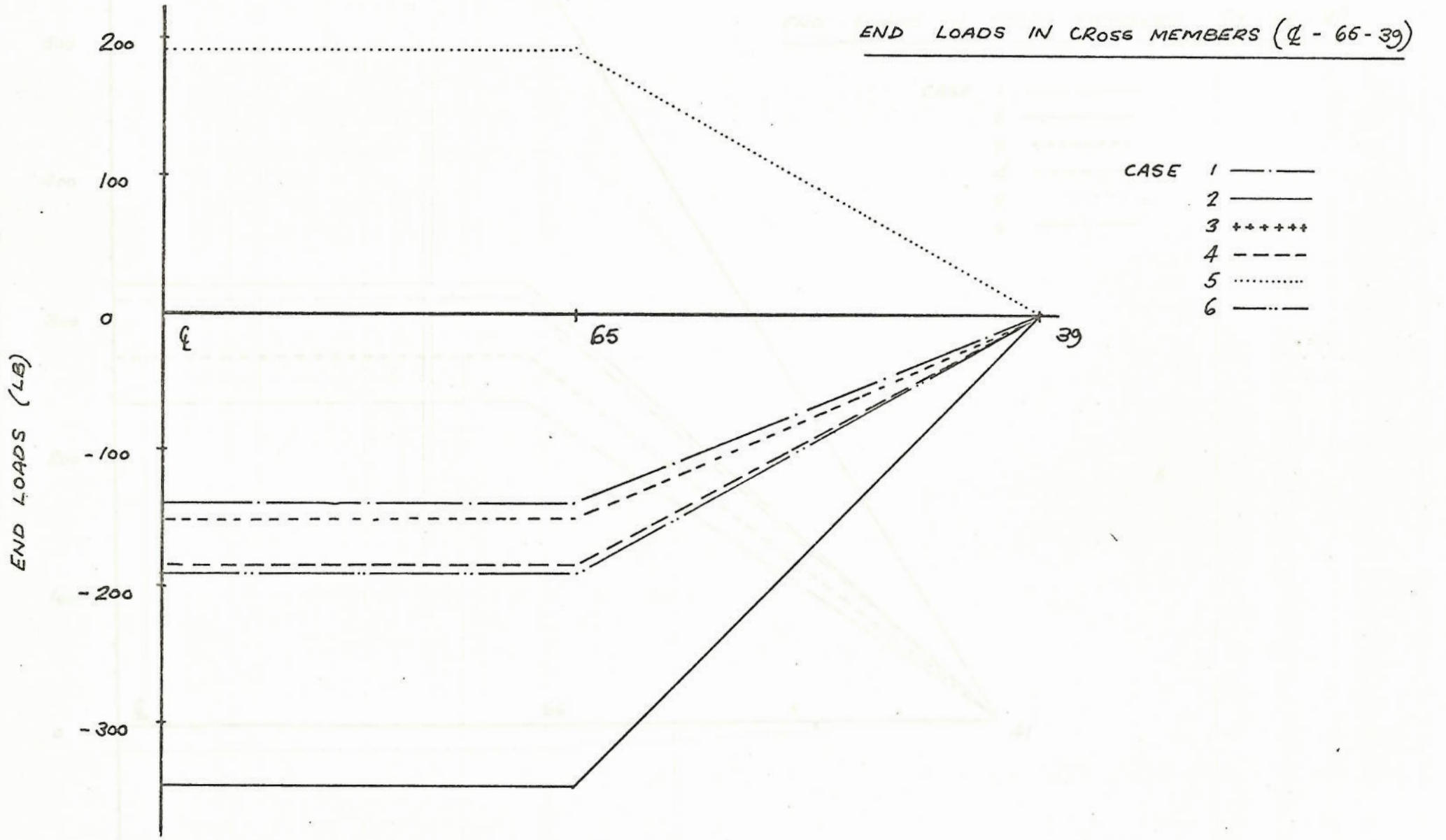
END LOADS IN CROSS MEMBERS (℄ - 66 - 39)
CASE 1
2
3
4
5
6
200
100
0
-100
-200
-300
END LOADS (LB)
℄
65
39

fig. 62

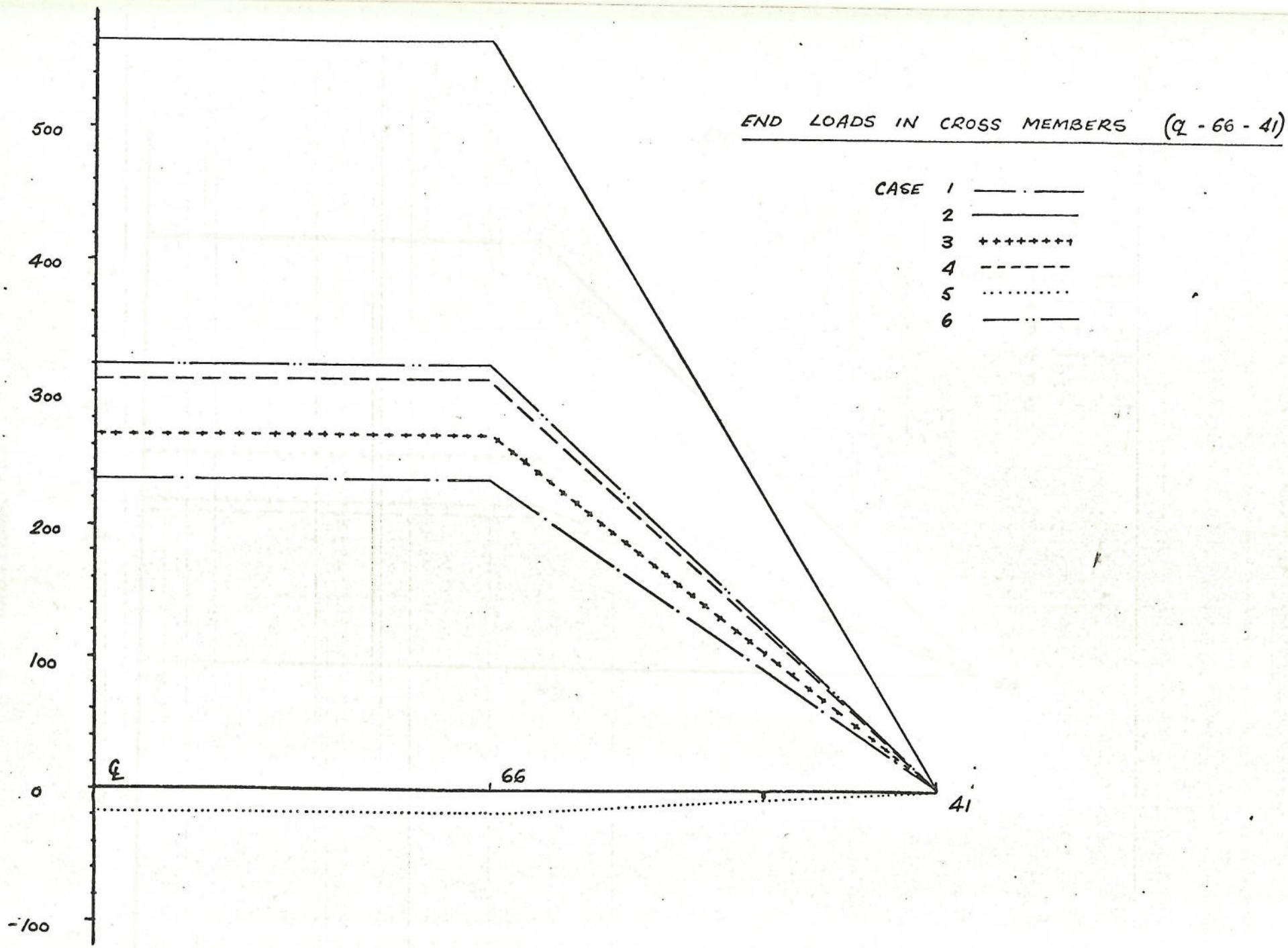
END LOADS IN CROSS MEMBERS (℄ - 66 - 41)
CASE 1
2
3
4
5
6
500
400
300
200
100
0
-100
END LOADS (LB)
℄
66
41

Fig. 63

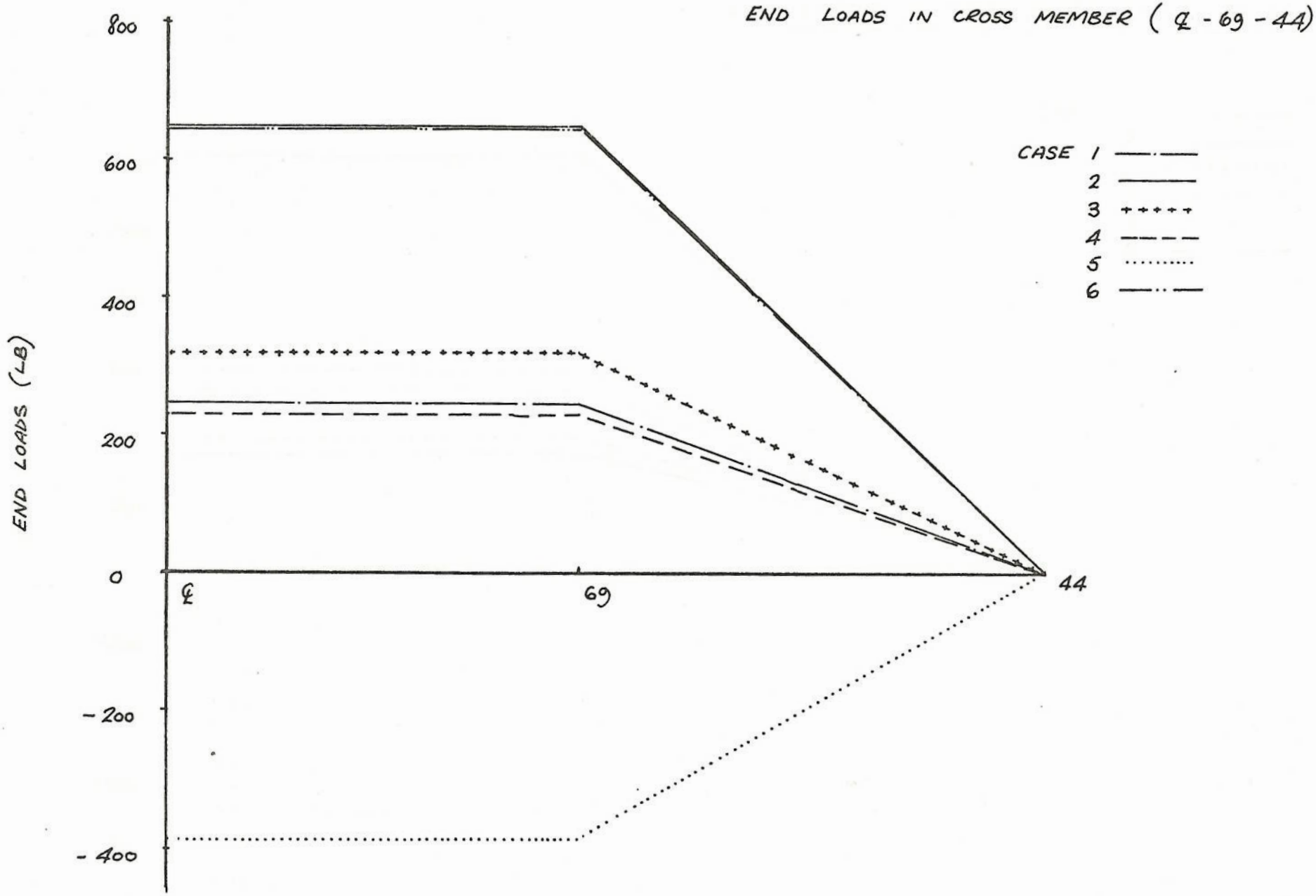
END LOADS IN CROSS MEMBER (℄ - 69 - 44)
800
600
400
200
0
- 200
- 400
END LOADS (LB)
℄
69
44
CASE 1
2
3
4
5
6

fig. 64

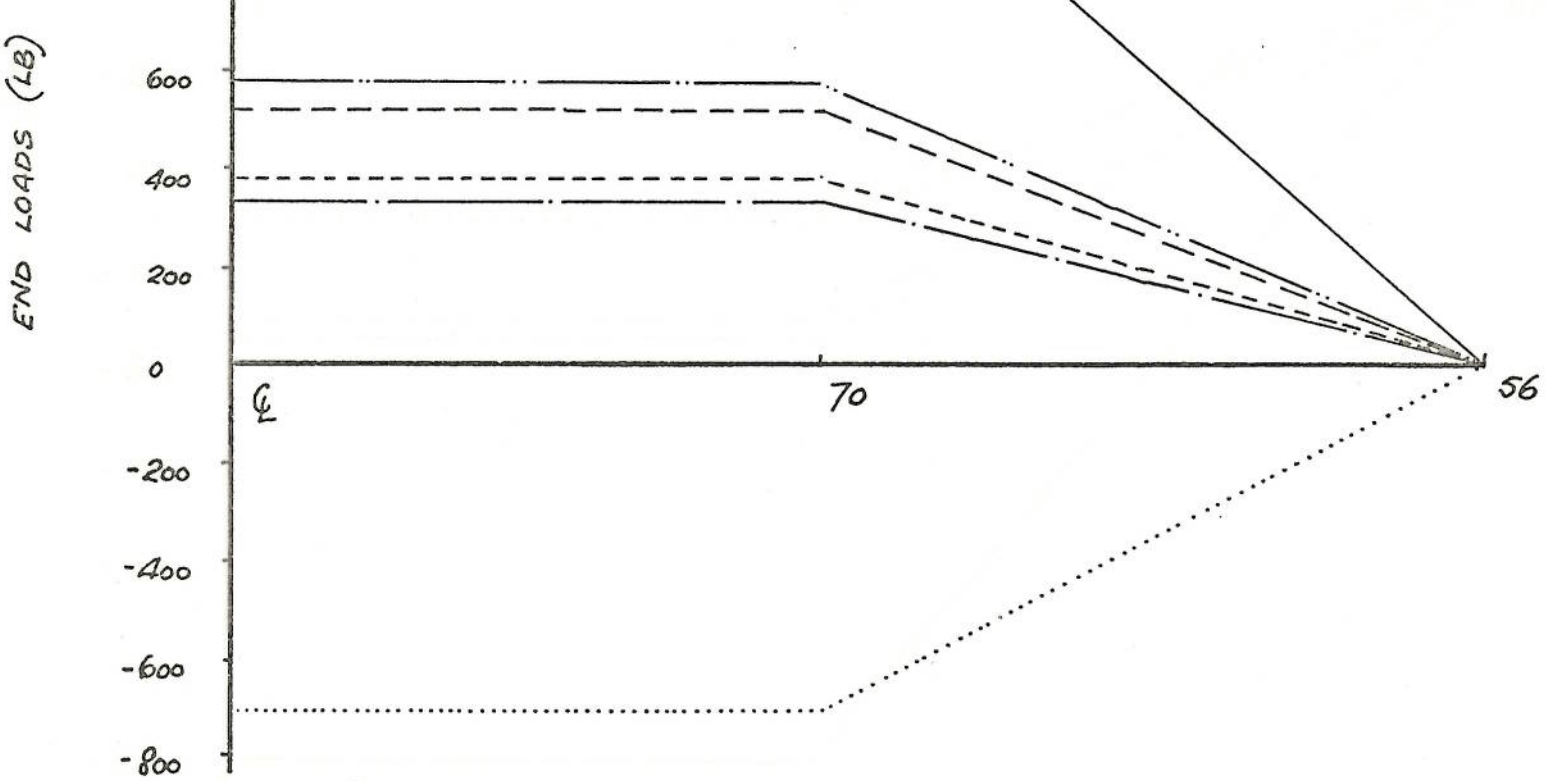

Fig. 65

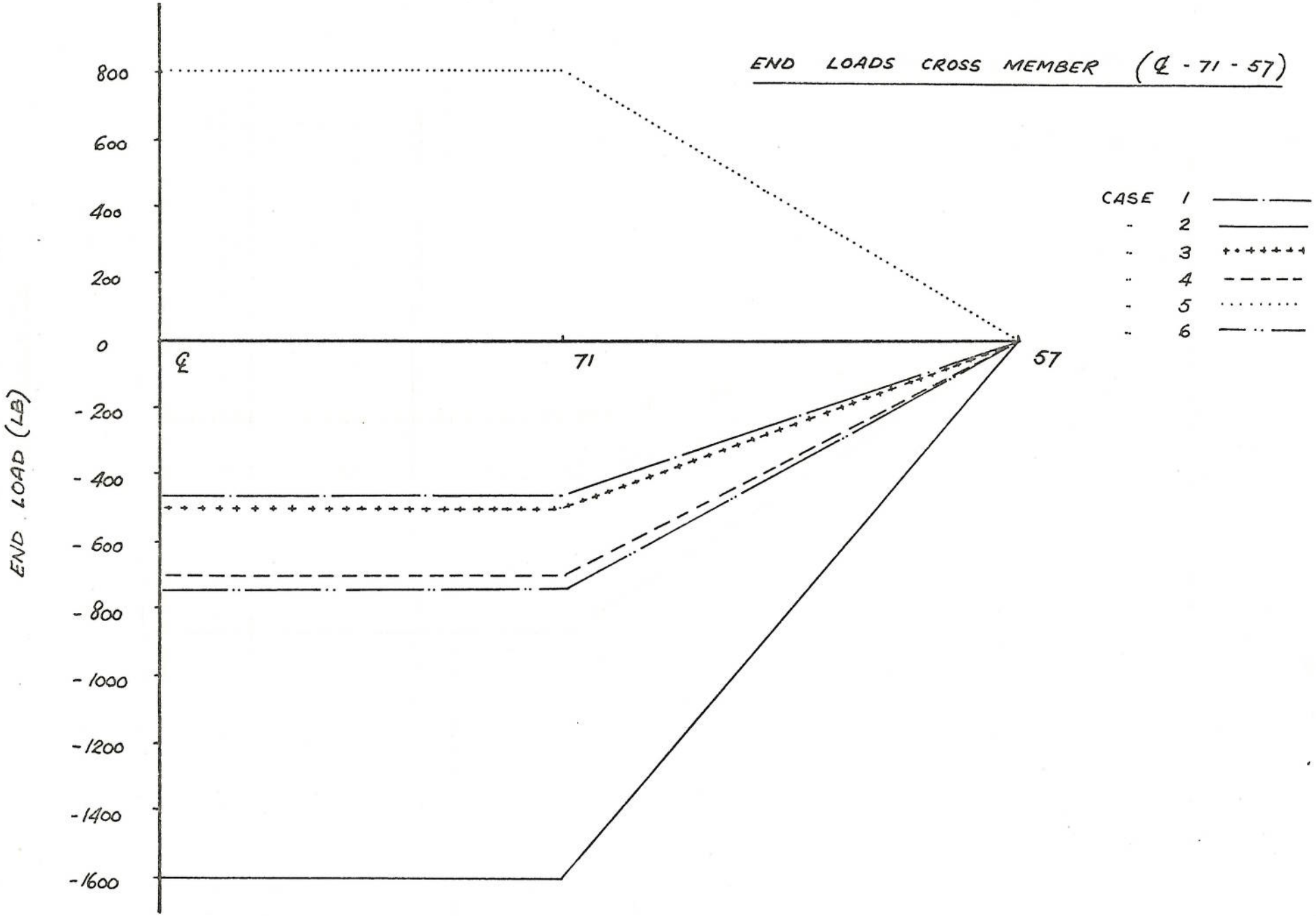
END LOADS CROSS MEMBER (℄ - 71 - 57)
CASE 1
2
3
4
5
6
800
600
400
200
0
- 200
- 400
- 600
- 800
- 1000
- 1200
- 1400
- 1600
END LOAD (LB)
℄
71
57

fig. 66

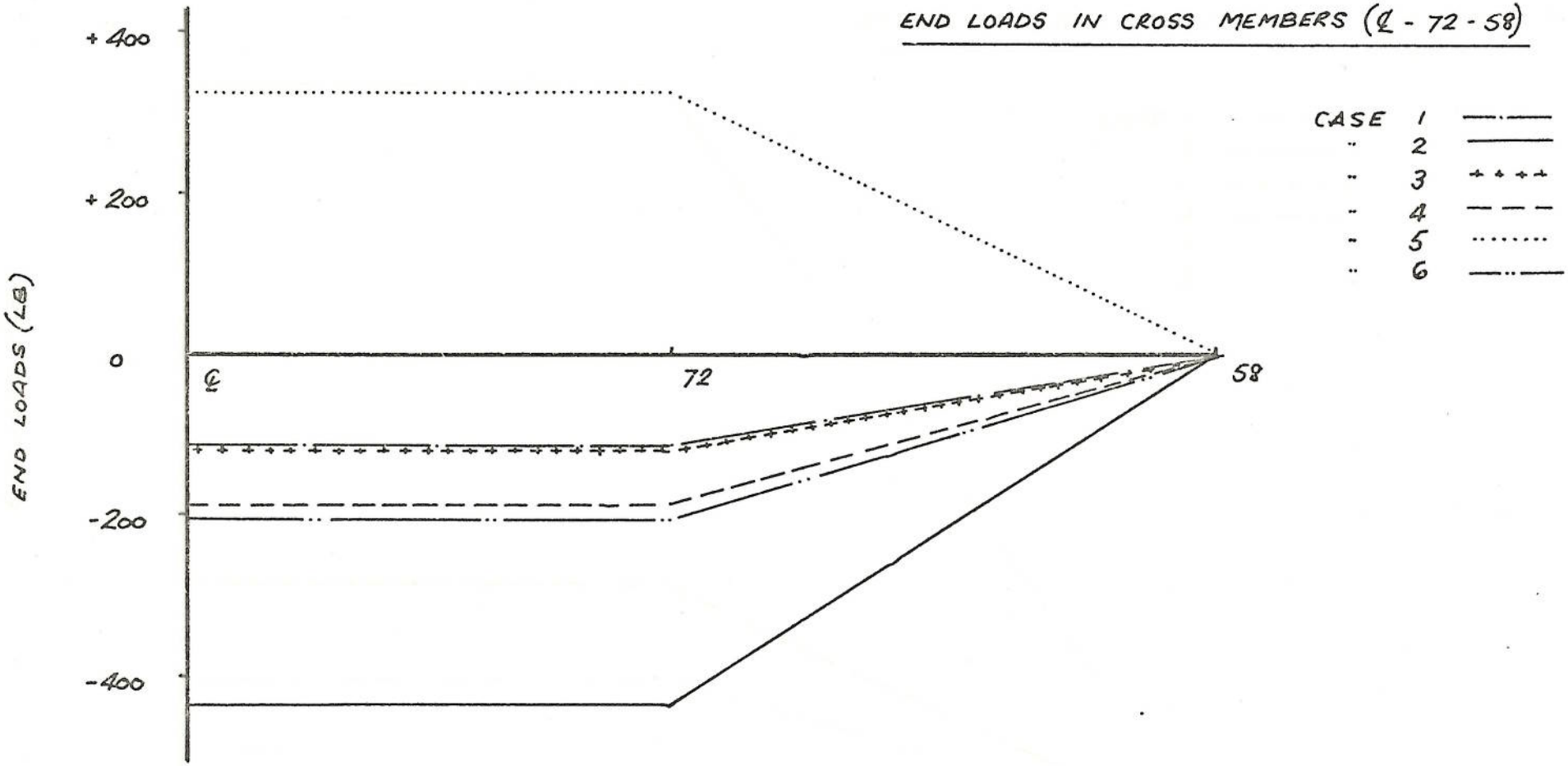
END LOADS IN CROSS MEMBERS (℄ - 72 - 58)
CASE 1
" 2
" 3
" 4
" 5
" 6
+400
+200
0
-200
-400
END LOADS (LB)
℄
72
58

fig. 67

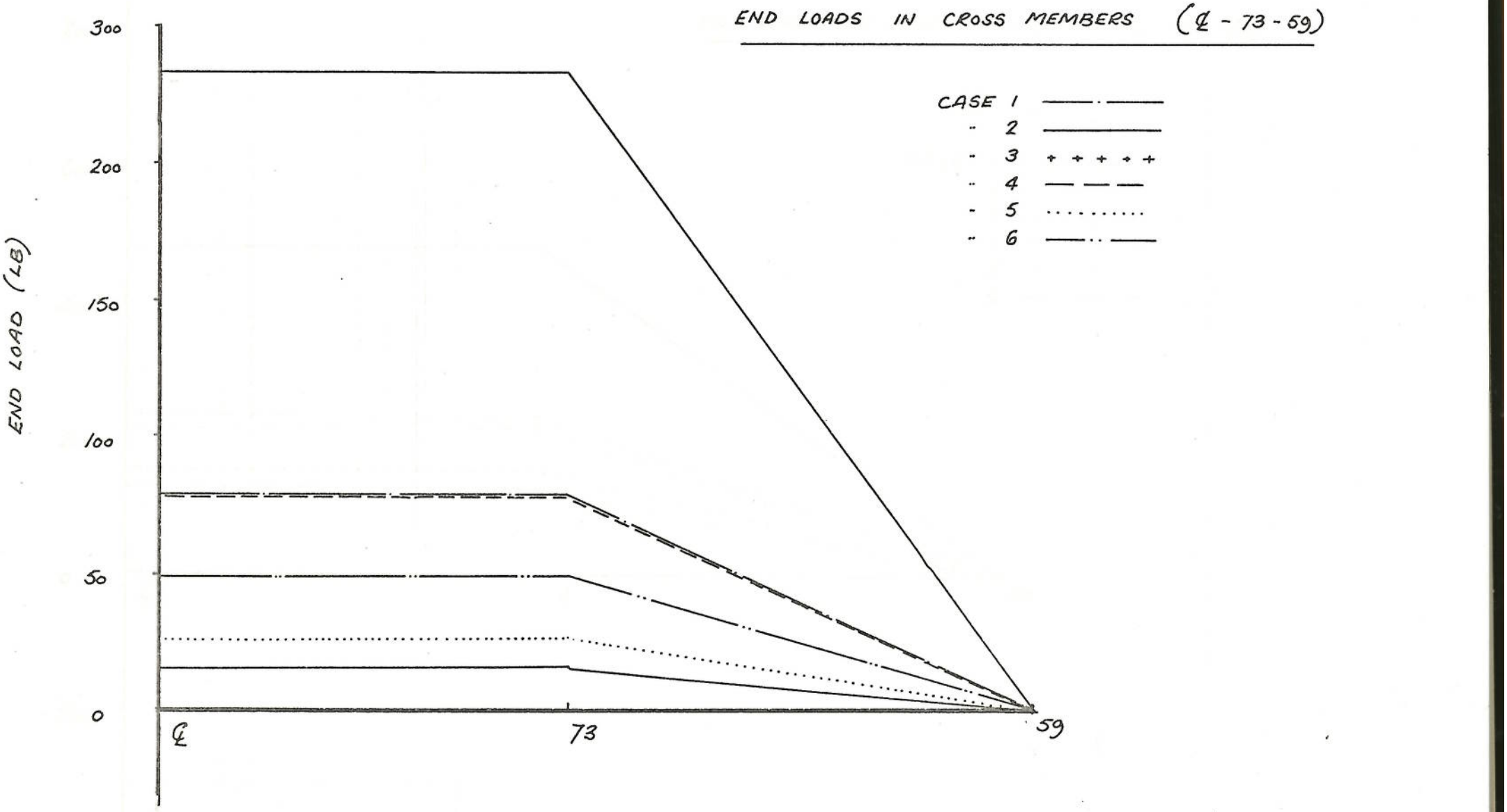
END LOADS IN CROSS MEMBERS (℄ - 73 - 59)
CASE 1
2
3
4
5
6
END LOAD (LB)
300
200
150
100
50
0
℄
73
59

fig. 68

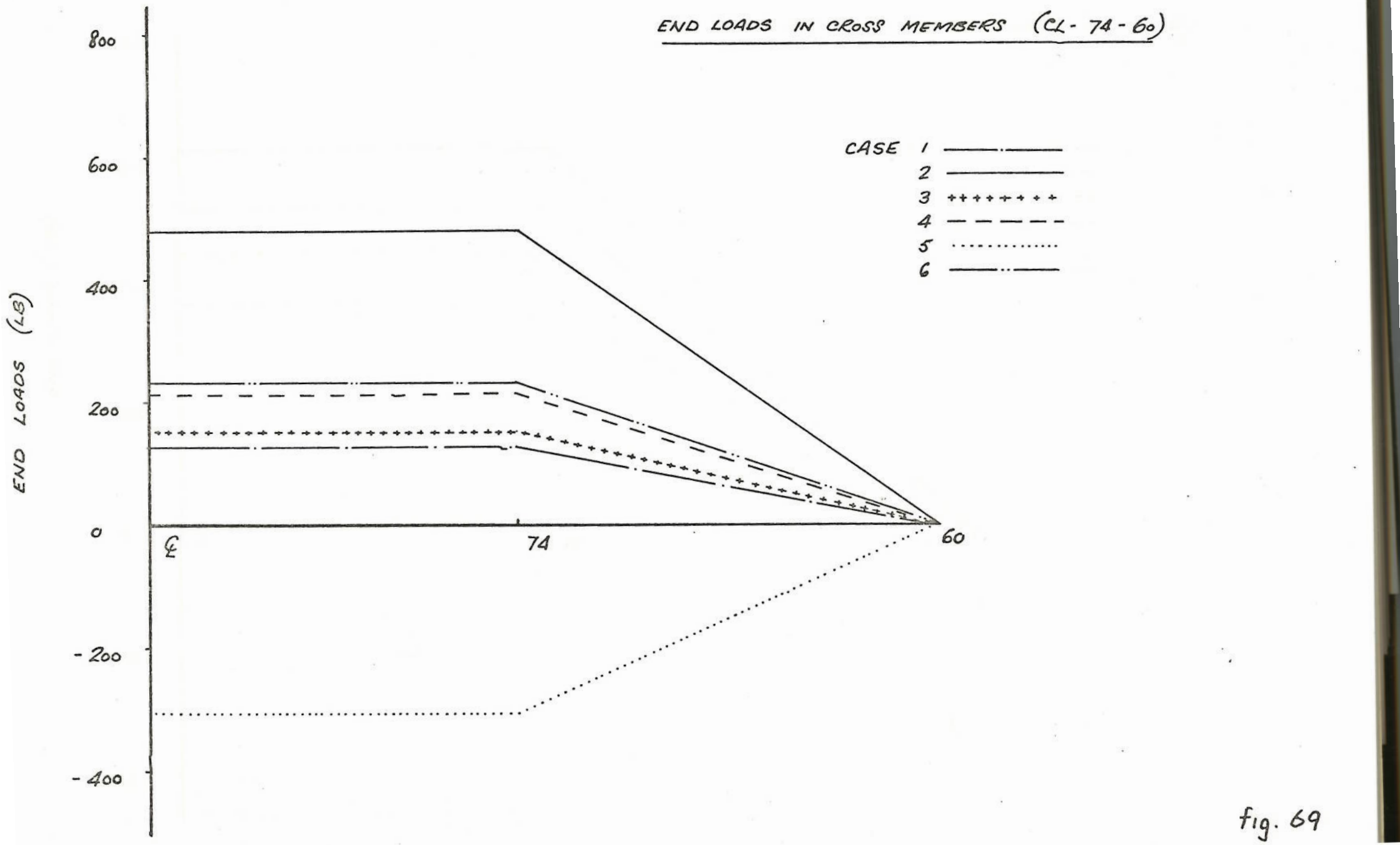
END LOADS IN CROSS MEMBERS (CL - 74 - 60)
CASE 1
2
3
4
5
6
800
600
400
200
0
- 200
- 400
END LOADS (LB)
℄
74
60

fig. 69

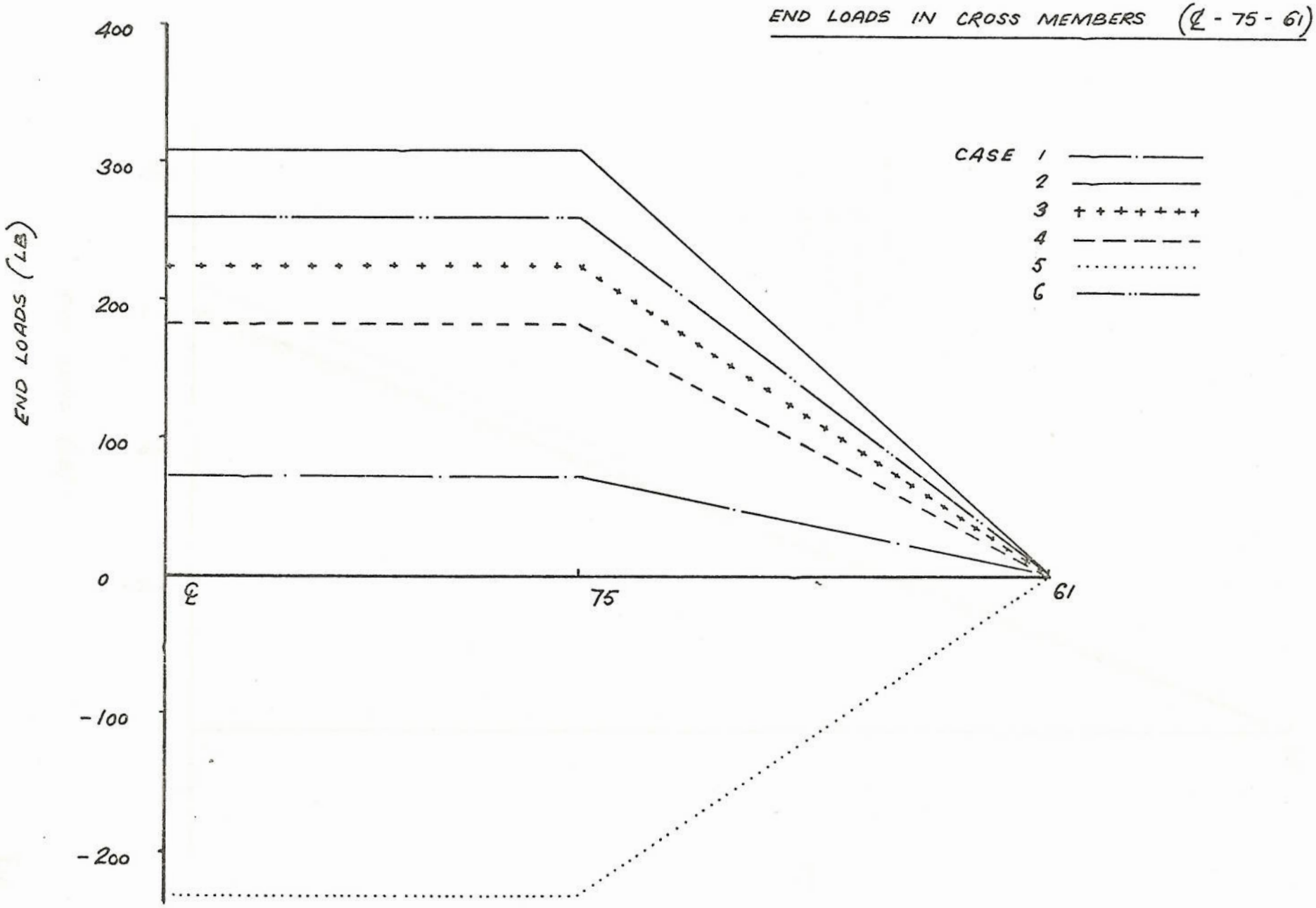
END LOADS IN CROSS MEMBERS (℄ - 75 - 61)
400
300
200
100
0
-100
-200
END LOADS (LB)
CASE 1
2
3
4
5
6
℄
75
61

Fig. 70

END LOADS IN INNER WING PANEL (1-65)

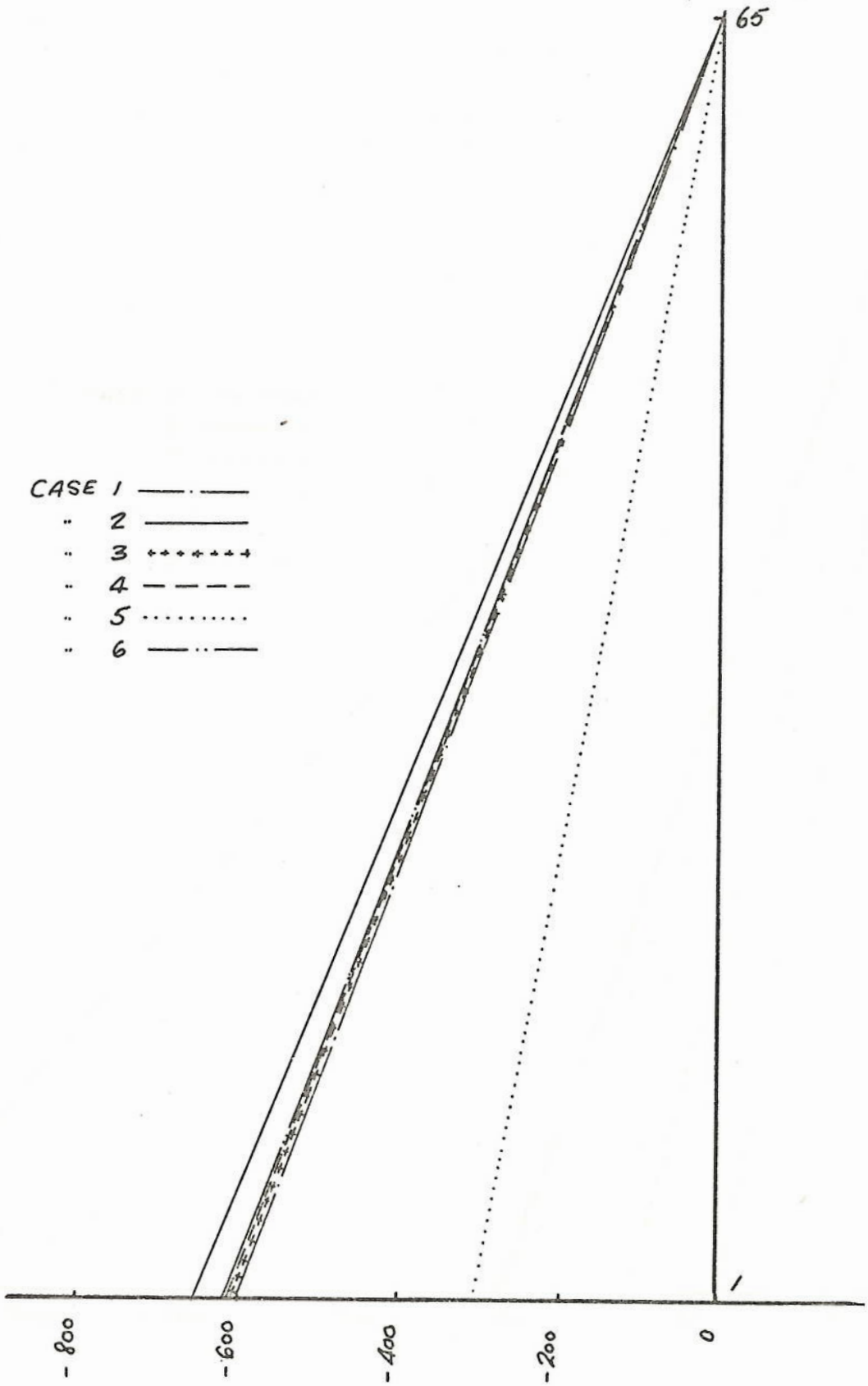

Fig. 71

END LOAD IN INNER WING PANEL (2-66)

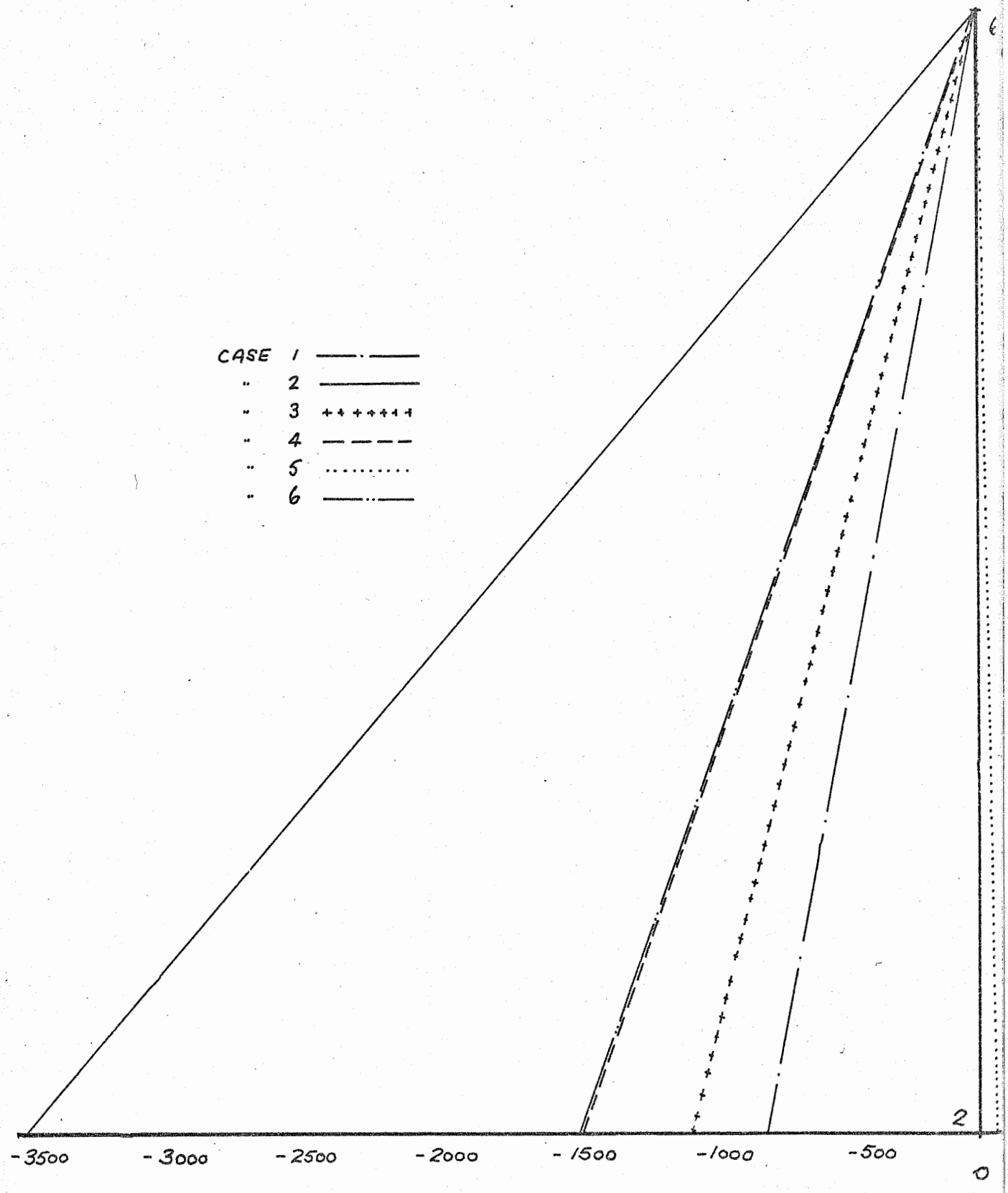

fig. 72

END LOADS IN INNER WING PANEL (3 - 67)

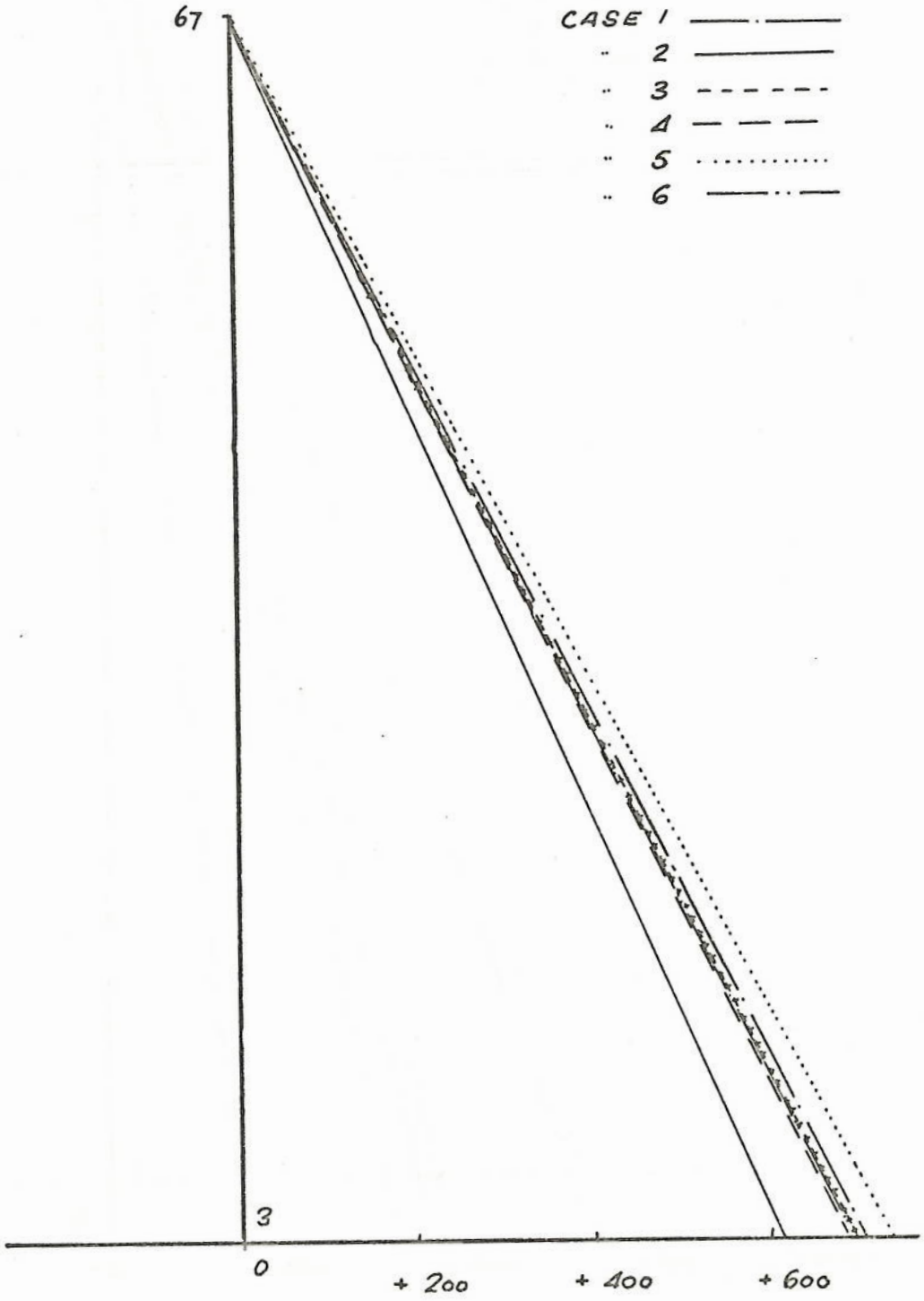

Fig. 73

END LOADS IN INNER WING PANEL (4 - 68)

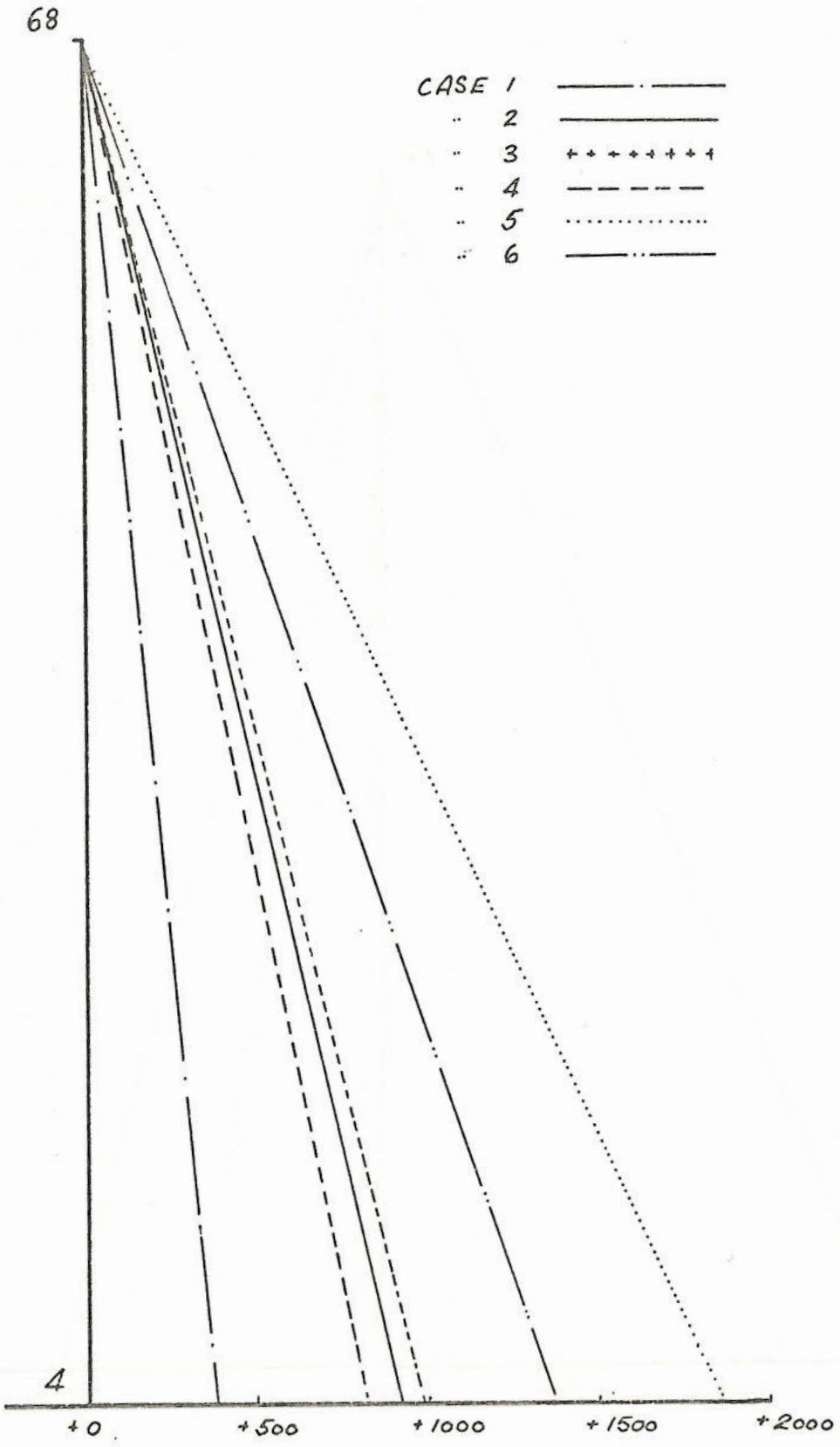

fig. 74

END LOADS IN INNER WING PANEL (5-69)

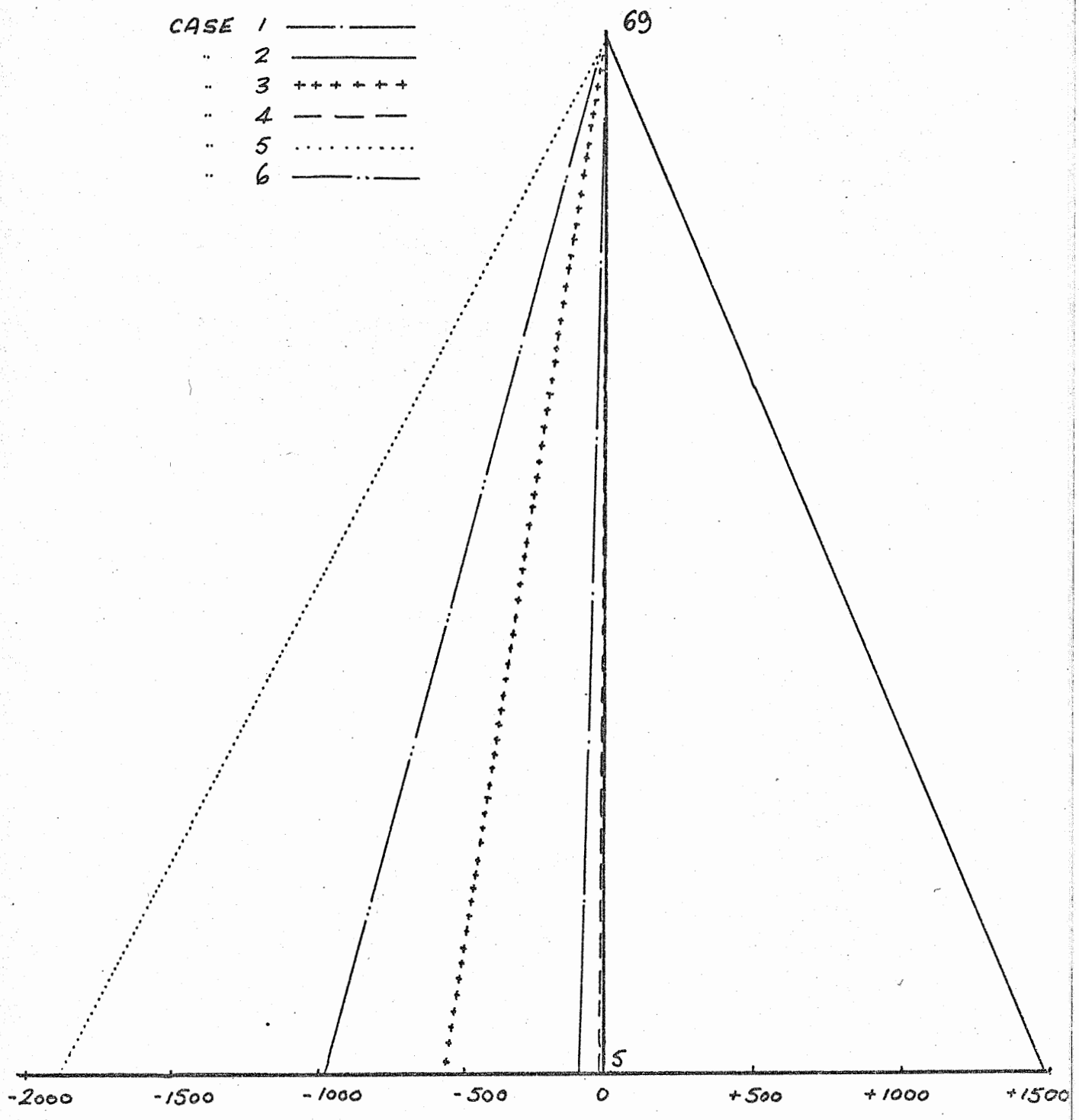

END LOAD (LB)

fig. 75

CASE 1

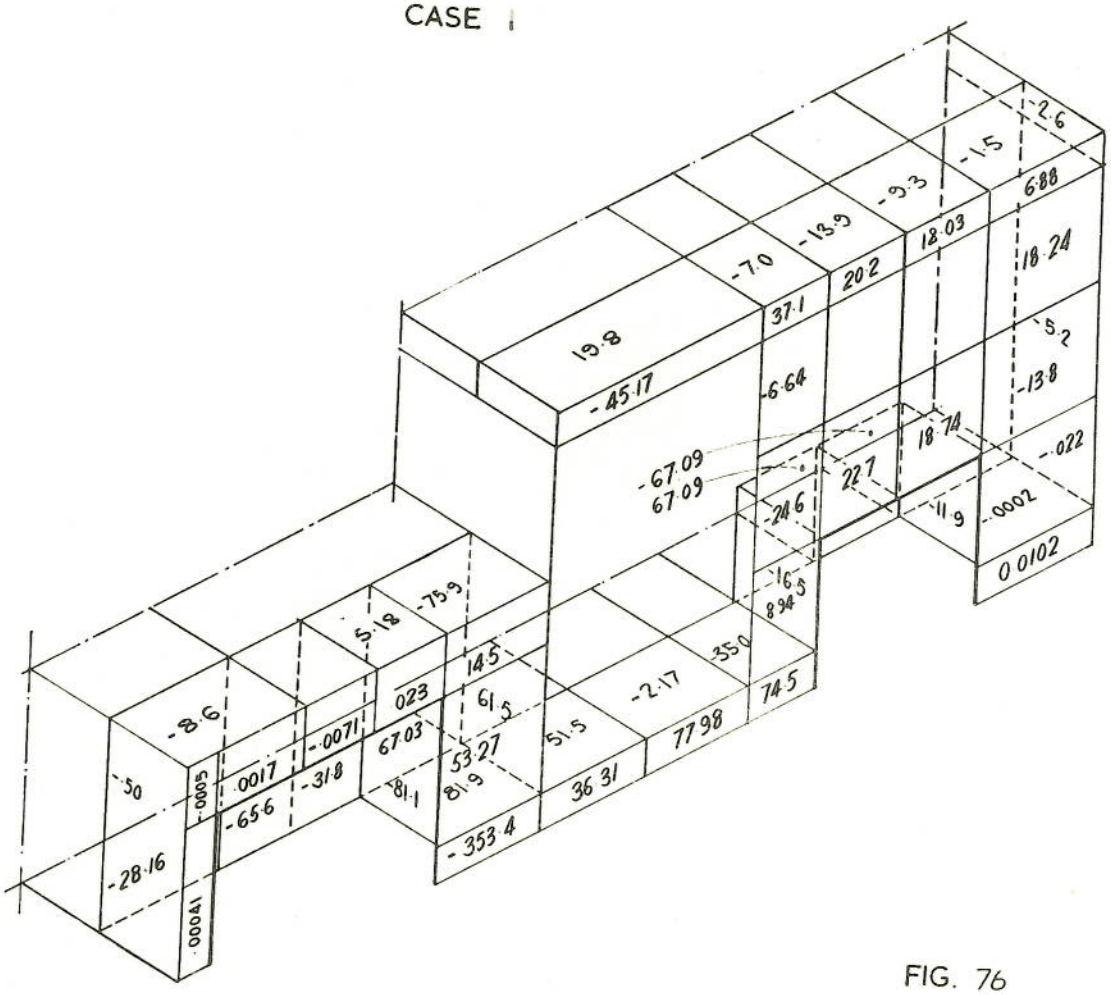

FIG. 76

CASE 2

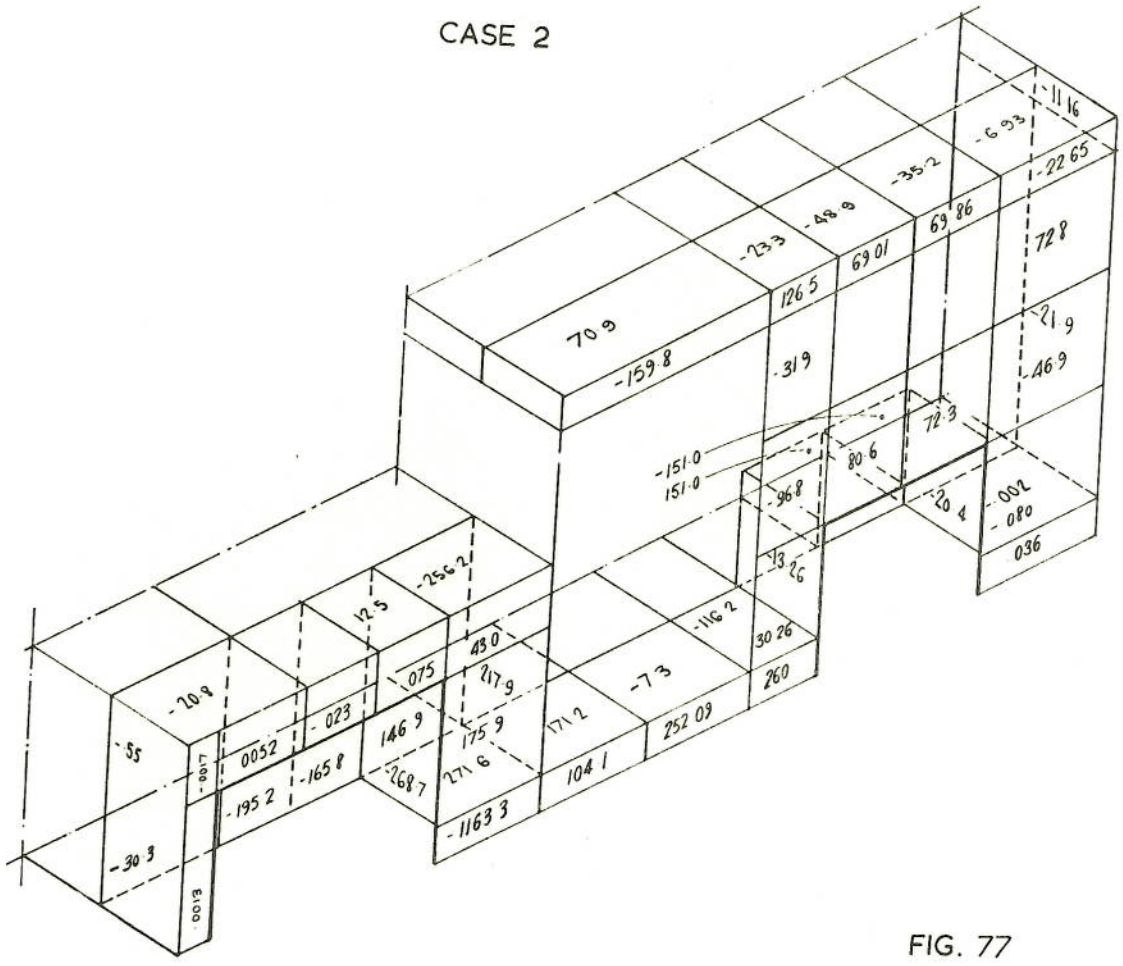

FIG. 77

CASE 3

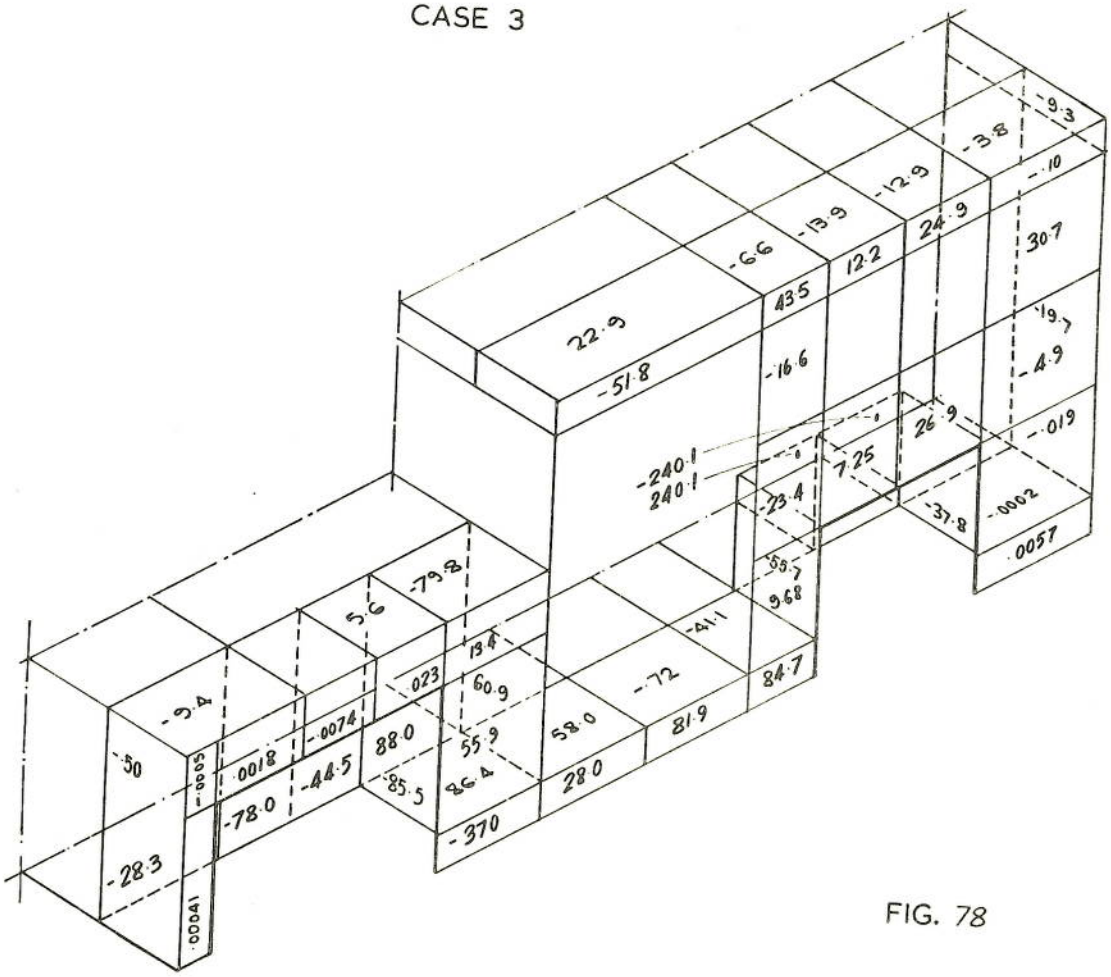

FIG. 78

CASE 4

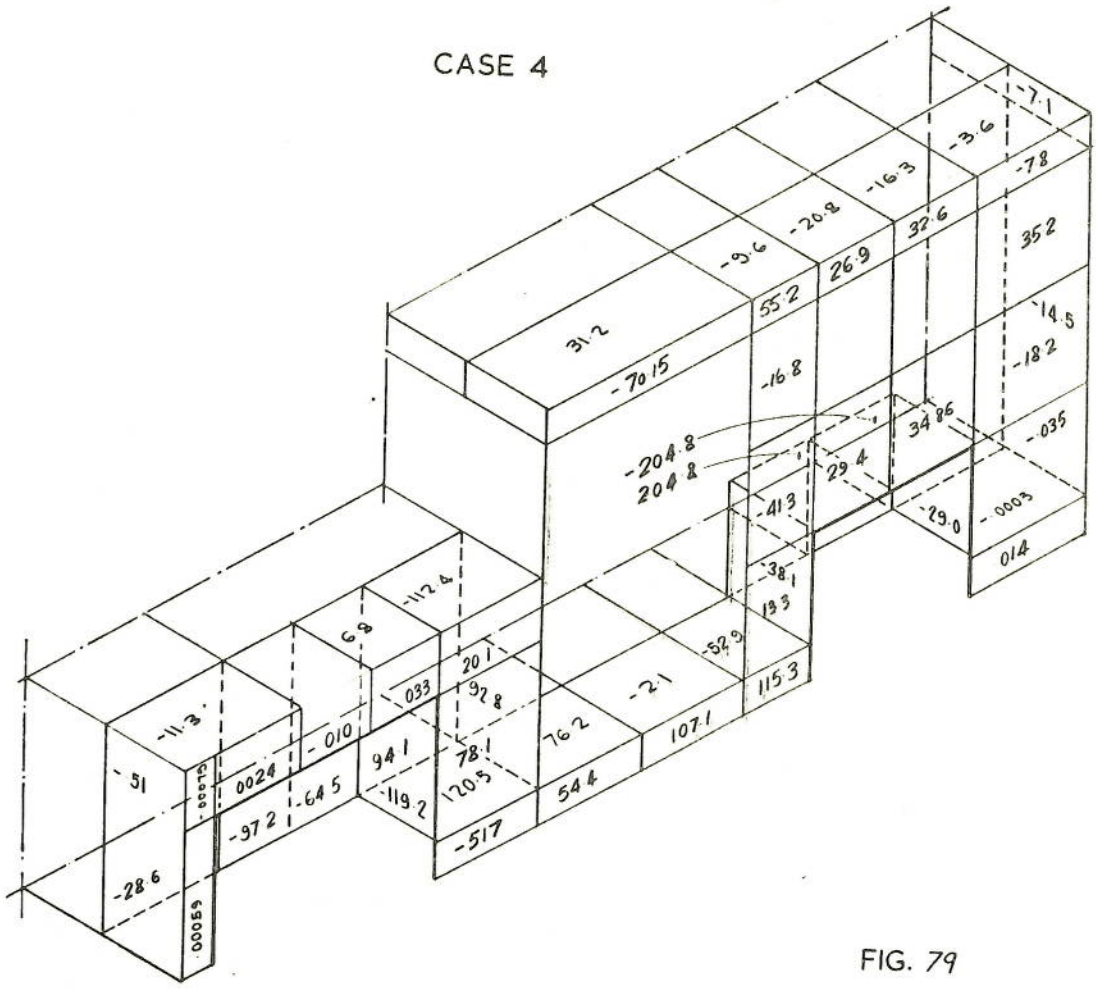

FIG. 79

CASE 5

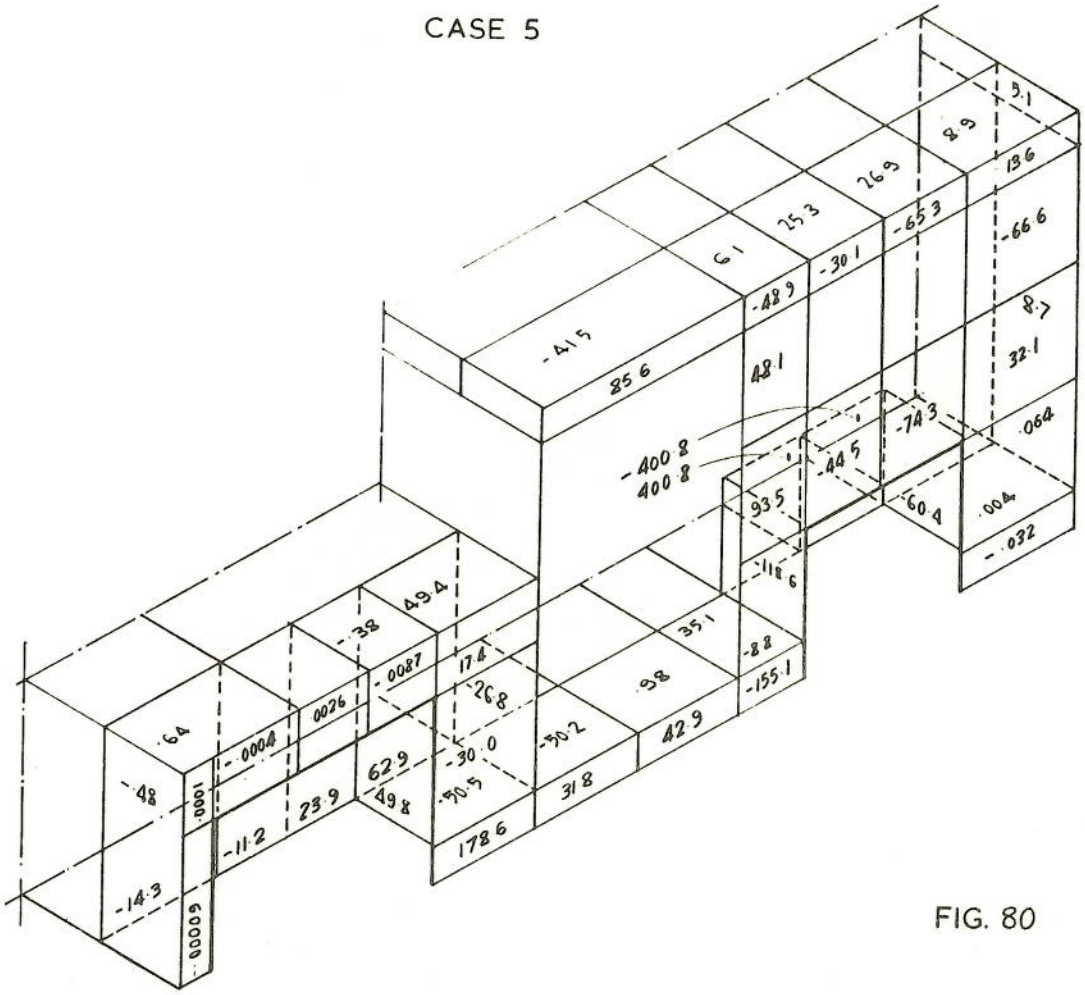

FIG. 80

CASE 6

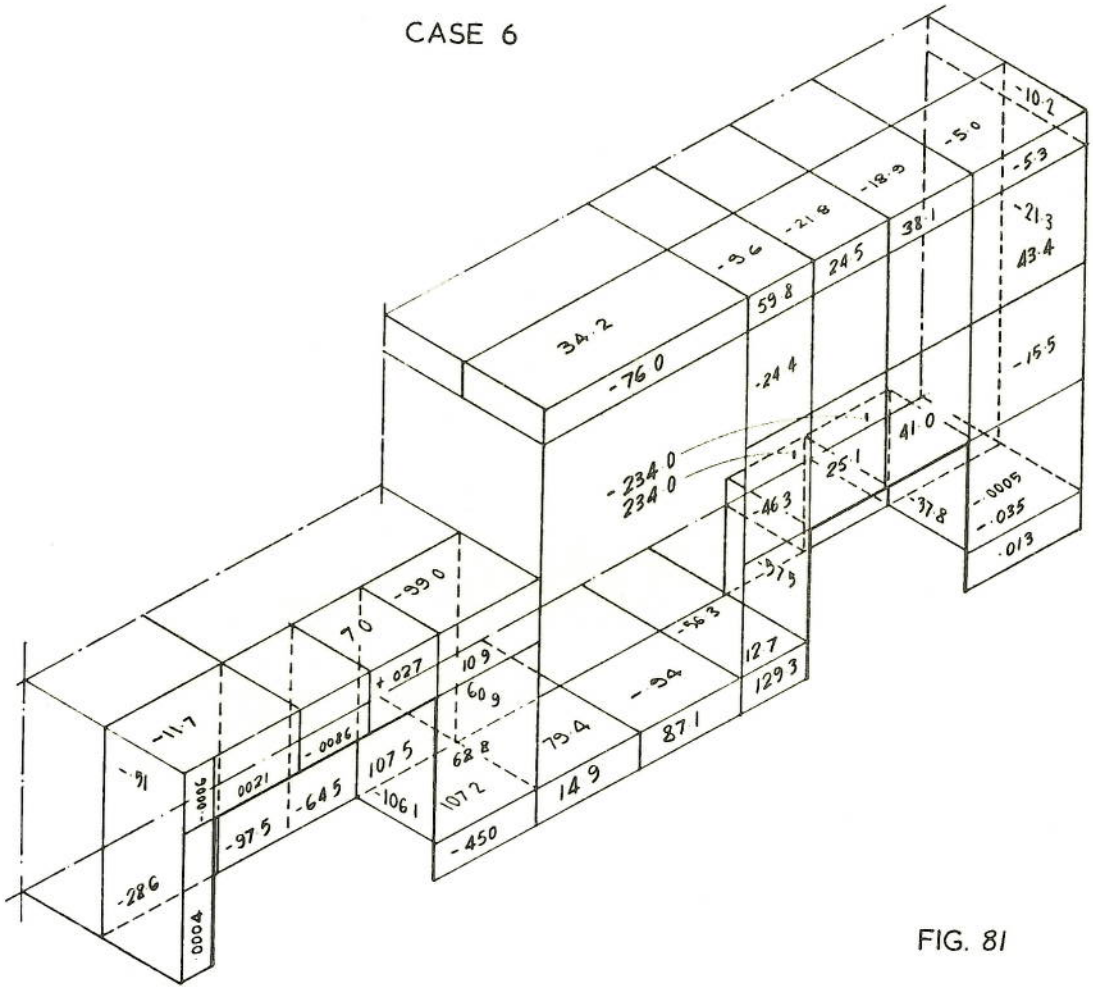

FIG. 81

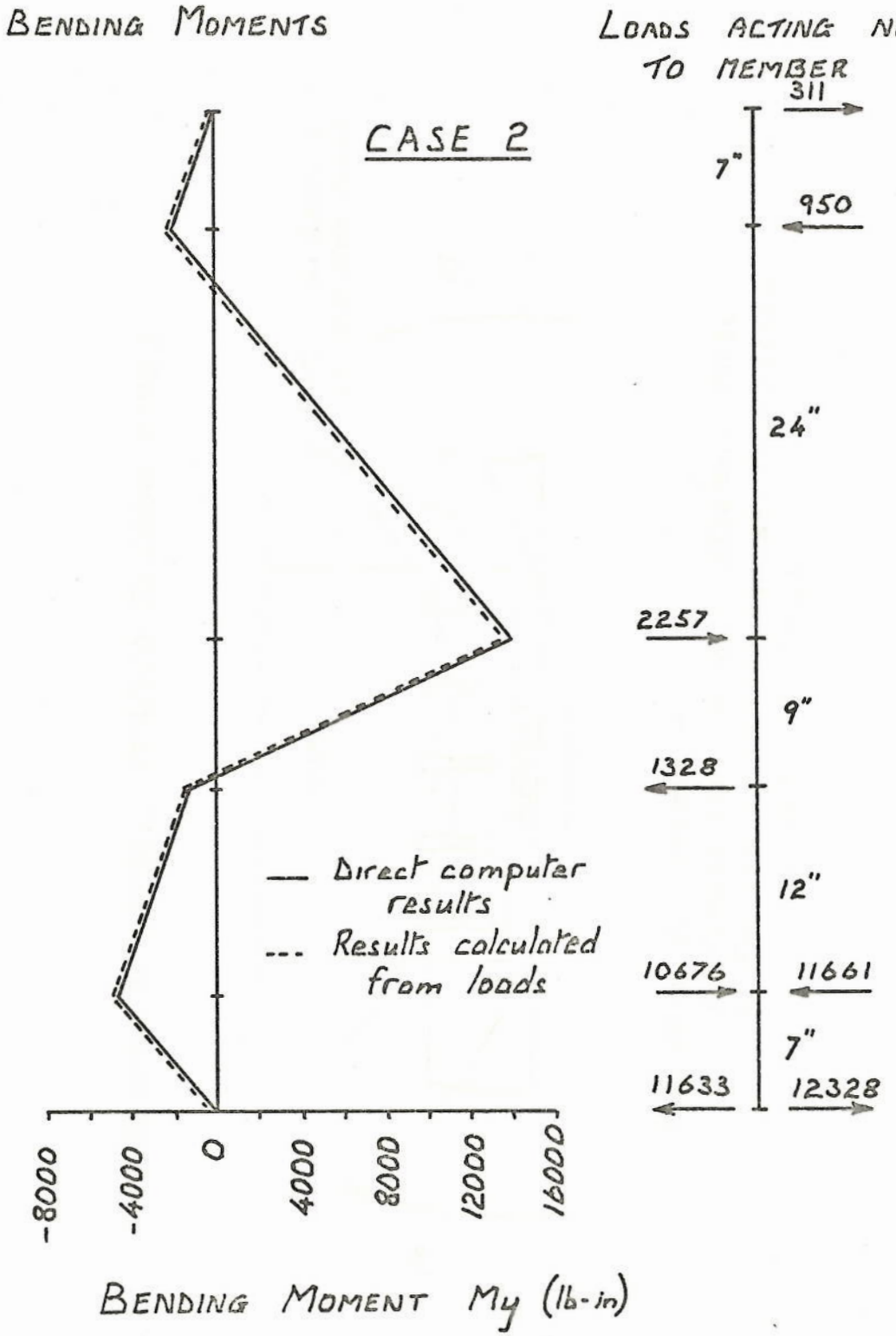

EQUILIBRIUM AND CROSS CHECKS FROM COMPUTER RESULTS FOR WINDSCREEN DOOR PILLAR

fig. 82

BENDING OF MEMBERS ATTACHED TO SHEAR PANELS

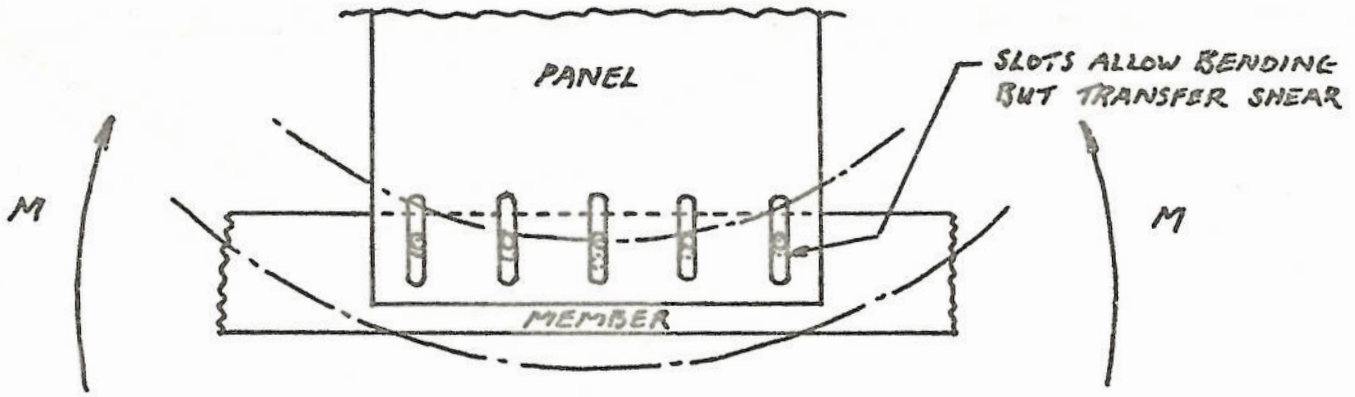

THEORETICAL ASSUMPTIONS :–

1. MEMBER BENDS WITHOUT DEFORMING PANEL
2. END LOAD IN MEMBER CAN BE TRANSFERRED TO SHEAR IN PANEL

fig. 83

DISPLACEMENT OF FLOOR BEAM FROM A BASE LINE THROUGH POINTS 2 AND 9 (AXLE CENTRE LINES)

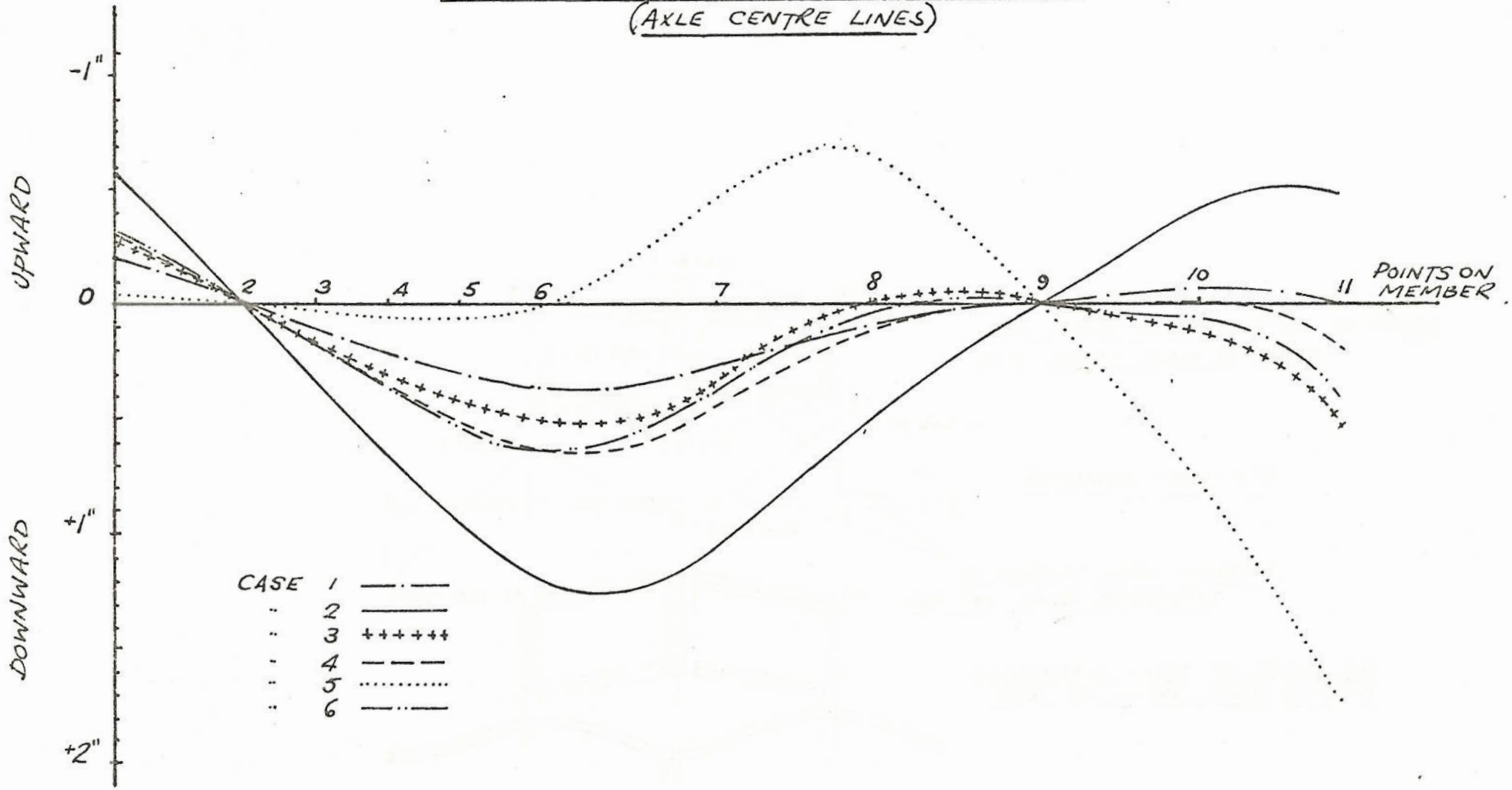

fig. 84

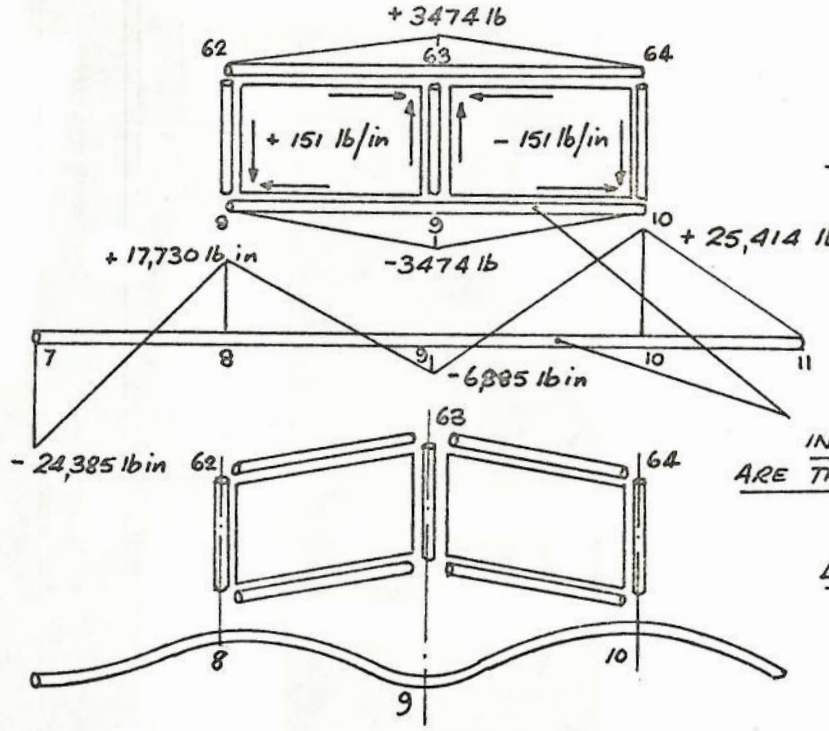

END LOADS IN HORIZONTAL MEMBERS AND SHEAR FLOW IN PANELS.

BENDING MOMENTS

IN PRACTICE THESE MEMBERS ARE THE SAME COMPONENT.

DEFLECTED FORM OF STRUCTURE DUE TO ABOVE LOAD SYSTEM.

FIG. 85

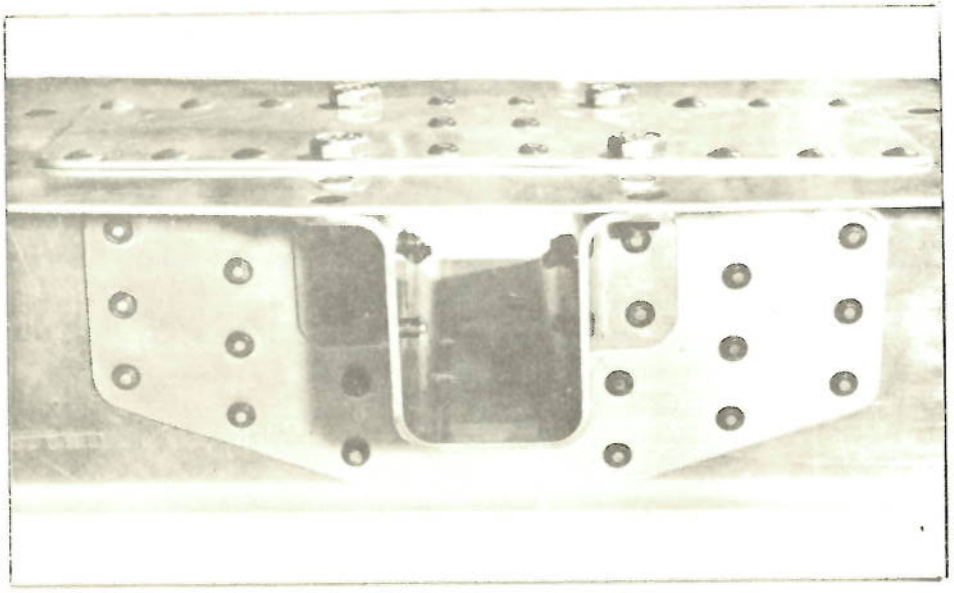

APP. IV. FIG. 1

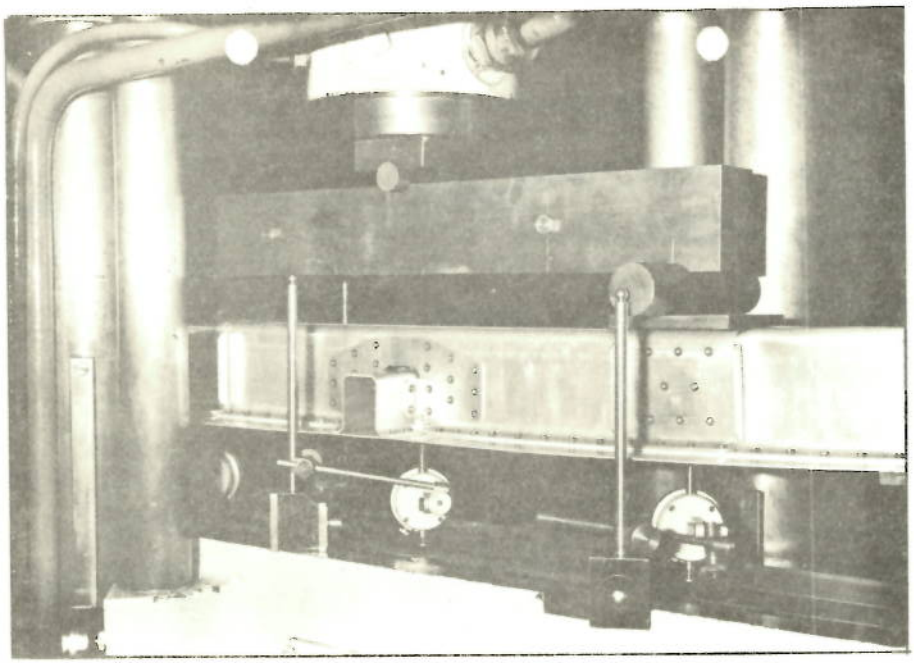

APP. IV. FIG. 2

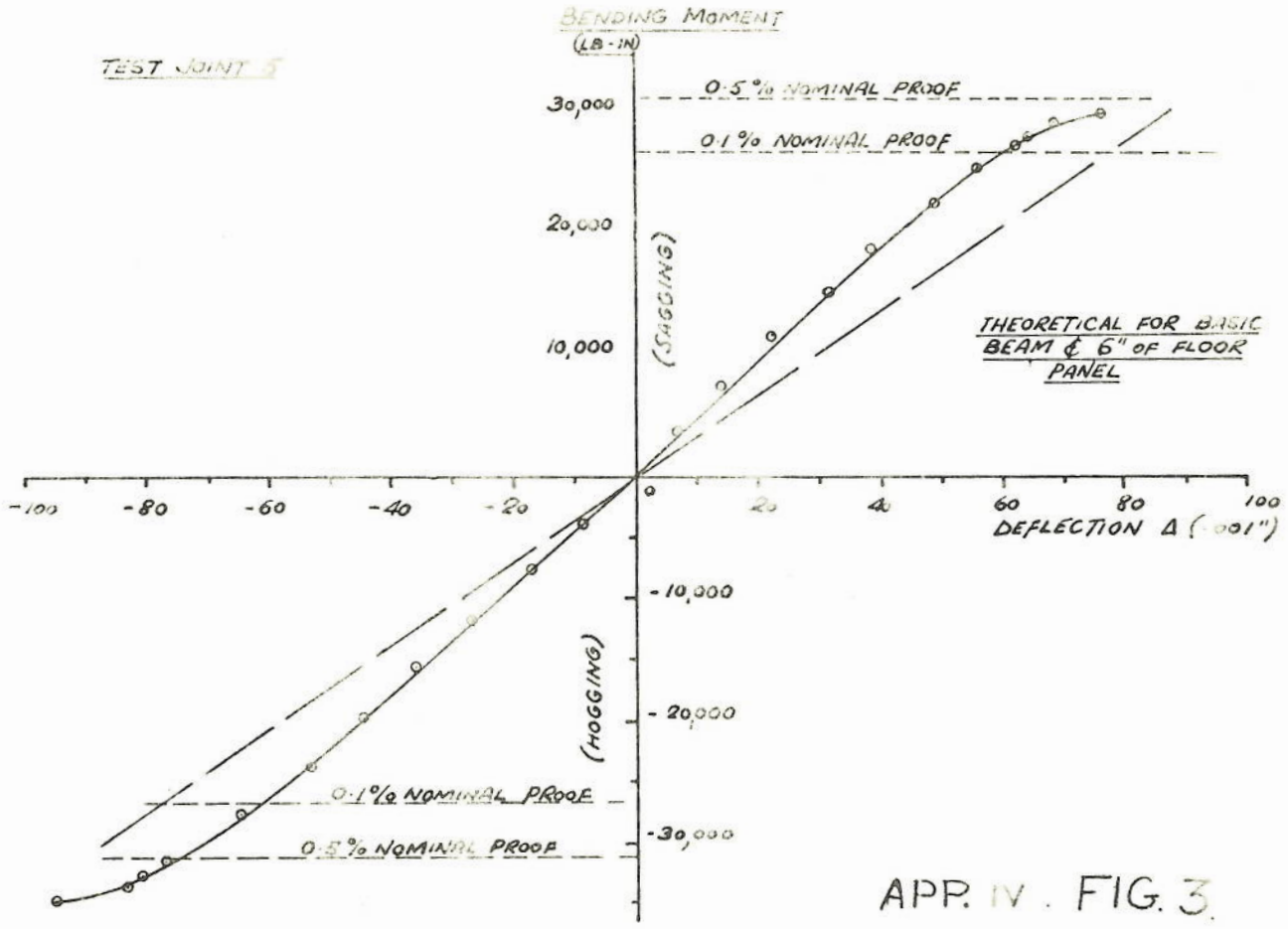

APP. IV . FIG. 3.

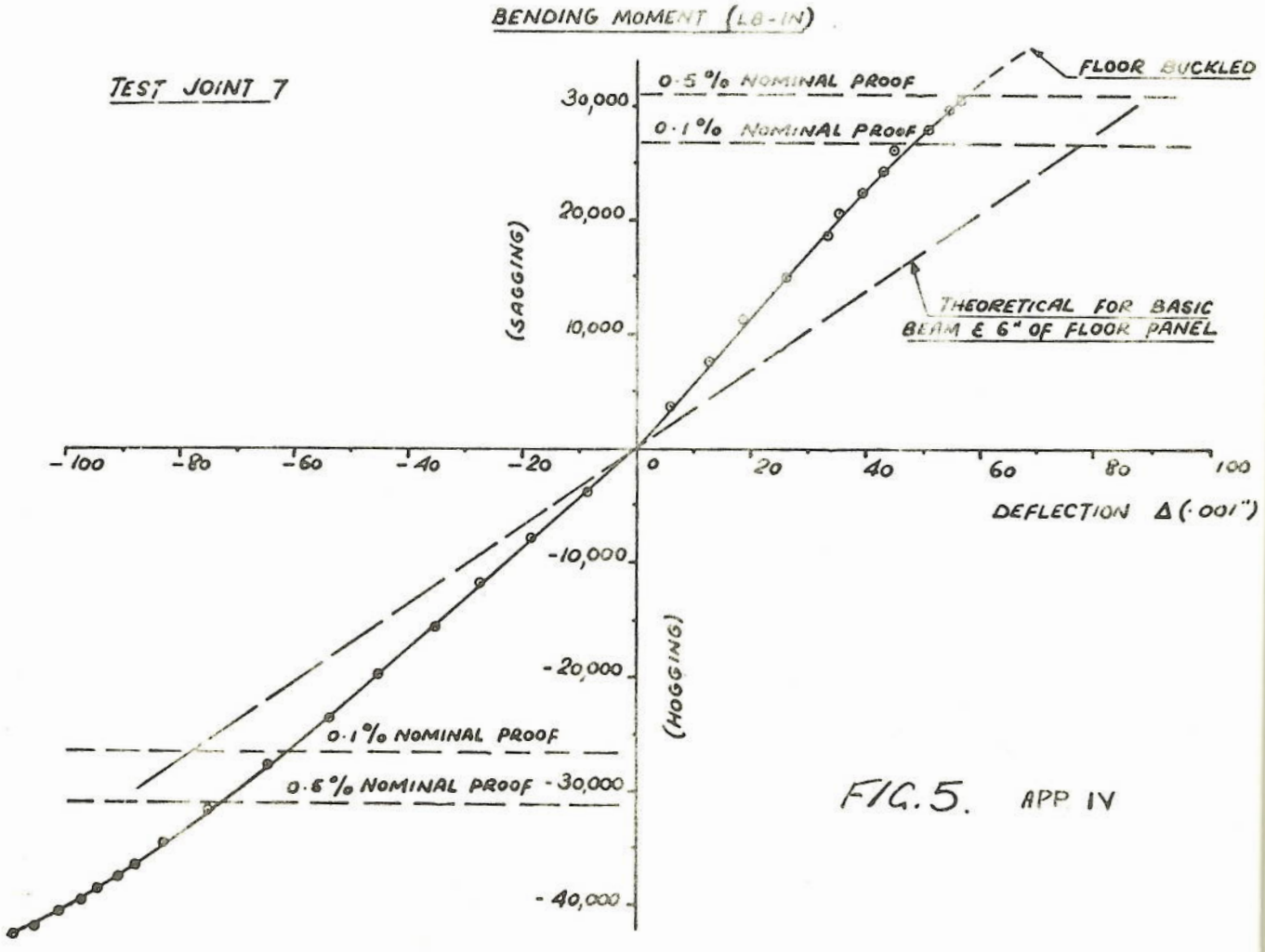

FIG. 5. APP IV

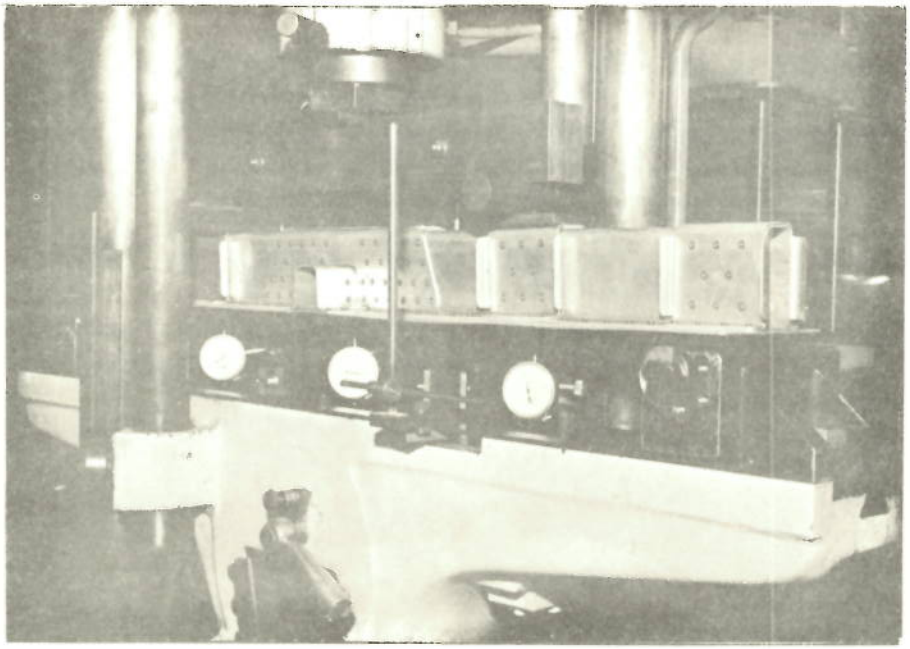

APP. IV FIG. 4

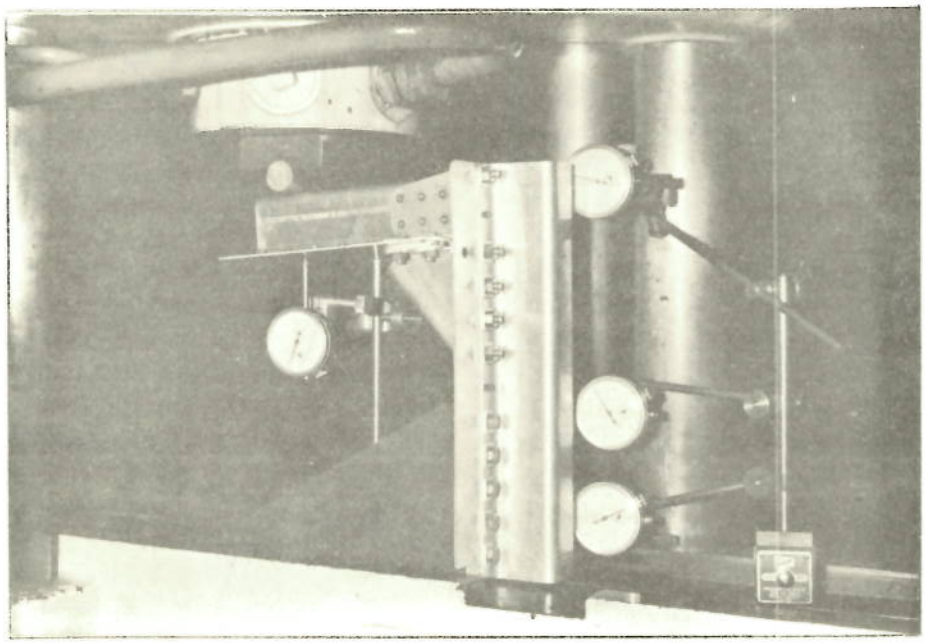

APP. IV. FIG. 5

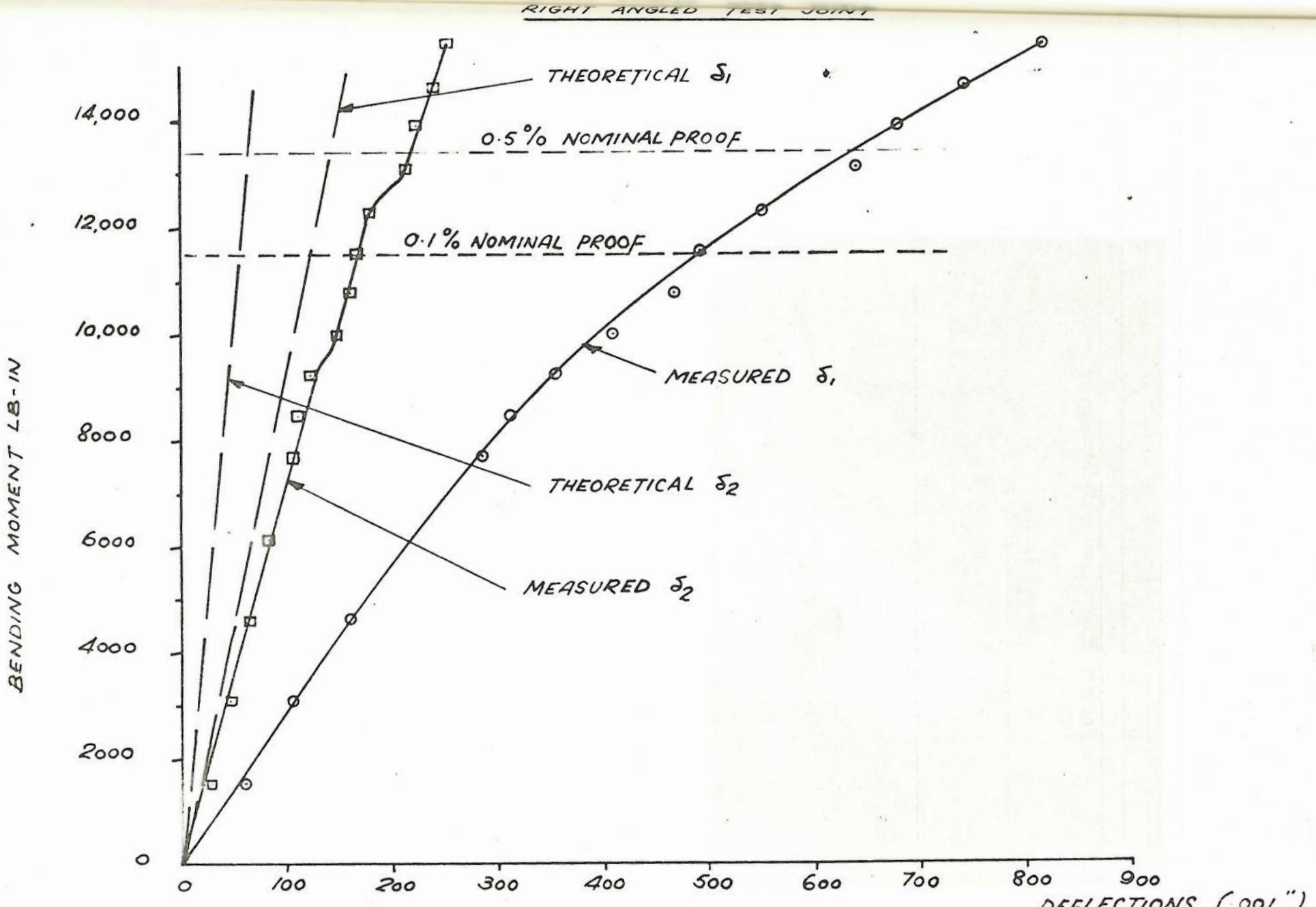
RIGHT ANGLED TEST JOINT
THEORETICAL δ_1
0·5% NOMINAL PROOF
0·1% NOMINAL PROOF
MEASURED δ_1
THEORETICAL δ_2
MEASURED δ_2
BENDING MOMENT LB-IN
14,000
12,000
10,000
8000
6000
4000
2000
0
0
100
200
300
400
500
600
700
800
900
DEFLECTIONS (·001")

APP. IV fig. 7

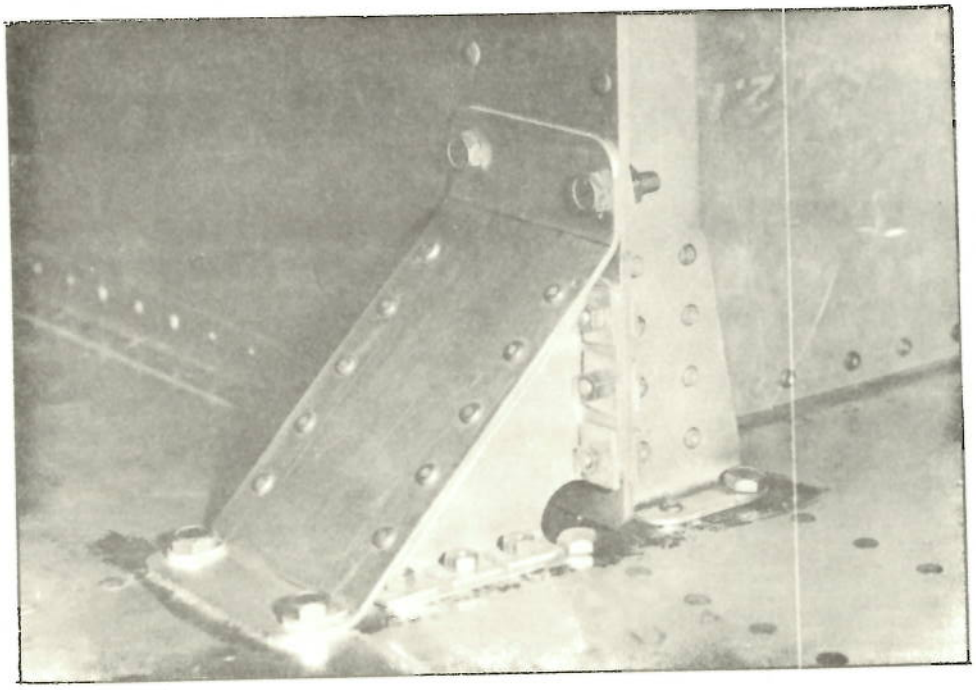

APP. IV FIG. 8